

Thesis title

**OPTIMISING THE DELIVERY AND MONITORING OF
PEPTIDE IMMUNOTHERAPY FOR TYPE 1 DIABETES**

Degree award title

PhD

Year of presentation

2015

Candidate name

Dr Danijela Tatovic

THESIS SUMMARY

Peptide immunotherapy for Type 1 diabetes aims to restore tolerance to self, whilst leaving the rest of the immune system intact. Once the right peptide is delivered to the right cell, it is important to closely monitor the effect of such a therapy, both in the regards to the immune and metabolic response.

Clinical trials are designed to test the effect of a drug at the end of the trial period, which can be years later. *Ex-vivo* human models are not subject to extensive regulatory requirements, and can rapidly provide proof of principle on the efficacy of a treatment, which can be then translated to the clinic.

I have shown that the skin organ bath culture is a useful system for studying treatment effects of variety of *ex-vivo* delivered agents. When used to optimise peptides delivery, it indicated a potential role of dry coated microneedles in targeting epidermal DCs, important because of their endogenous tolerogenic potential, which can be further modified by topical treatments and locally injected agents. Whether true tolerogenic potential can be achieved in such a way, is subject to further studies designed to optimise the type, dose and the duration of the treatment by the conditioning agent.

My data also suggested that lymph node fine needle aspiration biopsy is a feasible non-invasive method suitable for monitoring the cellular immune responses after antigen skin delivery. Subject to confirmatory study, it has a potential to find immediate application as an efficient and reliable tool for monitoring immune response after antigen-specific immunotherapy in clinical trials. Once recognised as 'immune responders' in such a way, participants in clinical trials can be subjected to the monitoring of the metabolic response to

the immune intervention, by measuring β -cell function via stimulated UCPCR as a non-invasive and more compliant-prone alternative to the standard MMTT.

DECLARATION

This work has not previously been accepted in substance for any degree and is not concurrently submitted in candidature for any degree.

This thesis is the result of my own independent work/investigation, except where otherwise stated. Other sources are acknowledged by explicit references.

Signed (candidate) Date

ABBREVIATIONS

Abbreviation	Explanation
5-TAMRA	5 - Carboxytetramethylrhodamine
AIRE	autoimmune regulator gene
ANOVA	Analysis of variance
AP-1	activator protein - 1
APC	Antigen presenting cell
APC dye	Allophycocyanin
ASI	Antigen-specific immunotherapy
AUC	Area under the curve
BCG	Bacillus Calmette–Guérin
BCIP/NBT	5-Bromo-4-chloro-3-indolyl phosphate/Nitro blue tetrazolium
BMI	Body mass index
BSA	Bovine serum albumin
C1R-A2 cells	HLA-A2 expressing, human plasma leukemia cell line
CCR	Chemokine receptor
CD	Cluster of differentiation
CI	Confidence interval
CLA	Cutaneous leukocyte antigen
CMV	Cytomegalo virus
cpm	counts per minute
CTLA-4	Cytotoxic T-lymphocyte antigen
Cy	Cyanine dye
DC	Dendritic cell
DC SIGN	Dendritic Cell-Specific Intercellular adhesion molecule-3-Grabbing Non-integrin (CD209)
DCCT	Diabetes Control and Complication Trial
DDC	Dermal dendritic cell
Dex-DC	Dexamethasone modulated dendritic cell
DI water	Deionized water

Abbreviation	Explanation
DIPP	Type 1 diabetes prediction and prevention project
DMEM	Dulbecco's modified Eagle medium
DMSO	Dimethylsulfoxide
DNA	Deoxyribonucleic acid
DNA-se	Deoxyribonuclease
DPT-1	Diabetes Prevention Trial 1
DTH	Delayed type hypersensitivity
EBV	Epstein Barr virus
EBVP1	Lytic protein BMLF-1 (280-288) Epstein-Barr virus peptide GLCTLVAML
EC	Epidermal cell
EDTA	Ethylenediaminetetraacetic acid
ELISA	Enzyme-linked immunosorbent assay
ELISPOT	Enzyme linked immunosorbent spot
EpCAM	Epithelial cell adhesion molecule
FCB	Flow-cytometry buffer
FCF	Flow-cytometry fixative
FCS	Foetal calf serum
FITC	Fluorescein isothiocyanate
FNA	Fine needle aspiration
Foxp3	Forkhead/winged-helix transcription factor box P3
FP1	HLA DR1 restricted cloned T cells, specific for hemagglutinin (306-318) Influenza A virus peptide PKYVKQNTLKLAT
FPIR	first phase insulin response
FSC	Forward scatter
G-CSF	Granulocyte colony stimulating factor
GAD	Glutamate-decarboxylase
GC	Glucocorticoid
GITR	Glucocorticoid-induced tumour necrosis factor receptor family-related gene
GLIS	Gli-similar

Abbreviation	Explanation
HAEP	HLA Epitope Analysis Programme
HEV	High endothelial venules
HLA	Human leukocyte antigen
HRP	Horseradish Peroxidase
HSP	Heat shock protein
i.d.	Intradermal
i.n.	Intranasal
i.v.	Intravenous
IA-2	Islet antigen-2, islet tyrosine phosphatase
IAA	insulin
IAPP	Islet amyloid polypeptide
ICA	insulin cell cytoplasmic antibodies
ICOS	inducible co-stimulator
IDO	Indolamine-2,3 dioxygenase
IFIH1 genes	Interferon induced with helicase C domain 1 gene
IFN- γ	Interferon γ
Ig	Immunoglobulin
IGRP	Islet-specific glucose-6-phosphatase catalytic subunit related protein
IL	Interleukin
IL-10p	Interleukin-10 pure
ILT	immunoglobulin like transcripts
INS gene	Insulin gene
LAG-3	Lymphocyte activation gene-3
LC	Langerhans cell
LD marker	Life/dead marker
LN	Lymph node
LNCs	Lymph node cells
MECLR	Mixed epidermal cell lymphocyte reaction
MFI	Mean fluorescent intensity

Abbreviation	Explanation
MHC	Major Histocompatibility Complex
MIP-1 β	Macrophage Inflammatory Protein 1 β
MLR	Mixed lymphocyte reaction
MM-UCPCR	Mixed meal stimulated UCPCR
MMP	Matrix metalloproteases
MMTT	Mixed meal tolerance test
MN	Microneedle
MNc	Microneedle coated with the coating solution only
MNpep	Microneedle coated with the peptide
mRNA	Messenger ribonucleic acid
NFAT-1	nuclear factor of activated cells -1
NF κ B	nuclear factor kappa-light-chain-enhancer of activated B cells
NOD mouse	Non-obese diabetic mouse
NP	Nanoparticle
NP IL-10	IL-10 attached to nanoparticle
NPPEs	naturally processed and presented peptide epitopes
PBMCs	Peripheral blood mononuclear cells
PBS	Phosphate buffered saline
PCR	Polymerase chain reaction
PDL	programmed death ligand
PE	Phycoerythrin
PerCP	Peridinin chlorophyll
PHA	Phytoheamagglutinin
PI	Proliferation index
PIT	Peptide immunotherapy
PTH	Parathyroid hormone
PTPN 22	T-cell protein phosphatase gene on chromosome 1
PVDF membrane	Polyvinylidene difluoride membrane
RD	Reagent diluent

Abbreviation	Explanation
REC	Research ethics committee
ROR γ T	RAR-related orphan receptor gamma
s.c.	Subcutaneous
s.l.	Sublingual
sCP	Serum C-peptide
SD	Standard deviation
SLC	Secondary lymphoid tissue chemokine
SSC	Side scatter
SST	Serum separator tubes
SST tubes	Serum separator tubes
STAT 1	signal-transducing activator of transcription 1
T1D	Type 1 diabetes
T2A2 cells	HLA-A2 expressing, antigen processing (TAP)-deficient human T-B lymphoblastoid hybrid cell line
TAE buffer	Tris-acetate-EDTA buffer
TCR	T cell receptor
TCR	T-cell receptor
TEDDY	Environmental Determinants of Diabetes in the Young
TEDDY Study	Trial of Environmental Determinants of Diabetes in the Young
T _{EMRA}	Effector memory RA positive T cells
TGF- β	Transforming growth factor β
TGF- β	Transfoming growth factor- β
Th1	T helper 1 cells
Th17	T helper 17 cells
Th2	T helper 2 cells
Th3	T regulatory cells type 3
TMB	Tetramethylbenzidine
TNF α	Tumour necrosis factor- α
Tr1	T regulatory cells type 1
Tregs	T regulatory cells

Abbreviation	Explanation
TU	Tuberculin units
Tuberculin PPD	Tuberculin protein purified derivative
uCP	Urinary C-peptide
UCPCR	Urinary C-peptide to creatinine
VEGF	Vascular endothelial growth factor
VIP	Vasoactive intestinal peptide
VitD3	Vitamin D3
VM	Viral mix
VNTR	variable numbers tandem repeat
ZnT8A	zinc transporter-8

ACKNOWLEDGMENTS

I would like thank my supervisors Prof. Colin Dayan and Prof. Susan Wong for supporting and guiding me during this project, and particularly for sharing their inspiring knowledge and enthusiasm for research.

I would like to thank my colleagues who helped me during this work, particularly Prof. James Birchall for his expertise in *ex vivo* human skin delivery and microneedle delivery, and Dr Philippa Young for performing fine needle lymph node aspirations.

I would also like to thank my parents, Mrs Ljubinka Tatovic and Mr Miroslav Tatovic, for their unconditional love and support throughout my life, my husband Prof. David Murphy and my daughter Miss Anja Babic for their love and for being my ultimate inspiration.

TABLE OF CONTENT

CHAPTER 1 INTRODUCTION.....	1
1.1 PATHOGENESIS OF TYPE 1 DIABETES.....	2
1.1.1 THE NORMAL IMMUNE RESPONSE.....	8
1.1.2 AUTOIMMUNITY IN TYPE 1 DIABETES.....	19
1.1.2.1 Genetic predisposition.....	21
1.1.2.2 Environment.....	23
1.1.2.3 β -cell epitopes.....	25
1.2 IMMUNE INTERVENTIONS IN TYPE 1 DIABETES.....	28
1.2.1 NON ANTIGEN-SPECIFIC INTERVENTIONS.....	29
1.2.2 ANTIGEN-SPECIFIC INTERVENTIONS.....	33
1.3 OPTIMISING IMMUNE INTERVENTIONS IN TYPE 1 DIABETES.....	35
1.3.1 WHEN AND WHAT TO GIVE?.....	36
1.3.2 HOW MUCH TO GIVE?.....	36
1.3.3 WHERE TO ADMINISTER?.....	37
1.3.4 WHOM TO TREAT?.....	37
1.3.5 HOW TO MONITOR EFFECT OF THE TREATMENT?.....	38
1.4 SUMMARY OF AIMS.....	41
1.4.1 TARGETING EPIDERMAL DENDRITIC CELLS IN PEPTIDE SKIN DELIVERY – RIGHT PLACE, RIGHT TOOL (CHAPTER 3).....	41
1.4.2 ENHANCEMENT OF THE TOLEROGENIC ENVIRONMENT IN PREPARATION FOR THE PEPTIDE IMMUNOTHERAPY (CHAPTER 4).....	41
1.4.3 METHODS FOR THE OPTIMAL MONITORING OF THE IMMUNE RESPONSE AFTER SKIN ANTIGEN DELIVERY (CHAPTER 5).....	42
1.4.4 ASSESSMENT OF STIMULATED UCPCR AS OPTIMAL METHOD FOR ESTIMATION AND MONITORING OF THE CHANGING B-CELL FUNCTION OVER TIME (CHAPTER 5).....	42
CHAPTER 2 MATERIALS AND METHODS.....	43
2.1 EX-VIVO METHODS FOR THE OPTIMAL TARGETING AND CONDITIONING OF SKIN DENDRITIC CELLS 44	
2.1.1 ISOLATION OF PERIPHERAL BLOOD MONONUCLEAR CELLS (PBMCs).....	44
2.1.2 ORGAN SKIN BATH CULTURE.....	44
2.1.3 MIXED LYMPHOCYTE REACTION (MLR).....	46
2.1.4 MIXED EPIDERMAL CELLS LYMPHOCYTE REACTION (MECLR).....	47
2.1.5 FLOW-CYTOMETRIC ANALYSIS.....	47
2.1.5.1 Phenotyping of the DCs in the epidermal cells single cell suspension.....	48
2.1.5.2 Phenotyping of the T cells harvested after 14-days long culture driven by epidermal cells with an without previous topical steroid exposure.....	50
2.1.5.3 HLA-A2 typing of the DCs in the epidermal single cell suspension.....	50
2.1.6 CYTOKINE DETECTION (ENZYME-LINKED IMMUNOSORBENT ASSAY – ELISA).....	51
2.1.6.1 Cytokine measurement in MLR and MECLR type reactions.....	51
2.1.6.2 IFN γ measurement in co-cultures of epidermal cells and HLA DR1 restricted FP1 specific cloned T-cells.....	53
2.1.6.3 MIP-1 β measurement in co-cultures of epidermal cells and HLA-A2 restricted EBVP1 specific cloned T-cells.....	53
2.1.7 MAGNETIC CELL SEPARATION.....	55
2.1.7.1 Naïve CD4 $^{+}$ T cell Isolation.....	55
2.1.7.2 CD4 $^{+}$ CD25 $^{+}$ CD127 $^{-}$ regulatory T cell isolation.....	56
2.1.8 EFFECT OF THE <i>EX VIVO</i> SKIN TREATMENT WITH IMMUNE-MODULATORY AGENTS.....	57
2.1.8.1 Steroid pre-treatment.....	57
2.1.8.2 Interleukin-10 (IL-10).....	58

In vitro assessment.....	59
Ex-vivo assessment.....	59
2.1.9 EFFECT OF THE <i>EX VIVO</i> SKIN TREATMENT WITH IMMUNE-MODULATORY AGENTS	60
2.1.10 PROTOCOL FOR GROWING CLONED T-CELLS	64
2.1.11 PROTOCOL FOR GROWING ANTIGEN-PRESENTING CELLS FOR STIMULATION OF CLONED T CELLS	67
2.1.12 PEPTIDE INJECTION TO THE SKIN IN THE ORGAN BATH CULTURE	67
2.1.12.1 Peptide injection via hollow microneedle.....	67
2.1.12.2 Peptide insertion via dry coated microneedle	69
The characteristics and the preparation of microneedles	69
Microneedle coating	70
Quantification of peptide delivery.....	70
Peptide administration.....	71
2.1.13 HLA-DR1 TYPING BY RAPID PCR.....	74
2.1.14 STATISTICS.....	76
2.2 <i>IN-VIVO</i> METHODS FOR THE OPTIMAL MONITORING OF THE IMMUNE RESPONSE AFTER ANTIGEN SKIN DELIVERY	77
2.2.1 ULTRASOUND GUIDED LYMPH NODE FINE NEEDLE ASPIRATION BIOPSY	78
2.2.2 IFN γ ELISPOT	78
2.2.3 PHENOTYPING OF THE LYMPH NODE CELLS AND PBMCs BY FLOW-CYTOMETRY.....	80
2.2.4 STATISTICS	82
2.3 <i>IN-VIVO</i> METHODS FOR THE EFFICIENT AND NON-INVASIVE ASSESSMENT AND MONITORING OF THE RESIDUAL B-CELL FUNCTION IN TYPE 1 DIABETES.....	83
2.3.1 MAIN STUDY	83
2.3.1.1 Setting and subjects	83
2.3.1.2 UCPCR stimulation	83
2.3.1.3 Standard MMTT.....	84
2.3.1.4 Home urine collections.....	84
a) Months 1 and 6 – home MM-UCPCR.....	84
b) Months 2, 3, 4 and 5 – home meal-UCPCR.....	84
2.3.1.5 Urine and serum samples.....	85
2.3.2 ADDITIONAL SAMPLES.....	86
2.3.3 STATISTICS	86
<u>CHAPTER 3 TARGETTING EPIDERMAL DENDRITIC CELLS IN PEPTIDE SKIN DELIVERY – RIGHT PLACE, RIGHT TOOL.....</u>	<u>88</u>
3.1 INTRODUCTION.....	89
3.1.1 OPTIMAL DELIVERY ROUTE FOR PEPTIDE IMMUNOTHERAPY (PIT).....	89
3.1.1.1 Histology of the human skin [142].....	90
Epidermis	90
Dermis.....	91
Hypodermis	91
3.1.1.2 Skin antigen-presenting cells (APCs)	91
3.1.2 OPTIMAL DELIVERY DEVICE FOR THE PEPTIDE IMMUNOTHERAPY	94
3.2 HYPOTHESIS	99
3.3 AIMS.....	99
3.4 RESULTS.....	100
3.4.1 ORGAN SKIN BATH CULTURE: AN <i>EX VIVO</i> METHOD TO INVESTIGATE SKIN DENDRITIC CELLS	100
3.4.2 PEPTIDE UPTAKE BY EPIDERMAL DCs AFTER INJECTION BY HOLLOW MICRONEEDLES.....	104
3.4.3 EBVP1 PEPTIDE UPTAKE BY EPIDERMAL DCs AFTER INSERTION BY DRY COATED MICRONEEDLES	111
3.5 SUMMARY OF FINDINGS.....	119

3.5.1	SKIN ORGAN BATH CULTURE	119
3.5.2	TARGETING THE RIGHT SKIN DCs	121

CHAPTER 4 ENHANCEMENT OF TOLEROGENIC ENVIRONMENT IN PREPARATION FOR PEPTIDE IMMUNOTHERAPY 126

4.1	INTRODUCTION.....	127
4.1.1	ROLE OF DCs IN MAINTAINING TOLERANCE TO SELF-ANTIGENS	127
4.1.1.1	Dendritic cells in immune defense	127
4.1.1.2	Dendritic cells in tolerance.....	128
4.1.2	PHARMACOLOGICAL MODULATION OF DCs TO ENHANCE TOLERANCE	129
4.1.2.1	Vitamin D and dexamethasone as immunomodulating agents	129
	In vitro and animal studies	129
	Human studies	130
4.1.2.2	Pharmacological modulation of skin dendritic cells	131
	Vitamin D3 and steroids	131
	IL-10	132
4.2	HYPOTHESIS	133
4.3	AIMS.....	133
4.4	RESULTS.....	134
4.4.1	TOPICAL STEROID TREATMENT	134
4.4.1.2	Effect of topical steroid (0.05% betamethasone w/w) on cell viability	134
4.4.1.3	Effect of topical steroid on dendritic cells surface markers.....	137
4.4.1.4	Effect of topical steroid on skin DCs ability to induce proliferation in Mixed Epidermal Cell Lymphocyte Reaction (MECLR)	142
4.4.2	EFFECT OF IL-10.....	151
4.4.2.1	Effect of in vitro added IL-10 on Mixed Lymphocyte Reaction.....	151
4.4.2.2	Effect of ex-vivo IL-10 skin injection on Mixed Epidermal Cell Lymphocyte Reaction	156
4.5	SUMMARY OF FINDINGS.....	158
4.5.1	EFFECT OF TOPICAL STEROID TREATMENT	158
4.5.2	EFFECT OF IL-10.....	161

CHAPTER 5 *IN-VIVO* METHODS FOR THE OPTIMAL MONITORING OF THE IMMUNE RESPONSE AFTER ANTIGEN SKIN DELIVERY 164

5.1	INTRODUCTION.....	165
5.1.1	ANATOMY AND HISTOLOGY OF THE LYMPH NODES.....	166
5.1.2	INTERPLAY BETWEEN SKIN AND THE LYMPH NODE DURING IMMUNE RESPONSE.....	168
5.1.2.1	Dendritic cells.....	169
5.1.2.2	T cells	170
5.1.2.3	T regulatory cells	171
5.1.3	MANTOUX TEST	173
5.2	HYPOTHESIS	176
5.3	AIM.....	176
5.4	RESULTS.....	177
5.4.1	LYMPH NODE ASPIRATE	179
5.4.2	RESPONSE AFTER TWO DAYS OF TUBERCULIN PPD INJECTION	189
5.4.2.1	Lymph node size	189
5.4.2.2	ELISPOT	189
5.4.2.3	Flow cytometry analysis.....	196
5.4.3	RESPONSE AFTER FIVE DAYS OF TUBERCULIN PPD INJECTION.....	200
5.4.3.1	Lymph node size	200
5.4.3.2	ELISPOT	200
5.4.4	MANTOUX NEGATIVE SUBJECTS	204

5.5 SUMMARY OF FINDINGS.....	205
CHAPTER 6 NON-INVASIVE ASSESSMENT AND MONITORING OF CHANGES IN B-CELL FUNCTION	211
6.1 INTRODUCTION.....	212
6.1.1 MEASURING RESIDUAL B-CELL FUNCTION	213
6.1.2 PRACTICAL APPLICATION OF TESTS FOR ESTIMATION OF RESIDUAL B-CELL FUNCTION.....	215
6.2 HYPOTHESIS	217
6.3 AIMS	217
6.4 RESULTS.....	218
6.4.1 MAIN STUDY	218
6.4.1.1 Standard mixed meal stimulation of β -cell insulin production	220
6.4.1.2 Correlation of hospital MM UCPCR with the diabetes related parameters	222
6.4.1.3 Collection of repeated home UCPCR values and change of β - cell function over time	223
6.4.1.4 Home meal stimulation of β -cell insulin production.....	225
6.4.2 ADDITIONAL SAMPLES.....	226
6.5 SUMMARY OF FINDINGS.....	228
CHAPTER 7 GENERAL DISCUSSION AND CONCLUDING REMARKS.....	231
7.1 SKIN ORGAN BATH CULTURE FOR THE ASSESSMENT OF OPTIMAL ANTIGEN SKIN DELIVERY	234
7.1.1 THE SKIN ORGAN BATH CULTURE MODEL	234
7.1.2 TARGETING EPIDERMAL DENDRITIC CELL IN THE PEPTIDE SKIN DELIVERY.....	236
7.1.3 ENHANCEMENT OF TOLEROGENIC ENVIRONMENT IN PREPARATION FOR PEPTIDE IMMUNOTHERAPY	239
7.2 MONITORING IMMUNOLOGICAL AND METABOLIC OUTCOMES	242
7.2.1 IMMUNE RESPONSE MONITORING AFTER SKIN ANTIGEN DELIVERY	242
7.2.2 MONITORING OF THE METABOLIC OUTCOME	244
REFERENCES	246
APPENDIX – SOURCES OF MATERIALS.....	263

LIST OF FIGURES

Figure 1-1. Development of Type 1 diabetes	3
Figure 1-2. Activation of naïve T cells.....	11
Figure 1-3. Interplay between genetic and environmental factors in the pathogenesis of Type 1 diabetes	25
Figure 1-4. Antigenic distribution of (a) CD4 and (b) CD8 T cell epitopes in autoimmune diabetes in humans and mice.	26
Figure 1-5. Targets of therapeutic agents used in immune intervention studies in Type 1 diabetes.....	29
Figure 2-1. Organ skin bath culture	45
Figure 2-2. Representative examples of ELISA standard curves.....	53
Figure 2-3. Representative example of MIP-1 β ELISA standard curve.	55
Figure 2-4. <i>Ex-vivo</i> topical application of the betamethasone cream	58
Figure 2-5. <i>Ex-vivo</i> injection and bleb formation of IL-10.....	59
Figure 2-6. Flow chart of the culture of the T cells stimulated by epidermal DCs with and without previous <i>in vivo</i> topical steroid exposure.....	61
Figure 2-7. Assessment of the suppressive capacity of the T cells previously stimulated by epidermal DCs with and without previous <i>in vivo</i> topical steroid exposure.	63
Figure 2-8. EBVP1 specific, HLA-A2 restricted cloned T-cells in the culture (day 9) ...	66
Figure 2-9. Hollow microneedle.	68
Figure 2-10. The shape and the dimensions of steel dry microneedle.....	70
Figure 2-11. Representative example TAMRA-EBVP1 standard curve.	71
Figure 2-12. Peptide administration into the skin explant via dry coated microneedle.	72
Figure 2-13. Experimental protocol for the assessment of the efficacy of peptide loading of skin dendritic cells	73
Figure 3-1. Histology of the human skin	90
Figure 3-2. Types of the dendritic cells.....	92
Figure 3-4. Flowcytometric analysis of the dendritic cells in the epidermal cell suspension	101

Figure 3-5. Flowcytometric analysis of the epidermal single cell suspension	102
Figure 3-6. Mixed Epidermal Cells Reaction proliferation (MECLR) driven by epidermal DCs.....	103
Figure 3-7. HLA DR1*0101-0103 typing.....	105
Figure 3-8. Sensitivity of HLA-DR1 restricted cloned T cells to FP1 peptide.....	105
Figure 3-9. IFN γ production by FP1 specific cloned T cells stimulated by HLA DR1 negative donors.....	106
Figure 3-10. IFN γ production by FP1 specific cloned T cells stimulated by HLA DR1 positive donors	108
Figure 3-11. IFN γ production by FP1 specific cloned T cells stimulated by HLA-DR1 positive donors	110
Figure 3-12. Efficacy of EBVP1 delivery via dry coated microneedle.....	112
Figure 3-13. Representative example of the expression of HLA A2	113
Figure 3-14. Sensitivity of HLA-A2 restricted cloned T cells to EBVP1 peptide.....	113
Figure 3-15. MIP1- β production by EBVP1 specific cloned T cells stimulated by HLA- A2 negative donors.....	114
Figure 3-16. MIP1- β production by EBVP1 specific cloned T cells stimulated by HLA- A2 positive donors.....	116
Figure 3-17. MIP1- β production by EBVP1 specific cloned T cells: microneedle vs intradermal delivery in HLA-A2 positive donors.....	118
Figure 4-1. Flowcytometric analysis of the viability of epidermal cells with and without topical steroid treatment.....	134
Figure 4-2. Viability of epidermal cells following exposure to the topical steroid treatment, flowcytometric analysis of the representative sample.	135
Figure 4-4. Viability of dendritic cells following the exposure to the topical steroid treatment, flowcytometric analysis of the representative sample	136
Figure 4-5. HLA DR expression on skin dendritic cells with and without topical steroid treatment.....	138
Figure 4-6. HLA DR expression on skin dendritic cells with and without topical steroid treatment, flowcytometric analysis of the representative sample.....	138
Figure 4-7. CD80 expression on skin dendritic cells with and without topical steroid treatment.....	13

Figure 4-8. CD80 expression on skin dendritic cells with and without topical steroid treatment, flowcytometric analysis of the representative sample.....	139
Figure 4-9. CD86 expression on skin dendritic cells with and without topical steroid treatment.....	140
Figure 4-10. CD83 expression on skin dendritic cells with and without topical steroid treatment.....	140
Figure 4-11. CD40 expression on skin dendritic cells with and without topical steroid treatment.....	141
Figure 4-12. Proliferation in MECLR driven by DCs with and without exposure to the topical treatment.....	143
Figure 4-13. IL-10 produced in the MECLRs driven by DCs with and without exposure to the topical treatment.....	144
Figure 4-14. IFN γ produced in the MECLRs driven by DCs with and without exposure to the topical treatment.....	145
Figure 4-15. IL-10/IFN γ ratio produced in the MECLRs driven by DCs with and without exposure to the topical treatment.....	146
Figure 4-16. Representative example of the flowcytometric analysis of the cells harvested after 14 days long incubation of the epidermal cells suspension (with and without <i>in vivo</i> steroid pre-treatment) and the allogeneic responder CD4+ naïve T cells	148
Figure 4-17. Effect of Tcells pre-stimulated by steroid exposed and untreated epidermal DCs, on proliferation and cytokine production	150
Figure 4-18. <i>In-vitro</i> effect of IL-10 on proliferation in MLR	151
Figure 4-19. <i>In-vitro</i> effect of IL-10 on IFN γ production in MLR	152
Figure 4-20. <i>In-vitro</i> effect of combined NP IL-10 and anti-IL-10 on proliferation and IFN γ production in MLR.	154
Figure 5-1. Anatomy of the axillary lymph nodes.....	167
Figure 5-2. Histology of the lymph node.....	168
Figure 5-3. Study progression flow chart.....	178
Figure 5-4. Lymph node aspirate	179
Figure 5-5. Representative example of gating strategy.....	180
Figure 5-6. Summary of the ratio of CD3 ⁺ /CD19 ⁺ cells in lymph node and blood	181

Figure 5-7. Summary of the ratio of CD4 ⁺ /CD8 ⁺ cells in lymph node and blood derived CD3 ⁺ population.....	181
Figure 5-8. Representative flow cytometric analysis of the CD4:CD8 ratio in the CD3 ⁺ population.	182
Figure 5-9. Flow cytometric analysis of CD45RA and CCR7 expression in the LN and in the blood	184
Figure 5-10. Flow cytometric analysis of CD45RA and CD69 expression in the LN and in the blood	185
Figure 5-11. Flow cytometric analysis of skin homing receptors in the LN and in the blood.....	187
Figure 5-12. Comparison of naïve vs memory	188
Figure 5-13. Lymph node cortex thickness at baseline and two days after Mantoux test.....	189
Figure 5-14. Representative example of the ELISPOT plate used for counting IFN γ producing cells in the suspension of lymph node aspirate cells (LNCs) before and two days after <i>in vivo</i> injection of Tuberculin PPD.	190
Figure 5-15. Representative example of the ELISPOT plate used for counting IFN γ producing cells in the suspension of PBMCs before and two days after <i>in vivo</i> injection of Tuberculin PPD	191
Figure 5-16. Summary of the ELISPOT response to <i>in vitro</i> Tuberculin PPD before and two days after <i>in vivo</i> injection.....	192
Figure 5-17. Summary of the ELISPOT response of LNCs to <i>in vitro</i> PHA, Tetanus toxoid and viral mix before and 48h after <i>in vivo</i> Tuberculin PPD injection.....	193
Figure 5-18. Summary of the ELISPOT response of PBMCs to <i>in vitro</i> control antigens before and two days after <i>in vivo</i> Tuberculin PPD injection.....	194
Figure 5-19. CD4 ⁺ /CD8 ⁺ ratio before and two days after Tuberculin PPD	196
Figure 5-20. Representative example of CD69 expression on blood and lymph node derived T cells before and two days after Tuberculin PPD injection.	198
Figure 5-21. Percentage of CD69 ⁺ cells on lymph node derived T cells before and two days after Tuberculin PPD injection.....	199
Figure 5-22. Lymph node thickness at baseline and five days after Mantoux test. Statistical test used: Wilcoxon signed ranked test.	200
Figure 5-23. Summary of the ELISPOT response to <i>in vitro</i> Tuberculin PPD before and five days after <i>in vivo</i> injection	201
Figure 5-24. Summary of the ELISPOT response of LNCs to <i>in vitro</i> PHA and Tetanus toxoid before and five days after <i>in vivo</i> Tuberculin PPD injection	202

Figure 5-25. Summary of the ELISPOT response of PBMCs to <i>in vitro</i> Tetanus toxoid before and five days after <i>in vivo</i> Tuberculin PPD injection	203
Figure 5-26. Summary of the baseline ELISPOT response of PBMCs to <i>in vitro</i> Tuberculin PPD at in Mantoux negative subjects	204
Figure 5-27. Interplay between skin and its regional draining lymph node following antigen skin delivery	209
Figure 6-1. Flow-diagram of participants' progress during the study.	219
Figure 6-2. Serum C-peptide and glucose levels during 120 min of MMTT	220
Figure 6-3. Peak serum C-peptide and AUC serum C-peptide during MMTT	221
Figure 6-4. Correlation between peak serum C-peptide and MM-UCPCR.	222
Figure 6-5. Correlation between peak serum C-peptide and fasting UCPCR measured from second morning void sample	222
Figure 6-6. Correlation of hospital MM UCPCR with diabetes related parameters .	223
Figure 6-7. MM-UCPCR change over 6 months	224
Figure 6-8. Correlation of peak serum C-peptide with home meal stimulated UCPCR (HM UCPCR).....	225
Figure 6-9. Correlation: Peak serum C-peptide and MM-UCPCR	226
Figure 6-10. Correlation: Change in the peak serum C-peptide and the change in the MM-UCPCR.	227
Figure 7-1. Dilemmas, answers and scope for the future in the optimisation of the efficacy of the peptide immunotherapy.....	233
Figure 7-2. Flow cytometry profile of the dermal dendritic cells. a) CD1a/HLA-DR staining; b) Langerin/CD1a staining; c) Langerin/CD1a staining.....	238

LIST OF TABLES

Table 1-1. Phenotyping of the T regulatory cells.....	16
Table 1-2. Protective and susceptibility MHC class II alleles in Type 1 diabetes	21
Table 2-1. Monoclonal antibodies for flow-cytometry – panels for the epidermal cells	49
Table 2-2. Role of the surface markers used for the flow-cytometric analysis of DCs.	49
Table 2-3. Monoclonal antibodies for flow-cytometry – panels for the T cells cultivated in the culture driven by steroid exposed and untreated ECs.....	50
Table 2-4. Monoclonal antibodies for flow-cytometry – panel for HLA-A2 typing.....	50
Table 2-5. Content of cloning media	64
Table 2-6. HLA DR1 and control primers characteristics.	74
Table 2-7. Components and quantities of PCR mixture: HLA-DR1 primer reaction and control primer reaction.	75
Table 2-8. Conditions of the PCR reaction.....	75
Table 2-9. Conditions for incubation of cells prior to placement in the ELISPOT plates.	79
Table 2-10. Monoclonal antibodies for flow-cytometry (baseline analysis) – panels for LNCs and PBMCs.	81
Table 2-11. Monoclonal antibodies for flow-cytometry (before and after Mantoux test) – panels for LNCs and PBMCs.....	82
Table 2-12. Time-line of urine sample collection for UCPCR after different stimuli...	85
Table 3-1. Microneedle types and mechanisms of drug delivery.....	96
Table 3-2. IFN γ production by FP1 specific cloned T cells co-cultured with epidermal cells (containing DCs) from HLA DR1 negative donors.	107
Table 3-3. IFN γ production by FP1 specific cloned T cells co-cultured with epidermal cells (containing DCs) from HLA DR1 positive donors..	109
Table 3-4. Efficacy of EBVP1 delivery via dry coated microneedle.....	112
Table 3-5. MIP1- β production by EBVP1 specific cloned T cells co-cultured with epidermal cells (containing DCs) from HLA-A2 negative donors.	115
Table 3-6. MIP1- β production by EBVP1 specific cloned T cells co-cultured with epidermal cells (containing DCs) from HLA-A2 positive donors.	117

Table 4-1. Flowcytometric analysis of the viability of epidermal cells with and without topical steroid treatment.	134
Table 4-2. Flowcytometric analysis of the epidermal cells solution with and without topical steroid.	135
Table 4-3. Surface markers used for the phenotyping of the epidermal DCs.....	137
Table 4-4. HLA DR expression on skin dendritic cells with and without topical steroid treatment	138
Table 4-5. CD80 expression on skin dendritic cells with and without topical steroid treatment.	139
Table 4-6. CD86 expression on skin dendritic cells with and without topical steroid treatment.	140
Table 4-7. CD83 expression on skin dendritic cells with and without topical steroid treatment.	140
Table 4-8. CD40 expression on skin dendritic cells with and without topical steroid treatment.	141
Table 4-9. Proliferation in MECLR driven by DCs with and without exposure to the topical treatment.....	143
Table 4-10. IL-10 produced in the MECLRs driven by DCs with and without exposure to the topical treatment..	144
Table 4-11. IFN γ produced in the MECLRs driven by DCs with and without exposure to the topical treatment.	145
Table 4-12. IL-10/IFN γ ratio produced in the MECLRs driven by DCs with and without exposure to the topical treatment.	146
Table 4-13. <i>In-vitro</i> effect of IL-10 on proliferation in MLR.	152
Table 4-14. <i>In-vitro</i> effect of IL-10 on IFN γ production in MLR.	153
Table 4-15. <i>In-vitro</i> effect of combined anti-IL10 and NP IL-10 on proliferation and IFN γ production in MLR.	155
Table 4-16. <i>Ex-vivo</i> effect of combined NP IL-10 and anti-IL-10 on proliferation and IFN γ production in MECLR.	157
Table 5-1. Comparison between distribution of cells in four stages of T cell activation in the LN and blood.	186
Table 5-2. CD69 expression calculated as MFI on blood derived and lymph node derived T cells.	197
Table 5-3. CD154 expression calculated as MFI on blood derived and lymph node derives T cells.	199

Table 5-4. HLA-DR expression calculated as MFI on blood derived and lymph node derives T cells.	199
Table 6-1. Abbreviations of the parameters used in the study.	218
Table 6-2. Demographic and diabetes related characteristics of the patients on entering the study.	220
Table 6-3. Comparison of patients with complete and incomplete data sets.....	224

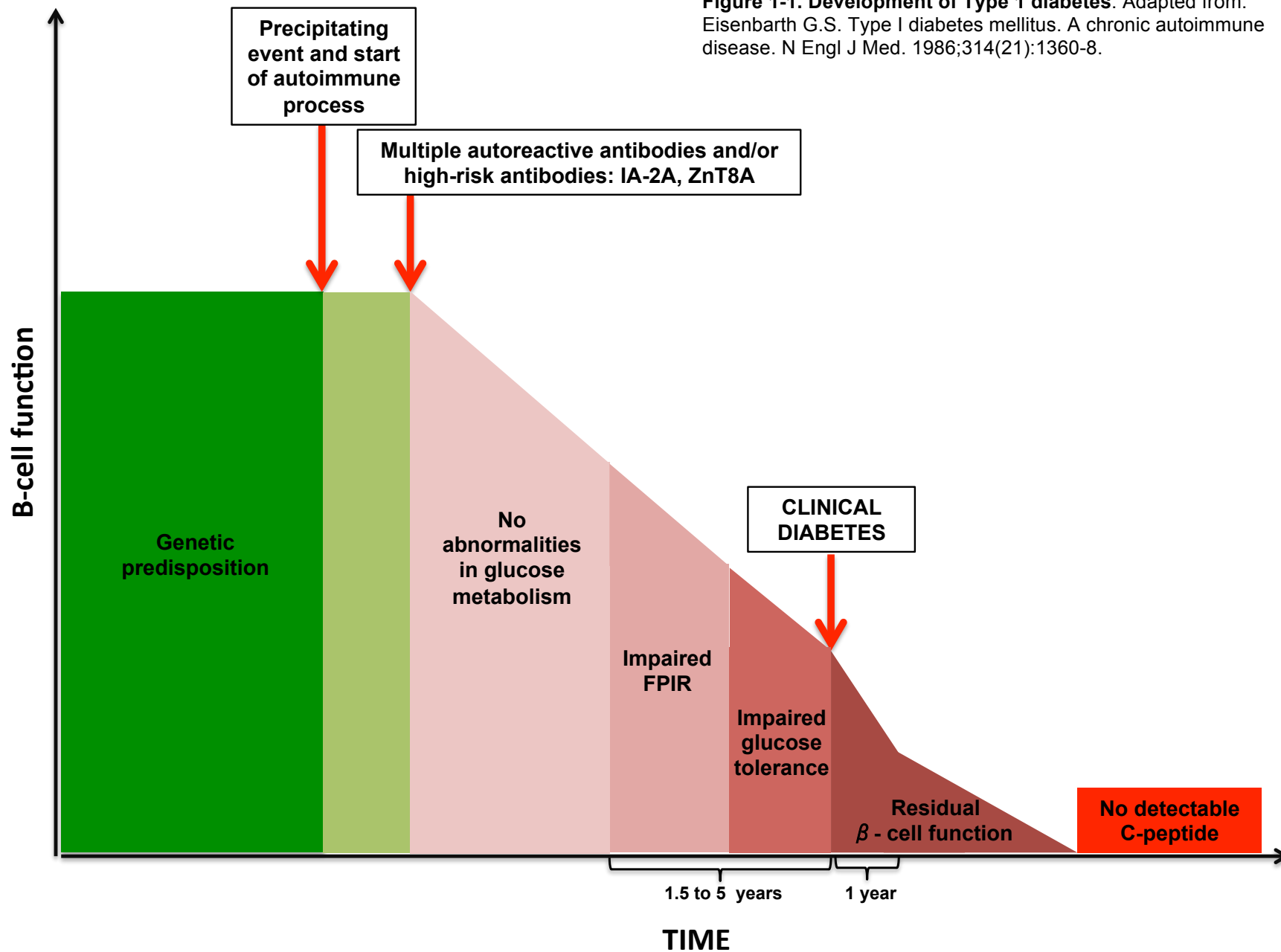
Chapter 1 INTRODUCTION

Despite nearly 100 years of experience and improvement in insulin replacement therapy, Type 1 diabetes (T1D) remains a challenge to control and manage from the perspectives of the patients, their families and their physicians. The implications of poor diabetes control involve acute life-threatening conditions, such as diabetic ketoacidosis and hypoglycaemia, and chronic complications, including heart disease, retinopathy, neuropathy and kidney disease. Understanding the aetiology and pathogenesis of T1D is crucial to base strategies to prevent and treat this life-changing and potentially fatal disease.

1.1 Pathogenesis of Type 1 diabetes

T1D is the result of selective immune-mediated attack on the insulin producing β -cells of the pancreas. This chronic destructive inflammation, influenced by various factors, exhibits variable severity in different individuals, from rampant insult in childhood, to the slowly developing disease encountered in some adults. In genetically predisposed individuals, immunological assault begins with one self-antigen and spreads to relevant others, leading to metabolic abnormalities, starting from attenuated first phase insulin response (FPIR) to intravenous glucose challenge, loss of glucose tolerance and, finally, clinical diabetes – **Figure 1-1**. [1, 2] It has been estimated that takes approximately 1.5 to 5 years from attenuated FPIR to diagnosis of Type 1 diabetes [3], at which point 50-80% of β -cell function has been lost. [4] It seems that the loss of β -cell function after diagnosis follows biphasic pattern, with faster decline in the first year after diagnosis, implying different intensity and/or type of metabolic and immunological factors in the early stage. [5]

Figure 1-1. Development of Type 1 diabetes. Adapted from:
Eisenbarth G.S. Type I diabetes mellitus. A chronic autoimmune
disease. N Engl J Med. 1986;314(21):1360-8.



Indeed, autoantibodies against pancreatic self-antigens, such as glutamate-decarboxylase (GADA), islet tyrosine phosphatase (islet antigen-2, IA-2A), insulin (IAA), and zinc transporter-8 (ZnT8A) are detectable in blood, years before clinical presentation of the disease. They can appear any time during life, but peak at one to three years of age in children who go on to develop early diabetes, and again in puberty, with the second wave of high incidence of T1D.[6-8] The rate of the autoimmune process varies significantly between individuals and can be influenced by factors such as HLA type, age, gender, the presence of insulin resistance and autoreactive antibodies.[2] The humoral response to pancreatic self-antigens, including changes in antibody number, type and concentration, gives us a valuable glance into the dynamic of this intriguing process. First to appear are usually IAA, followed by GADA, then IA-2A and ZnT8A. The latter usually represent more aggressive autoimmunity and are a critical turning point in the pathogenesis, announcing impending clinical diabetes. In addition to this intermolecular antigen spreading that is more likely to be sequential [9], it seems that the process shifts intra-molecularly as well, with antibodies to juxta-membrane parts of the IA-2A appearing first, followed by intracytoplasmatic tyrosine phosphatase epitopes later in the course of disease development. A study that analysed the antibody profile in children early after diagnosis observed an increase in the proportion of children with multiple antibodies, and antibodies suggestive of more aggressive autoimmunity, such as ZnT8 and IA-2 β , over a period of 20 years.[10] These authors speculated that an increase in body mass index (BMI) of children might be a contributing factor, leading to the role of insulin resistance and consequent apoptosis of β -cells leading to more widespread

antigen exposure. However, findings in the BABYDIAB study did not support the role of increasing BMI in the development of the autoimmunity.[11]

Although seroconversion peaks early in life, it seems that the first antibody can appear any time between the ages of one and 60 years, according to some early observations.[9] A number of studies, mainly involving children and young adults, tried to understand and predict the rate of progression to clinical diabetes from this early seroconversion. In a study involving the siblings of patients with T1D aged 16 to 39 years, it was calculated that the 5-year risk of developing the disease increased from 13% in individuals with one or more detectable antibodies, to 34% in people with three or more. In another study, the majority of children with multiple antibodies progressed to diabetes within 15 years, and even faster if they seroconverted at very young age, three years and younger.[12] But, the presence of certain antibodies increased the risk even further, such as that individuals with positive IA-2A had a risk of developing diabetes in 5 years as high as 59%.[13] This was in agreement with the finding of the prospective TEDDY study where, alongside a first degree relative with T1D, the combination of IA-2A, GADA and IAA, was found to be a risk factor for early development of T1D, as well as the combination of GADA and IAA.[14] However, it seems that after seroconversion, children with certain genotypes (carriers for risk alleles in CD25, IL2, INS, IFIH1 genes, see below) progress quicker than others.[15]

In an attempt to link the dynamic of the humoral autoimmunity to the metabolic status in pre-diabetic phase of T1D, the Type 1 diabetes prediction and prevention project (DIPP), conducted in genetically predisposed children aged one to five years, found that decreased FPIR during intravenous glucose

challenge is an early metabolic predictor of the imminent diabetes, which was correlated with the presence of insulin cell cytoplasmic antibodies (ICA), multiple antibodies and their titers. However, approximately half of the children did not present with the clinical diabetes during the four years long follow up, suggesting the role of immune and/or metabolic compensation mechanisms operating in some individuals, that certainly contribute to the variety in the duration of the pre-diabetic stages.[16]

When combined with antibody status, diminished FPIR increased the risk of progression to clinical diabetes in the large ICARUS cohort of the first degree relatives with positive ICA (85% within 5 years) [17] and in a Finnish study where a combination of low FPIR and positive antibodies increased the risk of developing T1D to 92%, in comparison to only 66% when FPIR was not considered.[18]

Although the role of B-cells is emerging as a significant contributor in the pathogenesis of T1D, the cellular autoimmunity is still seen as the main culprit in this process that takes place in the islets of the Langerhans.

In the non-obese diabetic (NOD) mouse model, it has been shown that the disease progression correlates with the degree of insulitis, the inflammatory process in the islet of Langerhans.[19] It is difficult to establish the same temporal character of the histological changes in humans, but post-mortem material from patients early in the disease showed various degrees of insulitis with cell infiltrate consisting predominantly of CD8 T cells, with CD4 T cells, B cells and macrophages also present.[20] Another study using pancreatic biopsies from recently diagnosed patients showed that affected pancreatic

cells hyper-expressed Major Histocompatibility Complex (MHC) class I, which, together with the degree of insulinitis, correlated with deteriorating glycaemic control.[20, 21]. This hyper-expression of class I was recently confirmed in nPod samples, together with single and multiple CD8 T cell autoreactivities using tetramer technology.[22] Frozen sections of pancreata from patients with Type 1 diabetes stained positive for glucose transporters, suggesting capacity of remaining β -cells to sense glucose years after diagnosis[23], which is in line with some preservation of C-peptide in selected number of patients with T1D, all pointing towards chronicity of the process. However, it is likely that the autoimmunity changes its nature with time and moves from the insult mediated by single-specificity islet-autoreactive T-cells towards one involving multiple islet reactive species, which is possibly a consequence of the apoptotic process that could contribute to disease progression.[22] This is in line with the well-documented presence of single and multiple seroconversion discussed earlier.

To explain the process underlying this chronic inflammation, almost 30 years ago Botazzo¹ postulated that environmental attack results in the release of β -cell antigens that are then taken up by macrophages, presented to T cells, leading to the activation of T helper cells, which in turn activate B cells to produce antibodies, as well as activation of cytotoxic T cells. A constant influx of new information over time has broadened this concept to reveal very a complex, but only partially understood, interplay between the immune system, the environment and the β -cell. Before going into further details of T1D

¹ Botazzo GF. Lawrence lecture. Death of beta cell: homicide or suicide? Diabet Med 1986; 3:119-130.

pathogenesis, it is helpful to review our current understanding of several key events occurring during a normal immune response[24].

1.1.1 The normal immune response

Mature recirculating T cells that have not yet encountered their specific antigen are known as **naïve T cells**, which fall into two main categories: CD4 and CD8 cells, depending which co-receptor molecule they express. When the naïve T cell meets its respective antigen, presented to it as MHC-peptide complex on the surface of the antigen presenting cell (APC), it becomes an activated **effector T cell**, ready to perform various functions contributing to the removal of an antigen. At the same time as providing effector T cells, this primary immune response generates **memory T cells** that afford protection when the same antigen is encountered at a later stage.

Activation of the naïve T cells is step-by-step process that can be separated in 3 parts (Figure 1-2):

- **Signal 1** is provided during the interaction of T cell receptor (TCR) and the MHC-peptide complex on the APC; this process is facilitated by co-receptor molecules on the T cells: CD4 or CD8. CD4 cells recognise their antigen in the context of MHC class II (expressed by professional APCs), whilst the CD8 cell requires antigen to be presented in the context of MHC class I (expressed on all cells).
- Interaction of co-stimulatory molecules on the APC (B7.1 or CD80, B7.2 or CD86, CD40) and their ligands on the T cell (CD28 for B7.1 and B7.2 and CD40L for CD40) delivers **signal 2**; this step is important for clonal expansion of T cells, mainly through an increase in the

production and the responsiveness to IL-2. Another T cell co-stimulatory molecule, known as inducible co-stimulator (ICOS), binds to its ligand (LICOS) on activated dendritic cells and monocytes, and stimulates proliferation of an activated clone through production of cytokines other than IL-2. Interestingly, T cells express CTLA-4, an additional receptor for B7 molecules, which contrary to CD28, delivers an inhibitory signal to the activated T cell.

Another molecule, known as programmed death ligand- 1 (PD-1), also mediates inhibitory T cell proliferation signals. It binds to specific ligands: PD-L1, constitutively expressed on variety of cells, and PD-L2, exclusively expressed on activated APCs during inflammation. The interplay between stimulatory and inhibitory signals regulates T cell responses.

Also, immunoglobulin like transcripts (ILTs 2, 3 and 4) are members of the immunoglobulin gene super-family. They are expressed on dendritic cells. When they bind to their ligands on the T cells, the cascade of the intracellular signaling starts that causes T cell anergy and/or induction of allospecific T regulatory cells. [25]

- Finally, cytokines that govern differentiation into various types of effector cells induce **signal 3**, rendering the activation process complete.

The crucial moment in this process is the increase in the production and responsiveness to IL-2. The initial encounter with the appropriate antigen in the presence of co-stimulatory signals induces the synthesis of IL-2, as well

as the α -chain of the IL-2 receptor, known as CD25. Naïve T cells express a low sensitivity variant of the IL-2 receptor that consists only of β - and γ -chains. Binding of α -part to the rest of the receptor complex, upon cell activation, increases sensitivity to IL-2 and propels the cells into the proliferation. On the other hand, an increase in the production of IL-2 is achieved by induction of transcription factors such as NFAT-1 (nuclear factor of activated cells -1), AP-1 (activator protein - 1) and NF κ B (nuclear factor kappa-light-chain-enhancer of activated B cells), which bind to the promoter region of IL-2 gene. In addition, stabilisation of the otherwise unstable IL-2 mRNA in the naïve T cells, contributes to the increased production of IL-2.

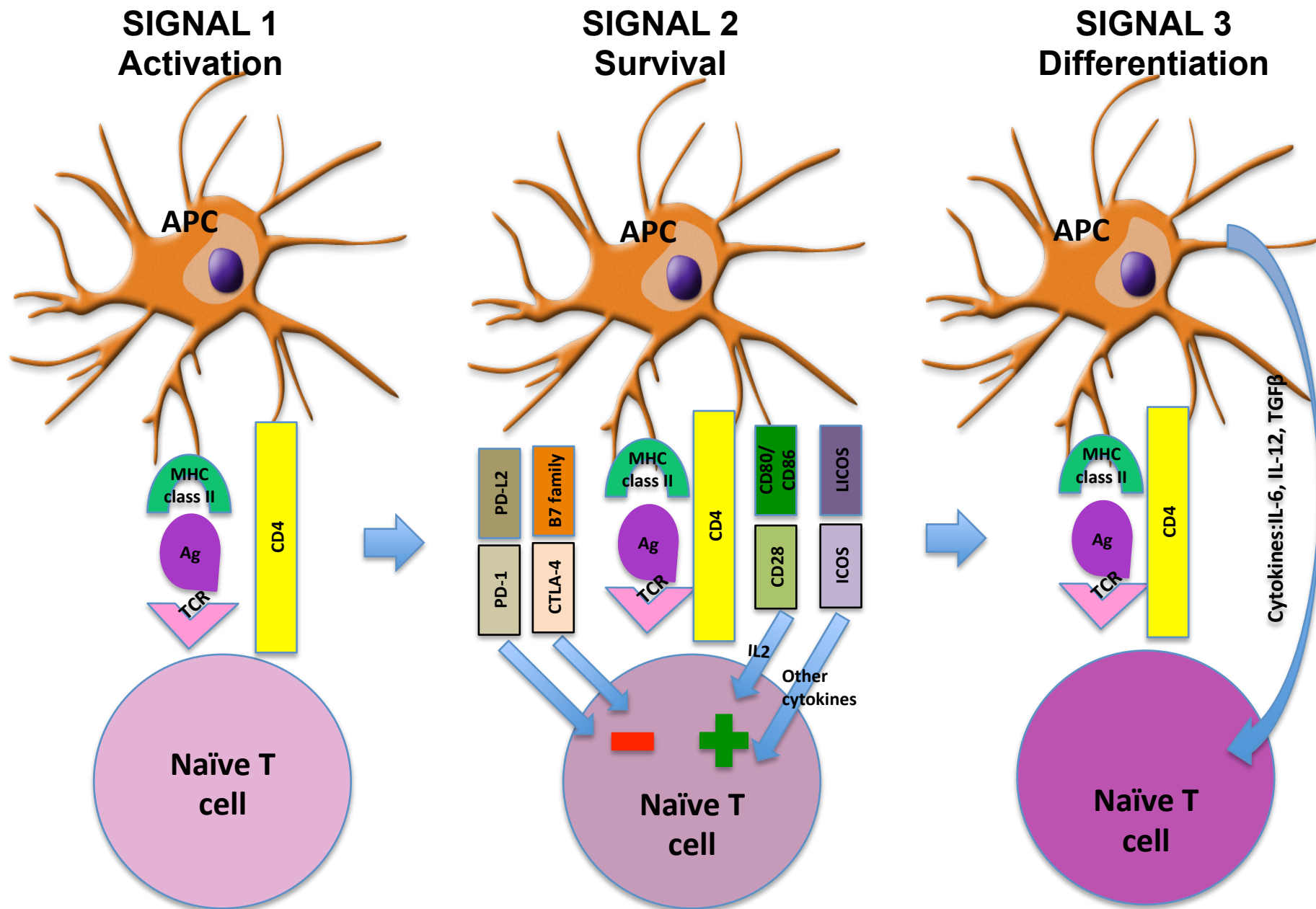


Figure 1-2. Activation of naïve T cells. Adapted from Murphy, K., et al., *Janeway's immunobiology*. 7th ed. 2008, New York: Garland Science. xxi, 887 p.

CD8 naïve cells differentiate into cytotoxic T cells, capable of killing their target cells during defense against intracellular pathogens, such as viruses. Because their effector functions are so destructive, they require more co-stimulatory activity to become activated. This can be achieved by mature dendritic cells that have intrinsic co-stimulatory activity capable of stimulating CD8 cells to produce IL-2 that drives their own proliferation and differentiation. Another way to provide this additional co-stimulatory activity is through the CD4 cell, that binds the antigen on the same APC (presenting both MHC class I and II) as CD8.

Unlike the CD8 cell, CD4 naive cells can differentiate into a number of different effector cells:

- T helper type 1 cells (Th1) are responsible for activating macrophages and facilitating the process of phagocytosis of intracellular bacteria, during which they produce IFN- γ and TNF- α . The signal 3 for their differentiation comes from APCs producing IL-12 and IFN- γ , which activates signal-transducing activator of transcription 1 (STAT 1) that, in turn, activates transcription factor tbet (t-box expressed in T cells), which is responsible for promoting the transcription of the IFN γ gene in the T cell, as well as the IL12 receptor, hence determining the fate of the cell towards Th1 pathway.
- T helper type 2 cells (Th2) are mainly involved in facilitating B cell function, after differentiation governed by IL-4 through activation of the STAT6 and GATA-3 transcription factors. They produce IL-4, IL-5, IL-10 and IL-13.

- T helper 17 cells (Th17) receive differentiation signal 3 through a different transcription factor, ROR γ T, which is activated in an environment rich in TGF- β , IL-6 and IL-21[26]. This results in the expression of the receptor for IL23, committing the cell to the Th17 pathway, which requires IL-23. These cells are induced early in the adaptive immune response to extracellular bacteria during which they stimulate a neutrophil response through production of IL-17.
- Regulatory T cells (Tregs) have the main function of suppressing immune responses. They differentiate after exposure to cytokines such as TGF- β and IL-10. Tregs are described in detail later in this chapter.

Focusing defense solely on foreign antigens and, at the same time, maintaining tolerance to “self” is extremely important process that continuously takes place during the development of normal immune response. It is viewed as multi-step process. It starts with the central tolerance in the thymus, which involves deletion of the T-cells that strongly react with self-antigens expressed on thymic epithelial cells. Many autoreactive T-cells, whose TCR weakly reacts with endogenous antigens, escape this control checkpoint. Other mechanisms, known as peripheral tolerance, are in place to eliminate these cells from the periphery. They include:

- 1) peripheral deletion of self-reactive T-cells by apoptotic cell death;
- 2) anergy, a mechanism during which effector T-cells are made functionally unresponsive due to failure to fully activate upon encounter with their respective antigen. [27]

3) Tregs, part of the CD4 lymphocyte family, that have the ability to suppress potentially deleterious activities of effector T-cells.

Many studies have suggested that Tregs, or their dysfunction, maybe responsible for uncontrolled autoreactive T cells in the periphery. For this reason they are seen as promising therapeutic target and have been the focus of research into autoimmune diseases over the past decade. The concept is based on the hypothesis that an increase in the number and/or function of Tregs can achieve targeted immunomodulation without generalised suppression.

The large population of Tregs, formerly known as natural Tregs, is mainly generated in the thymus following encounters with organ-specific ligands that are ectopically expressed on the thymic epithelial cells – thymus derived Tregs (tTregs).[28, 29] They represent approximately 10-15% of the CD4 positive population in the human blood. These are CD4 positive cells that express CD25 (α -chain of the IL-2 receptor) and the transcription factor FoxP3, which affects the interaction between AP-1 and NFAT at the level of the IL-2 promoter, preventing transcriptional activation of IL-2 gene. [24]

Thymic selection is not the only way that Tregs cells can be created. There is evidence that naïve T cell can be converted into “induced” Tregs in the periphery as a part of the adaptive immune response. According to the new nomenclature, these are peripherally derived Tregs (pTregs)[29] that include several subtypes:

- CD4+CD25+Foxp3+ pTregs can be generated following administration of low dose agonist peptide and/or a lack of co-stimulation, i.e. “subimmunogenic” conditions. [30, 31]
- Tr1 cells are a distinct type of pTreg in regards to their phenotype (CD4+CD25-IL-10+), cytokine dependent mode of action (rich in IL-10 and low in IL-4) and migratory behavior, in comparison to the CD4+CD25+Foxp3+ cells. Data in mice suggest that they mediate their actions through production of IL-10, and can be induced by repeated *in vivo* intranasal administration of antigenic peptide or repetitive administration of IL-10 and rapamycin.[32]
- Th3 cells produce IL-4, IL-10 and TGF- β , and populate the mucosal immune system where they can be activated through antigen presentation, particularly in the gut, as evidenced by a study in mice in which oral insulin favoured the generation of TGF- β producing Th3 cells. [33]

It is important to mention that the new nomenclature[29] also distinguishes *in vitro*-induced Tregs (iTregs), recognising the limitations of translating the *in vitro* models to the *in vivo* conditions.

There have been numerous attempts to characterise Tregs phenotypically. The most widely used markers are presented in the Table 1-1.

Marker	Description	Expression in Tregs	Reference
CD25	α -chain of the high affinity IL-2 receptor, which enables Tregs to respond to the much lower concentrations of IL-2 in comparison to the effector T cells and NK cells.	↑	[34], [35]
CTLA-4	Cytotoxic T lymphocyte-associated antigen-4 binds B7 molecules, delivering tolerogenic signal to APC.	↑	[36], [37],
GITR	Glucocorticoid-induced tumour necrosis factor receptor-related gene has suppressive effect on T cell proliferation.	↑	[38]
LAG-3	Lymphocyte activation gene-3 is a homolog of CD4 that binds MHC class II and exhibits suppressive effects on T cell.	↑	[39]
CD127	IL-7 receptor	↓	[40]
Foxp3	Forkhead/winged-helix transcription factor box P3 affects the interaction between AP-1 and NFAT at the level of IL-2 promoter, preventing transcriptional activation of IL-2 gene.	↑	[41], [42], [43]

Table 1-1. Phenotyping of the T regulatory cells.

All of these markers that are presently used to define Tregs, are also general T-cell activation markers, suggesting that activation is required for a T cell mediated suppression, but not offering definitive phenotyping of these cells. [44] As a consequence, attempts to show reduced number of Tregs in Type 1 diabetes lead to inconsistent data due to variability in the strategies defining

Treg populations, influence of age and duration of diabetes.[33] This makes them even less reliable marker for monitoring disease progression, with or without immune intervention.

Identifying and studying antigen-specific Tregs is even more challenging, given their low frequency of 1 in 10^4 or 1 in 10^5 PBMCs.[45] A sensitive cytokine ELISPOT assay, that detects peptide-specific IL-10 secreting cells at frequencies as low as 1 in 10^5 [46], gives the potential to monitor at least some of the actions of these cells through their functionality, rather than phenotype. Tetramer technology is another approach to address this issue, promising superior sensitivity in detecting HLA class I CD8⁺ T cell epitopes (preproinsulin and GAD), compared to ELISPOT, in patients recently diagnosed with Type 1 diabetes.[47] On the other hand, more unstable class II tetramers, although successful in detecting proinsulin and GAD epitopes, were discordant with ELISPOT method, suggesting that these assays detect different populations of CD4⁺ cells.[48]

That brings us to the importance of understanding the mechanism through which Tregs achieve suppression. It seems that antigen bearing APCs simultaneously engage with the naïve or effector T cells and the Tregs, which then work at several levels to halt self-reactivity or control overstimulation by the foreign. Tregs can influence priming and the effector stage of the immune process by acting on APCs and T cells alike. Activation of Tregs, and the suppression they mediate, is antigen-specific [49], although they may be able to suppress effectors with different antigen specificity.[50] It seems that they have several modes at their disposal, depending on environment:

- Cytokine production, such as IL-10 [51] and TFG- β - [52], through which they modulate activation of the T cells, acting both on APC and T cell level.
- Direct cell contact involving the release of granzyme inducing apoptosis in the target cells, such as CD4+ and CD8+ T cells, CD14+ monocytes and immature and mature dendritic cells [53]. The concept of granzyme induced apoptosis was also documented in human clones originating from patients with Type 1 diabetes, where antigen-restricted interaction between APC, effector T cells and Tregs was halted through granzyme induced killing of the antigen-bearing APC by Treg, but not “bystander” presenters.[54]
- Treg activation of indolamine-2,3 dioxygenase (IDO) metabolism when their CTLA-4 binds to CD80 or CD86 on antigen presenting cells (APC). This results in a reduced amount of tryptophan that prevents activation of effector T-cells.[55]

The generation of different subtypes of the Tregs with their different modes of action is not a mutually exclusive process during the encounter with the antigen. The predominance of a certain pTreg probably depends on the type of antigen, the conditions around its presentation and the type of the tissue where the process takes place. As an illustration, Tregs express L-selectin receptor CD62L, which together with CCR7 enables them to home in on their respective antigen draining lymph nodes. However, they are also capable of travelling into the inflamed tissue by expressing markers such as $\alpha_E\beta_7$ integrin in mice, which enables them to execute control of the effector response triggered by the inflammation.[56] It is possible that the suppression early in

the process requires a more gentle approach, such as cytokine modulation of APCs and T cells, whilst primed and activated effectors need more radical approach consisting of killing the culprit T cells or APCs that triggered them.

Antigen presenting cells also play important role in this process, and there is ample data to suggest a capacity of DCs to induce T cell tolerance. This is particularly important for the efficacy of the antigen-specific immunotherapy delivered in the skin, given the abundance of tolerogenic APCs and Tregs in this organ, and this will be explored in detail in Chapters 4 and 5.

1.1.2 Autoimmunity in Type 1 diabetes

The autoimmunity process starts in the thymus, where peptides of peripheral antigens (including insulin) [57] are presented in the context of MHC molecules by medullary thymic epithelial cells to T cells, leading to the deletion of the majority, but not all, autoreactive T cells. The autoimmune regulator gene (AIRE) encodes a protein that plays an important role in the tissue-restricted antigen expression by thymic epithelial cells, an important pillar of self-tolerance. Indeed, patients with defective AIRE develop autoimmunity, which affects the parathyroid and adrenal glands, and many other organs, including pancreatic β -cell leading to T1D. It has been postulated that AIRE may function as a regulator of the expression of the insulin gene in thymus via an INS-VNTR (variable numbers tandem repeat) element. Polymorphisms in the VNTR region affect the propensity to Type 1 diabetes, with haplotypes associated with a lower expression of insulin in the thymus causing higher propensity to the disease.[58]

Tregs are produced alongside other effector cells and their balance is crucial for maintaining tolerance to 'self' in the periphery. The insulin producing β -cell produces target antigens, but also process them creating peptides that are taken up by APCs, either as a whole (dead β -cells) or as granules of β -cells, for further processing and presentation to the effector T cells. In the next step, the autoreactive T cell, with its T cell receptor (TCR) recognises the endogenous peptide in the context of the MHC class. There is no doubt that CD4 cells orchestrate this process with, according to some evidence, a predominantly Th1 response, but also involving multiple arms such as cytotoxic T cells, cytokine production, B cell activation etc.[59]. It is most likely that the final insult is executed by the autoreactive cytotoxic CD8 cell that kills β -cell wrongly perceived as foreign.

It is intriguing to understand why is β -cell such an "easy victim" of the imbalanced immune system, when many other neighbouring cells in the pancreas that produce similar array of antigens, remain intact in autoimmune diabetes. A vulnerability of the β -cell to the stress-induced changes during local infections, it's increased sensitivity to cytokine-mediated killing and hyperexpression of class I molecules once immunity has been initiated, are some of the potential explanations.[59] A number of studies have focused on β -cell biology to identify the etiology of the cell-specific killing in T1D, and these have been recently reviewed. [59]

The focus of this text is the approach of immune interventions, based on the concept that the disastrous reactivity to 'self' in T1D is the result of immune dysregulation, rather than the β -cell itself. It involves the presence of a sufficient number of autoreactive T cells that have escaped central or

peripheral control points, and/or lack a matching number of Tregs to counterbalance them, which will cause the destruction of the critical number of β -cells leading to T1D. The process is influenced by genetic predisposition, environmental factors and targeted antigens.

1.1.2.1 Genetic predisposition

It is clear that T1D diabetes develops in genetically predisposed individuals and the major risk factor is a first-degree family history of Type 1 diabetes.[60] In the Diabetes Prevention Trial -1 (DPT-1), islet autoimmunity developed particularly in the siblings of affected individuals.[61] Interestingly, almost all of susceptibility genes associated with Type 1 diabetes are connected to the immune system. Amongst them, HLA class II region on chromosome 6 has been studied the most.[60] These genes encode the MHC complex responsible for antigen presentation. It is very well known that certain MHC class II alleles are strongly associated with the disease, whilst others provides protection (Table 1-2).

Susceptibility alleles	Protective alleles
HLA-DRB1*03:01	HLA-DRB1*15:01
HLA-DRB1*04:01	HLA-DRB1*14:01
HLA-DRB1*04:02	HLA-DRB1*07:01
HLA-DRB1*04:05	HLA-DQB1*06:02
HLA-DQA1*03:02	HLA-DQB1*05:03
HLA-DQB1*03:02	HLA-DQB1*03:03

Table 1-2. Protective and susceptibility MHC class II alleles in Type 1 diabetes [62]

However, the combinations of certain alleles define a haplotype risk. Analysis of over 600 Caucasian families determined a number of susceptible, neutral, and protective DR-DQ haplotypes. The most susceptible haplotypes were DRB1*0301-DQA1*0501-DQB1*0201, DRB1*0405-DQA1*0301-DQB1*0302, DRB1*0401-DQA1*0301-DQB1*0302, and DRB1*0402-DQA1*0301-DQB1*0302 haplotypes. The most protective haplotypes were DRB1*1501-DQA1*0102-DQB1*0602, DRB1*1401-DQA1*0101-DQB1*0503, and DRB1*0701-DQA1*0201-DQB1*0303.[63]

The HLA Epitope Analysis Programme (HAEP) studied HLA epitopes associated with propensity or resistance to Type 1 diabetes, and found that they appear in alleles previously known to be associated with the disease. In addition, individuals diagnosed with diabetes at young age were found to carry the highest number of high-risk epitopes and the lowest number of protective epitopes. The opposite was true for the individuals that developed diabetes at an older age.[64]

Other genes have also been associated with an increased risk of Type 1 diabetes, such as the insulin gene on chromosome 11 (INS), which shows polymorphism in its promoter region with shorter tandem repeat polymorphisms associated with risk and longer with protection; the CLTA-4 gene on chromosome 2; the T-cell protein phosphatase gene on chromosome 1 (PTPN 22), which downregulates immune responses by inhibiting TCR signaling; the CD25 gene on chromosome 10, which may affect Treg function; and the Interferon induced with helicase C domain 1 gene (IFIH1) on chromosome 2, which encodes an intracellular detector of viral RNA, the

reduced expression of which may protect from T1D.[65] A recent analysis tested over 20 additional regions, and identified further candidate genes such as IL-10, IL-19, IL-20, Gli-similar (GLIS) protein 3, CD69 and IL-27.[66]

1.1.2.2 Environment

Traditionally, it has been postulated that environmental agents, such as viruses, microbes, diet-related, anthropomorphic and psychosocial factors, trigger the onset of the disease in genetically susceptible individuals. However, a number of studies have failed to identify a clear culprit, amongst many studied, such as early exposure to cow's milk, breast feeding, enteroviral infections, timing of vaccinations, birth weight and vitamin D exposure. [67] [68]

One of the most studied factors has been viruses, particularly ones with tropism for pancreatic tissue, where they were investigated as possible triggers of autoimmunity, or direct perpetrators, lysing the β -cells. However, evidence for this is not substantial.[69] Rather than triggers, viruses could be facilitators of the autoimmunity. Enteroviral infections in children with positive autoreactive antibodies were shown to accelerate progression to clinical diabetes in the DAISY study.[70] On the other hand, particular gut microbiota may be protective. This "hygiene hypothesis" is supported by the finding that the incidence of Type 1 diabetes in Finnish children is six-fold higher than in ethnically and geographically matching Russian Karelian children, with documented equal frequency of the predisposing HLA DQ genotypes.[71] Modern hygiene standards, presumably practiced in economically developed Finland, more so than Karelia, reduce "protective" exposure to the environmental antigens. On the other hand, some studies showed increased

incidence of T1D in children with multiple infections during first years of life, but protective effect of pre-school care. They suggest that environmental factors can promote or attenuate disease dependent upon timing and quantity of exposure.[72] In this model, environmental factors are seen as modifiers rather than triggers of autoimmunity on a background of inherited immune dysregulation. [67]

Studies looking at the link between the exposure to cows milk and Type 1 diabetes did not provide consistent evidence, but a recent finding suggests that exposure in early infancy is associated with the disease, but only in carriers of a particular allele of the PTNPP22 gene.[73] It is possible that certain factors work in certain genotypes at certain times, further supporting the importance of the timing of the causative agents and their interplay with genetics.

Another promising modifying factor is vitamin D, with a number of observational[74] and one prospective study[75] indicating that exposure to high dose vitamin D reduces the incidence of diabetes in predisposed children.

The TEDDY Study (Environmental Determinants of Diabetes in the Young; <http://teddy.epi.usf.edu/>) is currently prospectively analyzing environmental factors that may be responsible for modifying disease incidence.

The importance of the environment is further reflected in the fact that the concordance for Type 1 diabetes is 30-50% in monozygotic twins and 8% in dizygotic.[68] It is clear that genetic predisposition plays significant, but not self-sufficient role in the pathogenesis of T1D. It should rather be viewed as a framework on which environment works to either accelerate or attenuate

processes leading to autoimmunity. The speculation is that strong predisposing genetics needs only gentle influence from the environment to propel an individual to diabetes, whilst mild susceptibility or even protective genotype, requires much stronger insult or number of them to facilitate progression to the disease – Figure 1-3.

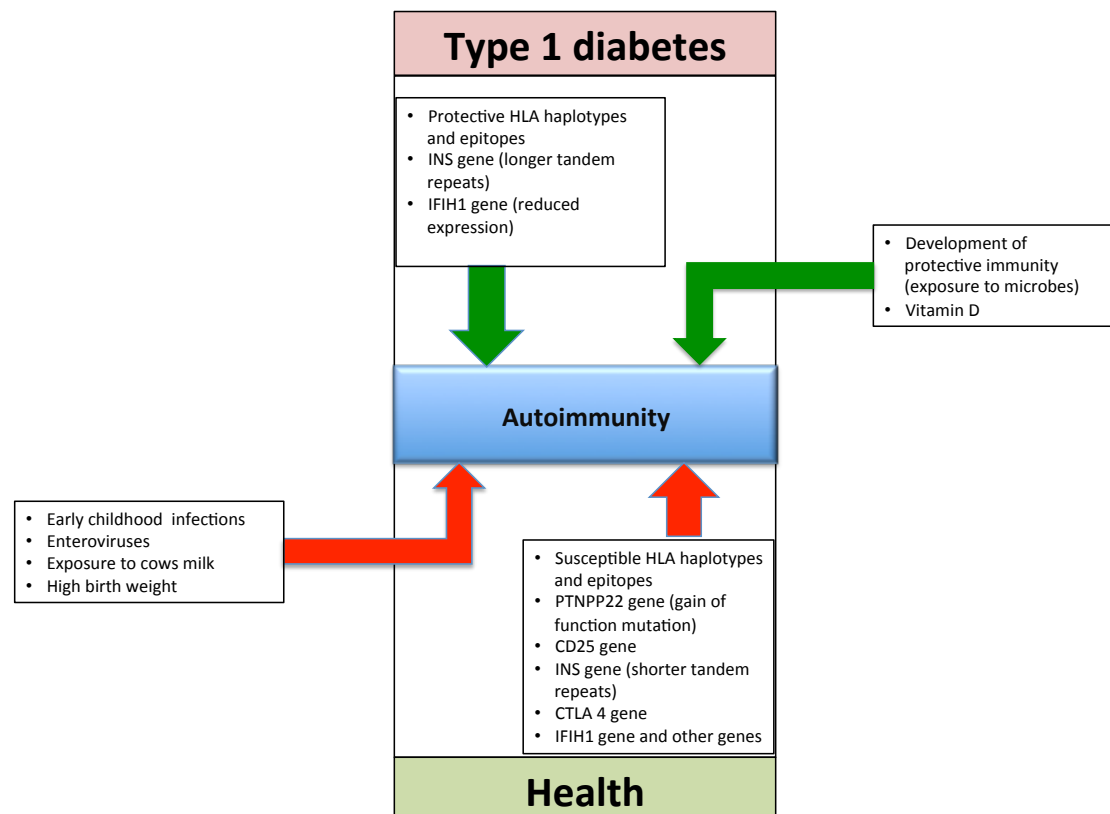


Figure 1-3. Interplay between genetic and environmental factors in the pathogenesis of Type 1 diabetes. Factors offering protection from T1D are indicated with the green arrows; predisposing factors are indicated with the red arrows.

1.1.2.3 β -cell epitopes

Alongside hereditary susceptibility and environmental modifiers, important players in the autoimmunity process are targeted antigens in the β -cell. Autoantibodies in T1D are generally regarded as a marker of autoimmunity, and whilst their role in pathogenesis is not clear, their target antigens have

been the focus of studies trying to identify epitopes of autoreactive T cells. In mouse and man, insulin and proinsulin are common targets of T cells of patients with Type 1 diabetes. [76] Whilst proinsulin is a major source of target epitopes for autoreactive CD8 cells in humans, CD4 cells tend to target epitopes residing mainly in GAD65, IA2, proinsulin. Antigens such as heat shock protein (HSP) 60 and 70, islet-specific glucose-6-phosphatase catalytic subunit related protein (IGRP) and islet amyloid polypeptide (IAPP) are the less common source of target epitopes in human – Figure 1-4.[77]

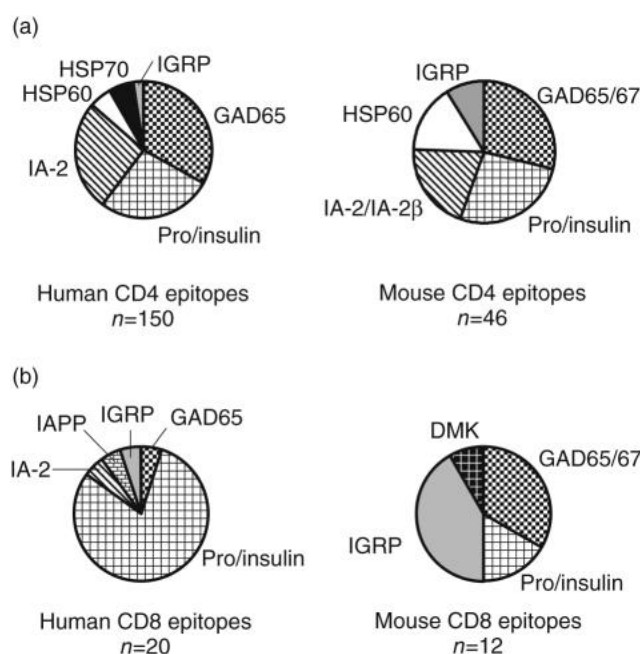


Figure 1-4. Antigenic distribution of (a) CD4 and (b) CD8 T cell epitopes in autoimmune diabetes in humans and mice. Adapted from Di Lorenzo, T.P., M. Peakman, and B.O. Roep, Translational mini-review series on type 1 diabetes: Systematic analysis of T cell epitopes in autoimmune diabetes. Clin Exp Immunol, 2007. 148(1): p. 1-16.

Amongst this wide array of candidate epitopes, it is difficult to precisely establish which are the relevant or “real” targets responsible for the pathogenesis. In mouse models, it is possible to imply strict criteria and consider an epitope essential only if it could be shown that genetic ablation of

its expression led to the protection from disease[77], which has been achieved with murine pre pro insulin 1.[78] However, it is impossible to apply this criterion in human studies, and some of the work in identifying relevant epitopes came from studies using elution of epitopes peptides from HLA complexes of patients with T1D. This methodology used recombinant versions of known target antigens, such as IA-2 and PI, which were then delivered to the APCs of certain HLA type known to be prevalent in patients with T1D. After processing by APCs, peptides were acid eluted and separated by reverse phase HPLC. The presence of T cell reactivity to naturally processed and presented peptide epitopes (NPPEs) obtained in such a way was further tested by high sensitivity ELISPOT assay in patients with T1D and compared with healthy controls.[46, 79] This is how proinsulin C19-A3 came into the light[46], which was then followed by clinical trial designed to establish its safety [80] and efficacy.

In the study assessing GAD65, different epitopes were designed based on the GAD65 GenBank sequence. The reactivity to these epitopes was further tested by tetramer technology. It was surprising to find that patients and healthy subjects did not differ in the presence or absence of autoreactive T cells to GAD65 epitopes, but the magnitude of the response was much higher in patients, suggesting a higher percentage of activated T cells in the disease.[81]

In addition, it is likely that the initial loss of tolerance is targeted against a particular epitope of the given antigen (insulin or GAD in humans), but is later spread over time in the inflamed tissue to other epitopes within the given antigen (intramolecular or epitope spreading).[82-84],[59]

1.2 Immune interventions in Type 1 diabetes

Starting from the concept that autoimmunity is a dominance of unwanted autoreactive effector T cells over Tregs, many immune intervention studies have aimed to restore the balance. They target various arms and molecules involved in the immune process, as shown in Figure 1-5.[85] Non-antigen specific immune interventions fit into the picture by performing global immunosuppression that will abolish autoreactive cells, together with many other innocent by-standers. More subtle in their approach, antigen-specific interventions (ASI) aim to restore tolerance to self by inducing antigen-specific Tregs, whilst leaving the function of the rest of the immune system intact. One very optimistic view is that to achieve suppression, we may not need to know or administer the initiating autoantigen, or multiple antigens. Induction of Tregs, whatever their specificity, may induce bystander immunomodulation through production of protective cytokines, or promoting tolerogenic antigen presentation.[76, 86]

Timing of immune intervention trials spans from primary prevention in genetically high-risk individuals, with no detectable autoimmunity, to secondary prevention in people who have detected islet cell autoantibodies and, finally, tertiary prevention, aimed to preserve residual β -cell function after diagnosis of diabetes, which may have impact on control and complications of T1D later in life. Primary prevention trials involving oral insulin in subjects with high titer of islet cell antibodies showed promising preliminary results [87]. In addition, administration of nasal insulin showed good safety and tolerability records.[88] This was not confirmed in the DIPP trial in which nasal insulin

was administered in the large cohort of high-risk infants or their siblings.[89] The concept of primary and secondary prevention is challenging in regards to the need for the large-scale population screening, the balance of safety and efficacy, as well as the impact of the alternative approach of not treating. In addition, recent review of the various studies points towards the lack of consistent in achieving delay or prevention of diabetes.[90, 91] These are some of the reasons why the prevention concept shifted its focus towards tertiary prevention.

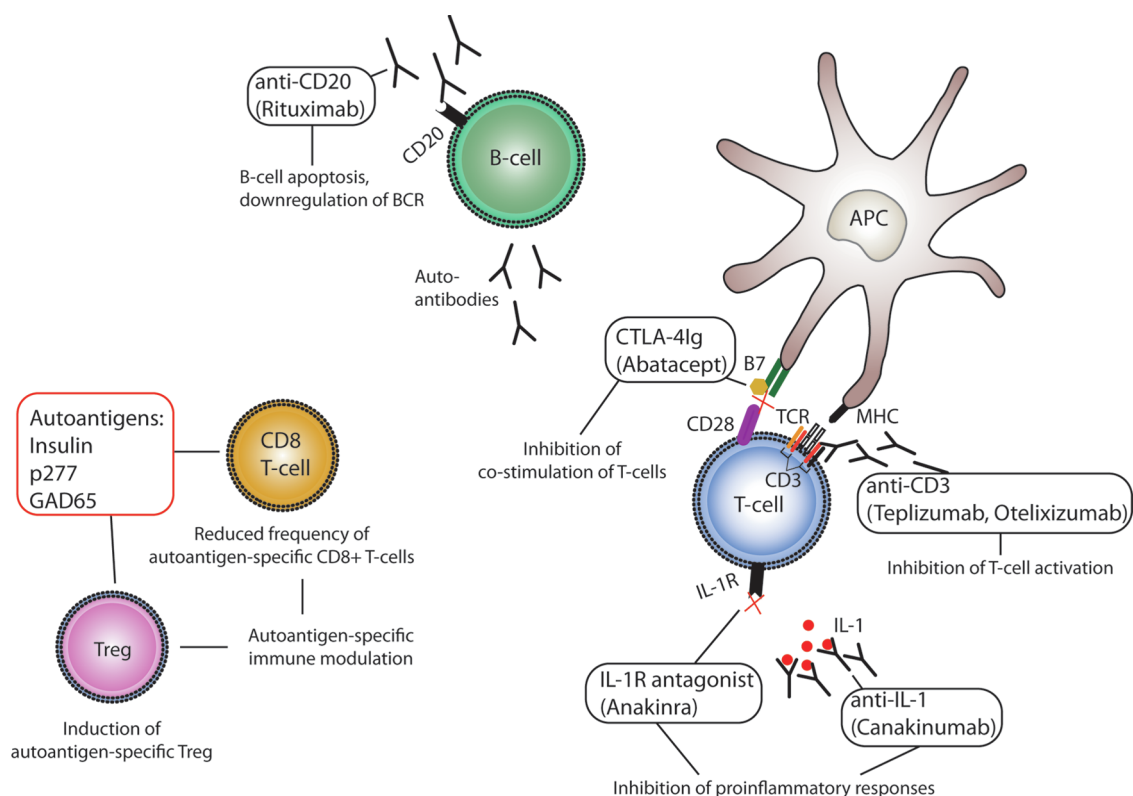


Figure 1-5. Targets of therapeutic agents used in immune intervention studies in Type 1 diabetes. Adapted from Ryden, A.K., et al., Non-antigenic and antigenic interventions in type 1 diabetes. Hum Vaccin Immunother, 2013. 10(4).

1.2.1 Non antigen-specific interventions

Studies on immune intervention in T1D started with cyclosporine, a peptide of fungal origin with a potent immunosuppressive capacity through inhibition of T

cell activation. Although this agent was rendered unacceptable for this purpose due to serious side effects, and the need for repetitive dosing, it proved the concept that T-cell directed immunosuppression is capable of preserving β cell function and insulin production. [92, 93]

However, studies using different immunosuppressants, mycophenolate mofetil and daclizumab, a monoclonal antibody targeting CD25, which is widely used in transplantation, did not preserve β -cell function in T1D. This approach may be a double-sided sword, in which by targeting $CD4^+CD25^+$ Tregs, daclizumab destroys T-cells important for maintaining self-tolerance.[94]

All together, these observations suggested the need for more targeted immunotherapies and led to anti-CD3 monoclonal antibodies against CD3 molecules expressed on the surface of T cells as a part of the TCR complex. These antibodies have been successful in preventing transplant rejections, but had the significant side effect of causing cytokine-storm.[95] Their modification to reduce Fc receptor binding affinity led to the reduction in side-effects, but retained immunosuppression.[96] Two of these antibodies have been developed for use in the immune interventions: teplizumab and oteelixizumab.

Teplizumab, was promising in arresting the loss of β -cell function, in both children and adults, when administered within 6 weeks of diagnosis, an effect that extended up to two years of follow-up.[97, 98] The effect was individual, with a number of patients showing decline in β -cell function after two years. This was particularly the case in a study that included a younger cohort, known to have more aggressive disease and some thymus function that can

regenerate autoimmunity. However, an effect of immune regulation was detected in some patients, including significant increases in the amount of IL-10 and IL-5 in the serum, as well as an increase in the number of FOXP3⁺CD8⁺ Tregs. [99]

In the Protégé study on the efficacy of teplizumab, which involved patients diagnosed 4-12 months before enrolment in the study, the treatment group showed reduced decline in C-peptide after two years, with most of the effect observed in patients with recent T1D onset.[100] The same effect was replicated in a larger study, although the trial did not meet its endpoints, which were focused on diabetes control (HbA1c level and insulin requirement) that is, unlike C-peptide level, dependent on manipulation by physicians and patients.[101] However, younger patients with good metabolic control and higher C-peptide levels had better therapeutic benefit.[102]

Otelxizumab failed to show benefit in β -cell preservation in a larger study [103], despite promising results of a higher dose otelxizumab in a smaller cohort, extending up to 18 months of follow up after a single treatment.[104] Interestingly, a subgroup of patients showing the most benefits, extending up to 48 months, were the younger ones and those with the highest β -cell function at diagnosis. [105]

Another approach is based on the observation that stimulation of T-cells through the TCR complex without co-stimulation (interaction of CD28 on T cells and B7 molecules on APC) leads to T cell inactivation. Modulating co-stimulation would, in theory, affect only T cells that have their antigen-specific receptors engaged. This is the basis of trials studying the CD28 homologue,

cytotoxic T-lymphocyte antigen 4 immunoglobulin (CTLA4-Ig), also known as abatacept. It selectively binds the B7 molecules on the APC, interfering with APC – T-cell interaction and inhibiting T-cell.

Indeed, when abatacept was tried in patients with recent onset Type 1 diabetes, it showed limited β -cell preservation properties early in the disease, but not after prolonged treatment.[106] A possible explanation for the failure in this later stage is that main wave of T cell activation happens earlier in the disease. For this reason, the drug is now been investigated in a secondary prevention trial.[85]

The success of rituximab, a monoclonal anti-CD20 antibody directed against B cells, in rheumatoid arthritis, indicated the possibility for its use in diabetes. The rationale for this approach is to affect a large population of cells with antigen presenting properties, such as B cells. A phase II trial showed initial improvement in stimulated C-peptide, and HbA1c and insulin requirement, particularly in younger patients, but the effect that did not sustain over the 12 months follow-up.[107] An interesting analysis of the rituximab responders indicated that they showed enhanced responses to diabetes-associated target antigens. The authors speculated that rituximab enabled recovery of β -cell function through interruption of pathogenic T cell recruitment via surface immunoglobulin-captured autoantigens. This effect was transient and post-treatment recovery of B cells enabled targeting of new antigens leading to the recovery of autoimmunity and decline in C peptide levels.[108] Although difference was seen in the frequency of the different T cell populations in this study, including Tregs, in another trial involving patients with vasculitis,

rituximab was associated with higher level of follicular T cells and Tregs in comparison to conventional treatments.[109]

The rationale for targeting cytokine IL-1 β or its receptor is based on the fact that these receptors are highly expressed on β -cells, and that hyperglycaemia promotes the binding of IL-1 β to its receptor, which can lead to β -cell apoptosis.[110] Despite a solid background, efficacy of anakinra, a human IL-1 receptor antibody, and canakinumab, a human IL-1 receptor antagonist, has not been observed in the clinic.[111]

Combination therapy of low dose IL-2 and rapamycin in humans, contrary to the success in mice, worsened β -cell function, despite an increase in Treg number.[112] This suggests the need for fine-tuning of the immune system in order to promote tolerance and reduce inflammation at the same time.

The choice of these therapies has to be influenced by their immunosuppressive effect. For example, it has been suggested that abatacept decreases the magnitude of antibody responses to recall vaccination.[113] There were also some concerns of progressive multifocal leukoencephalopathy with rituximab[114], although full clinical presentation was not observed after four treatment doses in Type 1 diabetes, not excluding the theoretical possibility for the disease the case for the long term treatment.[115]

1.2.2 Antigen-specific interventions

Antigen-specific immunotherapy (ASI) is a manipulation designed to deliver β -cell autoantigens via a route and regime that will restore immunological tolerance to the β -cell and thus halt further immune-mediated β -cell damage.

As previously discussed, one of the major autoantigens considered for use in ASI is proinsulin[46], the precursor molecule of the hormone insulin and therefore many ASI strategies are insulin/proinsulin based. Amongst ASI approaches, peptide immunotherapy (PIT) is a strategy in which specific peptide sequences of β -cell autoantigens that are targeted by autoreactive T lymphocytes are administered in an attempt to restore immunological tolerance.[116]

One of the first trials in the field of ASI interventions was a GAD–alum trial. GAD65 is one of the major autoantigens in Type 1 diabetes, hence the large interest in the therapeutic application of this agent. For the purpose of the human trial, it was combined with an aluminum hydroxide adjuvant called alum, known to preferentially induce Th2 responses[117] and promote Treg expansion[85], which can potentially be beneficial in Type 1 diabetes reversal. Administration of GAD-alum in children within 18 months of diagnosis, showed less decline in fasting and stimulated C-peptide only in patients treated within 6 months of diagnosis.[118] This was not confirmed in another trial using GAD-alum in children and adults within 100 days of diagnosis, which showed no effect on stimulated C-peptide [119], and also in the latest Phase III trial.[120] Looking back, this is not surprising, as GAD prevented diabetes in animal models, but never reversed diabetes in the later stage of developed disease. It was therefore probably too optimistic to expect that GAD will reverse diabetes in humans. In addition, GAD alum used in clinical trials was never preclinically tested in animal models. It has only recently been shown to have no efficacy in NOD and B6 diabetes models.[121] The dose of GAD in the human trial was probably not the reason for the failure, as people

mounted detectable antibody response, but alum may not be the right adjuvant. It showed T helper type 2 – dominated cytokine response that did not result in protective cell populations.[122]

A more successful trial (DiaPep277), involving s.c. administration of HSP60 derived peptide (p277, amino acids 437-460) in adults within 6 months of diagnosis, slowed glucagon stimulated C-peptide decline in adults [123], but not in children [124]. These pilot results in adults were confirmed in the Phase III trial that showed not only slower decline in β -cell function, but also improvement in HbA1c independent of insulin dose. Interestingly, the beneficial effect on C-peptide was evident only when glucagon was used as a stimulus, but not standard mixed meal.[125] This provides the ground for skepticism, given the difference in sensitivity to glucose during stimulation by these two agents.[126]

An interesting trial, involving administration of plasmid-encode proinsulin in subjects with Type 1 diabetes, showed better preservation of C-peptide in the selected treated group, but the effect disappeared after withdrawal of the treatment. Alongside the metabolic effect, reduction of proinsulin-specific CD8 cells was also detected. Plasmid based therapies open a new potential in combining antigen encoding gene with the genes encoding suppressive cytokines such as IL-4 and IL-10 inhibiting Th1 response.[127]

1.3 Optimising immune interventions in Type 1 diabetes

Experience over the past years taught us that achieving and proving the efficacy of immune intervention depends on number of factors that have to fit

together like a jigsaw puzzle for the treatment to be successful and to be recognized as such.

Design and monitoring of the “ideal” immune intervention trial in Type 1 diabetes requires addressing number of issues.

1.3.1 When and what to give?

With a more advanced autoimmune process, immune intervention may be less effective. Antigen-specific tolerance would be easier to induce in the earliest stages of the disease, with a broader approach needed later in the pathogenesis, when the polyclonal repertoire develops. This is certainly the case at the time of diagnosis, and possibly even earlier, when multiple antibodies are detected in pre-diabetic individuals, indicating intermolecular spreading. As previously discussed, GAD prevented diabetes in animal models, but never reversed diabetes in the stage of developed disease. It was not surprising that the effect was not consistent in humans with developed disease.

It is possible that, at this late stage, multiple antigen therapy is needed. Alternatively, a dual approach therapy of systemic immunosuppression with, for example, monoclonal anti-CD3 antibody followed by antigen specific immunotherapy, maybe the optimal combination. This approach was effective in the NOD mouse model, when anti-CD3 treatment was combined with the intranasal proinsulin peptide.[128]

1.3.2 How much to give?

Finding the optimal balance between side effect and an adequate dose sufficient to elicit substantial effect on immunity is of paramount importance.

Taken wrongly, it can compromise the whole trial and the future of an otherwise promising drug, as was the case with oteixizumab in a Phase III trial.

Antigen specific immunotherapies for the induction of immune tolerance were successful in animal models, but less so in the clinic. Difficulties encountered in translating the dose may be explanation for these less promising results. Dose titration in humans requires a reliable monitoring tool of the immune response, and cannot simply be based on the presence or the absence of metabolic outcome.

1.3.3 Where to administer?

Apart from skin delivery, other possible routes for administration of antigen-specific immunotherapy are the intranasal, the sublingual, the subcutaneous and the intravenous. Skin is most preferred route due to its accessibility and the abundance of cells, such as potent APCs and Tregs that can take up delivered peptide and send an antigen-related tolerogenic message to the rest of the immune system. The optimal mode of skin administration, taking into account depth and potential pro-inflammatory impact of delivery, will be discussed in Chapter 3.

1.3.4 Whom to treat?

Immune interventions work better in people with higher insulin production, which was certainly the case with the monoclonal anti-CD3 antibody trials. Some people with T1D have an aggressive and strong autoimmune process capable of fast β -cell destruction. Others have mild disease that progressively destroys β -cells over number of years, and some exhibit remitting/relapsing disease.[129] Identifying the mode and severity of the autoimmune process in

each patient is an important basis for choosing the right type, intensity and the right timing of immunotherapy. Supportive of this are the findings that the DiaPep277 trials worked in people with an HLA type associated with less aggressive disease and only in adults, but not in children with rapidly progressing autoimmunity.[130]

1.3.5 How to monitor effect of the treatment?

Effective immune interventions in T1D would an elicit immune response that can potentially be evident promptly after administration of the agent, and more long-term metabolic outcomes, such as an effect on β -cell function, and glycaemic control.

The majority of trials have focused on β -cell function as a gold standard measure of efficacy. β -cell function is expressed as stimulated serum C-peptide, with standardised mixed meal used as a stimulus in most trials. Interestingly, the DiaPep277 study showed an effect only when serum C-peptide production was stimulated with glucagon, but not a standardised mixed meal, indicating the influence of a difference of sensitivity to glucose during these two types of stimulation.[126] No other studies have routinely used both stimulations, so it remains to be clarified which one is a more sensitive method for the assessment of β -cell function in clinical trials.

In addition, there is some recent evidence suggesting that β -cell function can be assessed by measuring urinary C-peptide production after standardised mixed and random meals.[131] The simple and non-invasive nature of this method makes it a good candidate for the estimation of β -cell function in trials. This will be discussed in detail in Chapter 6.

Although a positive effect on glycaemic control is the most desirable one to be recorded in any trial on T1D, it is not the most reliable one as it can be influenced by other factors not necessarily related to the intervention. Indeed, HbA1c and insulin dose are affected by starting residual β -cell function, the patient's compliance with the medication, quality of care etc. Changing the outcome from the effect on β -cell function, that gave promising results in earlier stages of the teplizumab trial, to the effect on glycaemic control in Phase III, resulted in failure to reach study outcomes, probably due to the reasons discussed above.[101]

Separately from metabolic outcomes, effects on immune system are important to record, as some patients may experience one without another. In addition, immune outcomes would, by definition, happen earlier than metabolic outcomes, which would help to identify responders and/or guide dose adjustments. However, detection of the effect on immune processes in the blood following antigen specific immunotherapy has been a challenge for many trials, and to this day no ideal marker for monitoring immune and therapeutic efficiency has been established.[132] Detection of cellular immune responses to self-antigen in the blood is very difficult, as the frequency of cells responding to any given antigen is very low (less than 1 in 10,000 cells).[45] Irrespective, the accessibility of blood makes it the most commonly used source of immune cells in human studies. On the contrary, in murine models, lymphoid organs, such as spleen and lymph nodes, are usually used to harvest cells and monitor immune interventions.

It is becoming more and more clear that simple administration of candidate antigen with various frequencies, followed by monitoring of the metabolic

outcome, is ineffective to achieve and record efficacy in halting autoimmune response in Type 1 diabetes.

Firstly, the site and mode of the delivery, including the choice of optimal delivery device and co-administration of agents that will facilitate the generation of the tolerogenic response, has to be carefully considered and planned.

Secondly, choosing the right monitoring tool of the immune and metabolic response is equally important because, without evident effect, any potential benefit of the ASI may be missed. The immune response needs to be detected with the minimally invasive, but sufficiently sensitive tool, but also in the site where immune process takes place, which is not the blood but the lymph node (or local tissues), as known from murine studies. On the other hand, assessment of β cell function requires a test acceptable and sensitive enough to identify rapid changes in C-peptide production. Such a test would help in identifying patients with rapid decline of insulin production as excellent candidates for intensive therapeutic interventions, as well as responders to the treatment.

1.4 Summary of aims

This project is focussed on, firstly, establishing the optimal means and conditions for antigen skin delivery in order to achieve tolerance and, secondly, establishing the optimal tool to monitor immune and metabolic responses to a given treatment.

1.4.1 Targeting epidermal dendritic cells in peptide skin delivery – right place, right tool (Chapter 3).

1. To study the targeting of epidermal DCs by peptide delivered by hollow microneedles.
2. To study the targeting of epidermal DCs by peptide delivered by dry coated microneedles.

1.4.2 Enhancement of the tolerogenic environment in preparation for the peptide immunotherapy (Chapter 4)

1. To study the effect of topical steroid pretreatment on tolerogenic potential of skin DCs
2. To study the effect of pretreatment of intradermally injected IL-10, alone or attached to gold nanoparticles, on tolerogenic potential of skin DCs.

1.4.3 Methods for the optimal monitoring of the immune response after skin antigen delivery (Chapter 5)

1. To assess feasibility and to optimise methods for monitoring immune response in the draining lymph nodes after intradermal antigen skin delivery in comparison to PBMCs isolated from the blood of the same subject at the same time.

1.4.4 Assessment of stimulated UCPCR as optimal method for estimation and monitoring of the changing β -cell function over time (Chapter 5)

1. To confirm in our center that standard mixed-meal stimulated UCPCR correlates well with gold standard MMTT.
2. To determine whether stimulated UCPCR can be used to monitor changing β - cell function over time.
3. To determine which form of stimulation is optimal for this purpose.

Chapter 2 MATERIALS AND METHODS

2.1 *Ex-vivo* methods for the optimal targeting and conditioning of skin dendritic cells

2.1.1 Isolation of peripheral blood mononuclear cells (PBMCs)

PBMCs were isolated by Ficoll-Paque Plus gradient centrifugation from healthy donors with full ethical approval (REC number 05/MRE06/57) and after informed consent. [133]

Samples were collected in heparinized tubes (0.5ml of 1000 units/ml Na-heparin per 20 ml of blood) and mixed with 25ml of warm RPMI 1640 per 20 ml of blood. The mixture was layered on Ficoll-Paque Plus (15 ml of the mixture on 10 ml of Ficoll-Paque Plus) and centrifuged on 400xg for 40 min on ambient temperature. Supernatants, containing serum and PBMCs, were aspirated, washed twice in RPMI 1640 and finally re-suspended in 10% (v/v) human serum in RPMI 1640 supplemented with 0.5mM L-glutamine, 50IU/ml penicillin, 0.05mg/ml streptomycin and 0.1mg/ml neomycin.

2.1.2 Organ skin bath culture

An organ skin bath culture system was developed and optimised for the *ex-vivo* study of various treatment effects (antigen delivery and pre-treatment with immunomodulatory agents) on the human skin dendritic cells assessed by means of flow cytometry and functional assays.

Skin samples were obtained from female patients aged 19-82 years, following mastectomy or breast reduction with full ethical approval (SE Wales Local Research Ethics Committee, reference number 08/WSE03/55) and informed consent. Skin without obvious pathological findings, and that was surplus to diagnostic histopathology requirements, was excised and transported to the laboratory on ice in organ culture medium comprising Dulbecco's modified

Eagle medium (DMEM) supplemented with 50 IU mL⁻¹ penicillin and 50µg mL⁻¹ streptomycin.

Subcutaneous adipose tissue was removed by blunt dissection to yield full-thickness skin, which was exposed to treatment depending on the experiment.

Circular biopsy punches of the treated skin were obtained by using a disposable 8mm biopsy punch. Punches were then cultured at the air-liquid interface in cell culture inserts with perforated bottoms in a 24-well plate (Figure 2-1) in DMEM supplemented with 50 IU mL⁻¹ penicillin and 50µg mL⁻¹ streptomycin at 37°C in an atmosphere of 5% (v/v) CO₂/95% (v/v) air for 24h.[134]

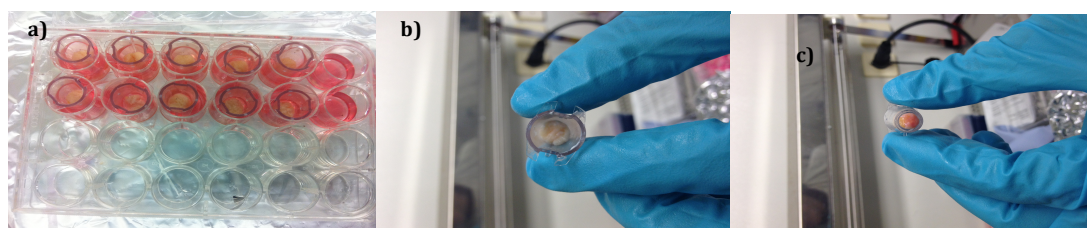


Figure 2-1. Organ skin bath culture: a) 24-well plates with well inserts creating air-liquid interface; b) top aspect of the insert with the skin punch; c) bottom aspect of the insert with the skin punch.

After the incubation (duration varied depending on the experiment), the skin was taken out of the culture and the bulk of the lower dermis was removed by blunt dissection. The remaining tissue containing epidermis and upper dermis was immersed in enzyme solution containing Dispase II (2 units/ml), Collagenase I (197units/ml) and Deoxyribonuclease I (DNA-se I) from bovine pancreas (20 units/ml) in RPMI 1640 for 1 h on 37°C. Epidermal sheets were mechanically separated from the rest of the dermis and transferred in the

0.25% (w/v) trypsin solution in phosphate buffered saline (PBS) for 30 min at 37°C.[135]

After incubation, the remnants of the epidermal sheets were pipetted up and down to increase cell yield, centrifuged at 400xg for 10 min and re-suspended in DNase I (0.85units/ml) in 10% (v/v) fetal calf serum (FCS) in PBS for 1h at 37°C.

Single cell suspensions were subsequently centrifuged at 400xg for 10 min and re-suspended in the appropriate solution depending on the experimental procedure.

2.1.3 Mixed Lymphocyte Reaction (MLR)

γ -irradiated (2000 rad) PBMCs (200,000 live cells/well) from one donor were incubated with allogeneic PBMCs (200,000 live cells/well) in 10% (v/v) human serum in RPMI 1640 supplemented with 0.5mM L-glutamine, 50IU ml⁻¹ penicillin, 0.05mg ml⁻¹ streptomycin and 0.1mg ml⁻¹ neomycin (complete RPMI 1640) in a 96-well plate at 37°C and 5% (v/v) CO₂/95% (v/v) air. Each well contained 200 μ l of medium.

The number of cells was counted in a haemocytometer after staining with trypan blue (1:3 dilution in PBS).

After 96h of culture, 100 μ l of medium was collected from the surface and stored at -20°C for cytokine detection at the later date. 1 μ Ci [³H] thymidine was added to each well, and the incorporation of radioactivity was measured after 16h using a β -microplate scintillation counter. [136]

2.1.4 Mixed Epidermal Cells Lymphocyte Reaction (MECLR)

To assess the functional capacity of the skin dendritic cells, epidermal cells (50,000 live cells/well, containing dendritic cells) were incubated with allogeneic PBMCs (200,000 live cells/well) in complete RPMI 1640 in a 96-well plate, at 37°C and 5% (v/v) CO₂/95% (v/v) air. Each well contained 200µl of medium.

The number of cells was counted in the haemocytometer after staining with trypan blue (1:3 dilution in PBS).

After 96h of culture, 100µl of medium was collected from the surface and stored at -20°C for cytokine detection at the later date. 1µCi [³H] thymidine was added to each well and the incorporation of radioactivity was measured after 16h using β-microplate scintillation counter. [137]

2.1.5 Flow-cytometric analysis

Before staining, cells were filtered through a 70µm cell strainer. For viability, a near-IR fixable Live/Dead Cell Stain was used (APC Cy7 channel). The stain reacts with amines, which are available both on the cell surface and in the interior of the dead cells with compromised membranes, giving bright fluorescence. Amines on the live cells with the intact membranes are available only at the surface, giving less bright colour intensity and easy distinction from the dead cells. Epidermal cells were re-suspended in 1µl/1000 cells of 0.1% (v/v) Live/Dead stain in PBS and incubated for 30 min in the dark at 4°C.

The cells were centrifuged at 400xg for 5 min, re-suspended in the solution of flowcytometry antibodies in flow-cytometry buffer (FCB) (Section 2.1.5), and

incubated for 20 min in the dark at 4°C. Staining was performed in a 100µl volume with up to 1×10^5 cells/test.

Simultaneously, in some experiments and for the compensation purposes, the appropriate species matching compensation beads were incubated with each dye separately under the same conditions.

After incubation, centrifuging at 400xg and re-suspending in FCB twice, additional step of 20 min long incubation with biotinylated fluorochrome was included in some experiments (Section 2.1.5). Otherwise, in some experiments, flow-cytometry fixative (FCF) was added to cell solutions (FCB:FCF=1:2), but not to the compensation beads. Cells were analysed on a FACS Canto II flow cytometer (BD biosciences) and data was processed using FlowJo software version 8.8.6 (Leland, Stanford).

I used this protocol for the following purposes:

2.1.5.1 Phenotyping of the DCs in the epidermal cells single cell suspension

The following test tubes were used:

- Test tube containing cells stained with Live/Dead stain only
- Test tube containing cells stained with antibodies listed in the Panel A
(Table 2-1, Table 2-2)
- Test tube containing cells stained with antibodies listed in the Panel B
(Table 2-1, Table 2-2)
- Test tubes containing compensation beads stained with each dye separately and unstained beads

Panel A			Panel B		
Marker	Dilution	Manufacturer	Marker	Dilution	Manufacturer
Pacific Blue anti-human CD1a	1:20	E-bioscience, Hatfield, UK	Pacific Blue anti-human CD1a	1:20	E-bioscience, Hatfield, UK
AF488* anti-human CD207	1:50	Dendritics, Lyon, France	FITC anti-human CD40	1:50	E-bioscience, Hatfield, UK
PE anti-human Epcam-	1:50	E-bioscience, Hatfield, UK	PE anti-human CD83	1:50	E-bioscience, Hatfield, UK
APC anti-human CD86	1:50	BD Pharmigen, Oxford, UK			
biotin anti-human CD80 (+anti-biotin PerCPy5.5)	1:50 (1:50)	BD Pharmigen, Oxford, UK (E-bioscience, Hatfield, UK)	PerCPy5.5 anti-human HLA-DR-	1:100	BD Pharmigen, Oxford, UK
Near-IR fixable Live/Dead stain	see text	Invitrogen, Paisley, UK	Near IR fixable Live/Dead stain	see text	Invitrogen, Paisley, UK
PeCy7 Anti-human CD11c	1:100	E-bioscience Hatfield, UK	PeCy7 Anti-human CD11c	1:100	E-bioscience Hatfield, UK

Table 2-1. Monoclonal antibodies for flow-cytometry – panels for the epidermal cells

*Later in the project PE anti-human CD207 (dilution 1:30) used for some studies, Biolegend, London, UK

Marker	Role
CD1a	Membrane glycoprotein, role in non-peptide glycolipid antigen presentation to T cells
CD207	Member of C-type lectin family, role in processing pathway through capture and internalization of its ligands (mannose, N-acetylglucosamine etc.)
Epcam	Epithelial cell surface antigen involved in the cells adhesion
CD86	Ligand for CD28 and CD152 (CTLA-4), involved in T cell co-stimulation
CD80	Ligand for CD28 and CD152 (CTLA-4), involved in T cell co-stimulation
CD11c	Glycoprotein expressed by dendritic cells, important for cell-cell contact by binding to its ligands such as fibrinogen
CD40	Co-stimulatory protein, required for activation of APCs upon binding to its ligand CD154 on lymphocytes
CD83	Trans-membrane protein, marker of maturity of dendritic cells, involved in regulation of T cell development
HLA-DR	MHC class II, trans-membrane protein, essential for T antigen presentation

Table 2-2. Role of the surface markers used for the flow-cytometric analysis of DCs.

2.1.5.2 Phenotyping of the T cells harvested after 14-days long culture driven by epidermal cells with an without previous topical steroid exposure

The following test tubes were used:

- Test tube containing cells stained with Live/Dead stain only
- Test tube containing cells stained with antibodies listed in the Panel A
(Table 2-3)
- Test tubes containing compensation beads stained with each dye separately and unstained beads

Panel A		
Marker	Dilution	Manufacturer
V450 anti-human CD3	1:30	Invitrogen, Paisley, UK
eFluor®506 viability dye	1:500	E-bioscience, Hatfield, UK
FITC anti-human CLA	1:30	Biolegend, London, UK
PE anti-human CD127	1:10	Miltenyi Biotec, Surrey, UK
APC anti-human CD25	1:10	Miltenyi Biotec, Surrey, UK
Per CP Cy 5.5 Anti-human CD8	1:30	Biolegend, London, UK

Table 2-3. Monoclonal antibodies for flow-cytometry – panels for the T cells cultivated in the culture driven by steroid exposed and untreated ECs.

2.1.5.3 HLA-A2 typing of the DCs in the epidermal single cell suspension

The following test tubes were used:

- Test tube containing cells stained with Live/Dead stain only
- Test tube containing cells stained with Live/Dead stain and FITC anti-human HLA-A2 antibody (Table 2-4)

Marker	Dilution	Manufacturer
FITC anti-human HLA-A2	1:50	Biolegend, London, UK
Near-IR fixable Live/Dead stain	see text	Invitrogen, Paisley, UK

Table 2-4. Monoclonal antibodies for flow-cytometry – panel for HLA-A2 typing

2.1.6 Cytokine detection (Enzyme-linked immunosorbent assay – ELISA)

2.1.6.1 Cytokine measurement in MLR and MECLR type reactions

Production of pro-inflammatory cytokine Interferon γ (IFN γ) and pro-tolerogenic Interleukin 10 (IL-10) was measured in the supernatants of MLR or MECLR reactions by using ELISA (Human IFN γ ELISA Ready-Set-Go! and Human IL-10 ELISA Ready-Set-Go!; E-bioscience, Hatfield, UK).

The kit consists of the following reagents:

- Capture antibody: Purified anti-human IFN γ (250x); Purified anti-human IL-10 (250x)
- Standard (Recombinant human IFN γ protein - 1 $\mu\text{g ml}^{-1}$, reconstituted in the 1xassay diluent to prepare top standard solution (500pg ml^{-1}); Recombinant Human IL-10 protein – reconstituted in 1xassay diluent to prepare top standard solution (300pg ml^{-1}))
- Detection antibody; biotin-conjugated anti human IFN γ (250x), biotin-conjugated anti human IL-10 (250x)
- Enzyme: Avidin-Horseradish Peroxidase (HRP) – 250x
- 5xassay diluent, reconstituted in deionized water to make 1xassay diluent
- Substrate solution: 1xtetramethylbenzidine (TMB) solution
- 10xELISA coating buffer, reconstituted in deionized water to make 1xELISA coating buffer.

The following incubation steps were performed:

- The ELISA plate was coated with 100µl/well of capture antibody in coating buffer (1:250) and left overnight at 4°C.
- Blocking with 1xassay diluent and incubation at ambient temperature for 1h.
- Two-fold serial dilutions of the top standard (500pg ml⁻¹ for IFN γ and 300pg ml⁻¹ for IL-10) were made down to lowest standard concentration of (7.8pg ml⁻¹ for IFN γ and 4.7pg ml⁻¹ for IL-10), by using 1xassay diluent. Fifty µl/well of standard dilutions and samples (including sample dilutions 1:1, 1:10 and 1:20 in 1xassay diluent) were added to the plate and incubated for 2h at ambient temperature.
- 100 µl/well of detection antibody diluted in 1xassay diluent (1:250) was added to the plate and incubated at ambient temperature for 1h.
- 100 µl/well of avidin-HRP diluted in 1xassay diluent (1:250) was added to the plate and incubated at ambient temperature for 30 min.
- Finally 100µl of substrate solution was added to each well and incubated up to 15 min. 100µl of 2M H₂SO₄ was added to each well to stop the reaction. The plate was read at 450nm on a microplate spectrophotometer.

Each incubation step, with the exception of the last one, was completed by the thorough wash of the wells with 200µl/well of wash buffer (5x).

Optical density values were transformed to the cytokine concentration on the basis of the respective standard curves (Figure 2-2).

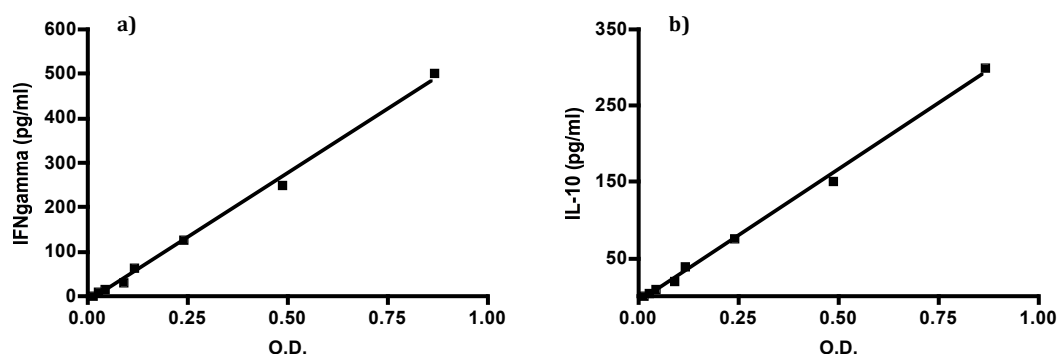


Figure 2-2. Representative examples of ELISA standard curves: a) IFN γ : standard curve range 4 – 500 pg/ml; b) IL-10: standard curve range 2 – 300 pg/ml.

2.1.6.2 IFN γ measurement in co-cultures of epidermal cells and HLA DR1 restricted FP1 specific cloned T-cells

IFN γ in the supernatants of co-cultures of epidermal cells and HLA DR1 restricted FP1 specific cloned T-cells was measured by the use of the exactly same IFN γ ELISA kit and protocol as described in the part 2.1.6.1 of this section.

2.1.6.3 MIP-1 β measurement in co-cultures of epidermal cells and HLA-A2 restricted EBVP1 specific cloned T-cells

Production of Macrophage Inflammatory Protein 1 β (MIP-1 β) in the supernatants of co-cultures of epidermal cells and HLA-A2 restricted EBVP1 specific cloned T-cells, was measured by ELISA (human CCLR/MIP-1 β , DuoSet® Development System, R&D Systems, Abingdon, UK).

The kit consists of the following reagents:

- Capture antibody, reconstituted in PBS to 180 μ g/ml stock concentration

- Detection antibody, reconstituted in Reagent Diluent - RD (see below) to 9µg/ml stock concentration
- Human MIP-1β standard, reconstituted in RD to the top concentration of 1000ng/ml, which was used to make 2-fold serial dilutions (7 in total)
- Streptavidin-HRP

Additional required solutions were:

- Wash Buffer - 0.05% Tween®20 in PBS
- Reagent Diluent (RD) – 1%BSA
- Substrate Solution: 1:1 mixture of Colour A reagent (H₂O₂) and Colour reagent B (tetramethylbenzidine)
- Stop solution: 2M H₂SO₄.

The following incubation steps were performed:

- The ELISA plate was coated with 100µl/well of capture antibody in PBS (1µg/ml) and left overnight at ambient temperature.
- Blocking with 300µl/well of RD and incubation at ambient temperature for 1h.
- Two-fold serial dilutions of the top standard (1000pg ml⁻¹) were made down to lowest standard concentration of (15.6 pg ml⁻¹), by using RD. Fifty µl/well of standard dilutions and samples (including sample dilutions 1:1 and 1:2 in RD) were added to the plate and incubated for 2h at ambient temperature.

- 100 µl/well of detection antibody diluted in RD (50ng/ml) was added to the plate and incubated at ambient temperature for 2h.
- 100 µl/well of Streptavidin-HRP diluted in RD (1:200) was added to the plate and incubated at ambient temperature for 20 min.
- Finally 100µl of substrate solution was added to each well and incubated up to 20 min. 100µl of 2M H₂SO₄ was added to each well to stop the reaction. The plate was read at 450nm on a microplate spectrophotometer.

Each incubation step, with the exception of the last one, was completed by the thorough wash of the wells with 200µl/well of wash buffer (5x).

Optical density values were transformed to the cytokine concentration on the basis of the respective standard curves (Figure 2-3).

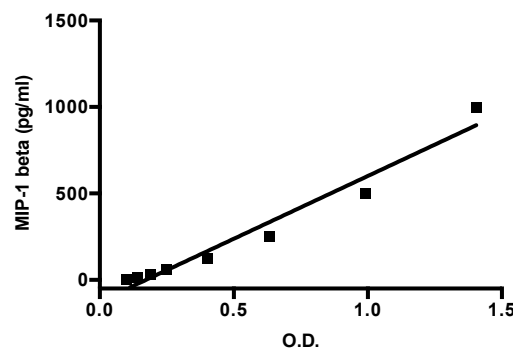


Figure 2-3. Representative example of MIP-1 β ELISA standard curve. Standard curve range 16 – 1000 pg/ml.

2.1.7 Magnetic cell separation

2.1.7.1 Naïve CD4⁺ T cell Isolation

I used Miltenyi Naïve CD4⁺ Isolation Kit II, which included the following steps:

- PBMCs were resuspended in 40µl of MACS buffer per total of 10⁷ cells and incubated for 10min. (2-8°C) with 10µl of Naïve CD4⁺ T cell Biotin-

Antibody Cocktail II (against CD8, CD14, CD15, CD16, CD19, CD25, CD34, CD36, CD45RO, CD56, CD123, TCR γ/δ , HLA-DR and CD235a) per 10^7 cells.

- After incubation, cells were washed by adding 1ml of buffer per 10^7 cells, centrifuged at 300xg for 10 min and resuspended in 80 μ l of buffer per 10^7 cells; then further incubated for 15 min. at 2-8°C with 20 μ l of Anti-Biotin Microbeads per 10^7 cells.
- Cell were washed and centrifuged as previously described, and resuspended in 500 μ l of buffer.
- After priming the MS column placed in the magnetic field with 500 μ l of MACS buffer, cell suspension was passed through the column followed by washing step (3x500 μ l).
- Follow-through containing unlabeled cells was collected as naïve CD4⁺ T cells.

During the procedure all buffers and cell suspensions were kept cold and sufficient time was allowed for the column reservoir to become empty before proceeding with the another step.

2.1.7.2 CD4⁺CD25⁺CD127⁻ regulatory T cell isolation

I used Miltenyi CD4⁺CD25⁺CD127⁻ Isolation Kit II, which included the following steps:

- PBMCs were resuspended in 40 μ l of MACS buffer per total of 10^7 cells and incubated for 5min. (2-8°C) with 10 μ l of CD4⁺CD25⁺CD127⁻ biotin-Antibody Cocktail II per 10^7 cells.

- After 5 min, 30µl of buffer and 20µl of Anti-Biotin Microbeads was added per 10^7 cells for further incubation for 15 min. at 2-8°C.
- After incubation, the volume was adjusted to a minimum of 500µl of buffer.
- After priming the LD column placed in the magnetic field with 2ml of MACS buffer, cell suspension was passed through the column followed by washing step (2x1ml).
- Total effluent of cell suspension was collected as population depleted from non-CD4⁺ and CD127^{high} cells.
- Cells were washed and resuspended in 90µl of buffer per 10^7 of cells and incubated at 2-8°C for 15 min. with 10µl of CD25 MicroBeads II per 10^7 .
- After priming, the MS column placed in the magnetic field, with 500µl of MACS buffer, cell suspension was passed through the column followed by washing step (3x500µl).
- Column was removed from the magnetic field and flushed with 1ml of buffer to remove magnetically labeled cells that were desired CD4⁺ CD25⁺CD127⁻ cells.

During the procedure all buffers and cell suspensions were kept cold and sufficient time was allowed for the column reservoir to become empty before proceeding with the another step.

2.1.8 Effect of the *ex vivo* skin treatment with immune-modulatory agents

2.1.8.1 Steroid *pre-treatment*

Betamethasone dipropionate cream 0.05% (w/v) (treatment) or PBS (control) was applied to the skin in the organ bath culture (Figure 2-4).



Figure 2-4. Ex-vivo topical application of the betamethasone cream

After 24h of incubation at the air-liquid interface at 37°C, the epidermis was enzymatically separated and single cell suspension was obtained as described in Section 2.1.2.

The effect of the steroid pre-treatment on DCs was studied by identifying their phenotype by flow cytometry (Section 2.1.5) and by assessing their ability to stimulate proliferation of PBMCs in the Mixed Epidermal Cells Lymphocyte Reaction - MECLR (Section 2.1.4).

Production of pro-inflammatory cytokine IFN- γ and pro-tolerogenic Interleukin IL-10 was measured in the supernatants of these reactions by using ELISA (Section 2.1.6).

2.1.8.2 Interleukin-10 (IL-10)

Immuno-modulatory agents used in this set of experiments were:

- Pure human recombinant IL-10, reconstituted as carrier free at the concentration of $50\mu\text{g ml}^{-1}$ in PBS – **IL-10^P**
- Human recombinant IL-10 attached to gold nanoparticles, stock containing $62.5\mu\text{g ml}^{-1}$ IL-10 and $227\mu\text{g ml}^{-1}$ gold – **NP IL-10**

- Control: pure gold nanoparticles, stock containing $325 \mu\text{g ml}^{-1}$ of gold–**NP**.

In vitro assessment

The effect of IL-10 was assessed *in vitro* by adding IL-10^p or NP-IL10, with and without $10\mu\text{g ml}^{-1}$ of human anti-IL-10 antibody, to MLR type cultures (Section 2.1.3). I used a range of IL-10 concentrations, starting from 0.1ng ml^{-1} and increasing 10 fold to 100ng ml^{-1} .

The effect on MLR was assessed by measuring proliferation and the production of IFN γ (ELISA) as described in Sections 2.1.3 and 2.1.6.

Ex-vivo assessment

A $50\mu\text{l}$ solution containing $10\mu\text{g ml}^{-1}$ of IL-10^p, NP IL-10 or NP was injected via standard intradermal 26G needle (Figure 2-5), creating a bleb measuring approximately 5-7mm. This was followed by punch biopsy around the bleb. Three injections/punches were performed per condition.



Figure 2-5. Ex-vivo injection and bleb formation of IL-10.

After 4h of incubation at the air-liquid interface at 37°C , the epidermis was enzymatically separated and single cell suspensions were obtained as described in Section 2.1.2.

The effect of injected IL-10 on DCs was studied by assessing their ability to stimulate proliferation of PBMCs in the MECLR (Section 2.1.4). Production of the cytokine IFN- γ and IL-10 was measured in the supernatants of these reactions by using ELISA (Section 2.1.6).

2.1.9 Effect of the *ex vivo* skin treatment with immune-modulatory agents

The study, approved by South West 3 Research Ethics Committee, UK, involved healthy volunteers aged 22-46 years with no history of any skin condition and no current or recent use of topical or systemic steroid, vitamin D preparation or any other potentially immunomodulatory therapy.

Participants applied DiproSone® cream, 12 hourly for four days, to the medial aspect of one arm (with other arm left untreated) prior to receiving two 50 μ l intradermal injections of 0.9% saline, one at each site of blister formation performed 6-18h later.

Skin suction blisters were performed by gradually applying negative pressure (up to 50kPa) from a suction pump machine VP25 through a suction blister cup with a 15 mm hole in the base for two to six hours until a unilocular blister had formed within the cup. The blister roof was removed by using a surgical blade and prepared for obtaining single epidermal cell suspension the same day, as described above. The procedure of suction blisters was performed by Dr Mohammad Ali Alhadjali – Figure 2-6.

Epidermal cells obtained from blister donor (donor A) from untreated skin (EC-c) and steroid treated skin (EC-s) were co-cultured with allogeneic donor (responder B) CD4⁺CD45RA⁺ naïve T cells for 2 weeks, in in 10% (v/v) human serum in RPMI 1640 supplemented with 0.5mM L-glutamine, 50IU ml⁻¹

penicillin, 0.05mg ml^{-1} streptomycin and 0.1mg ml^{-1} neomycin (complete RPMI 1640) in a 48-well plate at 37°C and 5% (v/v) CO_2 /95% (v/v) air. Each well contained $1000\mu\text{l}$ of medium. The final expansion phase includes addition of recombinant human 20 IU/ml IL-2 on day 7 – Figure 2-6.

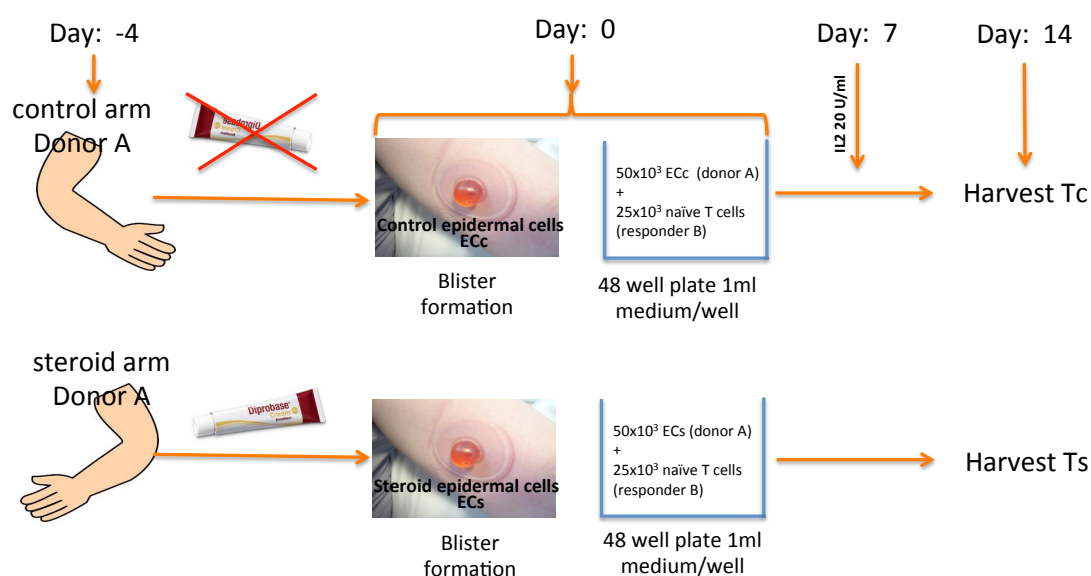


Figure 2-6. Flow chat of the culture of the T cells stimulated by epidermal DCs with and without previous *in vivo* topical steroid exposure. ECc – epidermal cells originated from the untreated arm; ECs – epidermal cells originated from the steroid treated arm; Tc – T cells originated from the culture stimulated by ECc. Ts – T cells originated from the culture stimulated by ECs.

The suppressive capacity of T cells expanded in such a way (Tc from co-culture with ECc, and Ts from co-culture with ECs) was assessed by their ability to suppress proliferation in the co-culture containing irradiated PBMCs from donor A and responder CD4⁺CD45RA⁺ naïve T cells from responder B in 10% (v/v) human serum in RPMI 1640 supplemented with 0.5mM L-glutamine, 50IU ml⁻¹ penicillin, 0.05mg ml⁻¹ streptomycin and 0.1mg ml⁻¹ neomycin (complete RPMI 1640) in a 96-well plate at 37°C and 5% (v/v) CO₂/95% (v/v) air. Each well contained 200µl of medium – Figure 2-7. After 96h of culture, 100µl of medium was collected from the surface and stored at -20°C for cytokine detection at the later date. 1µCi [³H] thymidine was added to each well, and the incorporation of radioactivity was measured after 16h using a β-microplate scintillation counter.

Efficacy of suppression was compared to the one achieved by addition of CD4⁺ CD25⁺ CD127⁻ natural regulatory T cells (Treg) from donor B to the co-culture containing irradiated PBMCs from donor A and responder CD4⁺CD45RA⁺ naïve T cells from responder B.

CD4⁺CD45RA⁺ naïve T cells were isolated from PBMCs by magnetic depletion of non-T helper cells and memory CD4⁺ T cells. CD4⁺ CD25⁺ CD127⁻ natural regulatory T cells (Treg) were isolated from PBMCs in the two step process involving: first, magnetic depletion of non- CD4⁺ and CD127^{high} cells, and the second, a positive selection of magnetically labelled CD4⁺ CD25⁺ CD127⁻ Treg.

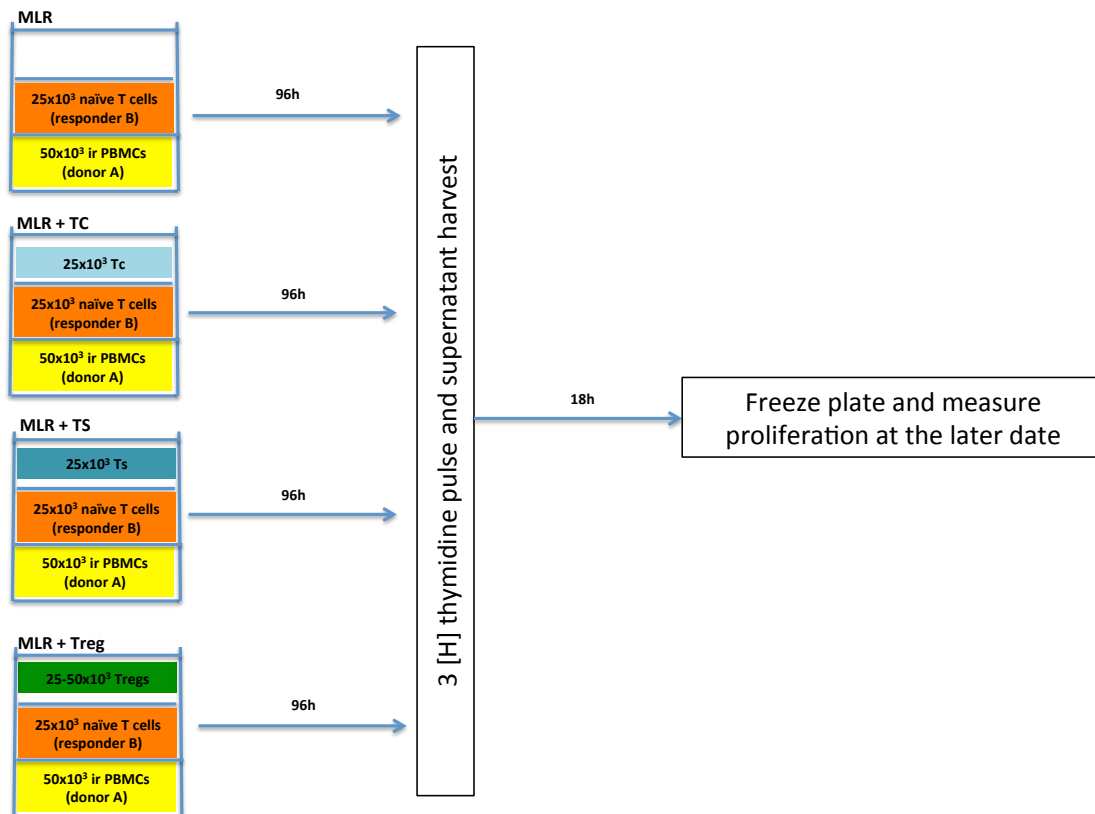


Figure 2-7. Assessment of the suppressive capacity of the T cells previously stimulated by epidermal DCs with and without previous *in vivo* topical steroid exposure. The content of wells in the 96 well plate is shown. MLR – Mixed lymphocyte reaction; Ir PBMCs – donor A PBMCs irradiated by 2000rad; Tc – T cells originated from the culture stimulated by ECc. Ts – T cells originated from the culture stimulated by ECs; Tregs – CD4+ CD25+CD127 – T cell from donor B.

2.1.10 Protocol for growing cloned T-cells

Cloning medium	Content of the medium
Cloning medium 1	10% (v/v) AB serum in RPMI 1640 (supplemented with 0.5mM l-glutamine, 50IU/ml penicillin, 0.05mg/ml streptomycin and 0.1mg/ml neomycin), containing PHA (1µg/ml), IL 2 (20IU/ml) and IL15 (50IU/ml)
Cloning medium 2	10% (v/v) AB serum in RPMI 1640 (supplemented with 0.5mM l-glutamine, 50IU/ml penicillin, 0.05mg/ml streptomycin and 0.1mg/ml neomycin), containing IL 2 (200IU/ml) and IL15 (50IU/ml)

Table 2-5. Content of cloning media

HLA DR1 restricted cloned T cells, specific for hemagglutinin (306-318) Influenza A virus peptide PKYVKQNTLKLAT (**FP1**) and HLA-A*0201 (HLA-A2) restricted cloned T cells, specific for lytic protein BMLF-1 (280-288) Epstein-Barr virus peptide GLCTLVAML (**EBVP1**) were grown in cycles lasting 14 ± 3 days. The cloned T cells were the kind gift of Dr A. Godkin (Clinical Reader, Cardiff University, Institute of Infection and immunity) and Prof. A. Sewell (Professor, Cardiff University, Institute of Infection and immunity).

The cycle started with the stimulation of 1×10^6 cloned T cells with a total of 10×10^6 γ -irradiated PBMCs (3000 rad) from 3 different allogeneic donors in 20ml of cloning medium 1 (Table 2-5) for 7 days in T25 cell culture flasks tilted at 25°. On day 7, cells were harvested, washed in RPMI 1640 and transferred to 24-well plates, at a density of $2-4 \times 10^6$ /well in 2ml of cloning medium 2 (Table 2-5).

From day 9 to day 14 ± 3 , 50% of the medium 2 was changed every 3 days. The cells were half-split if the density exceeded $3-4 \times 10^6$ /well. During this

period, cloned T cells were ready to respond to peptide-loaded skin DCs -

Figure 2-8.

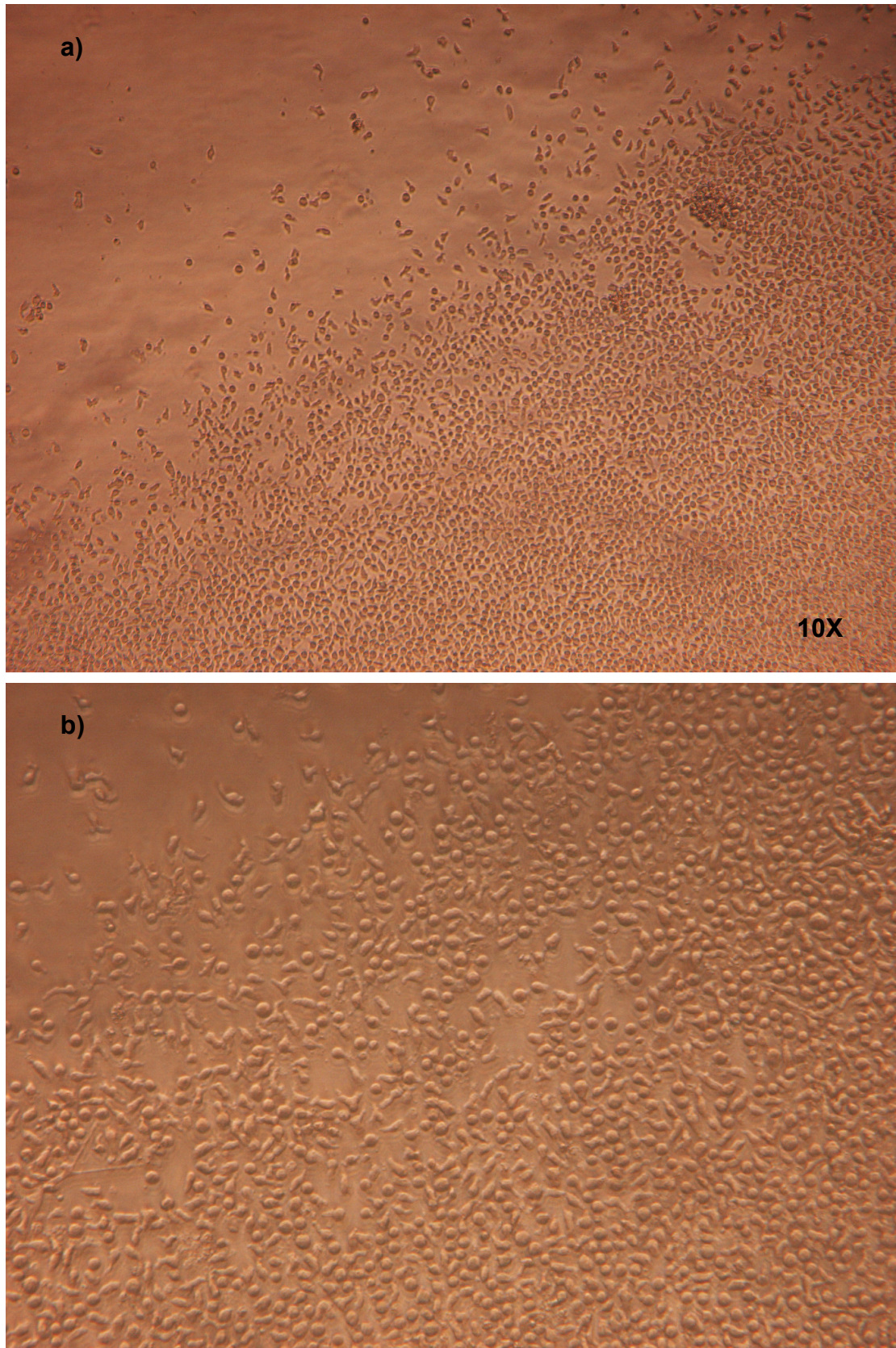


Figure 2-8. EBVP1 specific, HLA-A2 restricted cloned T-cells in the culture (day 9)

2.1.11 Protocol for growing antigen-presenting cells for stimulation of cloned T cells

Cells were grown 10% (v/v) FCS supplemented RPMI in upright T75 flasks at 37°C and 5% (v/v) CO₂/95% (v/v) air, at density of 0.2-0.4x10⁶/ml. 50 % of medium was changed every 3 days. Cells were half split if the density exceeded optimal. I grew 3 types of cells under the described conditions:

- HLA DR1 expressing, EBV transformed B cells
- HLA-A2 expressing, antigen processing (TAP)-deficient human T-B lymphoblastoid hybrid cell line – T2A2 cells
- HLA-A2 expressing, human plasma leukemia cell line - C1R-A2 cells

2.1.12 Peptide injection to the skin in the organ bath culture

A system was developed to study peptide loading of DCs with different delivery methods, based on antigen specific responses of the cloned T cells.

2.1.12.1 Peptide injection via hollow microneedle

Ten µg of FP1 in a 50µl volume was injected by hollow microneedle or standard 26G intradermal needle into *ex-vivo* skin explants (Figure 2-9). Blebs measuring approximately 5mm were created, followed by punch biopsy around the bleb. Three injections/punches were performed per condition including untreated skin.



Figure 2-9. Hollow microneedle. MicronJet 600 Needle, device containing 3x0.6mm length; NanoPass Technologies Ltd., Nes Ziona, Israel.

After 4h of incubation in the organ bath culture at 37°C, single cell suspension was obtained as per protocol (Section 2.1.2), and co-cultured with HLA DR1 restricted, FP1 specific cloned T cells for 12h. The measure of the response was the production of IFN- γ in the supernatants of these reactions, harvested after incubation period and quantified by ELISA (Section 2.1.6).

Cultures with cells derived from HLA DR1 positive skin donors were used as a treatment group, whilst cultures with cells derived from HLA DR1 negative skin donors were used as a negative control.

The positive controls in this experiment was a culture of FP1 specific cloned T cells with *in-vitro* added FP1 (0.5 μ M) with or without EBV transformed HLA DR1 expressing B cells.¹

HLA DR1 typing was performed by using rapid PCR on epidermal cells derived from skin explants.

¹ In some experiments only cultures of cloned T-cells (without APCs) with *in vitro* added peptide were used, given the ability of cloned T cells to present peptide to each other.

2.12.1.2 Peptide insertion via dry coated microneedle

The characteristics and the preparation of microneedles

Microneedles were made by wire-electrical discharge machining from stainless steel plates. Preparation of microneedles for optimal delivery is the subject of PhD thesis of Xin Zhao. The following paragraph will describe this process in brief. To deburr and clean microneedle edges and to make the tips sharp, microneedles were electropolished in a solution containing glycerin, 85% ortho-phosphoric acid and water in ratio of 6:3:1 by volume. Electropolishing was performed in a 300ml glass container at 70°C and stirring rate of 150rpm. A copper plate was used as a cathode, while microneedles acted as anode. The anode was vibrated at a frequency of 10Hz throughout the electropolishing process using a custom built vibrating device to help to remove gas bubbles generated at the anodic surface during electropolishing. A current density of 1.8mA/mm² was applied for 15min to electropolish the microneedles. Subsequently, microneedles were cleaned by dipping alternatively three times in the de-ionised water and 25% nitric acid for 30s each. This was followed by another washing step in hot running water and a final wash in running de-ionised water. Microneedles were dried using compressed air before storing in the air tight container until the later use.

Microneedles were arranged into the array consisting of 10 needles – Figure 2-10. Each needle in the array has pyramidal shape with following dimensions: 500µm long, 200µm wide in the base and 100µm thick. Due to the electropolishing process, the length of the needles reduced to 400µm.

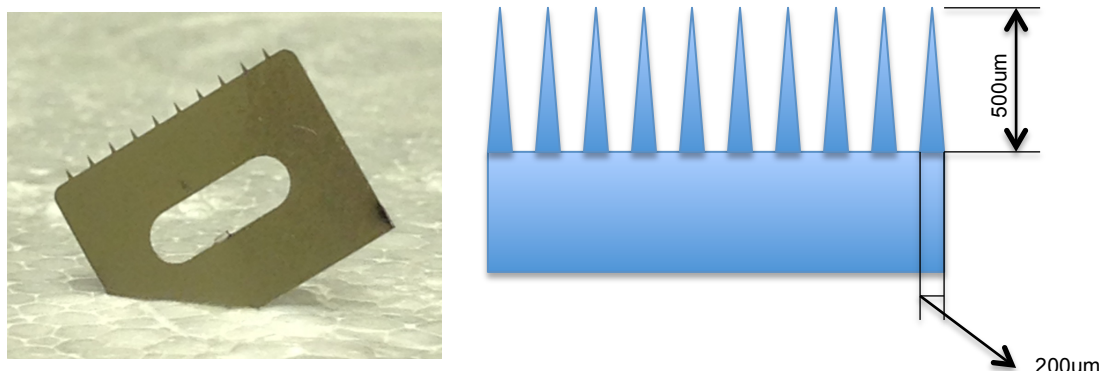


Figure 2-10. The shape and the dimensions of steel dry microneedle.

Microneedle coating

Microneedle arrays consisting of ten 400µm long polished needles were coated with 11.8µg EBVP1 peptide dissolved in 1µl of vehicle solution of glacial acetic acid, 2-methylbuten-2-ol and 20mg/ml, PVA 2000 (10:5:2, by volume) or 1µl of vehicle solution without peptide. Microneedles were repetitively dipped into the solution kept at the pipette tip until all the solution was used. After coating, needles were left to dry for 10 min. and kept at -80°C for the use in less than 24h.

Quantification of peptide delivery

I used 5-TAMRA labeled EBVP1 peptide to assess amount of peptide delivered to the skin during 15 min long insertion of the dry coated microneedle. Microneedle array was coated with 11.8µg of TAMRA-EBVP1 in 1µl of vehicle solution as described above, left to dry and inserted into the skin *ex-vivo* for 15 min. After insertion needles were washed in 100µl of 50%DMSO in DI water for 15 min. The amount of peptide left on the needle was quantified on the basis of the concentration of peptide in the washing

solution by using spectrophotometry. Example of the standard curve is shown in Figure 2-11. The comparison was made to the amount washed from non-inserted needles.

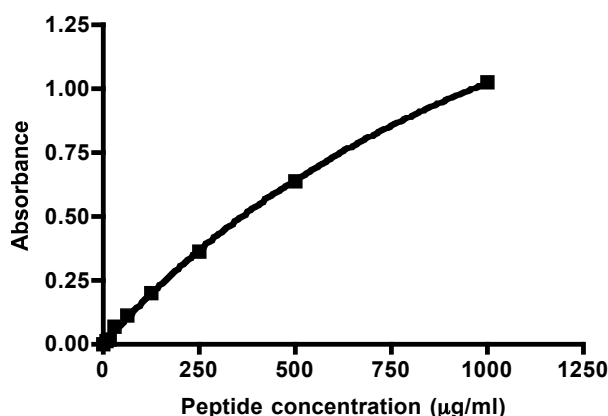


Figure 2-11. Representative example TAMRA-EBVP1 standard curve.

Peptide administration

11.8 µg of EBVP1 was inserted into the skin explants via microneedle and kept *in situ* for 15 min – Figure 2-12. Skin explants were also treated with microneedle coated with vehicle solution only (the same conditions as for peptide coated needles) or injected with 11.8 µg of peptide dissolved in 50µl of PBS from 5mM stock solution (20% DMSO and 80% DI water) via standard 26G needle. One punch was obtained per condition including untreated skin.

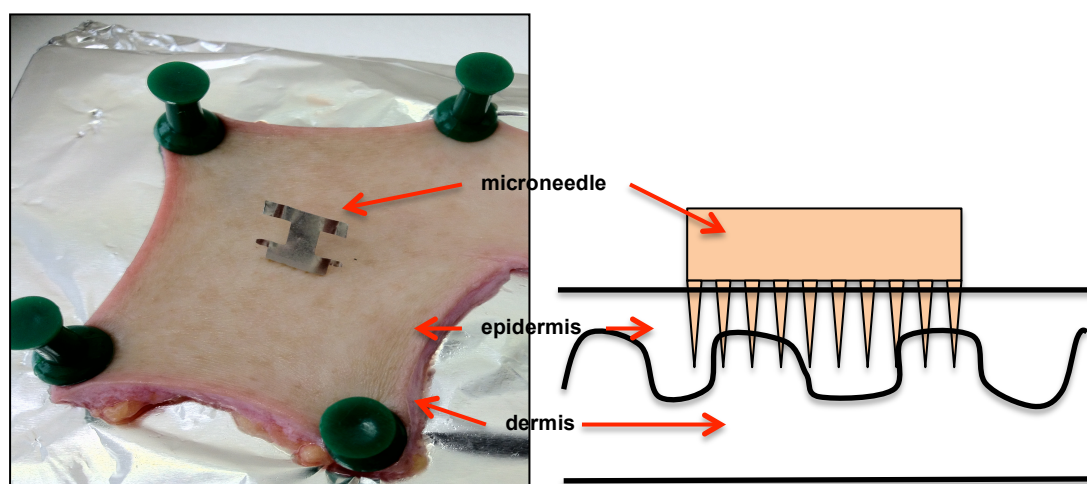


Figure 2-12. Peptide administration into the skin explant via dry coated microneedle.

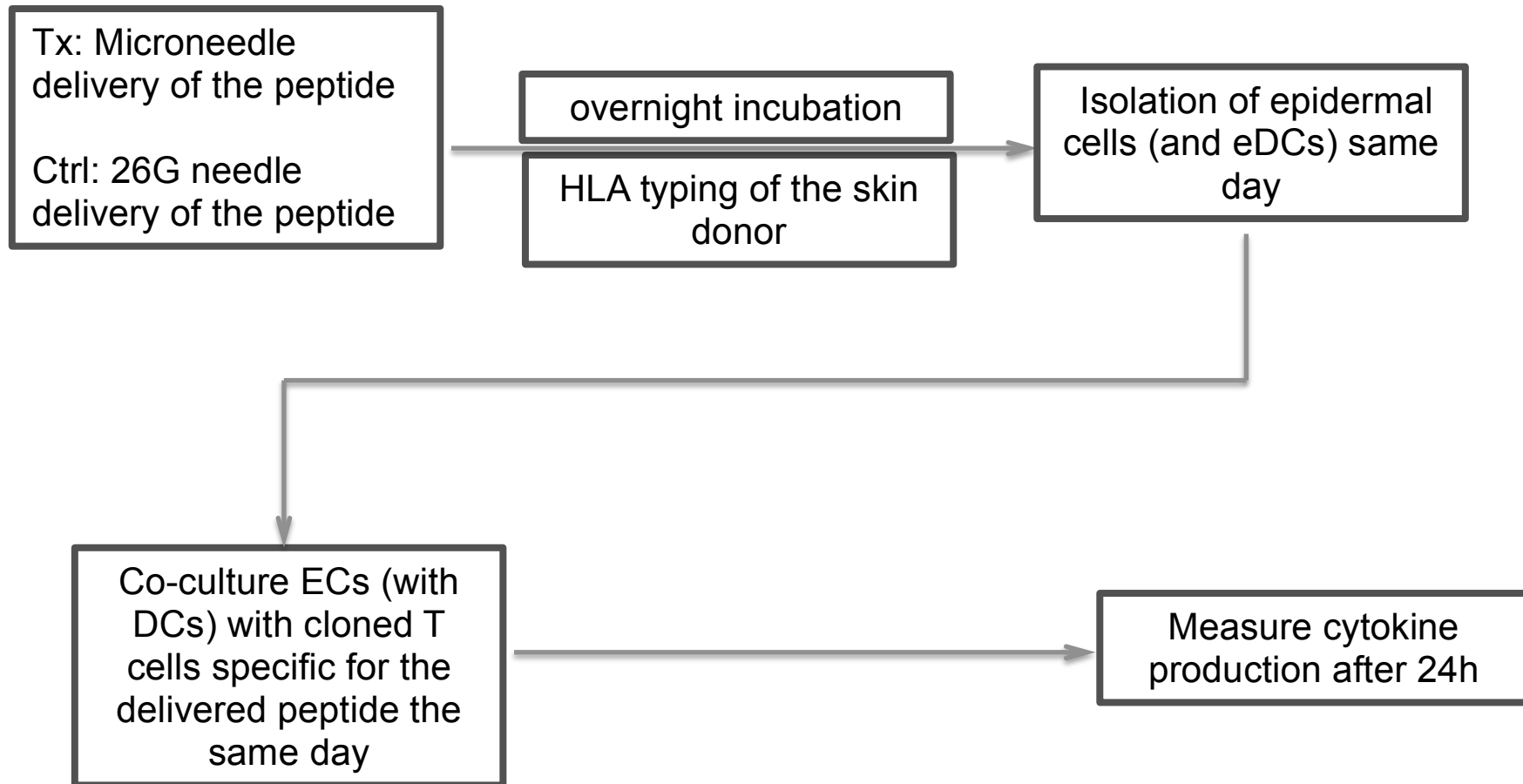
After overnight incubation in the organ bath culture at 37°C, single cell suspension was obtained as per protocol (Section 2.1.2), and co-cultured with HLA A2 restricted, EBVP1 specific cloned T cells for 12h. The measure of the response was the production of MIP-1 β in the supernatants of these reactions, harvested after incubation period and quantified by ELISA (Section 2.2.3).

Cultures with cells derived from HLA-A2 positive skin donors were used as a treatment group, whilst cultures with cells derived from HLA-A2 negative skin donors were used as a negative control. The positive controls in this experiment were a culture containing EBVP1 specific cloned T cells with *in-vitro* added EBVP1 (1 μ M) with or without T2A2 HLA-A2 expressing cells.

HLA-A2 typing was performed by flowcytometric analysis of epidermal cells derived from skin explants. Positive control in the analysis was HLA-A2 typing of the T2A2 cells.

A flow-diagram of study protocol is shown in the **Figure 2-13**.

Figure 2-13. Experimental protocol for the assessment of the efficacy of peptide loading of skin dendritic cells



2.1.13 HLA-DR1 typing by rapid PCR

I used the Phusion[®] Human Specimen direct PCR kit to identify the HLA DR1 status of the skin donors. The PCR was performed directly from the 0.5mm skin biopsy punch or control single cell suspension (HLA-DR1 expressing, EBV transformed B cells) without prior DNA purification.

Primers used in the reaction were originally obtained in 100µM (Table 2-6).[138] They were brought to 25µM concentration by adding sterile DI water.

Gene	Name	Sequence (5'3')	Size (bp)	Alleles
DR1	5'01 P1	TTG TGG CAG CTT AAG TTT GAA T	255	DRB1*0101-0103
	3'047 P2	CTG CAC TGT GAA GCT CTC AC		
	3'048 P3	CTG CAC TGT GAA GCT CTC CA		
Control 1	5'C	TGC CAA GTG GAG CAC CCA A	796	THIRD INTRON - DRB1 GENES
Control 2	3'C	GCA TCT TGC TCT GTG CAG AT		

Table 2-6. HLA DR1 and control primers characteristics.

Using the Harris Uni-Core[™] skin-sampling tool, 0.5mm punches were taken from the skin sample and placed directly into the 0.2ml Eppendorf tube with pre-prepared PCR mixture (Table 2-7). In control tubes, 2µl of single cell suspension (Table 2-7) or master mixture was added instead of the skin punch.

The components of the PCR mixture with HLA-DR1 primers and control primers were separately prepared as per Table 2-7. The quantities of the mixture components were multiplied accordingly, to pre-prepare master mixture for three individual 20µl reactions, including:

- 1) human donor skin sample;
- 2) control (HLA-DR1 expressing, EBV transformed B cells);

3) master mix only tubes.

	HLA-DR1 primer reaction	Control primer reaction	
Components	Volume	Volume	Final concentration
H2O	6.4µl	6.8µl	
2XPhusion® Human Specimen PCR Buffer	10µl	10µl	1x
Primer 1	0.4µl	x	0.5µM
Primer 2	0.4µl	x	0.5µM
Primer 3	0.4µl	x	0.5µM
Ctrl primer 1	x	0.4µl	
Ctrl primer 2	x	0.4µl	
Phusion® Human Specimen DNA Polymerase	0.4µl	0.4µl	
Sample	2µl	2µl	

Table 2-7. Components and quantities of PCR mixture: HLA-DR1 primer reaction and control primer reaction.

The reactions were performed on PTC-200 thermal cycler under conditions listed in the Table 2-8.

	Time	Temperature	N of cycles
Lysis	5min	98°C	1
Denaturation	10s	98°C	35
Annealing	16s	65°C	
Extension	18s	72°C	
Final extension	1min	72°C	1

Table 2-8. Conditions of the PCR reaction

When cooled, 3µl of Orange G loading buffer was added in each 20µl tube.

2% w/v agarose gel in 1xTAE buffer was mixed and microwaved until it became clear. After 2-3 min of cooling, 2µl 1% w/v ethidium bromide solution was added to 50µl of warm gel, mixed and placed in the casting tray with the comb to cool.

The gel was loaded with 10µl of sample per well, with the first well filled with 100bp DNA ladder and run for 55 min at 80V.

2.1.14 Statistics

Wilcoxon Signed Rank test or paired samples t test was performed to test the differences between paired measurements, whilst Mann Whitney U test was used for unpaired samples. For comparison of three or more samples One-way ANOVA was used and for the consecutive measurements, Repeated Measures ANOVA. For testing correlation, I used Spearman or Pearson correlation, depending on the distribution of the tested samples. Analysis was performed by using Prism GraphPad 4.0a for Macintosh. *P* values of less than 0.05 were considered significant. Results were expressed as mean±SD.

2.2 *In-vivo* methods for the optimal monitoring of the immune response after antigen skin delivery

This study was a single centre, before-after study of the optimisation of the detection of the immune response to intradermally delivered Tuberculin PPD in healthy volunteers. There were no untreated controls.

The study was approved by South East Wales REC (reference number 12/WA/0249) and involved healthy volunteers recruited from Cardiff University and Cardiff and Vale HB, who signed informed consent prior to the enrollment in the study.

Participants had pre-treatment blood sample and axillary lymph node fine needle aspiration biopsy (LN FNA), followed by injection of single dose of 2TU tuberculin PPD by hollow microneedle. The injection was administered intradermally in the forearm, contralateral to the initial LN FNA. Participants with a positive reaction (induration at the site of tuberculin PPD injection of greater than 5mm in diameter, 48-72h after injection)³ had a post-treatment blood sample and axillary LN FNA, ipsilateral to the injection site, 3-5 days after injection.

I used ELISPOT for the detection of IFN γ producing CD4 cells (blood and LN derived) in response to Tuberculin PPD as a read out (Section 2.2.2). The cells (LN derived and PBMCs) were also analysed for the change in the number, type and the expression of surface markers on flowcytometry.

³ Public Health England. Tuberculosis: the green book, Chapter 32, updated April 2013.

2.2.1 Ultrasound guided lymph node fine needle aspiration biopsy

Using aseptic technique, local anaesthesia and ultrasound guidance, a 21G needle was inserted into the axillary lymph node and up to 10µl of fluid aspirated.[139] The procedure was performed by consultant radiologist, Dr Philippa Young. The fluid was immediately transferred to 3ml of complete RPMI 1640 and transported to the laboratory at ambient temperature.

The number of white cells in the LN sample was counted in a haemocytometer after staining with trypan blue (1:3 dilution in PBS) and 4% (v/v) acetic acid to eliminate red blood cell contamination.

Simultaneously taken blood samples were processed for PBMCs extraction as described in Section 2.1.1.

2.2.2 IFN γ ELISPOT

PVDF plates previously treated with 35% (v/v) ethanol and washed with PBS (5x), were coated with IFN γ capture antibody (1:200 dilution in PBS) and incubated at 4°C for 18 h. [45, 140]

The next day, wells were blocked with 1% (w/v) BSA for 1h at 37°C, followed by addition of cell suspension at a density of 10^5 /100µl AIM-V medium per well for LNCs, and 10^6 /100µ AIM-V for PBMCs, in 2-3 replicate wells depending on cell availability.

Prior to placement in the ELISPOT plates, cells (LNCs or PBMCs) were incubated overnight with the study (Tuberculin PPD) and control antigens (PHA and tetanus toxoid) at various concentrations in complete RPMI 1640 in polypropylene round bottom tubes (Table 2-9), at 37°C and 5% (v/v) CO₂/95%

(v/v) air. PHA and the mixture of viral peptides used as another control antigen, were added directly to the plates with the responder cells, without pre-incubation period. Mixture of viral peptides included containing flu matrix protein (MP)₅₈₋₆₆ (GILGFVFTL), cytomegalovirus (CMV) pp65₄₉₅₋₅₀₃ (NLVPMVATV) and Epstein-Barr virus (EBV) BMLF1₂₈₀₋₂₈₈ (GLCTLVAML).

Experimental condition	<i>In vitro</i> added antigen	Final concentration	Note
1	No added antigens		background
2	Tuberculin PPD	0.05µg/ml	Only with frozen PBMCs, if repeat exp. needed due to strong response
3	Tuberculin PPD	0.5µg/ml	
4	Tuberculin PPD	0.05µg/ml	
5	Tetanus toxoid	0.5U/ml	Negative control
6	flu matrix protein (MP) ₅₈₋₆₆ (GILGFVFTL)	20nM	Negative control
7	cytomegalovirus (CMV) pp65 ₄₉₅₋₅₀₃ (NLVPMVATV)	20nM	Negative control
8	Epstein-Barr virus (EBV) BMLF1 ₂₈₀₋₂₈₈ (GLCTLVAML)	20nM	Negative control
9	PHA	1µg/ml	Positive control

Table 2-9. Conditions for incubation of cells prior to placement in the ELISPOT plates.

Plates were incubated overnight for 20h at 37°C.

The next day, cells were discarded and plates washed with the wash buffer and PBS. The incubation steps that followed included:

- Biotinylated IFN γ detection antibody (1:100 dilution in 10%FCS), 90µl/well – 1h at 37°C
- ExtrAvidin® -Alkaline Phosphatase (1:5000 dilution in 0.5% FCS), 100µl/well – 1h at ambient temperature
- 5-Bromo-4-chloro-3-indolyl phosphate/Nitro blue tetrazolium BCIP/NBT as a substrate for the alkaline phosphatase activity (1 tablet in 10ml of DI water), 100 µl/well – 10-12 min in the dark at ambient temperature

Each incubation step, with the exception of the last one, was completed by the thorough wash of the wells with 200µl/well of wash buffer (5x) and PBS (2x).

Reactions were stopped by adding DI water to the wells. Plates were left to dry overnight in the dark at ambient temperature and read on BioReader® at the later date.

First, the spots were counted as total number of spots per condition, summing all available wells and using customized settings in the BioReader (only spots with diameter $\geq 40\mu\text{m}$ were taken into account). Second, the number of background spots (spots from wells containing cells not-exposed to antigen) was subtracted from each condition. Third, the results are expressed as number of IFN γ producing cells per 2×10^5 cells.

2.2.3 Phenotyping of the lymph node cells and PBMCs by flow-cytometry

Single cell suspensions of lymph node cells obtained through lymph node fine needle aspiration biopsy (LNCs) and PBMCs were stained for flow-cytometry as described previously in Section 2.1.5, with the exception that staining was performed in 100µl of volume with up to 1×10^6 cells/test. The panels of flow-cytometry antibodies for phenotyping the cells at baseline are shown in the Table 2-10, whilst the panels for the assessment of changes before and after Mantoux test are shown in the Table 2-11.

The following test tubes were used:

- Test tube containing cells stained with viability stain only

- Test tube containing cells stained with antibodies listed in the Panel A
(Table 2-10, Table 2-11)
- Test tube containing cells stained with antibodies listed in the Panel B
(Table 2-10, Table 2-11)
- Test tube containing unstained compensation beads
- Test tubes containing compensation beads stained with each dye separately
- Separate test tube for the compensation of the viability dye: suspension of PBMCs containing 5×10^5 fresh cells and 5×10^5 cells, previously immersed in 80°C water bath for 20min.

Panel A			Panel B		
Marker	Dilution	Manufacturer	Marker	Dilution	Manufacturer
V450 anti-human CD3	1:30	Invitrogen, Paisley, UK	V450 anti-human CD3	1:30	Invitrogen, Paisley, UK
eFluor®506 viability dye	See text	E-bioscience, Hatfield, UK	eFluor®506 viability dye	See text	E-bioscience, Hatfield, UK
FITC anti-human CLA	1:30	Biolegend, London, UK	FITC anti-human CLA	1:30	Biolegend, London, UK
PE anti-human CCR7	1:30	Biolegend, London, UK	Biotin anti-human CCR8	7.8µg/ml	Gift from Dr McCully (CU, UK), origin ICOS Corporation (Seattle, USA)
			Streptavidin PE	1µl per 10^6 cells	Biolegend, London, UK
APC anti-human CD8	1:100	Biolegend, London, UK	APC anti-human CCR10	1:40	Biolegend, London, UK
PerCPCy5.5 anti-human CD69	1:100	Biolegend, London, UK	PerCPCy5.5 anti-human CD8	1:30	Biolegend, London, UK
APC Cy7 anti-human CD4	1:30	Biolegend, London, UK	APC Cy7 anti-human CD4	1:30	Biolegend, London, UK
PE Cy7 anti-human CD45RA	1:30	Biolegend, London, UK	PE Cy7 anti-human CCR4	1:30	Biolegend, London, UK

Table 2-10. Monoclonal antibodies for flow-cytometry (baseline analysis) – panels for LNCs and PBMCs.

Panel A			Panel B		
Marker	Dilution	Manufacturer	Marker	Dilution	Manufacturer
Pacific Blue anti-human CD19	1:100	Biologend, London, UK	V450 anti-human CD3	1:30	Invitrogen, Paisley, UK
eFluor®506 viability dye	See text	E-bioscience, Hatfield, UK	eFluor®506 viability dye	See text	E-bioscience, Hatfield, UK
FITC anti-human CD4	1:100	Biologend, London, UK	FITC anti-human CD4	1:100	Biologend, London, UK
			PE anti-human CD207	1:30	Biologend, London, UK
APC anti-human CD8	1:100	Biologend, London, UK	APC anti-human CD8	1:100	Biologend, London, UK
PerCPCy5.5 anti-human HLA DR	1:100	BD Pharmingen, Oxford, UK	PerCPCy5.5 anti-human CD69	1:100	Biologend, London, UK
			APC Cy7 anti-human CD154	1:30	Biologend, London, UK
			PE Cy7 anti-human CD1a	1:30	Biologend, London, UK

Table 2-11. Monoclonal antibodies for flow-cytometry (before and after Mantoux test) – panels for LNCs and PBMCs.

2.2.4 Statistics

Wilcoxon Signed Rank test was performed to test the differences between paired measurements. Analysis was performed by using Prism GraphPad 4.0a for Macintosh. *P* values of less than 0.05 were considered significant. Results were expressed as mean±SD.

2.3 *In-vivo* methods for the efficient and non-invasive assessment and monitoring of the residual β -cell function in type 1 diabetes

2.3.1 Main study

This pilot prospective observational study, approved by Berkshire Research Ethics Committee (reference number 10/H0505/87), was designed to assess stimulated urinary C-peptide in comparison to mixed-meal stimulated plasma C-peptide response in the same individual with Type 1 diabetes.

2.3.1.1 *Setting and subjects*

Seventeen non-obese, adult patients with type 1 diabetes (duration of ≤ 5 years) were recruited in the Bristol area (UK), through the South West Newly Diagnosed Diabetes Collection database, after signing informed consent. Inclusion criteria: age 18-45 years, normal renal function, HbA1c < 10% (86 mmol/mol), daily insulin requirement of < 0.8 units/kg/day and detectable β -cell function measured at a post-meal UCPCR.

2.3.1.2 *UCPCR stimulation*

Ensure Plus® (Abbott Nutrition, 6 ml/kg (max 360 ml)) was used as a Mixed Meal (MM) stimulant of β -cell insulin production, in both standard MMTT and standard mixed meal stimulated urinary C-peptide (uCP) measurements in hospital and at home.

For the home meal stimulus, the largest meal of the day was used. Patients were not asked to calculate or take a note of carbohydrate or protein content in their meal. [131]

2.3.1.3 Standard MMTT

Patients underwent a standard MMTT in the hospital after overnight fast.

They were asked to withhold taking long acting insulin on the morning of the hospital MMTT. They could take very short acting insulin up to 2 hours before the test and regular insulin up to 6 hours before the test. Test was conducted only if fasting value by capillary blood glucose was between 3.9-11.1mmol/l.

Serum samples for C-peptide (sCP) and glucose were collected at -10, 0, 15, 30, 60, 90 and 120 min. after Ensure Plus.

Urine samples were collected from the 2nd morning void before MM and 120 min after MM – hospital MM-UCPCR.

2.3.1.4 Home urine collections

Following the hospital MMTT, patients were asked to collect urine once monthly on 6 occasions at home (Figure 2-14):

a) Months 1 and 6 – home MM-UCPCR

Urine was collected at home 120 min. after Ensure Plus (taken after overnight fast and insulin dosing adjustments as with Standard MMTT) following pre-meal void, providing that the capillary blood glucose before the test was between 3.9 and 11.1 mmol/l.

b) Months 2, 3, 4 and 5 – home meal-UCPCR

Urine was collected at home 120 min after an evening meal of their choice following pre-meal void once a month. There was no requirement to withhold any insulin injections during the collection of urine after home meal stimulation.

Samples were collected irrespective of the level of the pre-meal capillary blood glucose.








Place	Hospital	Hospital	Home	Home	Home	Home	Home	Home
								
Test	Screen	Hosp. MMTT serum + UCPCR	Home MM-UCPCR month 1	Home meal UCPCR month 2	Home meal UCPCR month 3	Home meal UCPCR month 4	Home meal UCPCR month 5	Home MM-UCPCR month 6

Figure 2-14. Time-line of urine sample collection for UCPCR after different stimuli.

2.3.1.5 Urine and serum samples

Urine samples were collected in boric acid containers and transported to the laboratory at ambient temperature within 72h, for analysis by Diabetes Research Network Wales Laboratory, Swansea University.

Blood samples for glucose and C-peptide were collected in serum separator tubes (SST), allowed to clot, and centrifuged within 30 min. Serum was transferred into cryovials, kept at -20°C and sent frozen on dry ice for analysis by Diabetes Research Network Wales Laboratory, Swansea University.

Urine C-peptide, expressed as UCPCR in nmol mmol⁻¹, and serum C-peptide, expressed in pmol l⁻¹, were measured by ELISA.

2.3.2 Additional samples

Additional samples from 22 patients from MonoPepT1De were included in the analysis. This placebo controlled, double-blinded, randomized Phase Ib study, approved by NRES Committee South West – Exeter was designed to assess the safety of pro-insulin derived peptide C19-A3 in newly diagnosed patients with T1D within 100 days from first insulin injection.

These samples were used to assess correlation between change in residual β -cell function assessed by the production of serum C-peptide during standard MMTT and urinary C-peptide stimulated by standard Mixed Meal (see below) at baseline, after 3 and 6 months. Patients aged 18-45 years, possessed *0401 allele at the HLADRB1 gene locus, had starting peak serum C-peptide above 0.2 nmol/l on standard MMTT and positive at least one islet-cell autoantibody. The samples were analysed before unblinding.

2.3.3 Statistics

The study was powered on the ability to confirm a correlation between the peak sCP MMTT value and the 120minute UCPCR of ≥ 0.6 . Correlations below this level were not considered to be valuable. 25 paired sets of data were calculated to provide 90% power to detect as statistically significant correlations of 0.6 or more at the $p < 0.05$ level. I planned to recruit 30 participants to achieve a minimum of 20 complete sets of data. Due to slow recruitment of recently diagnosed patients satisfying the entry criteria, an interim analysis of results was conducted after 16 complete paired data sets had been obtained for the baseline correlation (17 subjects recruited). This showed a stronger correlation than the predicted minimum and, having

reached its primary end point, the study was concluded at this stage.

Non-parametric Spearman correlation was performed for correlating peak sCP during standard MMTT and stimulated UCPCR and for correlating area under the curve (AUC) sCP to peak sCP during standard MMTT.

The AUC was calculated for the 120 min. period of the standard MMTT using the sCP value at each time point.

The Wilcoxon signed rank test was performed to compare stimulated UCPCR between different time points over the follow up period.

All data are expressed as mean \pm SD. The difference was considered statistically significant if p value was < 0.05.

GraphPad Prism version 4.0a for Macintosh was used to for the analysis.

Chapter 3 TARGETTING EPIDERMAL DENDRITIC CELLS IN PEPTIDE SKIN DELIVERY – RIGHT PLACE, RIGHT TOOL

3.1 Introduction

3.1.1 Optimal delivery route for peptide immunotherapy (PIT)

In pursuing the goal of restoring tolerance to self-antigens responsible for autoimmunity in Type 1 diabetes, the choice of the delivery route is of paramount importance. Apart from epidermal and dermal skin delivery, other possible routes for PIT include the intranasal (i.n.), the sublingual (s.l.), the subcutaneous (s.c.) and the intravenous (i.v.). Skin has a number of advantages, including reliable dosing and absorbance of drugs (versus i.n and s.l.). In addition, completed Phase Ia trial of i.d. delivery of proinsulin C19-A3 peptide in Type 1 diabetes indicates safety of this route [116], which is in line with studies on PIT in clinical allergy [80]. Delivery into the skin has an advantaged over the s.c. route of a lower risk of hypersensitivity [141]. Furthermore, the skin is an easily accessible large organ with a well developed system of immune surveillance. Thus, the skin is an attractive candidate for the optimal delivery route of PIT.

3.1.1.1 Histology of the human skin [142]

Skin has three layers, from top to bottom: epidermis, dermis and hypodermis (Figure 3-1).

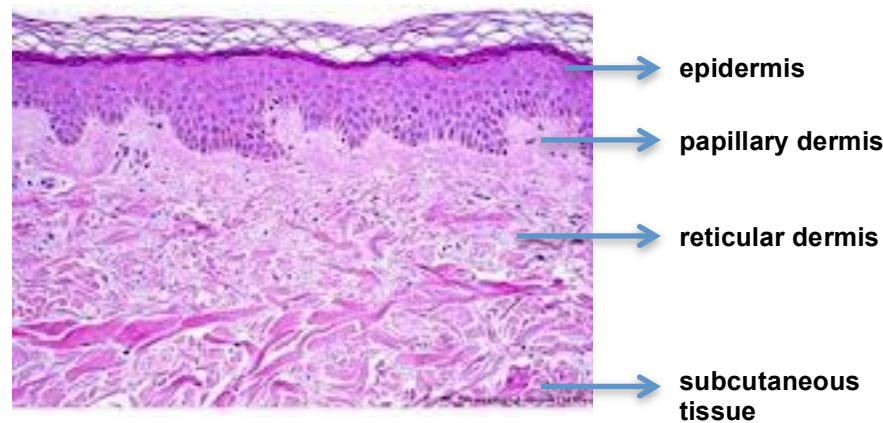


Figure 3-1. Histology of the human skin

Epidermis

The epidermis varies in thickness from 50µm on the eyelids to 1mm on the palms and soles. The most abundant cells in this layer are keratinocytes (90-95% of all cell types) that are arranged in several layers, from top to bottom: stratum corneum, stratum granulosum, stratum spinosum and stratum basale. Epidermal cells originate from mitotic divisions of stem cells of the basal layer and advance to the top over 30 days, undergoing morphological and biochemical differentiation (keratinisation). The other cells in this layer are: dendritic cells (DCs), are also known as Langerhans cells (LCs), representing 3-5% of the epidermal cells, which have a function of antigen presenting cells (APCs); melanocytes, which are melanin pigment containing cells that are scattered in the basal layer in the ratio of 1 melanocyte to every 4-10 basal keratinocytes; Merkel cells, which function as mechanoreceptors and exhibit neuroendocrine and epithelial features; and lymphocytes, which are

positioned mainly in the basal layer and represent less than 1.3% of epidermal cells [143].

Dermis

The superficial papillary dermis is arranged as upward projections that alternate with epidermal down-facing projections, which increases the surface of contact between the two layers. Deeper, reticular dermis is formed of coarser collagen bundles and a thicker elastic network. The dermis contains fibroblasts, dermal dendritic cells, mast cells and lymphocytes, as well as vessels and nerve endings, scattered around the network of collagen and elastic fibers.

Hypodermis

This is a fatty tissue that provides thermoregulation, insulation, mechanical protection and a nutritional store of energy.

3.1.1.2 Skin antigen-presenting cells (APCs)

Figure 3-2 gives an insight into the origin and function of different dendritic cells (DCs) that function as professional antigen presenting cells (APCs) throughout the body.

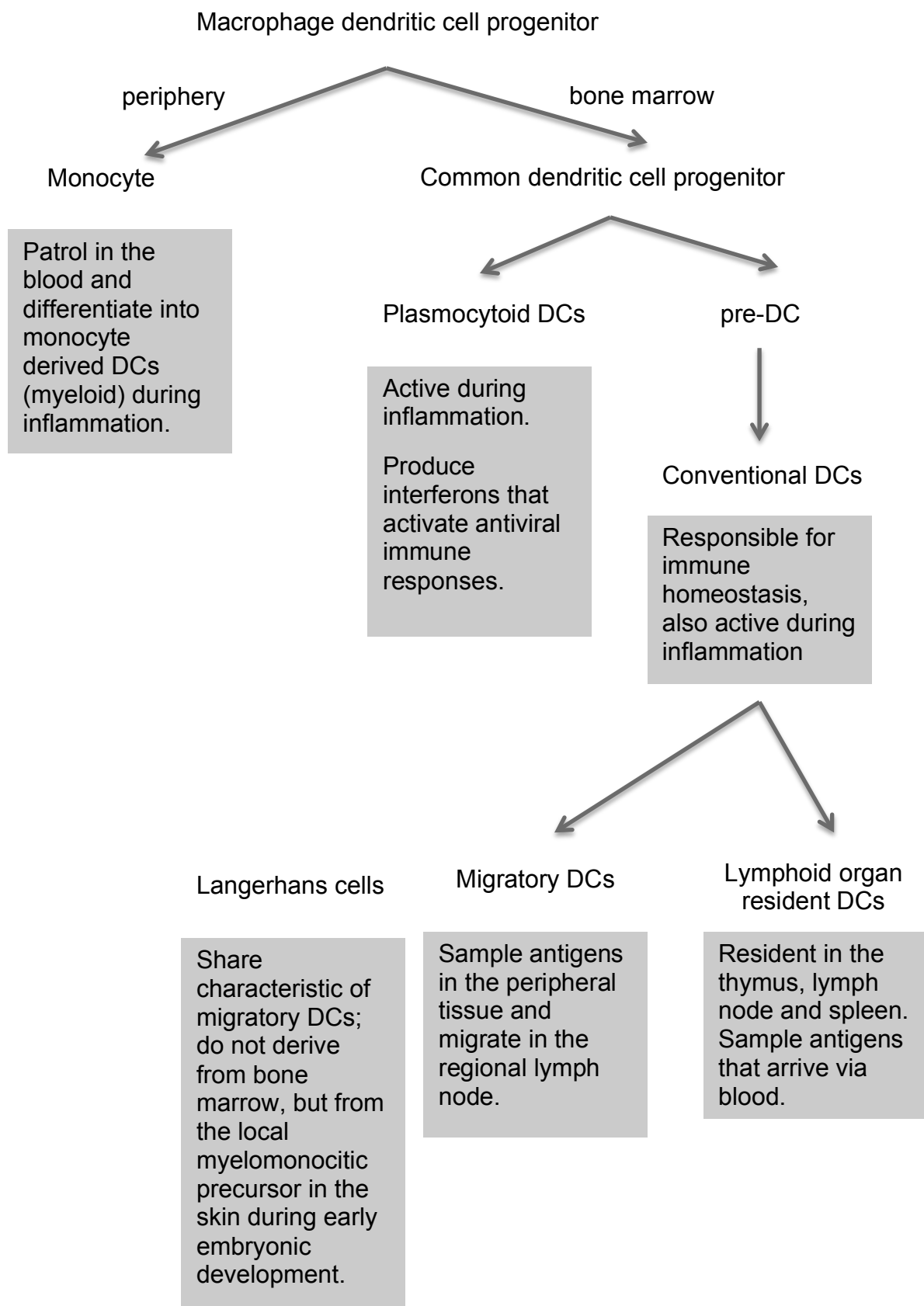


Figure 3-2. Types of the dendritic cells.[144]

Skin is the tissue rich in dendritic cells. They interact not only to provide efficient antimicrobial resistance, but also to maintain tolerance to self-antigens. One of the most studied type of skin APCs are the Langerhans cells (LC), which connect with each other through long dendritic projections creating an important immunological barrier in the suprabasal epidermis, where they mostly reside, representing 3-5% of all nucleated cells in this skin layer.[145] They are easily identified in the epidermis by the haematopoietic marker CD45 and MHC class II molecules.[146] They express lectin receptors, such as Langerin (CD207) [147] and CD205 [148], that have a role in the uptake of foreign pathogens. Adhesion molecules such as CD11c; E-cadherin [149] and EpCAM [150] connect LCs to neighboring keratinocytes. Another, surface marker, found only in humans is CD1a, a member of the CD1 protein family, presents microbial lipid antigens to T cells.[151] Although they don't share the same origin as conventional DCs, they exhibit similar behavior as migratory DCs. [144]

On the other hand, dermal dendritic cells express MHC class II and are mostly langerin negative, and do not express adhesion molecules such as EpCAM and E-cadherin.[152] Some dermal DCs also express lectin type receptor, such as DC-SIGN.[153] They are a much more diverse group, but two subpopulations of human dermal DCs can be characterised by their phenotype: one is CD1a^{high}/CD4⁺/DC-SIGN⁻/CD14⁻; the other is CD1a^{low}/CD4⁺/DC-SIGN⁺/CD14⁺. CD14⁺ dermal DCs have a number of functional differences to epidermal LCs, with the latter being more potent in the induction of CD8⁺ T-cell responses through IL-15, and the first playing a role in promoting antibody responses, either by directly acting on activated B

cells or by priming T follicular helper-like CD4⁺ cells.[154] They show similar characteristic of weak allogeneic stimulation as macrophages, suggesting common origin.[145] CD1a^{high} dermal DCs exhibit properties of both LCs and CD14⁺ dermal DCs.[154] Some studies suggest the existence of dermal langerin(+) DCs that can be distinguished from epidermal LCs by the CD103 expression in mouse.[155]

Apart from their role in antimicrobial defense, skin APCs have a role in maintaining self-tolerance. Little is known about the signals and factors that determine the perception of an antigen by an APC, originating from both sides of this interaction; that is, foreign to be fought versus self to be tolerated. In addition, elegant studies have attempted to define which subsets perform the role of maintenance of peripheral tolerance *in vivo* [156, 157], but the results are likely to be related to the particular transgenic model studied, and the relationship to human skin dendritic cell subsets remains uncertain.[158, 159] There are some suggestions from studies on human skin explants that LCs have a greater potential to elicit tolerogenic responses in responding T-cells [160], although data from humanised mouse model suggest existence of CD141⁺ subset of dermal DCs with tolerogenic properties as well.[161]

When delivering self-antigen into the skin to restore tolerance, it is important to target the area with the most abundant tolerogenic DCs. This goal can only be achieved with the right delivery device.

3.1.2 Optimal delivery device for the peptide immunotherapy

Most of our knowledge of immune responses following skin delivery comes from vaccine studies. Current convention is that most vaccines are delivered

to the muscle through the needle, where there is no abundance of immune cells and from where, due to the rich circulation, antigen is rapidly removed into the systemic circulation to trigger immune responses elsewhere. The most studied alternative is skin delivery to the dermis via a conventional needle. Skin delivery provides significant antigen dose reduction, as local uptake by numerous APCs is more efficient in comparison to conventional muscle administration.[162] Although superior to muscle, standard intradermal delivery places the antigen into the lower dermal layers with the sparser distribution of APCs that are less accessible to antigen in comparison to the rich network of LCs in the epidermis[145] that potentially can present antigen more efficiently and in more tolerogenic manner.

Due to its potential to deliver superficially to target APCs with less local irritation, microneedle technology could be valuable for the efficient delivery for peptide immunotherapy. Microneedles are needles of less 1000µm length that constituted with appropriate drug formulations, deliver into the skin more superficially than standard intradermal needles. A number of different microneedles categories are available, and can be divided into four major groups (Table 3-1).

Microneedle type	Mechanism of delivery
Solid microneedles	Pre-treatment of the skin to form pores through which subsequently topically applied drug will penetrate to reach deeper skin layers.
Coated microneedles	Needles carry the drug on their surface, such that it diffuses into the skin following insertion.
Dissolving microneedles	Needles are made of a polymer mixed with the drug of choice. The microneedle dissolves upon insertion into the skin.
Hollow microneedles	Needle is attached to a standard syringe, liquid drug is delivered through one or more projections. or Needles are attached to a reservoir filled with the liquid drug released once the microneedle is <i>in situ</i> at the desired place.

Table 3-1. Microneedle types and mechanisms of drug delivery

Peptides used in immunotherapy are large molecules that are not suitable for transdermal delivery, and are conventionally administered via hypodermic needle. Hollow microneedles were studied as an alternative.[163, 164] Also, the low doses of peptides required for immunotherapy allow delivery through coated and dissolving microneedles.

Some useful conclusions on pharmacokinetics can be drawn from animal studies on the use of solid [165], dissolving [166] and hollow microneedles [163] for insulin delivery that showed efficiency in lowering blood glucose. Consistent with the animal experiments, this type of needle in humans induced faster insulin absorption.[167, 168] Faster absorption of drugs via hollow microneedles most likely happens via dermal lymphatics.[169] Studies using parathyroid hormone (PTH) delivery via coated microneedles for the treatment of osteoporosis have progressed to Phase I and Phase II trials. A microneedle patch led to faster time to peak concentration and shorter half-life

of PTH than subcutaneous injection method with comparable improvement in bone mineral density.[170]

As with pharmacokinetics, studies on both animals and humans in the field of vaccine delivery can shed some light on immune responses after microneedle delivery. Hollow microneedles deliver antigen in a volume of liquid from the standard syringe; they are designed to target dermis and their reliability and dose-sparing effect in comparison to intramuscular delivery was tested using influenza vaccine administration.[164] Although potentially better in superficial delivery, due to their length (400-600 μ m vs approximate 200 μ m of human epidermal thickness), they largely miss the APC enriched area in the suprabasal epidermis. Microneedle arrays with short microprojections of approximately 100 μ m of length, dry coated with vaccine antigen, packed to an ultra high density (21.025/cm²), provide more reliable epidermal delivery.[171] A similar technology, using longer and less densely packed microprojections, failed to show comparable efficiency [172], suggesting that, in addition to length, it is important that an array is used that targets critical number of epidermal DCs that have approximate density of 500 cells per mm² in mice [173], with similar density in humans.

Another parameter to consider when choosing a delivery device is the level of injury to the skin caused by the injection or needle insertion. The larger extent of the injury during peptide delivery, the more probable is the pro-inflammatory response in the up-taking APCs that can send a wrong message to the responding T cell, steering away from the tolerance. This is of particular concern when dissolving microneedles are used because of the possibility that dissolved or degraded matrices have pro-inflammatory effects or other

side effects if devices are used frequently.[174] In comparison to hypodermic injection, influenza vaccine delivered by hollow microneedles induced more irritation in human subjects [175], although this can simply be due to more superficial and therefore more visible effects. Solid microneedles cause very mild skin irritation measured by erythema and blood flow. This effect is less prominent with shorter microneedles of 200µm length vs 400µm.[176] A study using nanopatch technology for influenza vaccine delivery suggested that that slow insertion of the array into the skin (less than 1m/s) causes significantly less cell death in comparison to other technologies.[177] In addition, invasive delivery may expedite traffic of LCs from the skin to the lymph node, which may have implications on shortening the beneficial local contact with the delivered antigen in the skin.[178]

For immunotherapy, it is clearly important that the presentation of antigen does not trigger or exacerbate existing autoimmune responses by inducing pro-inflammatory rather than tolerogenic signals. Preclinical studies suggest that peptide immunotherapy is most effective when the peptides are delivered to immature APCs that have not been activated by inflammatory stimuli.[179, 180] These cells regularly migrate to the draining lymph nodes and present self-antigens as part of the normal process of maintaining tolerance to self-antigens.[181, 182] The rich network of LCs in the suprabasal epidermis, with possibly greater potential for tolerance than other skin DC subsets, seem to be a logical target for peptide immunotherapy. The presence of adjuvant and the type of the antigen should also be taken into account. For example, large viral antigens induce immunity, rather than tolerance, despite efficient delivery to superficial LCs.[171]

3.2 Hypothesis

I hypothesise that microneedle technology has the potential to increase the efficacy of peptide delivery to epidermal DCs without causing significant local inflammation, in comparison to standard intradermal delivery.

3.3 Aims

1. To study the targeting of epidermal DCs by peptide delivered by hollow microneedles.
2. To study the targeting of epidermal DCs by peptide delivered by dry coated microneedles.

3.4 Results

3.4.1 Organ skin bath culture: an *ex vivo* method to investigate skin dendritic cells

Single epidermal cell suspensions obtained from skin explants described in Chapter 2, were analysed by using flow cytometry. The gating strategy of the analysis is shown in Figure 3-3. Relevant events were gated on an SSC-A/FSC-A graph (Figure 3-3 a), followed by gating on single cells only (FSC-A/FSC-H graph, Figure 3-3 b) and live cells, distinguished by the live/dead marker (Figure 3-3 c). The dendritic cells (DC) population was defined as CD1a⁺, HLA DR⁺ cells (Figure 3-3 d).

Once characterised in this way, further analysis of the DCs included staining for Langerin and CD11c. Staining with one antibody type (clone 923B7, rat) showed Langerin expression in only part of this population (Figure 3.3 e), but the use of another antibody (clone 10E2, mouse) later in the project, indicated that almost entire the DC population deriving from epidermal sheets express Langerin (Figure 3-4). However, CD11c was not expressed on these DCs, irrespective if the fixative was used during flow cytometric staining and despite staining by different antibodies derived from different clones.

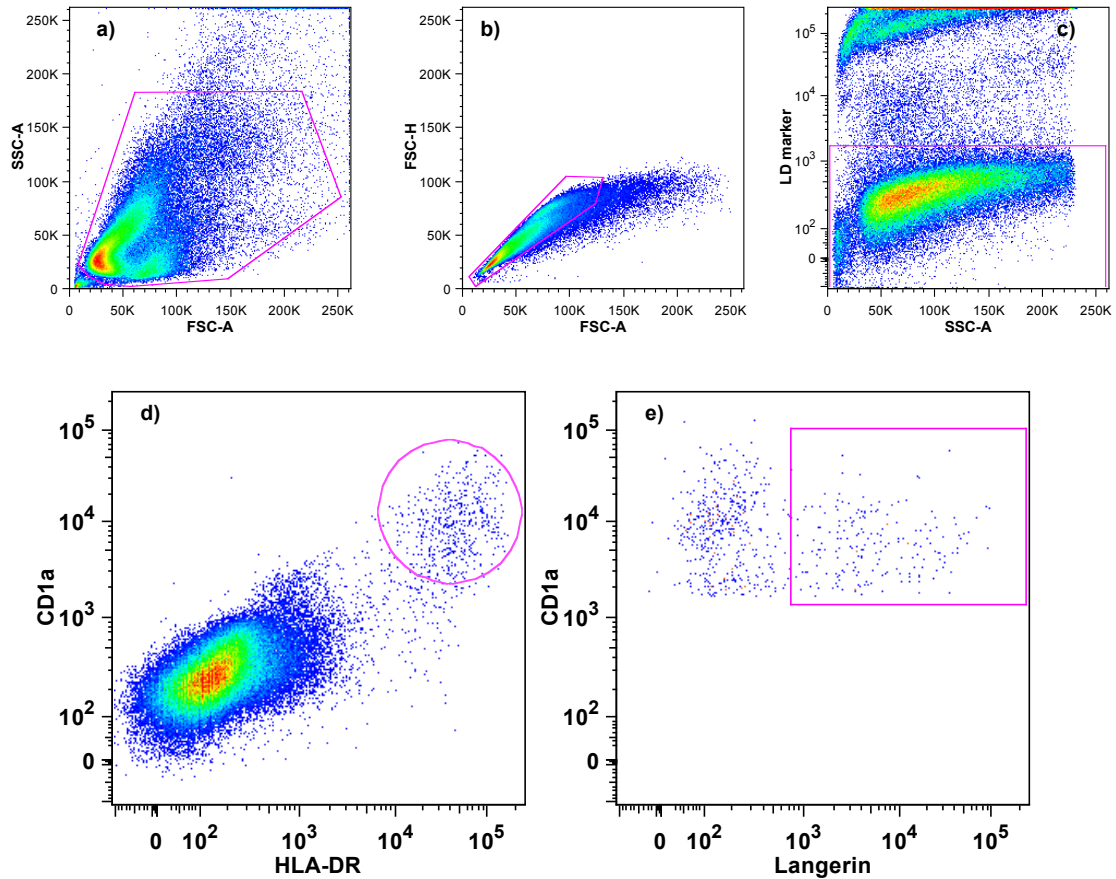


Figure 3-3. Flowcytometric analysis of the single epidermal cells suspension containing dendritic cells, gating strategy. a) Entire epidermal cell population; b) Gating on single cell events only; c) Epidermal cells negative for live/dead marker (APC-Cy7 channel) were characterised as live cells; d) $CD1a^+$ (Pacific Blue channel), $HLA\ DR^+$ (PerCP-Cy5.5 channel) cells from the live epidermal population were characterised as dendritic cells; e) Langerin staining (FITC channel) of $CD1a^+$, $HLA\ DR^+$ cells. FSC-H/A - forward scatter-height/area, SSC-A - side scatter-area, L/D marker – live/dead marker.

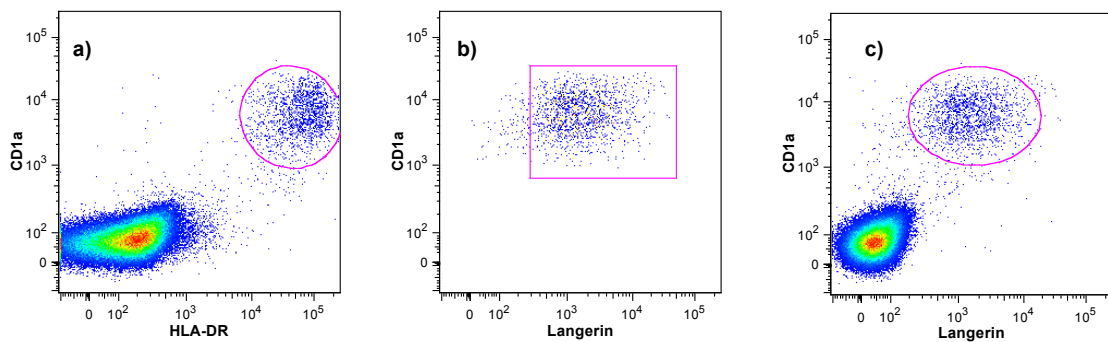


Figure 3-4. Flowcytometric analysis of the dendritic cells in the epidermal cell suspension. a) $CD1a^+$ (Pacific Blue channel), $HLA\ DR^+$ (PerCP-Cy5.5 channel) cells from the live epidermal population were defined as dendritic cells; b) Langerin staining with alternative antibody (PE channel) of $CD1a^+$ cells, $HLA\ DR^+$ cells; c) $CD1a^+$ (Pacific Blue channel), $Langerin^+$ cells from the live epidermal population.

Mean viability of epidermal cells was $33.7 \pm 20.5\%$ (Figure 3-5 a). The population of live epidermal cells contained on average $1.15 \pm 0.25\%$ of DCs defined as CD1a+, HLA DR+ cells (Figure 3-5 b).

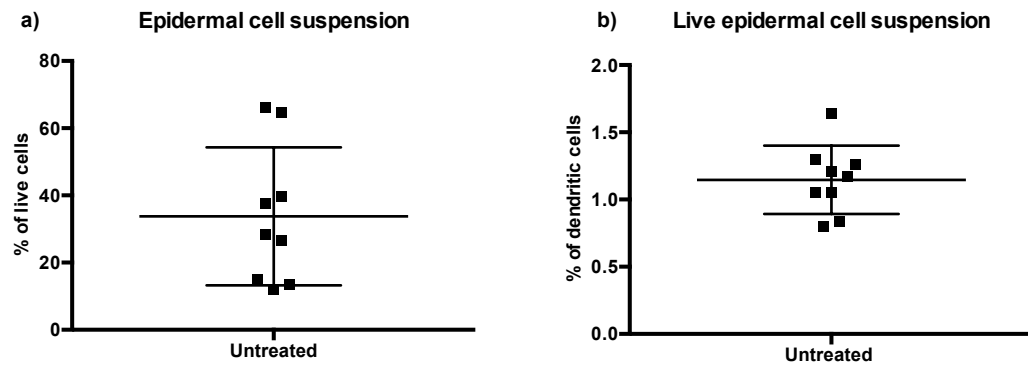


Figure 3-5. Flowcytometric analysis of the epidermal single cell suspension. a) percent of live cells in the epidermal cell suspension; b) percent of dendritic cells (CD1a+, HLA DR+) in the live epidermal cell suspension. N=9, results expressed as mean with SD, standard deviation.

To assess the functional capacity of DCs obtained, I co-cultured epidermal cells suspensions with allogeneic donor PBMCs in MECLR, as described in Chapter 2. The experiment, shown in Figure 3-6 a, suggested that 5×10^4 of ECs/well (estimated to contain around 500DCs) is sufficient to drive proliferation of 2×10^5 of allogeneic donor PBMCs. This was confirmed in a subsequent experiment (Figure 3-6 b) showing significant MECLR proliferation in comparison to background proliferation of PBMCs in 9 replicates.

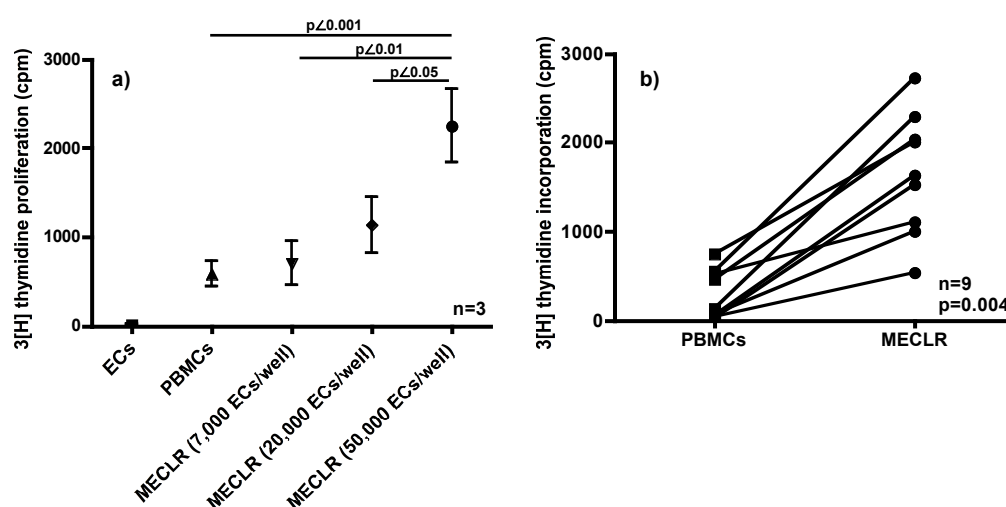


Figure 3-6. Mixed Epidermal Cells Reaction proliferation (MECLR) driven by epidermal DCs. a) titration of the optimal count of epidermal cells (ECs)/well in MECLR; statistical test used: One-way ANOVA ($p < 0.005$) with Bonferroni's Multiple Comparison post test. b) proliferation in MECLR with 50,000 ECs/well in comparison to PBMCs alone. PBMCs - peripheral blood mononuclear cells; statistical test used: Wilcoxon signed rank test.

3.4.2 Peptide uptake by epidermal DCs after injection by hollow microneedles

To assess ability of APCs to uptake injected antigen, ten µg of HLA-DR1 restricted hemagglutinin (306-318) Influenza A virus peptide PKYVKQNTLKLAT (**FP1**) was injected in the skin explant via hollow microneedles or standard 26G needles. Explants were subsequently incubated in the organ skin bath culture for 4h, followed by generation of the single cell suspension of the epidermal cells (Chapter 2), which were co-cultured with HLA DR1 restricted, FP1 specific cloned T cells for 12h. It is worth mentioning that the process of generating single epidermal cell suspension described in the Chapter 2, involved several washing steps, making the possibility of the existence of the free peptide in the cultures, negligible. The measure of the response was the production of IFN γ in the supernatants of these reactions, harvested after the incubation period and quantified by ELISA.

I used PCR analysis of skin to test for the expression of HLA DR1 in skin donors. I analysed samples from 20 different donors and detected 3 HLA-DR1 positive donors (217, 219 and 228). In addition, the first three consecutive donors that tested negative for HLA-DR1 (213, 214 and 221) were included in the experiment as negative controls – Figure 3-7. The rest of the negative donors were not included in further assays, i.e. co-cultures with the cloned T-cells., due to the limited availability of the cloned T cells.

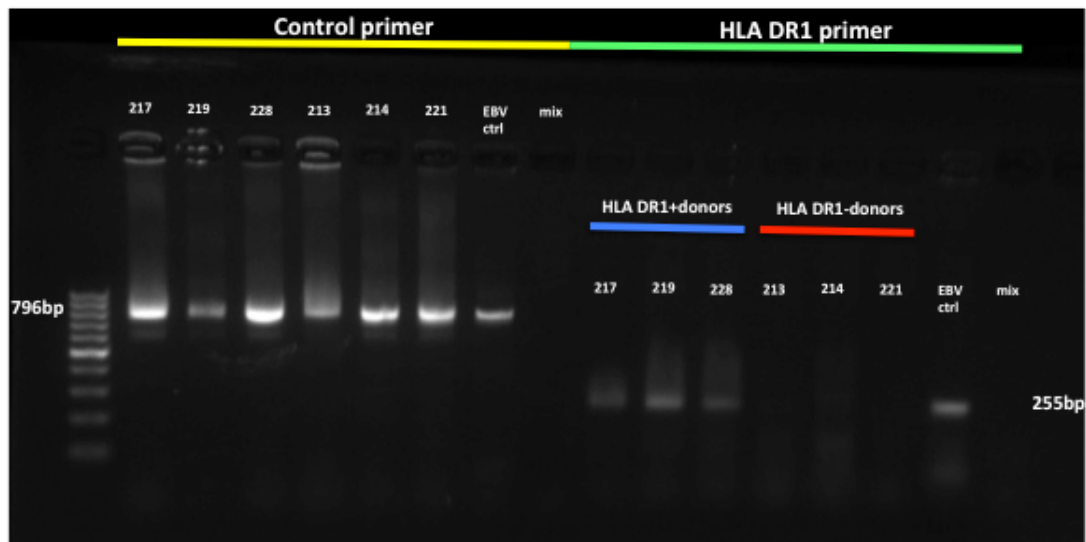


Figure 3-7. HLA DR1*0101-0103 typing. Positive donors: donors 217,219 and 228; negative donors: donors 213, 214 and 221; positive control: HLA DR1 expression EBV transformed B-cell line; mix: PCR master mix; control and HLA DR1 primer: see Chapter 2.

To assess baseline sensitivity of cloned T cells specific to FP1, I incubated the cells overnight at 37°C in 10% v/v FCS in RPMI containing increasing concentrations of FP1 and APCs (HLA DR1 expressing, EBV transformed B cells) in ratio 1:2 i.e. 6×10^4 APCs and 3×10^4 cloned T cells per well – Figure 3-8.

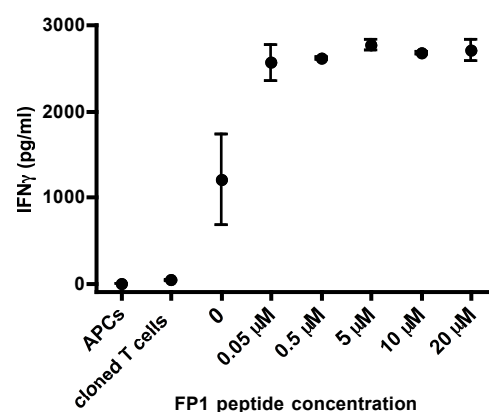


Figure 3-8 Sensitivity of HLA-DR1 restricted cloned T cells to FP1 peptide. Cloned T cells were incubated overnight with HLA DR1 expressing, EBV transformed B cells in ratio 1:2. IFN γ produced in these reactions was used as a measure of the clone stimulation. The mean and SD of the three separate experiments is shown in the graph.

When ECs from HLA DR1 negative individuals, loaded with FP1 peptide, were co-cultured with HLA DR1 restricted, FP1 specific cloned T cells, no additional stimulation of the cloned T-cells was observed in comparison to stimulation driven by untreated DCs, irrespective of the delivery device used, i.e. hollow microneedle or standard 26G needle. Stimulation was assessed by production of IFN γ by the cloned T-cells and expressed as ratio of IFN γ produced in cultures driven by FP1 loaded DCs and untreated DCs – Figure 3-9.

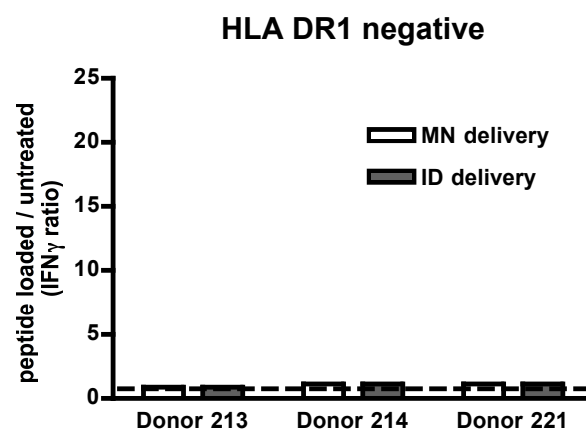


Figure 3-9. IFN γ production by FP1 specific cloned T cells stimulated by HLA DR1 negative donors. Stimulation expressed as IFN γ ratio derived from cloned T cells stimulated by FP1 loaded DCs/untreated DCs. MN delivery: FP1 injected into the skin explant by hollow microneedle; ID: FP1 injected into the skin by standard 26G needle.

	Donor 213 IFN γ pg/ml	Donor 214 IFN γ pg/ml	Donor 221 IFN γ pg/ml
APCs	0	0	14
Cloned Tcells	327	400	1129
EC UT	0	0	14
APCs+cloned Tcells	773	933	865
APCs+cloned Tcells+FP1 (<i>in vitro</i>)	19431	22352	17833
Cloned Tcells+FP1 (<i>in vitro</i>)	no data	no data	15010
EC UT + cloned Tcells	428	525	1246
EC MN + cloned Tcells	369	513	1334
EC ID + cloned Tcells	334	595	1283
N of replicates per donor	2	2	2

Table 3-2. IFN γ production by FP1 specific cloned T cells co-cultured with epidermal cells (containing DCs) from HLA DR1 negative donors. APCs: HLA DR1 positive EBV transformed B cell line; Cloned T cells: FP1 specific, HLA DR1 restricted cloned T cells; EC UT: epidermal cells derived from untreated skin; EC MN: epidermal cells derived from skin injected with FP1 by hollow microneedle; EC ID: epidermal cells derived from skin injected with FP1 by standard 26G needle; FP1 *in vitro*: FP1 added to the co-culture *in vitro*. IFN γ expressed in pg/ml; all experiments done in 2 replicate wells.

In contrast, when ECs from HLA DR1 positive individuals, loaded with FP1 peptide, were co-cultured with HLA DR1 restricted, FP1 specific cloned T cells, I observed an increase in the stimulation of the cloned T-cells, in comparison to stimulation driven by untreated DCs. The same trend was seen with each of the delivery devices used i.e. hollow microneedle or standard 26G needle -

Figure 3-10, **Table 3-3.**

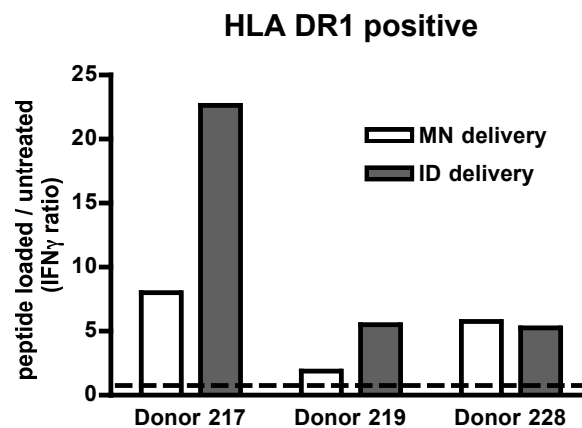


Figure 3-10. IFN γ production by FP1 specific cloned T cells stimulated by HLA DR1 positive donors. Stimulation expressed as IFN γ ratio deriving from cloned T cells stimulated by FP1 loaded DCs/untreated DCs. MN delivery: FP1 injected into the skin explant by hollow microneedle; ID delivery: FP1 injected into the skin by standard 26G needle.

	Donor 217 IFN γ pg/ml	Donor 219 IFN γ pg/ml	Donor 228 IFN γ pg/ml
APCs	7	69	0
Cloned Tcells	23	11	7
EC UT	8	16	0
APCs+cloned Tcells	39	169	7.3
APCs+cloned Tcells+FP1 (<i>in vitro</i>)	156	3444	9738
Cloned Tcells+FP1 (<i>in vitro</i>)	no data	no data	4818
EC UT + cloned Tcells	9	132	22
EC MN + cloned Tcells	65	228	125
EC ID + cloned Tcells	183	695	115.3
N of <i>in vitro</i> replicates per donor	2	2	2

Table 3-3. IFN γ production by FP1 specific cloned T cells co-cultured with epidermal cells (containing DCs) from HLA DR1 positive donors. APCs: HLA DR1 positive EBV transformed B cell line; Cloned T cells: FP1 specific, HLA DR1 restricted cloned T cells; EC UT: epidermal cells deriving from untreated skin; EC MN: epidermal cells deriving from skin injected with FP1 by hollow microneedle; EC ID: epidermal cells deriving from skin injected with FP1 by standard 26G needle; FP1 *in vitro*: FP1 added to the co-culture *in vitro*. IFN γ expressed in pg/ml; all experiments done in 2 replicate wells.

I compared IFN γ ratios obtained from HLA-DR1 negative donors to the ones measured in the reactions driven by HLA-DR1 positive donors, and found trend towards higher stimulation in positive donors with both delivery devices (ID^{neg}:0.99 \pm 0.15, ID^{pos}:11.08 \pm 9.92, p=0.1; MN^{neg}:0.99 \pm 0.11, MN^{pos}:5.18 \pm 3.09, p=0.1; Mann-Whitney test) – Figure 3-11.

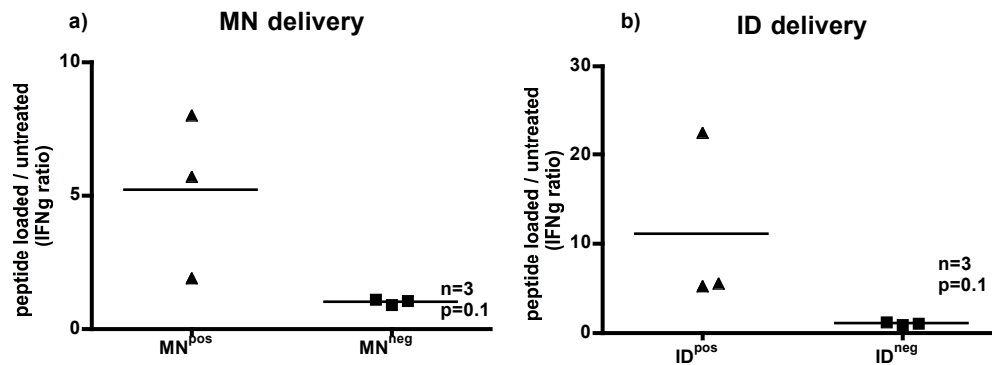


Figure 3-11. IFN γ production by FP1 specific cloned T cells stimulated by HLA-DR1 positive donors. Stimulation expressed as IFN γ ratio deriving from cloned T cells stimulated by FP1 loaded DCs/untreated DCs. a) MN^{pos/neg}: FP1 inserted into the skin explant by dry coated microneedle in HLA-DR1 positive or negative donors, respectively. b) ID^{pos/neg}: FP1 injected into the skin explant by standard 26G microneedle in HLA-DR1 positive or negative donors, respectively. Statistical test used: Mann-Whitney test.

3.4.3 EBVP1 peptide uptake by epidermal DCs after insertion by dry coated microneedles

I used similar system to assess ability of APCs to uptake antigen inserted into the skin *ex vivo*, via dry microneedles. However, this time I used HLA-A2 restricted clone, due to the much higher prevalence in the general population, hence higher probability to obtain skin samples originating from the donors, HLA matching the available cloned T cells.

Dry microneedles coated with 11.8µg lytic protein BMLF-1 (280-288) Epstein-Barr virus peptide GLCTLVAML (**EBVP1**) were inserted in the skin and kept in place for 15 min. As a control, 2µg or 11.8µg of the same peptide was injected into the skin via standard 26G needles. Explants were subsequently incubated overnight and processed to obtain single cell suspension as described in chapter 2. Single EC suspensions were co-cultured with HLA-A*0201 (HLA-A2) restricted cloned T cells, specific for EBVP1, for 12h.

To estimate the quantity of peptide retained in the skin, I used spectrophotometric analysis of the 5-TAMRA labeled EBVP1 peptide harvested from the needle before and after insertion (Chapter 2). It showed that only $17.0 \pm 1.4\%$ of the coated peptide remained in the skin after 15 min of insertion of the dry coated microneedle – **Figure 3-12**, Table 3-4.

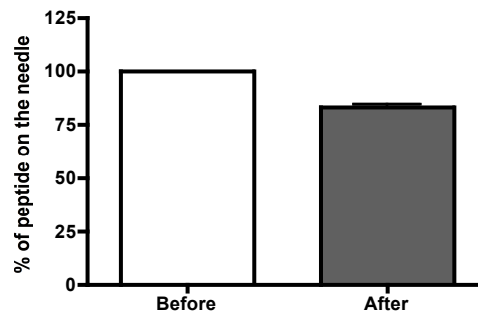


Figure 3-12. Efficacy of EBVP1 delivery via dry coated microneedle. The amount of peptide on the needle was quantified by the spectrophotometric analysis of 5-TAMRA labeled EBVP1 washed from the needle coated with 11.8µg of labeled peptide. Before: amount of peptide washed from the needle without insertion into the skin. After: amount of peptide washed from the needle after 15 min. long insertion into the skin.

Peptide	Before	After
Quantity (µg)	11.85±1.77	9.8±1.27
Percentage on the needle	100±0	83.0±1.4
N of replicates	3	3

Table 3-4. Efficacy of EBVP1 delivery via dry coated microneedle. The amount of peptide on the needle was quantified by the spectrophotometric analysis of 5-TAMRA labeled EBVP1 washed from the needle coated with 11.8µg of labeled peptide. Before: amount of peptide washed from the needle without insertion into the skin. After: amount of peptide washed from the needle after 15 min. long insertion into the skin.

I used flowcytometric analysis of the skin to test for the expression of HLA-A2 in skin donors. I analysed samples from 11 different donors and detected seven HLA-A2 positive donors. Four donors that tested negative for HLA-A2 were included in the experiment as negative controls. Figure 1-3 shows examples of flowcytometric analysis of HLA-A2 negative (a) and positive donors (b).

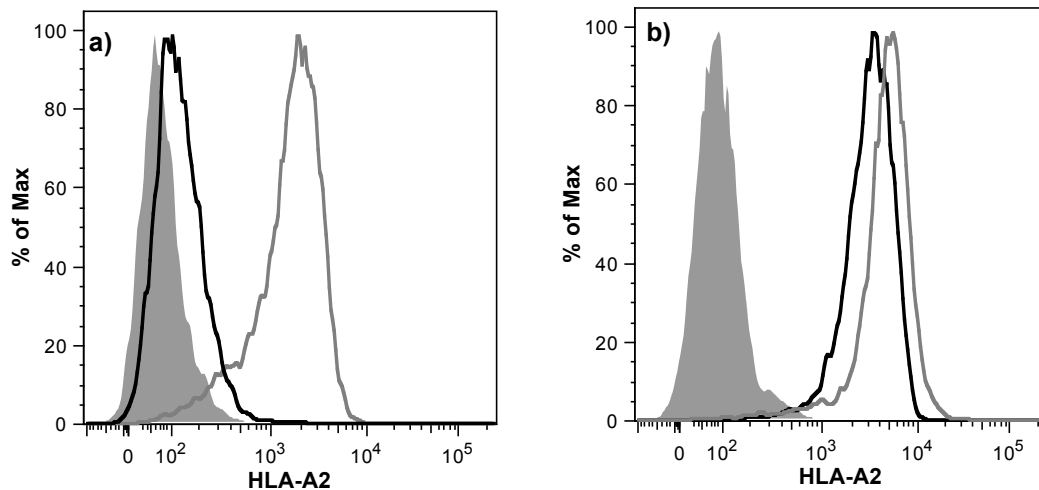


Figure 3-13. Representative example of the expression of HLA A2 (FITC channel): on the epidermal cells deriving from skin explants stained for HLA-A2 (black lines); on unstained epidermal cells deriving from the same skin explant - negative control (solid gray); on HLA A2 expressing human T2A2 cell line - positive control (dark gray lines). a) HLA A2 negative donor; b) HLA A2 positive donor.

To assess baseline sensitivity of cloned T cells specific to EBVP1, I incubated the cells overnight at 37°C in 10% (v/v) FCS in RPMI containing increasing concentration of EBVP1 and APCs (HLA-A2 expressing, antigen processing (TAP)-deficient human T-B lymphoblastoid hybrid cell line – T2A2 cells) in ratio 1:2 i.e. 6×10^4 APCs and 3×10^4 cloned T cells per well – Figure 3-14.

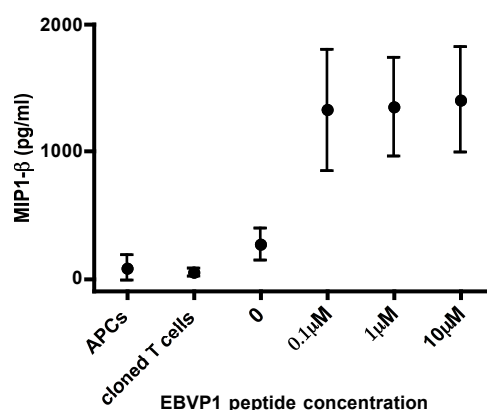


Figure 3-14. Sensitivity of HLA-A2 restricted cloned T cells to EBVP1 peptide. Cloned T cells were incubated overnight with HLA-A2 expressing, T2A2 cells in ratio 1:2. MIP1-β produced in these reactions was used as a measure of the clone stimulation. n=3

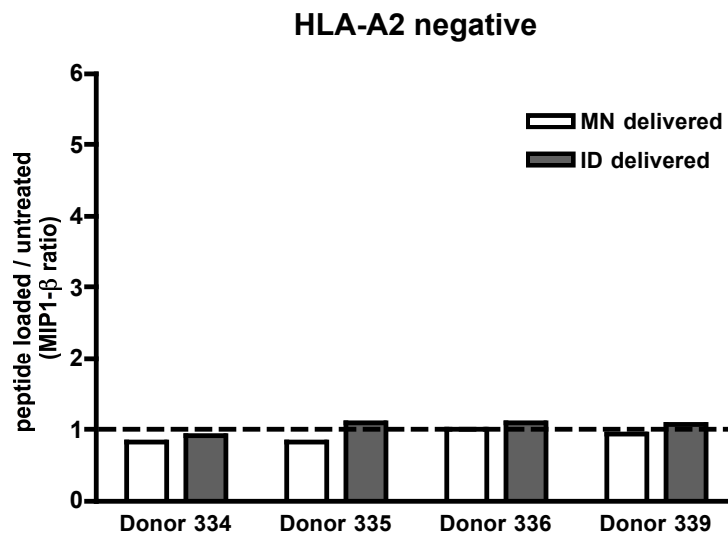


Figure 3-15. MIP1- β production by EBVP1 specific cloned T cells stimulated by HLA-A2 negative donors. Stimulation expressed as MIP1- β ratio deriving from cloned T cells stimulated by EBVP1 loaded DCs/untreated DCs. MN delivery: EBVP1 injected into the skin explant by dry coated microneedle; ID delivery: EBVP1 injected into the skin by standard 26G needle.

When ECs from HLA-A2 negative individuals, loaded with EBVP1 peptide, were co-cultured with HLA-A2 restricted, EBVP1 specific cloned T cells, no additional stimulation of the cloned T-cells was observed in comparison to stimulation driven by untreated DCs, irrespective of the delivery device used i.e. dry microneedle or standard 26G needle. Stimulation was assessed by production of MIP1- β by the cloned T-cells and expressed as ratio of MIP1- β produced in cultures driven by EBVP1 loaded DCs and untreated DCs – Figure 3-15, Table 3-5.

	Donor 334	Donor 335	Donor 336	Donor 339
	MIP1- β pg/ml	MIP1- β pg/ml	MIP1- β pg/ml	MIP1- β pg/ml
APCs	0	0	0	0
APC+ Cloned Tcells	40	40	43.5	46
EC UT	0	0	0	0
APCs+cloned Tcells+EBVP1 (<i>in vitro</i>)	764	650	641	375
EC UT + cloned Tcells	40	36.5	40	43
EC MNc + cloned Tcells	33	33	36.5	40
EC MNpep + cloned Tcells	33	33	40	40
EC stID + cloned Tcells	36.5	40	43.5	46
N of replicates per donor	2	2	2	2

Table 3-5. MIP1- β production by EBVP1 specific cloned T cells co-cultured with epidermal cells (containing DCs) from HLA-A2 negative donors. APCs: HLA-A2 expressing, T2A2 cells ; Cloned T cells: EBVP1 specific, HLA-A2 restricted cloned T cells; EC UT: epidermal cells deriving from untreated skin; EC MNc: epidermal cells deriving from skin into which microneedle coated with coating solution only was inserted; MNpep: epidermal cells deriving from skin into which microneedle coated with EBVP1 was inserted EC ID: epidermal cells deriving from skin injected with EBVP1 by standard 26G needle; EBVP1 *in vitro*: EBVP1 added to the co-culture *in vitro*. MIP1- β expressed in pg/ml; all experiments done in 2 replicate wells; some donors shared negative controls for cloned T cells and APCs as samples were processed on the same day.

I compared MIP1- β ratios obtained from HLA-A2 negative donors to the ones measured in the reactions driven by HLA-A2 positive donors, and found significantly higher stimulation with positive donors when microneedle delivery was used (MN^{neg} : 0.89 ± 0.08 , $n=7$; MN^{pos} : 2.50 ± 1.03 , $n=4$; $p=0.006$, Mann Whitney test) and a trend towards an increase when peptide was injected via standard 26G needle (ID^{neg} : 1.04 ± 0.09 , ID^{pos} : 1.86 ± 0.49 ; $p=0.05$, Mann Whitney test). This suggests exclusive stimulation when peptide is presented by the HLA matched donor –Figure 3-16, Table 3-6.

In this comparison, I only used intradermal injections of 2 μ g of peptide, as all HLA-A2 negative controls received this amount of peptide through i.d. delivery.

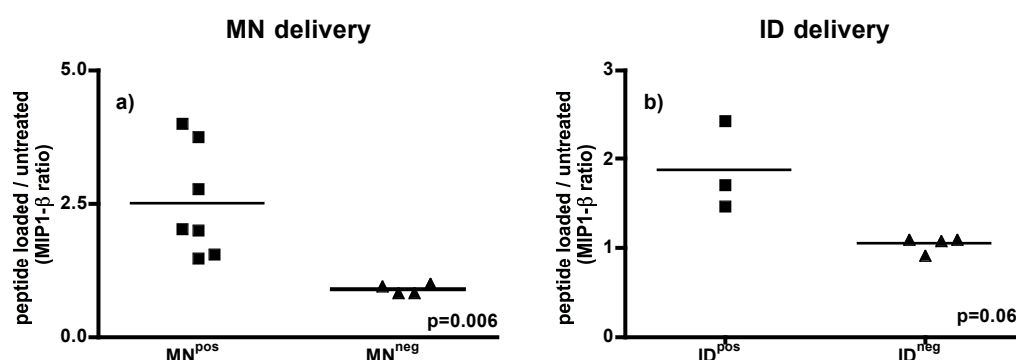


Figure 3-16. MIP1- β production by EBVP1 specific cloned T cells stimulated by HLA-A2 positive donors. Stimulation expressed as MIP1- β ratio deriving from cloned T cells stimulated by EBVP1 loaded DCs/untreated DCs. a) $MN^{pos/neg}$: EBVP1 inserted into the skin explant by dry coated microneedle in HLA-A2 positive or negative donors, respectively. b) $ID^{pos/neg}$: EBVP1 injected into the skin explant by standard 26G microneedle in HLA-A2 positive or negative donors, respectively. Statistical test used: Mann-Whitney test

	Donor295	Donor297	Donor305	Donor306	Donor337	Donor338	Donor340
	MIP1- β pg/ml	MIP1- β pg/ml	MIP1- β pg/ml	MIP1- β pg/ml	MIP1- β pg/ml	MIP1- β pg/ml	MIP1- β pg/ml
APCs	0	0	0	0	0	0	0
Cloned Tcells	798	631	171	171	50	50	46
EC UT	42	40	0	0	0	0	0
APCs+cloned Tcells+EBVP1 (<i>in vitro</i>)	3361	3320	1317	1317	489	489	375
Cloned Tcells+EBVP1 (<i>in vitro</i>)	no data	3450	no data	no data	no data	no data	no data
EC UT + cloned Tcells	333	552	229	410	43.5	40	43
EC MNc + cloned Tcells	429	599	236	425	40	40	40
EC MNpep + cloned Tcells	1326	2073	635	817	67	80.5	63.5
EC ID (2 μ g) + cloned Tcells	no data	no data			74	97	63.5
EC ID (11.8 μ g) + cloned Tcells			1128	1164			
N of <i>in vitro</i> replicates per donor	2	2	2	2	2	2	2

Table 3-6. MIP1- β production by EBVP1 specific cloned T cells co-cultured with epidermal cells (containing DCs) from HLA-A2 positive donors. APCs: HLA-A2 expressing, T2A2 cells; Cloned T cells: EBVP1 specific, HLA-A2 restricted cloned T cells; EC UT: epidermal cells deriving from untreated skin; EC MNc: epidermal cells deriving from skin into which microneedle coated with coating solution only was inserted; MNpep: epidermal cells deriving from skin into which microneedle coated with EBVP1 was inserted EC ID: epidermal cells deriving from skin injected with 2 μ g or 11.8 μ g EBVP1 by standard 26G needle; EBVP1 *in vitro*: EBVP1 added to the co-culture *in vitro*. MIP1- β expressed in pg/ml; all experiments done in 2 replicate wells; some donors shared negative controls for cloned T cells and APCs as samples were processed on the same day.

The greater efficacy of microneedle delivery in comparison to the delivery of 2 μ g peptide via standard 26G needle delivery was not confirmed when results of paired samples (MN and ID injection into the explant derived from the same donor) were analysed - Figure 3-17a, Table 3-6. However DCs showed suggestion toward more potent stimulation of the cloned T cells when higher dose of peptide was intradermally injected into the skin (10 μ g) in comparison to MN delivery – Figure 3-17b, Table 3-6.

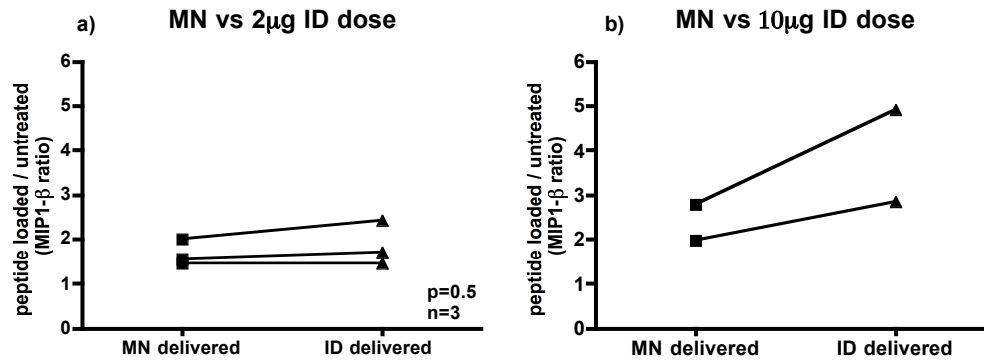


Figure 3-17. MIP1- β production by EBVP1 specific cloned T cells: microneedle vs intradermal delivery in HLA-A2 positive donors. Stimulation expressed as MIP1- β ratio deriving from cloned T cells stimulated by EBVP1 loaded DCs/untreated DCs. MN delivered: EBVP1 inserted into the skin explant by dry microneedle coated with 11.8 μ g of EBVP1. ID delivered: EBVP1 injected into the skin via standard 26G needle: a) 2 μ g injected intradermally; b) 11.8 μ g injected intradermally. Statistical test used: Wilcoxon signed rank test.

3.5 Summary of findings

1. Single epidermal cell suspension can be obtained from organ bath cultures, by using enzymatic digestion. This novel approach combines known steps to obtain epidermal cells, including sufficient DCs for phenotypic and functional characterization at the desired time-point, without the need for prolonged “walk-out” methods. This is important because we can use this as a surrogate for skin delivery *in vivo* and assess the effect in the precise moment in time.
 2. The phenotype of cells obtained is similar to those previous described in the epidermis – with the exception of CD11c, suggesting some damage of the DCs in the process.
 3. The DCs are functional as shown by their ability to stimulate allogeneic donor PBMCs in the MECLR with just 500 DCs driving the reaction. The functional capacity of enzymatically obtained epidermal DCs was previously only used in murine skin models, but not in models with human skin.
 4. The organ bath culture is viable for long enough to study uptake of antigen delivered into the skin and presentation to the T cells by epidermal DCs. This is a novel step in the translation studies, which has an alternative the murine studies that are limited by thinness of the murine skin, making it very difficult to assess delivery devices designed for humans.
 5. This set of experiments showed that both hollow and dry coated microneedles are comparable to standard intradermal 26G needles in targeting epidermal DCs, with some suggestion of superiority in the case of dry microneedles.
-

3.5.1 Skin organ bath culture

Dendritic cells obtained from the epidermal layer of skin explants are most likely Langerhans cells as evidenced by co-expression of unique classifier markers for skin DCs, such as HLA DR, CD1a and langerin. However, after staining with one flowcytometry antibody, expression of langerin is not evident in all DCs. This is maybe caused by membrane deformations in the process of langerin internalization [183], resulting in the unavailability of this particular epitope. Another possibility is the contamination of the sample with langerin(-)

dermal DCs during the epidermal separation process. This is less likely, given that the staining with another antibody indicates langerin expression by most CD1a+, HLA DR+ cells extracted from epidermal sheets.

Another problem encountered with the flowcytometric analysis of this population is the lack of the CD11c surface marker expression expected to be found in this population. It is possible that enzymatic epidermal separation followed by trypsinisation to obtain single cells suspension leads to cleavage of some surface markers, such as CD11c.

It is worth mentioning that the blood samples from the skin donors were not available, hence I did not have opportunity to compare MECLR reactions driven by epidermal APCs to the MLR reaction driven by blood derived APCs from the same individuals. Irrespective, impression was that the proliferation in the MECLR was weaker than what we would normally expect from the standard MLR. Lack of CD11c possibly affecting the function, together with the old age of the skin donors, the possibility of hypoxic injury to the DCs in the *ex-vivo* organ bath culture and previous cryopreservation of the responder PBMCs, can be explanation for the relatively low proliferation in these cultures. However, it has to be kept in mind that epidermal DCs obtained in such a way may also be in immature state and therefore less potent in driving MECLR reactions. Supportive of this explanation is the finding by Steinman et al. that epidermal DCs were able to drive proliferation comparable to splenic DCs only after maturation in culture.[184] Nevertheless, skin organ bath culture provides live and functional DCs suitable for the assessment of the ≤ 24 h long effect of different agents. It is thus a feasible *ex-vivo* prelude to *in-vivo* studies that are limited due to ethical considerations.

3.5.2 Targeting the right skin DCs

It is important to deliver the peptide for PIT in the optimal, minimally invasive way, to the correct antigen presenting cells that should be in the immature state and with the potential to transmit tolerogenic signal. The available data suggest that the best candidates for this role are skin Langerhans cells that are densely distributed in the suprabasal epidermis. In addition, their superficial position makes them available for topical immune-modulatory agents aiming to enhance PIT by increasing the tolerogenic potential of DCs without causing systemic effects of both peptide and tolerance enhancer.

I developed the system for the assessment of the delivery to the epidermal DCs, majority of which are LCs. This is expected based on the epidermal separation methodology and evidenced by the phenotype of the cells obtained in such a way.

I assessed hollow microneedles and dry coated microneedle compared to standard hypodermic needle intradermal injection as devices for this purpose. Dissolving microneedles were not considered in this project because of the concern that degraded matrices may exacerbate a pro-inflammatory effect. Delivery of antigens by pre-treatment of the skin to form pores by solid microneedles was also not considered due to difficulties in regards to quantification of antigen dose delivered. Antigen delivery in the liquid state through hollow microneedles allows precise quantification of dose delivered to the skin, whilst the estimated quantity of antigen delivered from the dry microneedle is less than 20% of the coated material. This depends on the solubility of the peptide and the degree of polishing of the needles (Xhao personal communication).

Targeting epidermal DCs was assessed by their ability to present delivered peptide to antigen- specific cloned T cells in the context of the right HLA type. The fact that both types of cloned T-cells were able to present their respective peptides to itself, means that they have ability to react to any free peptide present in the cultures, even in the absence of the HLA matched APCs. Lack of the stimulation of the cloned T-cell by the APCs originated from the HLA mismatched donors, indicated that there was no free or bound peptide in the cultures, as these cells were not able to capture and retain peptide after insertion into the skin, and any free peptide would have been eliminated during the washing procedures for the generation of single cell suspension. On the other hand, APCs of the right HLA type, captured *ex vivo* delivered peptide, retained it despite number of washing procedures, effectively presented it and stimulated cloned T cells.

The problem with experiments involving cloned T cells was variability of their sensitivity to respective peptides as evidenced by wide range of production of signature cytokines (IFN γ or MIP1- β). Clones had to be kept in an activated state to be ready for the unpredictable availability of skin samples (all skin samples were processed and used the same day without cryopreservation). That required maintaining the clones in the culture for many weeks, which may have led to loss of sensitivity. Also, cloned T cells were presented with peptide loaded DCs in various stages of activation of the T cells in their cycle ranging from 7 to 17 days from initial stimulation. The use of stimulation index i.e. normalization to untreated samples helped to overcome this problem to a certain extent and reduced large discrepancy between donors.

Data comparing FP1 peptide delivery by hollow microneedles to the standard intradermal delivery by 26G needles did not show any convincing difference between those two devices. Although the length of the microneedles should allow delivery in close proximity to the epidermis, the “jet” effect from the volume insertion is more likely to displace peptide solution deeper in the dermis. However, some presentation by epidermal DCs was detected with both devices. It is likely that FP1 peptide solution reached the epidermis through “flush back”, which was facilitated by the hydrophilic nature of this peptide (23% of hydrophilic residues, 38% of hydrophobic residues, 38% other residues; Peptide property calculator, GenScript, USA). The degree of “flushback” may be dependent on peptide solubility.

The use of FP1 specific cloned T-cells was limited by the rarity of the HLA DR1 type (1 in 9 people in general population) [185] to which this clone is restricted. This demanded screening of a large number of already limited skin donors. For this reason, I decided to use different cloned T-cells, specific for EBVP1 peptide, but restricted to class I HLA-A2 with 50% of individuals being carriers of this type.

Data comparing EBVP1 peptide delivery by dry coated microneedles to the standard intradermal delivery by 26G needles showed exclusive presentation when peptide was delivered in the right HLA context.

The data suggested that dry coated microneedles with the 500µm long projections are capable of targeting epidermal DCs. Although there was no difference to standard 26G needle delivery when comparable peptide dose

was injected in the skin explant of the same donor, comparison to HLA-A2 negative donors is suggestive of more efficient delivery via microneedles.

When higher dose was delivered via 26G needles, there was a trend of higher stimulation of cloned T cells, although numbers were small to draw any meaningful conclusions. However, with less than 20% of peptide delivered during skin insertion, efficacy of the delivery of this particular peptide from dry coated microneedle is low and represents a disadvantage, due to the possible influence of the individual properties of the skin, including the age of the recipient, which was not tested in this system. The explanation may be that EBVP1 is very hydrophobic peptide with 67% hydrophobic uncharged residues, 0% hydrophilic and 33% other residues (Peptide property calculator, GenScript, USA), which makes diffusion of the peptide to the tissue more difficult. This may not be an issue with other more hydrophilic peptides, such as proinsulin derived C19-A3 peptide, which is currently in clinical trial delivered via standard 26G needle. Another way to increase the quantity of peptide delivery from the microneedle is the use of arrays with larger number of needles that will allow a higher starting amount of peptide.

Overall conclusion from this set of experiments is that both hollow and dry coated microneedles are comparable to standard intradermal 26G needles in targeting epidermal DCs, with some suggestion of superiority in the case of dry microneedles. An additional advantage for the use of dry microneedles comes from the findings that they are less invasive and less painful delivery devices [186, 187] that offer the possibility of self-administration by patients [188], which is important advantage where there is a need for a chronic administration. Effect on pain is related to the reduction of depth of the

insertion and absence of the injected volume with the solid microneedles. In addition, solid microneedles potentially deliver more to the epidermal DCs than to the dermal. To further assess this speculation, the model should be developed to isolate dermal DCs from the skin bath culture and compare it to their epidermal counterparts. Taken together, these findings suggest that dry coated microneedles are potentially optimal delivery device for peptide immunotherapy. Future work will focus on increasing efficacy of delivery and the actual application in the administration of peptide immunotherapy in Type 1 diabetes.

This is a model that enables the *ex vivo* study of the antigen delivery and consequent uptake and presentation by skin DCs that offer excellent surrogate for the *in vivo* conditions, with obvious limitations discussed above, but without drug-related ethical considerations. That allows rapid assessments of the effect of various antigens delivered via different devices, which can be used as a robust step in translating novel therapies to clinic.

Chapter 4 ENHANCEMENT OF TOLEROGENIC ENVIRONMENT IN PREPARATION FOR PEPTIDE IMMUNOTHERAPY

4.1 Introduction

4.1.1 Role of DCs in maintaining tolerance to self-antigens

Dendritic cells (DCs) are professional antigen presenting cells, seen as a bridge between innate and adaptive immunity. They have a crucial role in the defense against 'foreign', but at the same time they patrol around the body, take-up and present peptides from dying cells and other self-antigens, maintaining tolerance to 'self'. [180] In the attempts to understand the intriguing mechanisms allowing this balance, two different opinions predominate. [189] One favours tolerogenic DC lineages such as CD8⁺ conventional DCs [190, 191] and plasmacytoid DCs. [191] Another emphasizes maturation of DCs as an important control point that propels DCs on the road of inflammation as opposed to tolerance. Possibility to modulate maturation of the DCs and affect self-antigen presentation and the autoimmune process, has been an important research focus.

4.1.1.1 Dendritic cells in immune defense

Upon encounter with the microbial agent, DCs mature through activation of Toll-like receptors [192] and TNF α receptors and CD40 ligand [193]. As a result, DCs increase expression of class II MHC [194], co-stimulatory molecules, such as CD80 and CD86 [195, 196], and increase production of growth factor IL-2 [197], chemokines [198] and cytokines, such as IL-12. [199] These phenotypic and functional changes render DCs capable of triggering pro-inflammatory immune response and efficient defense.

4.1.1.2 Dendritic cells in tolerance

On the other side, there is ample evidence to suggest capacity of DCs to induce T cell tolerance through generation of Tregs (Chapter 1). IL-10, TGF- β or IL-35 secreted by DCs are strongly implemented in this process.[200] *In vitro* data suggest that immature, monocyte-derived DCs are weak initiators of immunity, but when co-cultured with allogenic T-cells, they make them refractory to antigenic stimulation. This effect is partially blocked by anti-IL-10 antibodies, suggesting generation of Tr1 cells.[201] One of the proposed mechanisms through which immature DCs achieve suppression is low expression of MHC molecules and co-stimulatory factors.[202] Also, it has been suggested that suboptimal antigen presentation, together with increased indolamine 2,3-dioxygenase expression (IDO) by DCs leads to inhibition of T cell proliferation.[55] Another molecule, immunoglobulin-like transcript 3 (ILT3) works as an immune inhibitory receptor. It is selectively expressed on dendritic cells, and some other cells such as monocytes and macrophages. The extracellular domain of ILT3 binds to the T cells, sending inhibitory signals.[203] On the other hand, T cells, in particular Tregs can affect dendritic cells. LAG-3, transmembrane CD4-related protein that is expressed by Tregs upon activation, binds MHC class II on the APCs, modulating its function towards suppression.[204]

Considering the key role of DCs in the induction and activation of both effector T cells and Tregs, it is no surprise that discrepancies in DCs number, phenotype and function have been linked to pathogenesis of autoimmune diseases.[205, 206] It is encouraging that immuno-modulating therapies in

multiple sclerosis, for example, have been shown to restore DCs phenotype and function in non-specific manner.[206]

4.1.2 Pharmacological modulation of DCs to enhance tolerance

A number of authors have reported pharmacological modulation of DCs to enhance their tolerogenic potential.[207] Agents used include rapamycin, vitamin A, growth factors such as G-CSF, VEGF, VIP, cytokines such as IL-10 and hormones such as vitamin D and glucocorticoid (GC) dexamethasone.[208] *In vitro* IL-10 primed DCs showed tolerogenic profile and low T-cell activation properties, as well as generation of Tregs that strongly suppressed T cell reactivity [209] [32]

4.1.2.1 Vitamin D and dexamethasone as immunomodulating agents

In vitro and animal studies

Amongst listed, most commonly *in vitro* and *in vivo* studied agents are vitamin D3 and dexamethasone.

Vitamin D3 is known for its immunomodulating capacities that are mainly attributed to its action on DCs.[210, 211] Vitamin D3 primed DCs (vitD3-DCs) have stable immature phenotype featuring low expression of CD80, CD86 and CD40, as well as CD1a, CD83 and MHC class II.[212, 213] They produce IL-10 instead of IL-12 in the cultures. VitD3-DCs are able to prevent priming of naïve CD4 or CD8 T cells, induce apoptosis of effector T cells and induce antigen-specific Tregs from naïve T cells.[214, 215] There are several proposed mechanisms to explain these immunosuppressive effects. VitD3-DCs express high level of PDL1, which leads to low expression of co-stimulatory molecules and higher production of IL-10. This may be crucial in

inducing Tregs from naïve CD4⁺ cells.[215] There is evidence from another study that vitD3-DCs induce Tregs through increase in DCs IDO expression.[216]

Dexamethasone modulated DCs (dex-DCs) share the similar phenotype and functional status favoring induction of IL-10 producing cells over IFN γ producing cells.[215, 217-220] However Tregs generated with dexamethasone show features of IL-10 producing Tr1 and suppress in non-specific, bystander fashion, whilst effects of vitamin D3 are antigen-specific.[215]

When used combined, dexamethasone and vitamin D3 showed similar results as either agent alone [221], but retained antigen-specific suppression, which is the feature of vitD3-DCs. Other study suggested that Tregs induced by vitD3-DCs alone [222] and vitD3/dex-DCs [223] are more likely to generate Tr1 type Tregs. Direct killing of effector T cells is another possible mechanism of action of vitD3-DCs[212] and vitD3/dex-DCs.[224]

Variety seen between different studies can be attributed to difference in many factors, such as type and dose of the modulating agent and experimental conditions, but it seems that DCs have array of action modalities and their disposal that can be used depending on the environment.

Human studies

Systemically administered and inhaled glucocorticoids (GC) in patients with asthma are shown to increase circulating Tregs.[225] The similar results were repeated in several small studies on different autoimmune diseases [226-229], with one indicating that addition of vitamin D3 to GC improved outcome in

steroid resistant asthma.[229] However, large study involving over 50 patients, on effect of GC with and without vitamin D3 on asthma failed to show beneficial effect of adjuvants to specific-immunotherapy [230], as did the study looking at effect of systemic steroids in healthy individuals. [231]

Discrepancy in the results can be explained by heterogeneity of studied populations and difficulties in defining and monitoring target antigen presenting cell population and Treg population in blood.

4.1.2.2 Pharmacological modulation of skin dendritic cells

Vitamin D3 and steroids

As discussed in Chapter 1, skin is preferable route for administering antigen-specific immunotherapy (ASI) due to the abundance of DCs that are easily accessible both by antigens and modulating agents. Mode of antigen delivery as a way of promoting DC tolerance was discussed in Chapter 3. Here I discuss possibilities of pharmacological modulation of skin DCs through local administration of agents.

There is evidence from murine models that antigen-specific therapy administered subcutaneously (s.c.) was more effective when given in combination with s.c. dexamethasone.[232] However, subcutaneous way of delivery is more likely to achieve systemic effects due to proximity of skin vasculature. Authors went on to show that s.c. dexamethasone, as a tolerogenic adjuvant to immunotherapy, enriches CD11c low CD40 low macrophages in blood, which was suggestive of a systemic effect. [233]

The success of topical vitamin D3 in the treatment of T-cell mediated skin disease, psoriasis, is supportive of the concept of targeting local immune cells. It seems that when vitamin D3 is applied locally into the mouse skin, as an adjuvant to vaccine formulations, it targets skin DCs.[234] The Immunomodulatory effect of vitamin D3 in the skin is dependent on a subset of DCs. Whilst Langerhans cells (LCs) pretreated with vitamin D3 induce Foxp3⁺ Tregs in TGFβ dependent fashion, dermal DCs (DDCs) promoted Foxp3⁻ IL10⁺ Tregs, effect dependent on IL-10, despite comparable expression of vitamin D receptor between two subsets. [235]

IL-10

When administered to the skin explants, another modulating agent, IL-10, favoured migration of immature dermal DCs with functional qualities conducive to T cell tolerance.[236] This is consistent with recognised role of IL-10 in DCs biology, and encouraging for the approach of the local skin administration of IL-10. The potential limitation to this approach is difficulty in targeting skin DCs and creating IL-10 rich microenvironment in and around skin DCs as opposed to other skin resident cells.

Use of developing gold nanoparticles (NP) technology can overcome this problem. Gold nanoparticles are inert, non-toxic, and can be readily endocytosed by DCs and other phagocytic mononuclear cells.[237, 238] Even non-phagocytic T cells can load up to 10⁴ of these particles per cell.[239] This can significantly enhance uptake of antigens and bioactive molecules attached to them, such as peptides and IL-10 and enable administration of smaller “local immuno-modulating” IL-10 dose without systemic effects recognised when higher doses are used. [240, 241]

4.2 Hypothesis

I hypothesise that preconditioning of the skin DCs with agents such as topical steroid or intradermally injected IL-10 can enhance their tolerogenic responses.

4.3 Aims

1. To study effect of topical steroid pretreatment on tolerogenic potential of skin DCs
2. To study effect of pretreatment of intradermally injected IL-10, alone or attached to gold nanoparticles, on tolerogenic potential of skin DCs.

4.4 Results

4.4.1 Topical steroid treatment

4.4.1.2 Effect of topical steroid (0.05% betamethasone w/w) on cell viability

There was no significant difference in the proportion of live epidermal cells deriving from skin treated with PBS (untreated in further text) and live epidermal cells deriving from skin treated with topical 0.05% (w/w) betamethasone cream for 24h in the organ bath culture at 37°C in an atmosphere of 5% (v/v) CO₂/95% (v/v) (Figure 4-1, Table 4-1). Viability of cells was measured by live/dead marker on flow cytometry (Figure 4-2) and expressed as percentage of live cells out of the total number of cells in the single cell suspension obtained after incubation and as described in Chapter 2.

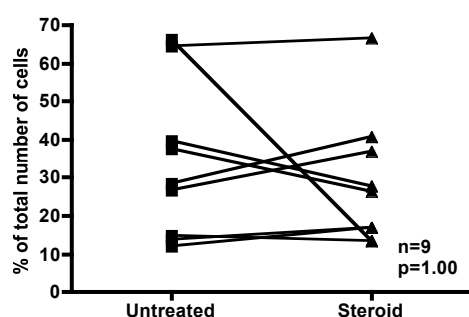


Figure 4-1. Flowcytometric analysis of the viability of epidermal cells with and without topical steroid treatment.

Untreated: % of live epidermal cells deriving from untreated skin. Steroid treated: % of live epidermal cells deriving from skin treated with 0.05% (w/w) betamethasone. Statistical test used: Wilcoxon signed rank test.

	Untreated	Steroid
Exp 1	13.6	16.9
Exp 2	12.1	16.8
Exp 3	66.3	13.3
Exp 4	26.6	36.7
Exp 5	28.3	40.5
Exp 6	39.7	27.6
Exp 7	14.9	13.2
Exp 8	37.6	26.2
Exp 9	64.6	66.7
N	9	9
Mean	33.7	28.7
SD	20.5	17.4

Table 4-1. Flowcytometric analysis of the viability of epidermal cells with and without topical steroid treatment.

Untreated: cells deriving from untreated skin; Steroid: cells deriving from skin treated with 0.05% (w/w) betamethasone; %: percent of live dendritic cells out of the total number of live epidermal cells. N: number of replicates; SD: standard deviation.

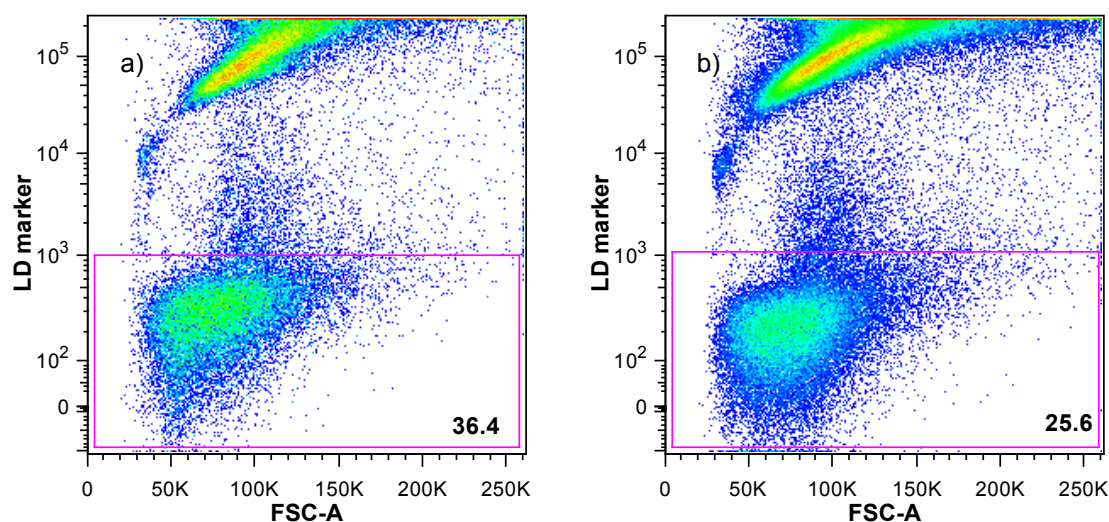


Figure 4-2. Viability of epidermal cells following exposure to the topical steroid treatment, flowcytometric analysis of the representative sample. Epidermal cells negative for live/dead marker (APC-Cy7 channel) were characterised as live cells; LD marker – live/dead marker; FSC-A – forward scatter - area; a) epidermal cells deriving from untreated skin; b) epidermal cells deriving from skin treated with 0.05% (w/w) betamethasone.

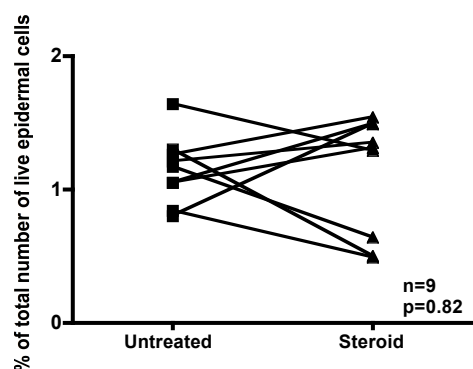


Figure 4-3. Analysis of the proportion of DCs in the epidermal cells solution with and without topical steroid treatment.

Untreated: % of live epidermal cells deriving from untreated skin. Steroid treated: % of live epidermal cells deriving from skin treated with 0.05% (w/w) betamethasone. Statistical test used: Wilcoxon signed rank test.

	Untreated	Steroid
Exp 1	1.05	1.31
Exp 2	0.80	1.49
Exp 3	1.64	1.29
Exp 4	1.30	0.50
Exp 5	1.17	0.64
Exp 6	1.21	1.35
Exp 7	1.05	1.49
Exp 8	0.84	0.49
Exp 9	1.26	1.54
N	9	9
Mean	1.15	1.12
SD	0.25	0.44

Table 4-2. Flowcytometric analysis of the epidermal cells solution with and without topical steroid.

Untreated: cells deriving from untreated skin; Steroid: cells deriving from skin treated with 0.05% (w/w) betamethasone; %: percent of the total number of live epidermal cells. N: number of replicates; SD: standard deviation.

There was no significant difference in the proportion of dendritic cells deriving from untreated skin and dendritic cells deriving from skin treated with topical 0.05% (w/w) betamethasone cream for 24h in the organ bath culture at 37°C in an atmosphere of 5% (v/v) CO₂/95% (v/v) (Figure 4-3, Table 4-2). Dendritic cells were characterized as CD1a⁺, HLA DR⁺ cells in the epidermal single cells suspension (Figure 4-4).

Viability was measured by live/dead marker on flow cytometry and expressed as percentage of live CD1a⁺, HLA DR⁺ cells out of the total number of live cells in the single cell suspension obtained after incubation and as described in Chapter 2. Gating strategy is described in Chapter 2.

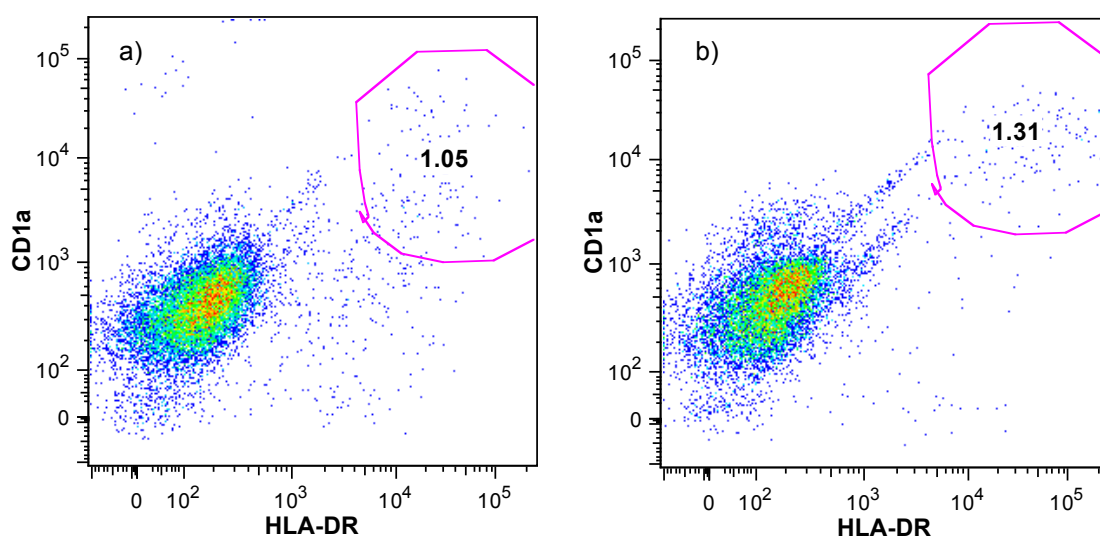


Figure 4-4. Viability of dendritic cells following the exposure to the topical steroid treatment, flowcytometric analysis of the representative sample. CD1a⁺, HLA DR⁺ cells from the live epidermal population were characterised as dendritic cells; a) dendritic cells deriving from untreated skin; b) dendritic cells deriving from skin treated with 0.05% (w/w) betamethasone.

4.4.1.3 Effect of topical steroid on dendritic cells surface markers

Surface markers used for phenotyping of the epidermal dendritic cells are shown in the **Table 4-3**.

Marker	Role
CD11c	Adhesion molecule, binds fibrinogen
CD1a	MHC class I like molecule, has specialised role in presentation of lipid antigens
CD207 Langerin	C-type lectin, uptake of foreign antigens
CD40	Binds CD40L (CD154), co-stimulatory molecule required for the activation of APCs
CD80	Co-stimulator, ligand for CD28 and CTLA-4
CD83	Marker of DCs maturation
CD86	Co-stimulator, ligand for CD28 and CTLA-4
Epcam	Adhesion molecule, connects LCs to the neighboring keratinocytes
HLA-DR	MHC class II molecule

Table 4-3. Surface markers used for the phenotyping of the epidermal DCs

DCs deriving from the skin pre-treated with topical steroid showed significantly lower expression of HLA-DR, expressed as Mean Fluorescent Intensity (MFI), in comparison to DCs from untreated skin (43419 ± 28858 , 23833 ± 15273 , $n=9$, $p=0.0039$) - Figure 4-5, Figure 4-6, Table 4-4.

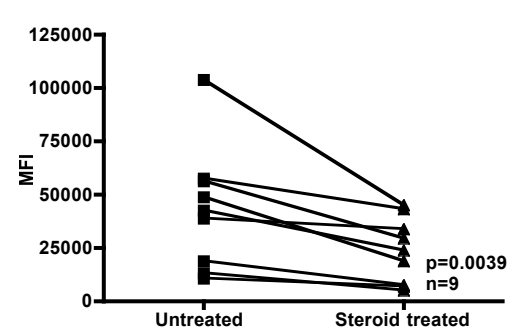


Figure 4-5. HLA DR expression on skin dendritic cells with and without topical steroid treatment. Untreated: dendritic cells deriving from untreated skin; Steroid treated: dendritic cells deriving from skin treated with 0.05% (w/w) betamethasone. MFI: Mean Fluorescent Intensity. Statistical test used: Wilcoxon signed rank test.

	Untreated	Steroid
Exp 1	18690.	7750.
Exp 2	10890.	7230.
Exp 3	104000.	45233.
Exp 4	13250.	5131.
Exp 5	42317.	23989.
Exp 6	48930.	18838.
Exp 7	57420.	42988.
Exp 8	39000.	33841.
Exp 9	56272.	29496.
N	9	9
Mean	43419	23833
SD	28858	15273

Table 4-4. HLA DR expression on skin dendritic cells with and without topical steroid treatment

Untreated: dendritic cells deriving from untreated; Steroid: dendritic cells deriving from skin treated with 0.05% (w/w); MFI: Mean Fluorescent Intensity, expressed in W/m²; N: number of replicates; SD: standard deviation.

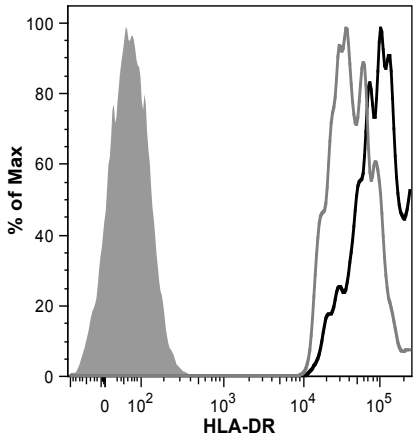


Figure 4-6. HLA DR expression on skin dendritic cells with and without topical steroid treatment, flowcytometric analysis of the representative sample. Expression of HLA DR (PerCP-Cy 5.5 channel) on the dendritic cells deriving from untreated skin (black lines) and skin treated with 0.05% (w/w) betamethasone (dark gray lines). Unstained sample used as control (solid gray).

Total steroid treatment induced significant reduction in the expression CD80 co-stimulatory marker (Figure 4-7, Figure 4-8, Table 4-5), whilst there was no significant reduction in the expression of other tested co-stimulatory markers CD86 (Figure 4-9, Table 4-6), CD83 (Figure 4-10, Table 4-7) and CD40 (Figure 4-11, Table 4-8).

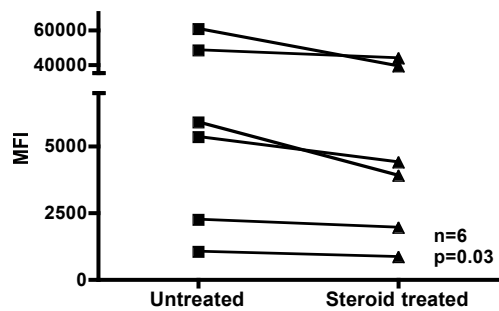


Figure 4-7. CD80 expression on skin dendritic cells with and without topical steroid treatment.

Untreated: dendritic cells deriving from untreated skin; Steroid treated: dendritic cells deriving from skin treated with 0.05% (w/w) betamethasone. MFI: Mean Fluorescent Intensity; Statistical test used: Wilcoxon signed rank test.

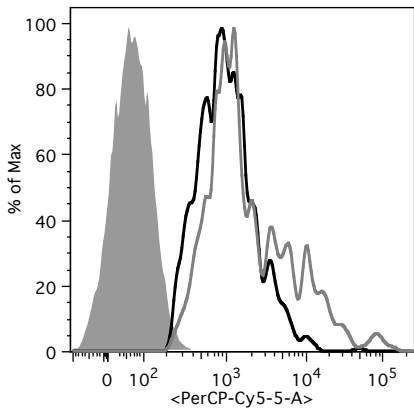


Figure 4-8. CD80 expression on skin dendritic cells with and without topical steroid treatment, flowcytometric analysis of the representative sample.

Expression of CD80 (PerCP-Cy 5.5 channel) on the dendritic cells deriving from untreated skin; (black lines) and skin treated with 0.05% (w/w) betamethasone (dark gray lines). Unstained sample used as control (solid gray).

	Untreated	Steroid
Exp 1	5905.	3924.
Exp 2	5366.	4427.
Exp 3	1034.	841.
Exp 4	2256.	1950.
Exp 5	48084.	44007.
Exp 6	60554.	39095.
N	6	6
Mean	3640	2786
SD	2368	1680

Table 4-5. CD80 expression on skin dendritic cells with and without topical steroid treatment.

Untreated: dendritic cells deriving from untreated skin; Steroid: dendritic cells deriving from skin treated with 0.05% (w/w); MFI: Mean Fluorescent Intensity, expressed in W/m²; N: number of replicates; SD: standard deviation

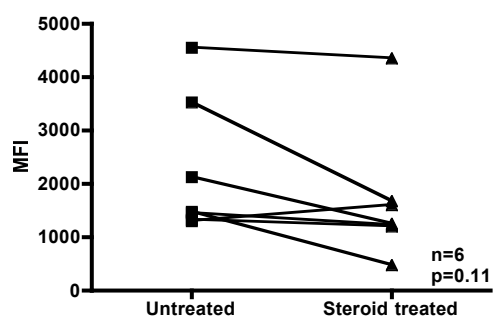


Figure 4-9. CD86 expression on skin dendritic cells with and without topical steroid treatment.

Untreated: dendritic cells deriving from untreated skin; Steroid treated: dendritic cells deriving from skin treated with 0.05% (w/w) betamethasone. MFI: Mean Fluorescent Intensity. Statistical test used: Wilcoxon signed rank test.

	Untreated	Steroid
Exp 1	1452.	1238.
Exp 2	1322.	1206.
Exp 3	1476.	491.
Exp 4	3535.	1691.
Exp 5	4560.	4356.
Exp 6	1297.	1611.
Exp 7	2118.	1256.
N	7	7
Mean	2251	1693
SD	1292	1237

Table 4-6. CD86 expression on skin dendritic cells with and without topical steroid treatment.

Untreated: dendritic cells deriving from untreated skin; Steroid: dendritic cells deriving from skin treated with 0.05% (w/w); MFI: Mean Fluorescent Intensity, expressed in W/m²; N: number of replicates; SD: standard deviation.

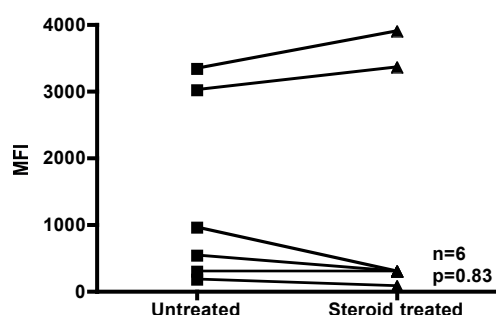


Figure 4-10. CD83 expression on skin dendritic cells with and without topical steroid treatment.

Untreated: dendritic cells deriving from untreated skin; Steroid treated: dendritic cells deriving from skin treated with 0.05% (w/w) betamethasone. MFI: Mean Fluorescent Intensity. Statistical test used: Wilcoxon signed rank test.

	Untreated	Steroid
Exp 1	3025.	3356.
Exp 2	3348.	3911.
Exp 3	180.	92.
Exp 4	307.	298.
Exp 5	965.	294.
Exp 6	548.	296.
N	6	6
Mean	1396	1375
SD	1417	1760

Table 4-7. CD83 expression on skin dendritic cells with and without topical steroid treatment.

Untreated: dendritic cells deriving from untreated skin; Steroid: dendritic cells deriving from skin treated with 0.05% (w/w); MFI: Mean Fluorescent Intensity, expressed in W/m²; N: number of replicates; SD: standard deviation.

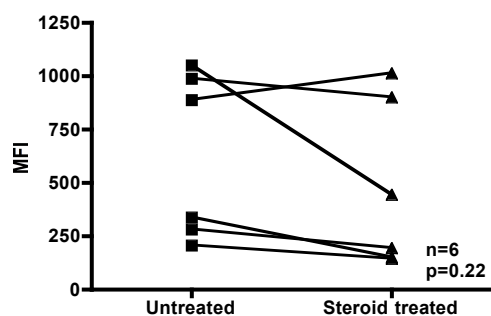


Figure 4-11. CD40 expression on skin dendritic cells with and without topical steroid treatment. Untreated: dendritic cells deriving from untreated skin; Steroid treated: dendritic cells deriving from skin treated with 0.05% (w/w) betamethasone. MFI: Mean Fluorescent Intensity; Statistic test used: Wilcoxon signed rank test.

	Untreated	Steroid
Exp 1	987.0	904
Exp 2	886.0	1012
Exp 3	1051	446
Exp 4	282	197.
Exp 5	340	150
Exp 6	206	144
N	6	6
Mean	625.3	475.5
SD	388.6	391.3

Table 4-8. CD40 expression on skin dendritic cells with and without topical steroid treatment.

Untreated: dendritic cells deriving from untreated skin; Steroid: dendritic cells deriving from skin treated with 0.05% (w/w); MFI: Mean Fluorescent Intensity, expressed in W/m^2 ; N: number of replicates; SD: standard deviation.

4.4.1.4 Effect of topical steroid on skin DCs ability to induce proliferation in Mixed Epidermal Cell Lymphocyte Reaction (MECLR)

Proliferation was expressed as proliferation index (PI), i.e. ratio of proliferation in the MECLR and unstimulated responder PBMCs, in order to correct for background originated from the some degree of the spontaneous PBMCs, often encountered with previously cryopreserved cells. I observed significantly lower proliferation rate measured by ³H thymidine incorporation (cpm) in 5-day long MECLR driven by DCs from steroid treated skin, expressed as PI (8.29 ± 6.35) comparing to the untreated (2.73 ± 1.39) - Figure 4-12, Table 4-9. The average baseline proliferation in the MECLR before steroid treatment was 1636 ± 861 cpm, with the responder PBMCs proliferation of 459.11 ± 463.4 cpm.

There was no proliferation from epidermal cells (untreated: 29.4 ± 10.5 , steroid treated: 49.9 ± 60.7).

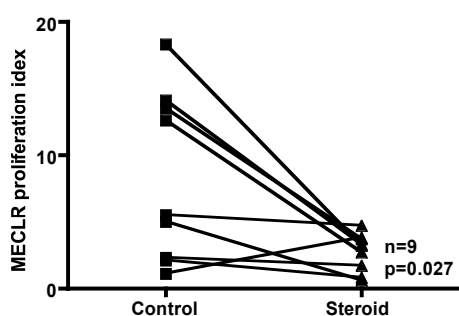


Figure 4-12. Proliferation in MECLR driven by DCs with and without exposure to the topical treatment. MECLR proliferation index (PI): Mixed Epidermal Cells Reaction proliferation/PBMC proliferation ratio; Untreated: MECLR PI driven by dendritic cells deriving from untreated skin; Steroid treated: MECLR PI driven by dendritic cells deriving from skin treated with 0.05% (w/w) betamethasone; Statistical test used: Wilcoxon signed rank test.

	Untreated (PI)	Steroid (PI)
Exp 1	2.12	0.83
Exp 2	5.03	0.62
	14.09	3.33
Exp 4	18.28	3.18
Exp 5	12.62	2.73
Exp 6	13.51	3.68
Exp 7	1.16	3.79
Exp 8	2.34	1.72
Exp 9	5.47	4.70
N	9	9
Mean	8.29	2.73
SD	6.35	1.39

Table 4-9. Proliferation in MECLR driven by DCs with and without exposure to the topical treatment. MECLR proliferation index (PI): Mixed Epidermal Cells Reaction proliferation/PBMC proliferation ratio; Untreated: MECLR PI driven by dendritic cells deriving from untreated skin; Steroid: MECLR PI driven by dendritic cells deriving from skin treated with 0.05% (w/w); N: number of replicates; SD: standard deviation.

Production of Interleukin 10 (IL-10) measured in the supernatants of MECLR reactions showed trend for lower levels in the reactions driven by steroid treated in comparison to untreated DCs, although it was not significantly different (Figure 4-13, Table 4-10). At the same time, the level of Interferon γ (IFN γ) was significantly lower (Figure 4-14, Table 4-11) and IL10/IFN γ ratio significantly higher (Figure 4-15, Table 4-12) in the supernatants of the reactions driven by steroid exposed DCs.

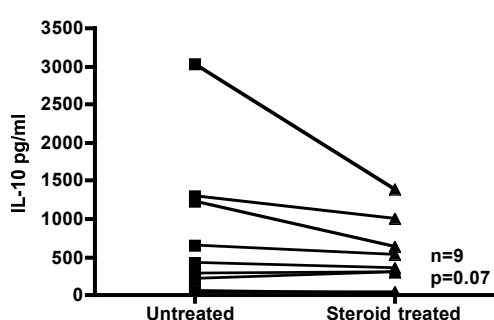


Figure 4-13. IL-10 produced in the MECLRs driven by DCs with and without exposure to the topical treatment. IL-10 – Interleukin 10 produced in the supernatants of MECLRs; Untreated: IL-10 from MECLRs driven by dendritic cells deriving from untreated skin; Steroid treated: IL-10 from MECLRs driven by dendritic cells deriving from skin treated with 0.05% (w/w) betamethasone; Statistical test used: Wilcoxon signed rank test.

	Untreated (IL10 pg/ml)	Steroid (IL10 pg/ml)
Exp 1	415.2	354.5
Exp 2	649.1	534.7
Exp 3	216.2	305.4
Exp 4	291.6	297.6
Exp 5	1238.3	637.6
Exp 6	1294.6	994.2
Exp 7	3040.4	1388.5
Exp 8	56.4	27.7
Exp 9	34.4	31.4
N	9	9
Mean	803.4	507.2
SD	958.5	444.6

Table 4-10. IL-10 produced in the MECLRs driven by DCs with and without exposure to the topical treatment. IL-10 – Interleukin 10 produced in the supernatants of MECLRs; Untreated: IL-10 from MECLRs driven by dendritic cells deriving from untreated skin; Steroid: IL-10 from MECLRs driven by dendritic cells deriving from skin treated with 0.05% (w/w) betamethasone; N: number of replicates; SD: standard deviation.

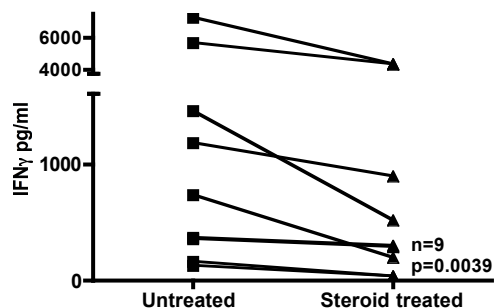


Figure 4-14. IFN γ produced in the MECLRs driven by DCs with and without exposure to the topical treatment. IFN γ – Interferon γ produced in the supernatants of MECLRs; Untreated: IFN γ from MECLRs driven by dendritic cells deriving from untreated skin; Steroid treated: IFN γ from MECLRs driven by dendritic cells deriving from skin treated with 0.05% (w/w) betamethasone; Statistical test used: Wilcoxon signed rank test.

	Untreated (IFN γ pg/ml)	Steroid (IFN γ pg/ml)
Exp 1	153.7	34.2
Exp 2	707.0	193.7
Exp 3	363.3	302.3
Exp 4	352.3	281.9
Exp 5	1438.0	530.6
Exp 6	7288.6	4347.7
Exp 7	5693.0	4378.9
Exp 8	1184.1	893.2
Exp 9	126.0	41.0
N	9	9
Mean	1928	1224
SD	2656	1804

Table 4-11. IFN γ produced in the MECLRs driven by DCs with and without exposure to the topical treatment. IFN γ – Interferon γ produced in the supernatants of MECLRs; Untreated: IFN γ from MECLRs driven by dendritic cells deriving from untreated skin; Steroid: IFN γ from MECLRs driven by dendritic cells deriving from skin treated with 0.05% (w/w) betamethasone; N: number of replicates; SD: standard deviation.

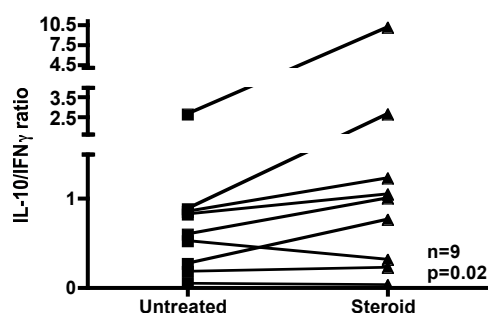


Figure 4-15. IL-10/IFN γ ratio produced in the MECLRs driven by DCs with and without exposure to the topical treatment. IL-10/IFN γ ratio – Interleukin 10/Interferon γ ratio produced in the supernatants of MECLRs; Untreated: IL-10/IFN γ ratio from MECLRs driven by dendritic cells deriving from untreated skin; Steroid treated: IL-10/IFN γ ratio from MECLRs driven by dendritic cells deriving from skin treated with 0.05% (w/w) betamethasone; Statistical test used: Wilcoxon signed rank test.

	Untreated (IL10/IFN γ pg/ml)	Steroid (IL10/IFN γ pg/ml)
Exp 1	2.70	10.36
Exp 2	0.92	2.76
Exp 3	0.60	1.01
Exp 4	0.83	1.06
Exp 5	0.86	1.20
Exp 6	0.18	0.23
Exp 7	0.53	0.32
Exp 8	0.05	0.03
Exp 9	0.27	0.76
N	9	9
Mean	0.76	1.92
SD	0.76	3.11

Table 4-12. IL-10/IFN γ ratio produced in the MECLRs driven by DCs with and without exposure to the topical treatment. IL-10/IFN γ ratio – Interleukin 10/Interferon γ ratio produced in the supernatants of MECLRs; Untreated: IL-10/IFN γ ratio from MECLRs driven by dendritic cells deriving from untreated skin; Steroid: IL-10/IFN γ ratio from MECLRs driven by dendritic cells deriving from skin treated with 0.05% (w/w) betamethasone; N: number of replicates; SD: standard deviation.

To explore this further, I wanted to clarify the mechanism by which steroid pretreatment affects DCs by flow-cytometric and functional assessment of T cell proliferation in response to DC stimulation, in particular focusing on evidence for Treg induction. Epidermal single cell suspension deriving from steroid treated skin from the donor A (untreated skin used as a control) was co-cultured for 14 days with allogeneic donor CD4⁺ naïve T cells (responder B), isolated from PBMCs through positive MACS column separation. The aim was to assess phenotype and the suppression capacity of T cells cultivated in such a way, on proliferation in the fresh co-culture of epidermal cells and PBMCs (the same pair of donors as the original culture). However, three replicates of this protocol resulted in low number of harvested cells insufficient to drive MECLR or to be analysed by flow cytometry. The conclusion was that DCs obtained from human skin explants are not potent enough to drive the reactions necessary for this experiment.

Instead, I used single epidermal cell suspension obtained from epidermal sheets generated through suction blister method (courtesy of Dr Alhadjali), following four day long *in vivo* topical steroid treatment of one arm, whilst the other arm was left untreated. Epidermal sheet was enzymatically digested as described with the *ex vivo* skin explants and the same suppression protocol was followed as described above and in the Chapter 2.

Representative example of the flowcytometric analysis of the cells obtained after 14 days of the incubation period is presented in the Figure 4-16.

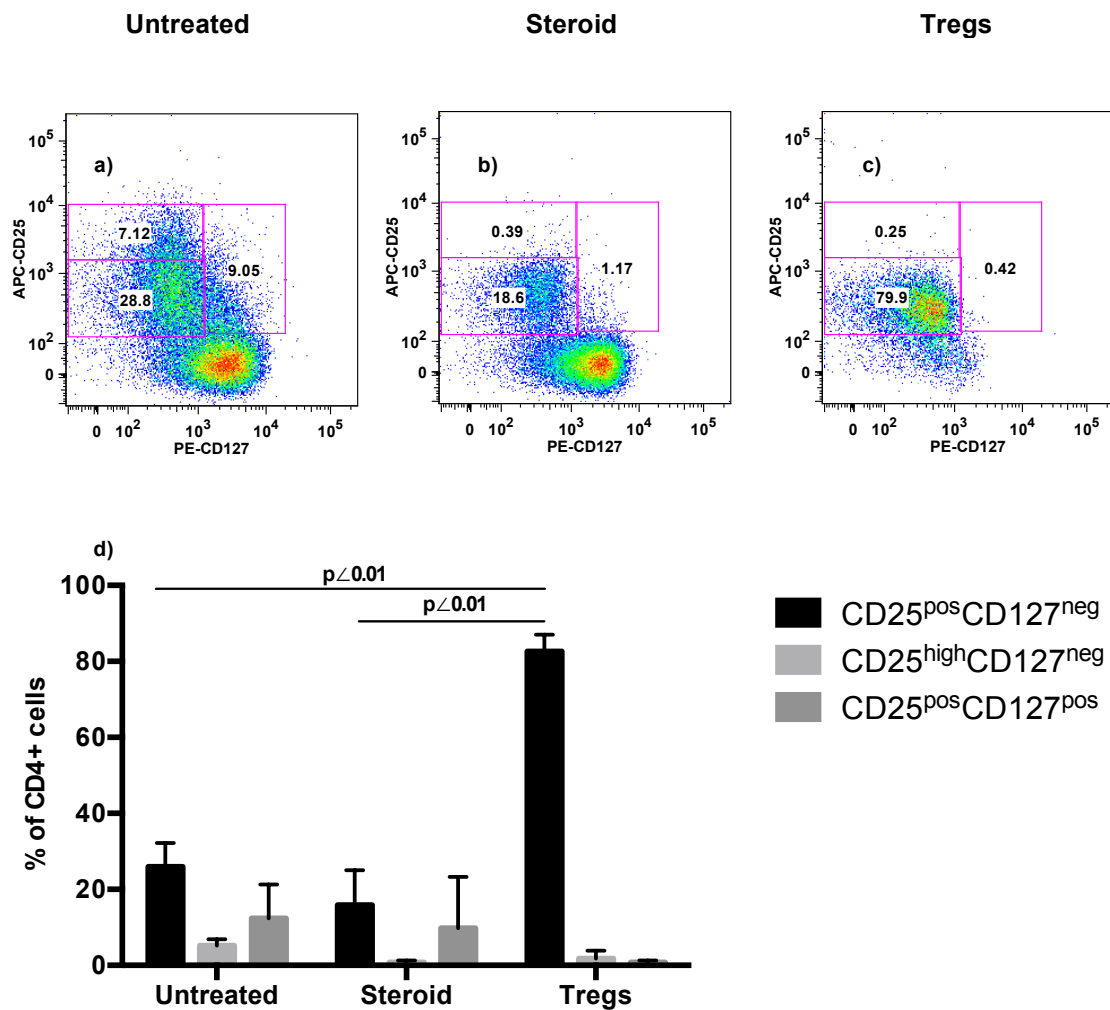


Figure 4-16. Representative example of the flowcytometric analysis of the cells harvested after 14 days long incubation of the epidermal cells suspension (with and without *in vivo* steroid pre-treatment) and the allogeneic responder CD4+ naïve T cells. Cells were gated on the live CD3+, CD4+ population. CD127 and CD25 staining is shown. a) harvest after stimulation by untreated epidermal cells; b) harvest after stimulation by steroid treated epidermal cells (*in vivo* exposure); c) CD127^{low}CD25^{pos} T cells extracted from the responder PBMCs through MACS separation; d) summary of the findings from 3 different cultures, expressed as the percentage of the CD4+ cells. Statistical test used: One-way ANOVA with multiple comparison post-test.

I assessed proliferation of the responder naïve T cells (responder B) stimulated in the MLR type cultures driven by blood derived APCs (irradiated PBMCs) from the original skin donor, donor A and compared it to the proliferation in the same donor-responder culture, but with added T cells harvested from the 14 days long incubation period with epidermal cells with (Ts) and without (Tc) *in vivo* steroid exposure. I observed higher proliferation in the cultures with added T cells (Tc and Ts) in comparison to the baseline MLR, with the trend towards higher proliferation in the culture with the Tc than Ts - Figure 4-17a.

IFN γ and IL-10 measured in the supernatants of these reactions showed similar pattern of higher levels in the cultures supplemented with Tc in comparison to Ts - Figure 4-17 c and d.

As a control, I used suppression capacity of the responder Tregs (defined as CD4⁺CD25^{pos}CD127^{low} T cells). In the two replicates, I only observed trend towards suppression when higher number of 50x10³ Tregs was used per well - Figure 4-17 b.

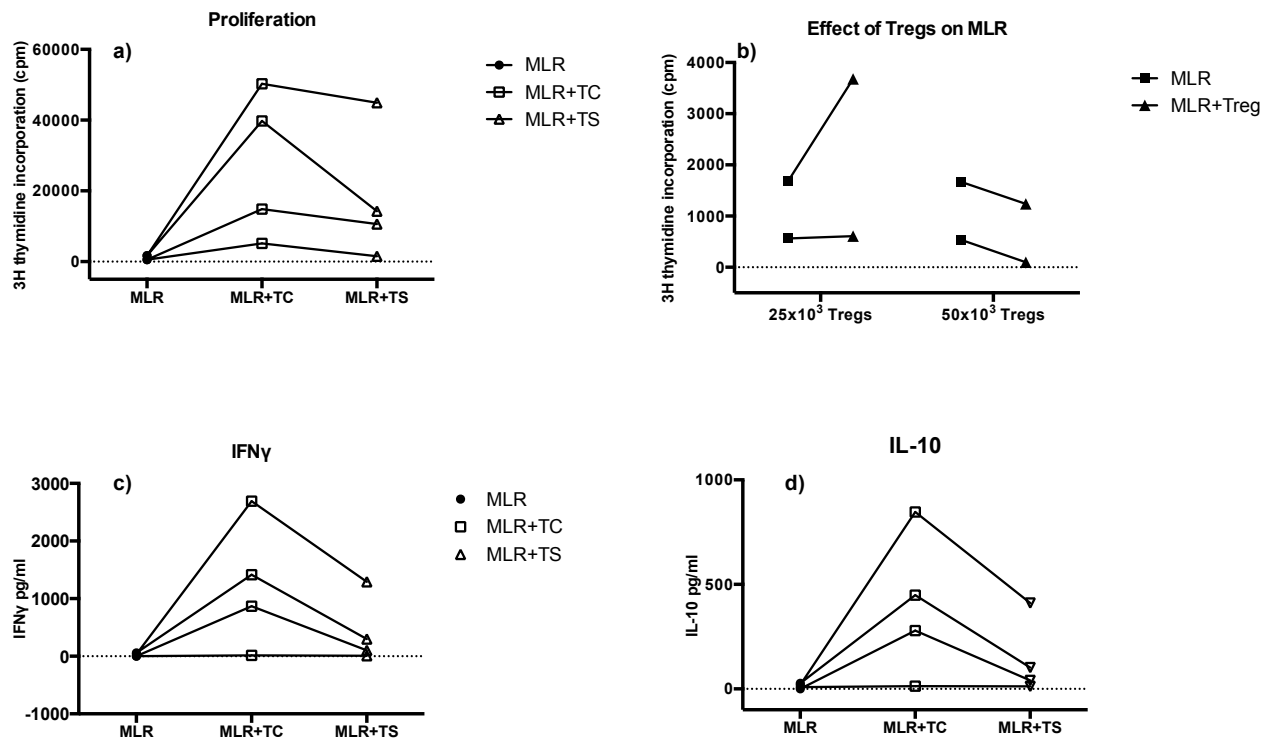


Figure 4-17. Effect of Tcells pre-stimulated by steroid exposed and untreated epidermal DCs, on proliferation and cytokine production. a) effect on proliferation; b) effect of Tregs used as a control; c) effect on IFN γ production; d) effect on IL-10 production. MLR – Mixed lymphocyte reaction; Tc – T cells originated from the culture stimulated by untreated epidermal cells; Ts – T cells originated from the culture stimulated by steroid treated epidermal cells; Tregs – CD4⁺ CD25⁺ CD127⁺ – T cell from responder B. Statistical test used: One-way ANOVA with multiple comparison post-test, no significant differences were observed.

4.4.2 Effect of IL-10

4.4.2.1 Effect of *in vitro* added IL-10 on Mixed Lymphocyte Reaction

Pure IL-10 (IL-10^p) and IL-10 non-covalently attached to the gold nanoparticles (NP IL-10) was added to MLR cultures to compare their capacity to reduce proliferation. [242]

Addition of both IL-10^p (Figure 4-18 a, Table 4-13) and NP IL-10 (Figure 4-18 b, Table 4-13) caused trend towards reduction of proliferation, proportional to the increasing IL-10 concentration.

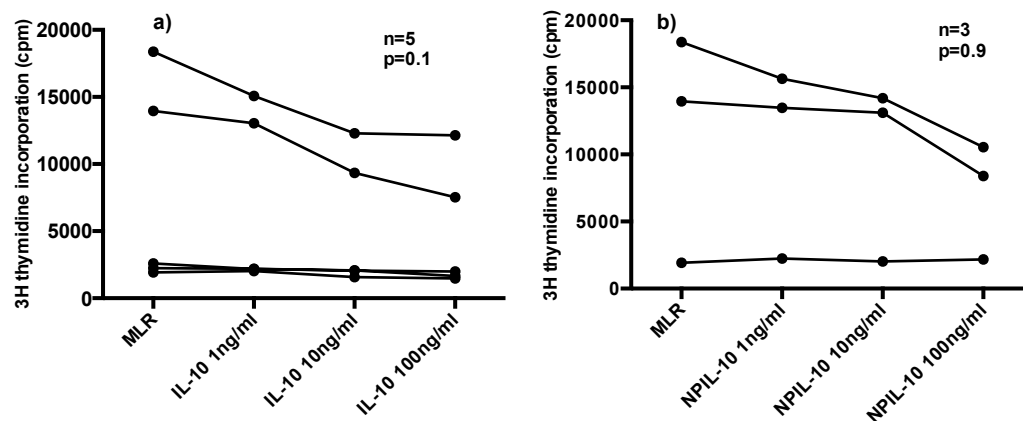


Figure 4-18. *In-vitro* effect of IL-10 on proliferation in MLR. MLR-proliferation without added IL-10; IL-10 1-100 ng/ml – proliferation with 1-100 ng/ml of IL-10 added in the culture; Statistical test used: Repeated measures ANOVA. a) effect of IL-10^p b) effect of NPIL-10. Each line represents data from the same donor-responder combination.

	IL-10 ^p 3H thymidine incorporation (cpm)	Reduction (%)	NPIL-10 3H thymidine incorporation (cpm)	Reduction (%)
rPBMc	568.0±291.8		571.3±375.2	
dPBMc	100.1±63.9		57.6±37.1	
MLR	7821±7779		11421±8509	
IL-10 1 ng/ml	6902±6576	11.75	10458±7193	8.4
IL-10 10 ng/ml	5466±5000	30.11	9776±6733	14.4
IL-10 1 ng/ml	6902±6576	11.75	10458±7193	8.4

Table 4-13. *In-vitro* effect of IL-10 on proliferation in MLR. MLR-proliferation without added IL-10; IL-10 1-100 ng/ml – proliferation with 1-100 ng/ml of IL-10 added in the culture; reduction – reduction of proliferation with increasing concentration of IL-10 in comparison to MLR without added IL-10, expressed in %.

When IFN γ concentration from the supernatants of these reactions was measured, only IL-10^p induced significant reduction of IFN γ , whilst only trend towards reduction was observed with NP IL-10 (Figure 4-19, Table 4-14).

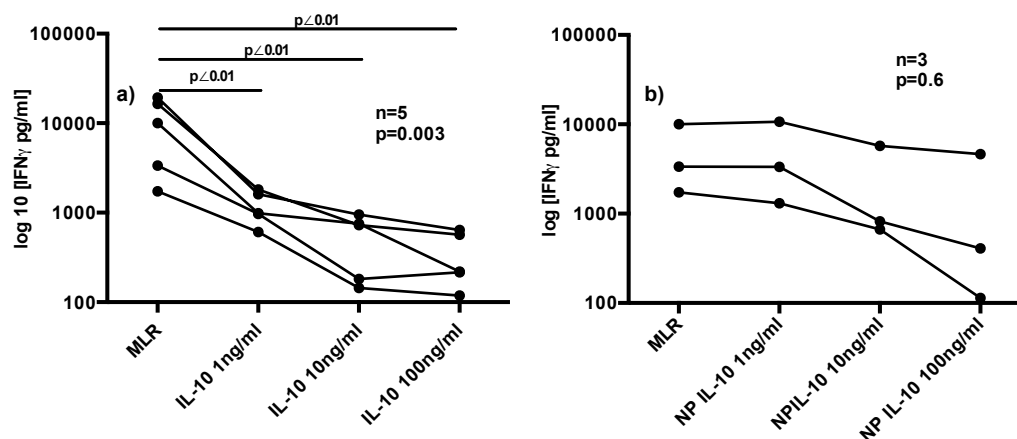


Figure 4-19. *In-vitro* effect of IL-10 on IFN production in MLR. MLR-proliferation without added IL-10; IL-10 1-100 ng/ml – proliferation with 1-100 ng/ml of IL-10 added in the culture; Statistical test used: Repeated measures ANOVA. a) effect of IL-10^p b) effect of NPIL-10. Each line represents data from the same donor-responder combination.

	IL-10 ^p IFN γ (pg/ml) mean \pm SD	Reduction (%)	NPIL-10 IFN γ (pg/ml) mean \pm SD	Reduction (%)
rPBMC	0 \pm 0		0 \pm 0	
dPBMC	7.5 \pm 16.7		12.4 \pm 21.5	
MLR	10175 \pm 7749		5046 \pm 4400	
IL-10 1 ng/ml	1198 \pm 500.5	88.2	5103 \pm 4915	-1.1
IL-10 10 ng/ml	552.2 \pm 366.6	94.6	2410 \pm 2888	52.2
IL-10 100 ng/ml	351.9 \pm 234.4	96.5	1724 \pm 2538	65.8

Table 4-14. *In-vitro* effect of IL-10 on IFN γ production in MLR. MLR-proliferation without added IL-10; IL-10 1-100 ng/ml – proliferation with 1-100 ng/ml of IL-10 added in the culture; reduction – reduction of proliferation with increasing concentration of IL-10 in comparison to MLR without added IL-10, expressed in %.

When anti-IL-10 was added in the cultures containing NP-IL-10, effect on proliferation and to some extent, IFN γ concentration was reversed, in comparison to the cultures without anti-IL-10 previously presented the Figure 4-18 a , Figure 4-19 (Figure 4-20, Table 4-15).

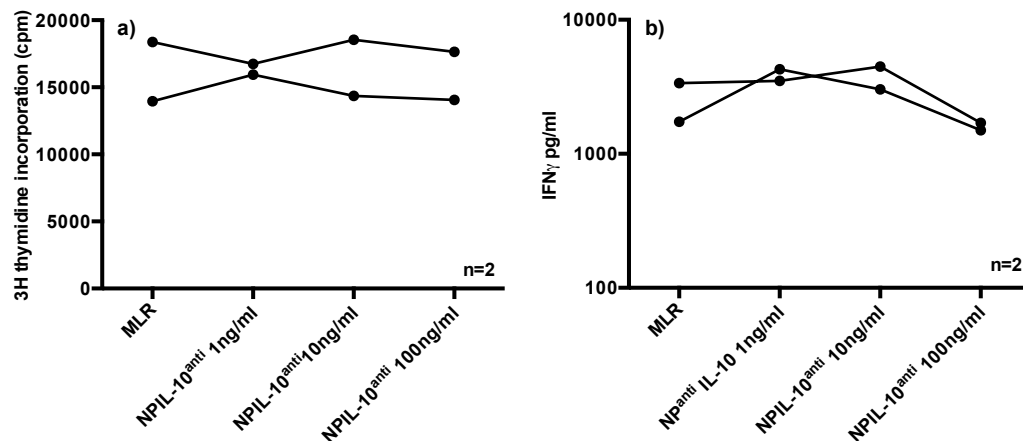


Figure 4-20. *In-vitro* effect of combined NP IL-10 and anti-IL-10 on proliferation and IFN γ production in MLR. MLR-proliferation and IFN γ production without added IL-10; IL-10 1-100 ng/ml – proliferation and IFN γ production with 100-1ng/ml of IL-10 added in the culture; ^{anti}- addition of anti-IL10 into the cultures; a) effect of proliferation in MLR b) effect on IFN γ production in MLR.

	3H thymidine incorporation (cpm)	Reduction (%)	IFN γ (pg/ml) mean \pm SD	Reduction (%)
rPBMc	686.5 \pm 449.5		0 \pm 0	
dPBMc	36.17 \pm 0.26		18.6 \pm 26.4	
MLR	16165 \pm 3125		2551.0 \pm 1151.0	
IL-10 1 ng/ml	16337 \pm 566	1.06	3887 \pm 554	-52.37
IL-10 10 ng/ml	16455 \pm 2957	-1.79	3754 \pm 1024	-47.16
IL-10 100 ng/ml	15852 \pm 2533	1.94	1599 \pm 144	37.32

Table 4-15. *In-vitro* effect of combined anti-IL10 and NP IL-10 on proliferation and IFN γ production in MLR. MLR-proliferation and IFN γ production without added IL-10; IL-10 1-100 ng/ml – proliferation and IFN γ with 1-100ng/ml of IL-10 added in the culture; reduction – reduction of proliferation and IFN γ production with increasing concentration of IL-10 in comparison to MLR without added IL-10, expressed in %.

4.4.2.2 Effect of ex-vivo IL-10 skin injection on Mixed Epidermal Cell Lymphocyte Reaction

On the basis of this proof of principle experiment, I proceeded to examine the effect of locally injected high dose IL-10 in the skin organ bath culture.

50µl of high concentration of 10µg/ml of IL-10 in both IL-10^p and NP IL-10 form and plain NP without IL-10, but with correspondent concentration of gold, was injected into the skin in the organ bath culture. After four hour long incubation, single cell suspension was performed as previously described. The suspension was co-cultured with mismatched PBMCs donors in the MECLR type of the reaction. Proliferation and IFN γ production was expressed as a ratio: modulated MECLR driven by DCs exposed to NP, NP IL-10 or IL-10^p / MECLR driven by untreated DCs. The average baseline proliferation and IFN γ production in the MECLR driven by DCs deriving from the untreated skin was 4659±5140 cpm and 7369±10468 pg/ml, respectively. Proliferation of responder PBMCs was 531.6±297.1 cpm, whilst production of IFN γ from these cells alone was below threshold of detection. Consistently with previous experiments, there was no proliferation or IFN γ production from epidermal cells alone.

Statistically non-significant trend towards reduction of proliferation was observed with IL-10^p only in two out of three donor-responder combinations in the MECLR, whilst reduction of IFN γ was suggestive in both IL-10^p and NP IL-10 modulated reactions in all MECLR (Figure 4-21, Table 4-16).

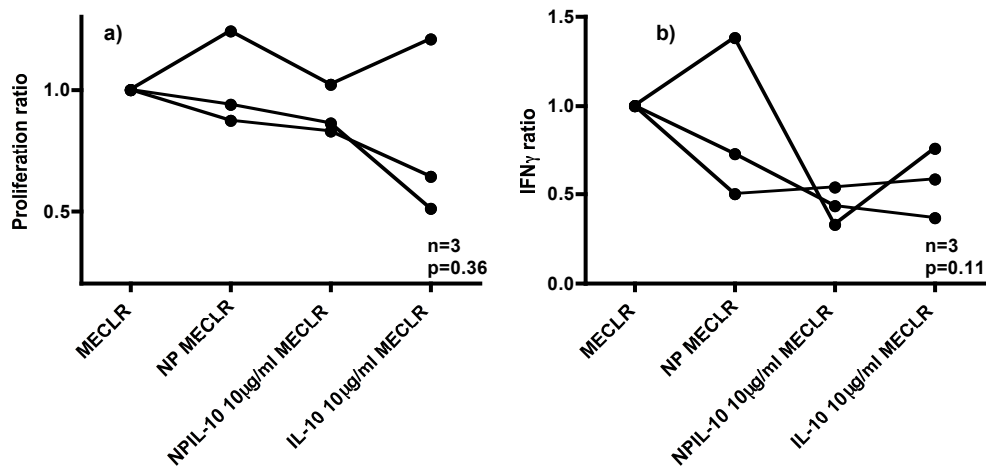


Figure 4-21. Ex-vivo effect of combined NP IL-10 and anti-IL-10 on proliferation and IFN γ production in MECLR. MECLR-proliferation ratio and IFN γ production ratio without added IL-10; NP MECLR - proliferation ratio and IFN γ production ratio in MECLRs driven by DCs exposed to plain NP; NP IL-10 10 μ g/ml MECLR - proliferation ratio and IFN γ production ratio in MECLRs driven by DCs exposed to NP IL-10; IL-10 10 μ g/ml MECLR - proliferation ratio and IFN γ production ratio in MECLRs driven by DCs exposed to pure IL-10^p. Statistical test used: repeated measures ANOVA. a) effect on proliferation ratio in MECLR b) effect on IFN γ production ratio in MECLR. Statistical test used: Repeated measures ANOVA.

	Proliferation ratio	IFN γ ratio
NP MECLR/MECLR	1.02 \pm 0.20	0.87 \pm 0.47
NP IL-10 10 μ g/ml MECLR/MECLR	0.90 \pm 0.10	0.44 \pm 0.11
IL-10 10 μ g/ml MECLR/MECLR	0.79 \pm 0.37	0.57 \pm 0.19

Table 4-16. Ex-vivo effect of combined NP IL-10 and anti-IL-10 on proliferation and IFN γ production in MECLR. NP MECLR/MECLR - proliferation ratio and IFN γ production ratio in MECLRs driven by DCs exposed to plain NP; NP IL-10 10 μ g/ml MECLR/MECLR - proliferation ratio and IFN γ production ratio in MECLRs driven by DCs exposed to NP IL-10; IL-10 10 μ g/ml MECLR/MECLR - proliferation ratio and IFN γ production ratio in MECLRs driven by DCs exposed to plain IL-10^p.

4.5 Summary of findings

1. Organ skin bath culture is a valuable *ex-vivo* system for studying effect of pharmacological modulation of skin DCs as evidenced by their viability and functional capacity to drive proliferation in MECLR after *ex vivo* application of treatments.
 2. Topical steroid treatment induces changes in the skin DCs responsible for their weaker capacity to activate responder T cells in the MLR type reactions. Although suggestive by the *ex vivo* model, *in vivo* data are less supportive of protolerogenic effects. Instead, generally weaker activation signal is more likely explanation for this phenomenon. This is in agreement by reduced expression of HLA-DR and some of the co-stimulatory molecules on skin DCs following *ex-vivo* steroid exposure.
 3. IL-10, both in pure and nanoparticle bound form, has a capacity to suppress activity in the MLR type reactions, particularly when assessed by IFN γ production. *In vitro* data are more robust, than the effect of the locally injected IL-10 in the skin organ bath culture, which may be subjects to the optimisation of the dose and duration of the treatment.
-

4.5.1 Effect of topical steroid treatment

Betamethasone cream (0.05% w/w) was chosen as a modulating topical steroid because of its equal potency to dexamethasone, whose ability to induce pro-tolerogenic changes in DCs was reviewed. In addition, our unpublished data suggest that when applied *in vivo*, this formulation has superior pro-tolerogenic effect on skin DCs in comparison to other agents including topical vitamin D3.

Topical steroid pretreatment for 24 hrs modulates skin DCs to express significantly less markers of functional maturity such as class II MHC and co-stimulatory molecule CD80, with a non-significant trend to reduction in CD86, and no change in the expression of CD40 and CD83. The possible explanation for the latter finding would be very subtle differences in individual markers, which does not exclude significant synergistic effect *in vivo*. Another

reason for non-significant reduction observed with some of the markers, is low background expression in otherwise non-inflamed skin.

DCs exposed to steroid pretreatment showed significantly weaker capacity to drive proliferation in MECLR. To support this finding, cytokines produced in these reactions showed a more tolerogenic profile (lower IFN γ production and higher IL10/IFN γ ratio) in MECLR driven by steroid exposed DCs comparing to control DCs. Important finding is that steroid affected mainly pro-inflammatory cytokine IFN γ , with no significant change of IL-10, though there was a trend in this direction.

To explore this further, I wanted to clarify the mechanism by which steroid pretreatment affects DCs, by studying phenotype and the suppression capacity of T cells cultivated after stimulus from steroid treated and untreated epidermal DCs, in particular focusing on evidence for Treg induction. However, three replicates of this protocol resulted in low number of harvested cells insufficient to drive MECLR or to be analysed by flow cytometry. The conclusion was that DCs obtained from human skin explants are not potent enough to drive the reactions necessary for this experiment. The potential reasons for this are: old age of skin donors, hypoxic injury to the DCs in the *ex-vivo* organ bath culture and injury to the DCs through enzymatic preparation of a single cell suspension.

To further develop this protocol, I used epidermal cells originated from the epidermal sheets generated through suction blister after four-day long *in vivo* application of the topical steroid. Idea was that DCs obtained in such a way are more viable and hence, more suitable to drive the reactions. I did not

observe suppression effect of T cells cultivated in such a way on baseline MLR, assessed by proliferation measured by ³H thymidine incorporation and production of IFN γ and IL-10 in the supernatants. The proliferation in the all baseline MLRs was low, most likely because of the low number of the responder naïve T cells (25×10^3 per well) in comparison to the usual number of 200×10^3 PBMCs in the standard MLR. Although, low starting point represented difficulty for observing further suppression, addition of the sufficient number of Tregs, used as a control, showed trend towards suppression.

In addition, flow cytometric analysis of the cultured T cells population, showed that only 20-30% of cells had Treg phenotype (CD25^{high}, CD127^{low}), which further reduced their probability to exhibit suppression. It is worth mentioning the possibility that some of these cells are simply activated T cells, not Tregs as such.

Probably the most important finding from this set of the experiments is the difference between proliferation in the cultures with added T cells stimulated by steroid exposed and untreated APCs. Given the proliferation rate in the baseline MLR, it is clear that this proliferation and cytokine production came from the harvested T cells upon second encounter with stimulator APCs (first time epidermal derived, second time blood derived). Generally lower proliferation in the steroid cultures together with lower IFN γ and IL-10 production, raises the possibility that steroid exposed DCs had lower ability to prime responder naïve T cells, which resulted in the weaker proliferation and cytokine production upon second stimulation with the same donor APCs.

Although *ex-vivo* model showed that topical steroid treatment induced phenotypic and functional changes in skin DCs supportive of their modulation into pro-tolerogenic profile, functional assays using DCs conditioned by *in vivo* topical steroid are suggestive of weaker activation signal coming from steroid exposed DCs, rather than induction of tolerance.

It is open to speculation that steroid administered in such a way and in such a dose and duration, may not be optimal for the tolerance induction. It is also worth mentioning that comparing the effect of the duration of treatment between *ex vivo* (24h) and *in vivo* (4 days) is not reliable due to the lack of circulation in the organ bath model. Future experiments with weaker steroid and titration of the optimal dose and the duration of the treatment are necessary to answer these questions.

4.5.2 Effect of IL-10

Interleukin-10, both pure and non-covalently attached to NP shows suppression of proliferation in MLR and production of IFN γ measured in the supernatants of these reactions. The effect was NP independent, as it could be counteracted by addition of anti IL-10 antibody. Although, IL-10 attached to NP retained its biological effect, IL-10 concentrations needed to achieve comparable suppression were ten fold higher with NP IL-10 than with IL-10^p. It is possible that biological activity of IL-10 is, to some extent altered by the chemical process of particle generation. Another explanation is that nanoparticles became promptly phagocytosed, which shortened the time for IL-10 activity through its extracellular receptors, although this is less likely given non-covalently bound IL-10. In addition, the link of IL-10 to NP might

have been unstable leading to the inaccuracy of the calculation of the free to bound cytokine ratio, making comparison to the free IL-10 even more difficult.

These *in vitro* reactions provided sufficient guidance to proceed with *ex-vivo* experiments on skin explants.

The injected dose of IL-10 was much higher than the injection of 10ng used in similar *ex vivo* models on tolerogenic effect on skin DCs [236], but still significantly lower than the dose that is expected to have systemic effect, for example 8µg/kg IL-10 used for the treatment of Crohn's disease. [241] DCs conditioned by locally injected IL-10^p and NP-IL10 for 4hrs, showed a suggestion of weaker capacity to drive proliferation in MECLR. When IFN γ production in these reactions was measured, the same trend was observed, although in some reactions plain NPs reduced the level of IFN γ as well.

The absence of strong suppression in the *ex vivo* model, previously observed *in vitro*, is most likely to be due to the large individual variation in the response to locally injected IL-10 on the background of a weaker MLR type reaction (MECLR). Other possible explanation is short duration of incubation to allow for the IL-10 effect, given that previous study incubated skin explants for 48h. An insufficient dose of locally injected IL-10 is less likely, as the same study showed effect with much smaller dose. In addition, the problem of the effect of plain NPs could have been solved by simultaneous injection of anti-IL10 antibody.[236] Optimisation of the protocol required a large number of replicates, which was not feasible at this stage due to limitation of the skin sample availability.

However, the *ex-vivo* trends on the background of the significant *in vitro* data, were suggestive that small dose of locally injected IL-10 has the potential to modulate skin DCs into pro-tolerogenic profile. Although anticipated dose-sparing benefit of NP IL-10 was not shown, *in vivo* tolerogenic potential of IL-10 can not be excluded, particularly if used as enhancer to peptide immunotherapy.

**Chapter 5 *IN-VIVO* METHODS FOR THE OPTIMAL
MONITORING OF THE IMMUNE RESPONSE AFTER ANTIGEN
SKIN DELIVERY**

5.1 Introduction

Alongside the importance of the optimal delivery of peptide immunotherapy, it is crucial to efficiently monitor its effect. Detection of a significant immune response in the blood following antigen specific immunotherapy (ASI) has been a challenge for many trials, and to this day no ideal marker for monitoring immune and therapeutic efficiency has been established.[132] Detection of cellular immune responses to self-antigen in the blood may be very difficult, as the frequency of cells responding to any given antigen is very low (less than 1 in 10,000 cells).[45] Irrespective, accessibility of the blood makes it the most commonly used source of immune cells in human studies. On the contrary, in murine models, lymphoid organs, such as spleen and lymph nodes, are usually used to harvest cells and monitor immune interventions. Here, I explore the concept of translating this approach into humans by using minimally invasive ultrasound guided fine needle aspiration (FNA) of the regional lymph node (LN), a technique commonly used in clinical practice for cancer diagnostics.[139]. To our knowledge, only one study to this date used lymph node biopsy to monitor response to transdermally applied myelin peptides for the treatment of multiple sclerosis, and showed increase in number of dendritic cells following antigen stimulation in the regional axillary lymph node.[243]

5.1.1 Anatomy and histology of the lymph nodes

Lymph nodes are secondary lymphoid organs, strategically positioned at the convergence of the lymphatic vessels that collect extracellular fluid (lymph) from peripheral tissues, where it is produced from filtration of the blood.

Relevant to this project are axillary lymph nodes regional to the arm because antigens are injected into the skin of the upper limb. They are divided into five groups depending on their draining area and their position relative to the other structures in the axilla (Figure 5-1)[244]:

1. The **lateral group** lies behind the axillary vein and drains the upper limb.
2. The **pectoral group** that drains most of the breast is situated at the inferior border of the pectoralis minor muscle.
3. The **posterior, or subscapular, nodes** are located in the posterior axillary fold and drain the posterior shoulder.
4. The **central group**, near the base of the axilla, receives the lymph from the previous three groups.
5. The **apical nodes** lie medial to the axillary vein and superior to the pectoralis minor muscle. The apical nodes receive the lymph from all the other groups and sometimes directly from the breast. They drain to subclavian trunks, which enter jugular-subclavian venous confluence or join common thoracic duct.

For the purpose of this project, we performed aspiration of the lateral group.

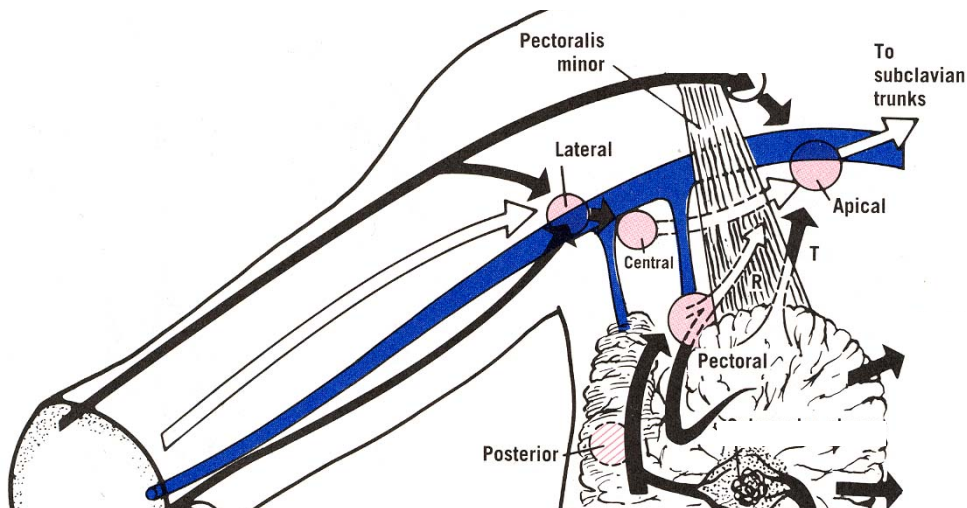


Figure 5-1. Anatomy of the axillary lymph nodes. Adapted from O’Rahilly R, Muller F, Carpenter S, Swenson R, eds. *Basic Human Anatomy*. Hanover, USA: Dartmouth Medical School, 2008. <http://www.dartmouth.edu/~humananatomy/>.

The histology of the lymph node is presented in the Figure 5-2. The lymph node is formed from two juxtapositioned zones, cortex and medulla.[24] The outer cortex primarily consists of B cells organised in follicles that become secondary follicles during the immune response with areas of rapid proliferation called germinal centers. They become dormant with the resolving immune process. Next to the outer cortex is a deeper cortex or paracortex, where T cells and dendritic cells (DCs) reside.

Arriving via afferent lymphatics from the peripheral tissue, lymph carrying soluble and cell bound antigens, passes through the lymph sinuses, before entering cellular paracortical areas. Naïve T cells arrive to the paracortex from the blood through specialised blood vessels known as high endothelial venules (HEV), attracted by the same chemokines, such as CCR7 that guided antigen presenting cells (APCs) from the peripheral tissue. This directed traffic enables the presence of all the relevant cells in the same place to enhance interaction of the T cells with the antigen in question. In the same way, B cells

deriving from the blood first pass through paracortex where they encounter antigens and helper T cells necessary for their activation. They then proceed to the outer cortex where they proliferate in the germinal centres. Lymph leaves the node via efferent lymphatic vessels in the medulla that also contains strings of macrophages and antibody secreting plasma cells, known as medullary cords.

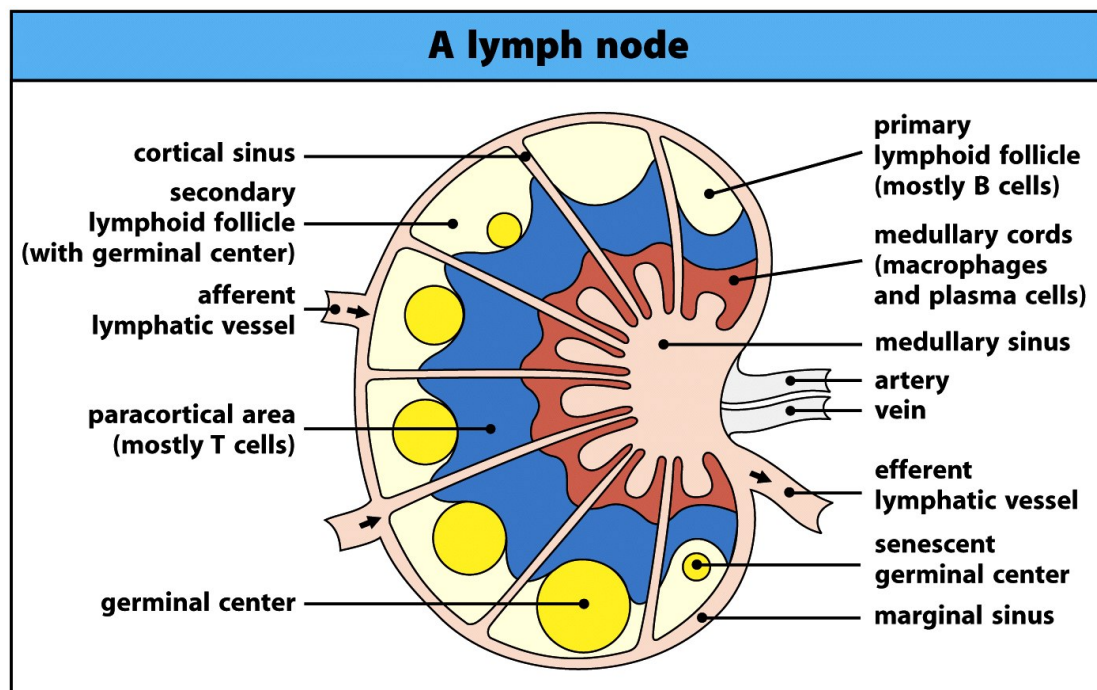


Figure 5-2. Histology of the lymph node. Adapted from Murphy K, Travers P, Walport M, eds. Janeway's Immunobiology. 7th Edition. New York: Garland Science, Taylor&Francis Group, LCC, 2008.

5.1.2 Interplay between skin and the lymph node during immune response

It is very important to understand the dynamic communication between peripheral tissue and its regional lymph node during the immune response, particularly one that develops after antigen skin injection. In this following section, I will consider the role of several cell groups involved in the process.

5.1.2.1 Dendritic cells

Soluble antigens are the first to arrive to the lymph node. They are followed by antigen bearing DCs, guided by chemotactic chemokines.[245] CCR7, a chemokine receptor known to mediate the mobilisation of skin DCs under inflammatory conditions, also controls homing from non-inflamed skin. In parallel to the expression of CCR7, migrating Langerhans cells (LCs) downregulate E-cadherin, molecule responsible for their adhesion to keratinocytes.[246] Timing of the arrival depends on the type of DCs, with more loosely connected dermal DCs arriving sooner than LCs, who require matrix metalloproteases (MMP), such as MMP-2 and MMP-9 to allow translocation through epidermal basal membrane.[247] Data from transgenic mice expressing photoconvertible dye indicate that approximately 5% of all DCs found in the skin-draining LNs arrive from the skin each day.[248] This is reflected in studies in humans, showing that DCs found in the skin draining LNs partially originate from the skin. Flowcytometric analysis of cancer-free human LNs excised during surgery for melanoma, showed two subsets of CD1a expressing cells: CD1a^{high}CD11c^{int}, with high intracellular expression of Langerin, most likely to be migratory skin LCs; and CD1a^{int}CD11c^{high}, migratory dermal DCs. Interestingly, CD1a⁺ cells despite their mature phenotype (high expression of CD80, CD83 and CD40), showed low potency in stimulating proliferation of allogeneic donor T cells. The other two subsets (CD11c⁺CD1a⁻) are most likely to be blood derived. They are distinguished by their variable expression of CD14 into CD14⁺ and CD14⁻. [249] Immunocytochemistry study on human lymph nodes, showed that CD1a⁺ cells (either Langerin positive or negative) are mainly localised in the paracortex of

the axillary lymph node, whilst CD14⁺ cells reside in the medullary areas and B cell zones. [250]

5.1.2.2 T cells

Another important player in this continuous conversation between skin and its LN are T cells. Naïve T cells arrive to LNs exclusively via HEV in the process involving CD62L, which allows CCR7 on T cells to engage with their ligand, secondary lymphoid tissue chemokine (SLC), expressed on endothelial cells.[251] This interaction facilitate homing of the naïve CD45RA⁺ T cells into the paracortex where they will meet antigen presented on the APC.

In parallel, memory cells are engaged in the process. There are two subsets of memory CD45RA⁻ T cells, distinguished on the basis of their expression of CCR7.[252]

CD45RA⁻CCR7⁻ cells, or effector memory cells, are less likely to home into the LN due to the lack of CCR7. They aim for the peripheral tissues where they arrive thanks to their high expression β 1 and β 2 integrins [253] and receptors for inflammatory chemokines such as CCR1, CCR3 and CCR5 [254, 255], necessary for homing into the inflamed tissues. There they target their antigen, being ready to quickly produce inflammatory cytokines such as IFN γ , IL-4 or IL-5.[252] On the other hand, CD45RA⁻CCR7⁺ cells or, central memory cells, are found in secondary lymphoid organs. Additionally equipped with CD62L to home in the LN, they probably share the same migratory routes via HEV into the LN as naïve T cells. They need a longer time to be activated and probably can function as a potent activator of the dendritic cells, through the rapid expression of a costimulatory molecule. They produce IL-2, but not IFN γ

upon stimulation. A small fraction of these blood cells express CD69 and CD25.[252]. On the contrary, a significant proportion of T cells in the lymph node, both naïve and memory, express CD69[256], which in this tissue is more likely to represent a retention rather than an activation marker.

The distinction between central and effector memory is not as clear in the skin. T cells specialised for entry into cutaneous sites are characterised by expressing high levels of CLA, a ligand for E-Selectin, CCR4 and CCR6.[257] The majority are CD45RA⁻CCR7⁻ effector memory cells, with predominant Th1 phenotype, but there is a proportion of CLA⁺ CCR7⁺ cells, which are known as “central memory skin homing cells” that can enter the skin, but most likely have access to the lymph nodes as well.[258] A significant proportion of skin memory cells express CD69. [259]

The skin is also a site of a vast number of T regulatory cells.

5.1.2.3 T regulatory cells

As discussed in the Chapter 1, T regulatory cells are responsible for the maintenance of self-tolerance, being tailored to recognise mainly self-antigens. It is believed that secondary lymphoid organs, i.e. lymph nodes are the place where T regs interact with their cognate antigens. Analysis of human inguinal LN showed that they comprise approximately 5-7% of CD4⁺ population. The majority of Tregs in human lymphoid tissues, defined as CD4⁺CD127⁻CD25⁺⁺Foxp3⁺ cells, are CD69⁺ CD45RA⁻ cells with Ki67⁺ phenotype and wide TCR repertoire. This implies that in healthy secondary lymphoid organs, Tregs are under constant polyclonal activation and expansion. Although

suppressive, they are not anergic as they produce IL-2, IL-10 and IFN γ . [256] One can speculate that LN Tregs are in the state of the continuous alert, surveying prolific T cell responses taking place in the lymph node, ready to suppress inappropriate self-reactive ones.

It is interesting to explore how do skin Tregs compare to their LN counterparts. They express high levels of CD25, L-selectin, Foxp3, GITR, intracellular CTLA-4, low CD69 levels and high levels of skin homing addressins such as CLA, CCR4 and CCR6. The suppression of the proliferation of CD25^{lo} T cells that skin Tregs mediate is dependent on cell-cell contact and unaffected by inactivation antibodies for IL-10 and TGF- β . [260]

Other studies also suggested the presence of memory regulatory T cells in the human skin. Approximately 20% of adult T cells in the skin express Foxp3, in contrast to only 5% in the blood and LN. The majority of adult skin Tregs are CD45RO⁺ effector memory type, whilst foetal skin has markedly reduced number of CD4⁺Foxp3⁺ cells, with significantly lower percentage of CD45RO expressing population. This indicates that these cells have seen their antigens outside the thymus and populated skin at some stage in life. [261] Supportive of the blood origin of skin Tregs is the finding of high expression of skin homing receptors CLA, CCR4 and CCR6 on peripheral blood Foxp3⁺. [262]

Interestingly, the majority of skin Tregs are CCR7⁻. They have no migratory capacity to traffic to regional lymph node as evidenced by experiments with transplanted human skin on immunodeficient NSG mice. [261]

It was shown that skin T regs, defined as CD4⁺Foxp3⁺CD25^{high}, accumulate in parallel with CD4⁺ effector cells upon *in vivo* Tuberculin PPD challenge (see

below). Authors debate about the origin of these cells. The previously mentioned finding that blood Foxp3^+ cells express skin homing receptors argues towards their blood origin, but proliferation of skin resident Tregs cannot be excluded. Another possibility is that they evolve from the responsive memory CD4^+ cells.[133]

5.1.3 Mantoux test

A potentially useful tool for understanding the interplay between the skin and its draining LN after antigen challenge, which has been used in the clinical practice for decades to test for the immunity against tuberculosis, is a Mantoux test. This is a classic CD4^+ mediated delayed type hypersensitivity (DTH) response to the intradermal injection of Tuberculin purified protein derivative (PPD), prepared from human strains of *M. tuberculosis*.[263]. With some exceptions, skin induration larger than 6mm in the transversal diameter, 48-72h from intradermal injection of Tuberculin PPD is considered to be positive reaction suggesting clinically significant immunity against TB.⁴

Histologically, the reaction starts just few hours after injection. It has two peaks: initial non-specific infiltration, present even in non-sensitised individuals, followed by specific one, found only in sensitised subjects.[263, 264] After 4-6h from injection, the majority of infiltrating cells are neutrophils [264], followed by T cells that begin to appear after 12h. [265] At 24h the majority of infiltrating cells are macrophages, whilst at 48h they are largely replaced by T cells, predominantly CD4^+ .[264, 265]

⁴ Public Health England. Tuberculosis: the green book, Chapter 32, updated April 2013.

It is not clear where this activation of PPD specific T cells takes place. There is some evidence that it actually happens *in situ* in the skin. A study looking at the expression of cellular marker of proliferation, Ki67 and shortening in the telomere length, indicative of cell's replicative history, in the skin cells after Mantoux test, detected proliferation only in the skin, but not in the blood. That was consistent with the increase in the PPD specific T cells in the skin only, 3 days after Tuberculin *in vivo* challenge.[266]

The possibility that PPD specific T cells from blood and skin are different entities also is suggested from a study looking at blood responses in healthy Mantoux negative individuals. T cells from some M. tuberculosis exposed or BCG vaccinated individuals with negative Mantoux can undergo blast cell transformation when incubated with Tuberculin PPD *in vitro*.[267] A study in people diagnosed with tuberculosis who have negative Mantoux test suggests the lack of the expression of skin homing antigen CLA as a possible cause. Blood derived PPD specific cells in these individuals are CLA⁻, in contrast to the Mantoux positive TB sufferers whose PPD specific cells are CLA⁺. These CLA⁻ also have lower capacity to produce IFN γ incubated with PPD.[268]

In summary, skin, a very efficient barrier to the outer world, is the home of twice as many T cells than in the peripheral circulation. These T cells have remarkable diversity in their TCR repertoire that is only slightly less than that of their peripheral blood counterparts [258]. Taken together with the skin's richness in dendritic cells, potent antigen presenters, we start to understand the importance of this active immune surveillance that can develop to either,

protective immunity or immune tolerance depending on the nature of the stimulus. Part of this interplay spills over into the regional lymph node. Capturing the immune response in the draining lymph node following antigen skin delivery is logical, but up until now, not developed as an approach in understanding and monitoring the immune process after therapeutic intervention. If proven effective, this approach has the potential to substantially accelerate the development of effective antigen specific therapy in humans.

5.2 Hypothesis

I hypothesise that an ultrasound guided fine needle lymph node aspiration can develop into an effective, but minimally invasive monitoring technique of the effect of the antigen skin specific immunotherapy in humans.

5.3 Aim

1. To assess feasibility and optimise methods for monitoring immune response in the draining lymph nodes after intradermal antigen skin delivery in comparison to PBMCs isolated from the blood of the same subject, drawn at the same time as lymph node aspiration.

5.4 Results

I recruited 25 healthy volunteers (21 female, 4 male) with the mean age of 28.9 ± 7.1 years. Detailed methods are given in Chapter 2. Lymph node aspirate from the first subject was used to obtain an initial estimate of number of cells available for analysis, their profile (number of CD4⁺, CD8⁺ and CD19⁺ cells) and viability, whilst the rest of the subjects (n=24) were included in the main part of the study. They were subjected to Mantoux test, with 15 of them being clinically positive i.e. induration larger than 6mm, 48h after Tuberculin PPD injection.

Samples from 12 Mantoux positive subjects were used in an ELISPOT assay designed to detect IFN- γ producing cells amongst lymph node cells (LNCs) and PBMCs before and after *in vivo* injection of 2 TU of Tuberculin PPD. Two time points were assessed: two and five days after injection, including 7 and 5 subjects, respectively.

Samples from the rest of the three Mantoux positive subjects were used for flow cytometric analysis of lymph node aspirate and PBMCs before and two days after *in vivo* injection of 2TU of Tuberculin PPD. I used pre-treatment samples from these subjects and additionally two Mantoux negative subjects for the general flow-cytometric analysis of the lymph node aspirate in comparison to PBMCs. Additional four subjects had more extensive flow cytometric analysis as described in the Chapter 2. Progress of the study is shown in the Figure 5-3.

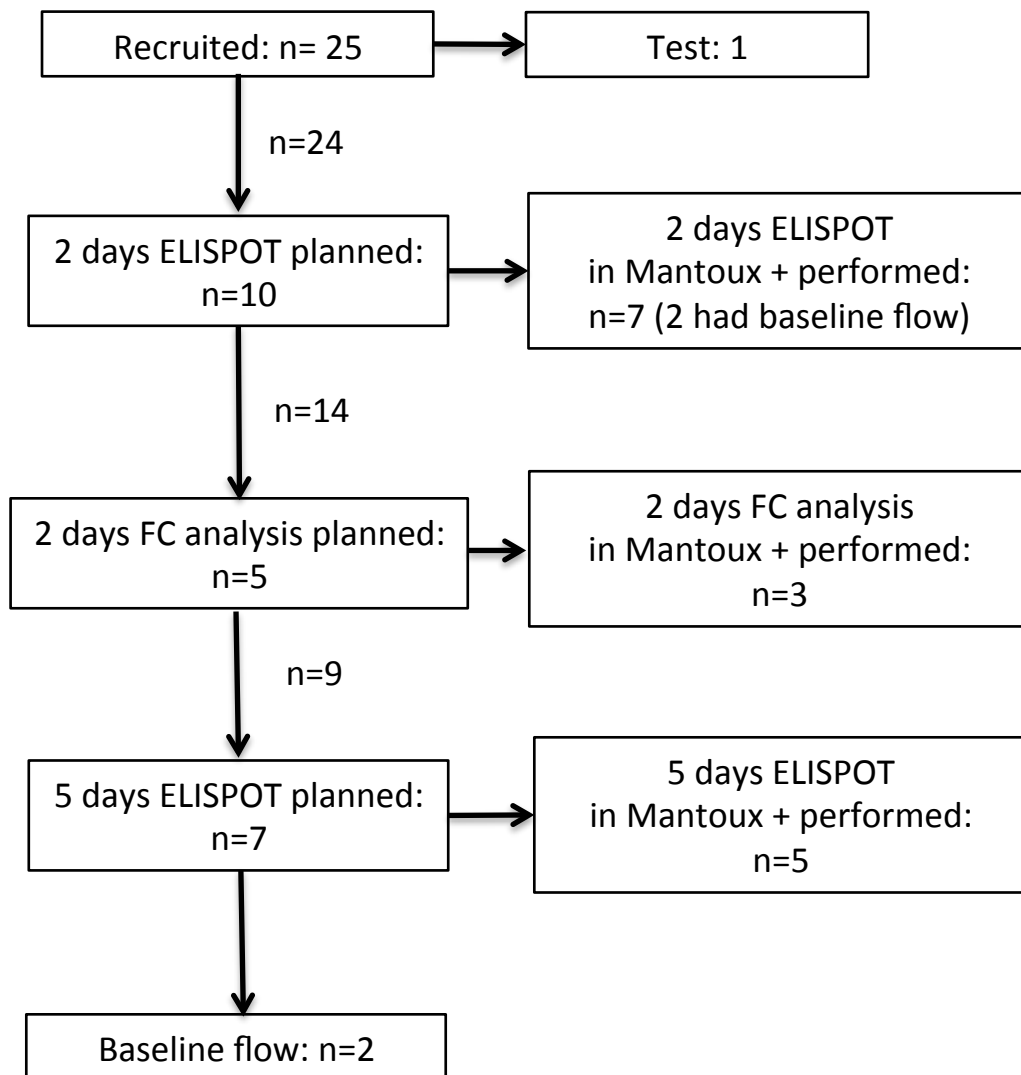


Figure 5-3. Study progression flow chart. Mantoux negative individuals were excluded from the second analysis after Tuberculin PPD injection. 2 days ELISPOT: ELISPOT before and 2 days after Tuberculin PPD; 2 days FC analysis: flow cytometry analysis before and 2 days after Tuberculin PPD; 5 days ELISPOT: ELISPOT before and 5 days after Tuberculin PPD.

5.4.1 Lymph node aspirate

I obtained on average of $3.3 \pm 2.1 \times 10^6$ white cells per aspirate, calculated from 39 analysed samples (15 Mantoux positive individuals had baseline sample and the sample after Tuberculin PPD, whilst seven Mantoux negative participants had only baseline sample, as did the subjects who had baseline flow cytometric analysis only) - Figure 5-4a. There was no significant correlation between the cortex diameter and the aspirate count – Figure 5-4b.

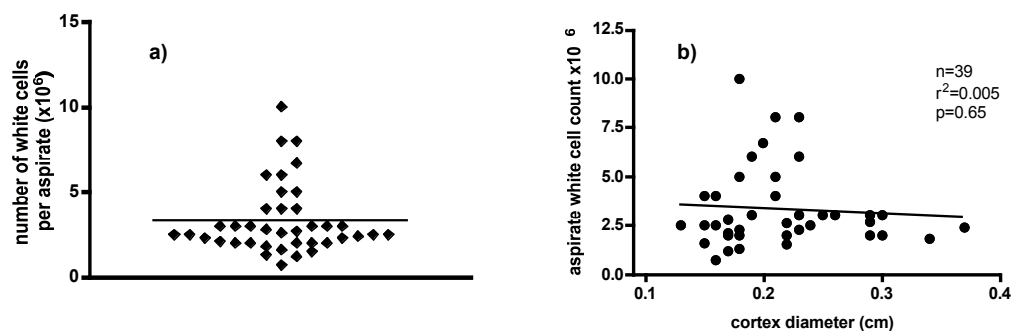


Figure 5-4. Lymph node aspirate. a) average number of white cells per LN aspirate. The cells were counted after staining with trypan blue with addition of 4% acetic acid to eliminate red blood cell contamination. N=39. b) correlation between aspirate white cell count at the diameter of the aspirated lymph node cortex. Statistical test used: Pearson's correlation.

First, the cells were analysed on flow cytometry. As shown in Figure 5-5, the majority of blood and lymph node derived lymphocytes were live. The LN aspirate contained a significant percentage of red cell contamination, although it was possible to identify the position of the lymphocyte gate, with clear CD3⁺ population. In order to preserve as many cells of interest as possible, I did not use any red cell elimination method.

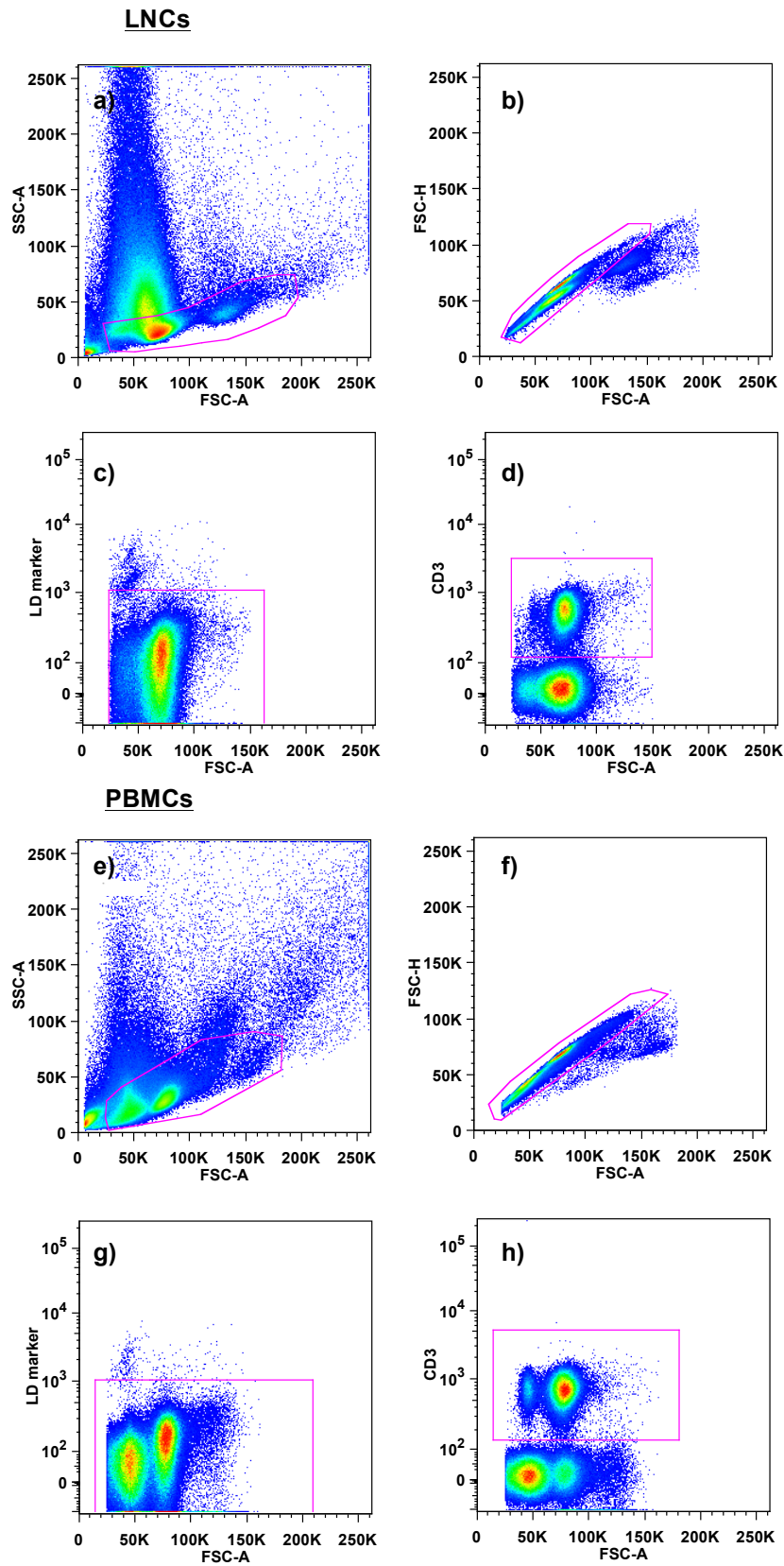


Figure 5-5. Representative example of gating strategy. a) lymphocyte gate in the LN aspirate; b) singlets gate in the LN derived lymphocytes; c) live cell gate amongst the LN derived lymphocytes; d) CD3⁺ lymph node derived lymphocytes; e) lymphocyte gate amongst PBMCs; f) singlets gate in the blood derived lymphocytes; g) live cell gate amongst blood derived lymphocytes. h) CD3⁺ blood derived lymphocytes.

The ratio of CD3⁺ vs. CD19⁺ appeared more in favour of CD3⁺ cells, in the blood (13.1 ± 3.7) than in the lymph node (4.4 ± 2.8), but the difference was not statistically significant – Figure 5-6.

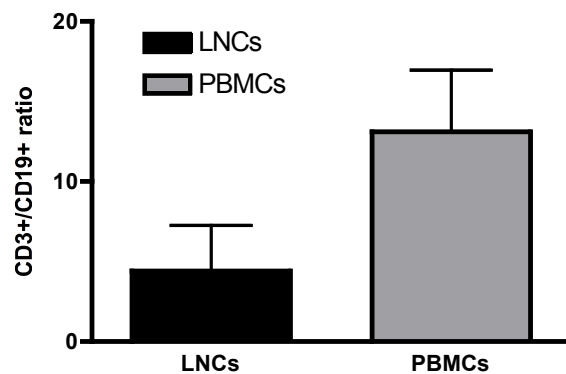


Figure 5-6. Summary of the ratio of CD3⁺/CD19⁺ cells in lymph node and blood. Statistical test used: Wilcoxon signed ranked test.

Although the predominance of CD4⁺ cells was obvious in both blood derived (CD4:61.9±8.1%; CD8:26.5±5.3%) and lymph node derived CD3⁺ cells (CD4:79.6±9.9%; CD8:15.3±6.7%), this was significantly more marked in the lymph node aspirate (n=12, p=0.02) – Figure 5-7.

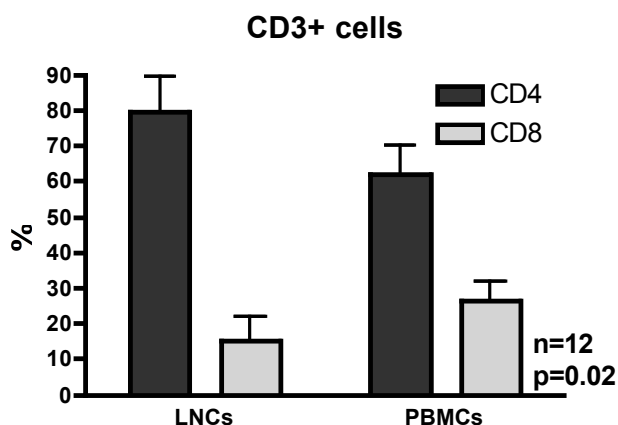


Figure 5-7. Summary of the ratio of CD4⁺/CD8⁺ cells in lymph node and blood derived CD3⁺ population. Statistical test used: Fisher's exact test.

Figure 5-8 shows an example of the distribution of CD4⁺ and CD8⁺ cells amongst CD3⁺ population of both LNCs (a) and PBMCs (b).

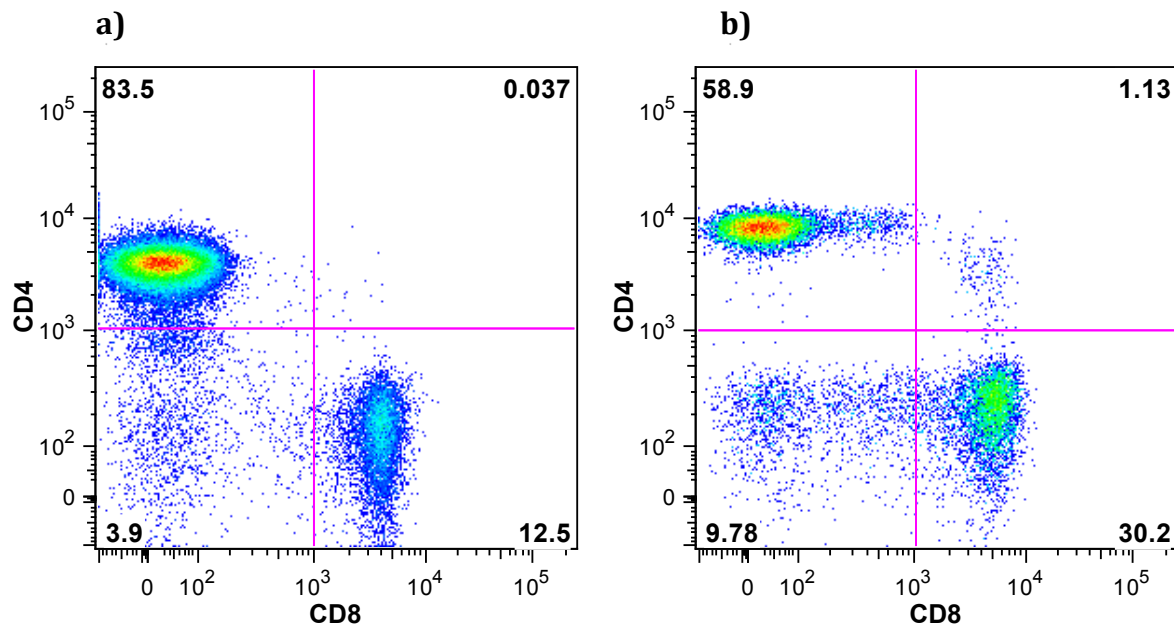


Figure 5-8. Representative flow cytometric analysis of the CD4:CD8 ratio in the CD3⁺ population: a) lymph node derived; b) blood derived.

Next, I analysed four matching LN and blood samples for the expression of CD45RA and CCR7 to establish the distribution of naïve and memory T cells. The CD45RA+CCR7+ cells were characterised as naïve, CD45RA+CCR7- as (effector memory CD45RA+) T_{EMRA} cells, CD45RA-CCR7+ as central memory cells and CD45RA-CCR7- cells as effector memory cells. There were significantly less CD8+ T_{EMRA} cells in the LN samples, even when CD8+ population only, was taken into account. Another difference was trend towards more marked predominance of central to effector memory in the LN, again more consistent in the CD8+ population - Figure 5-9.

Analysis of CD69 expression revealed significant higher proportion of CD69+ cells in the LN, in both, CD4+ and CD8+ population. When combined presentation of CD69 and CD45RA was looked at, I was able to distinguish four different populations of T cells: population I – CD69- naïve cells (CD45RA+CD69-), population II – CD69+ naïve cells (CD45RA+CD69+), population III – CD69+ memory (CD45RA-CD69+) and population IV – CD69- memory (CD45RA-CD69-). Percentage of CD69- cells, both naïve and memory, was significantly higher in blood, whilst CD69+ naïve and memory were significantly more represented in the lymph node. This similar pattern was observed in CD3+, CD4+ and CD8+ populations – Figure 5-10, Table 5-1.

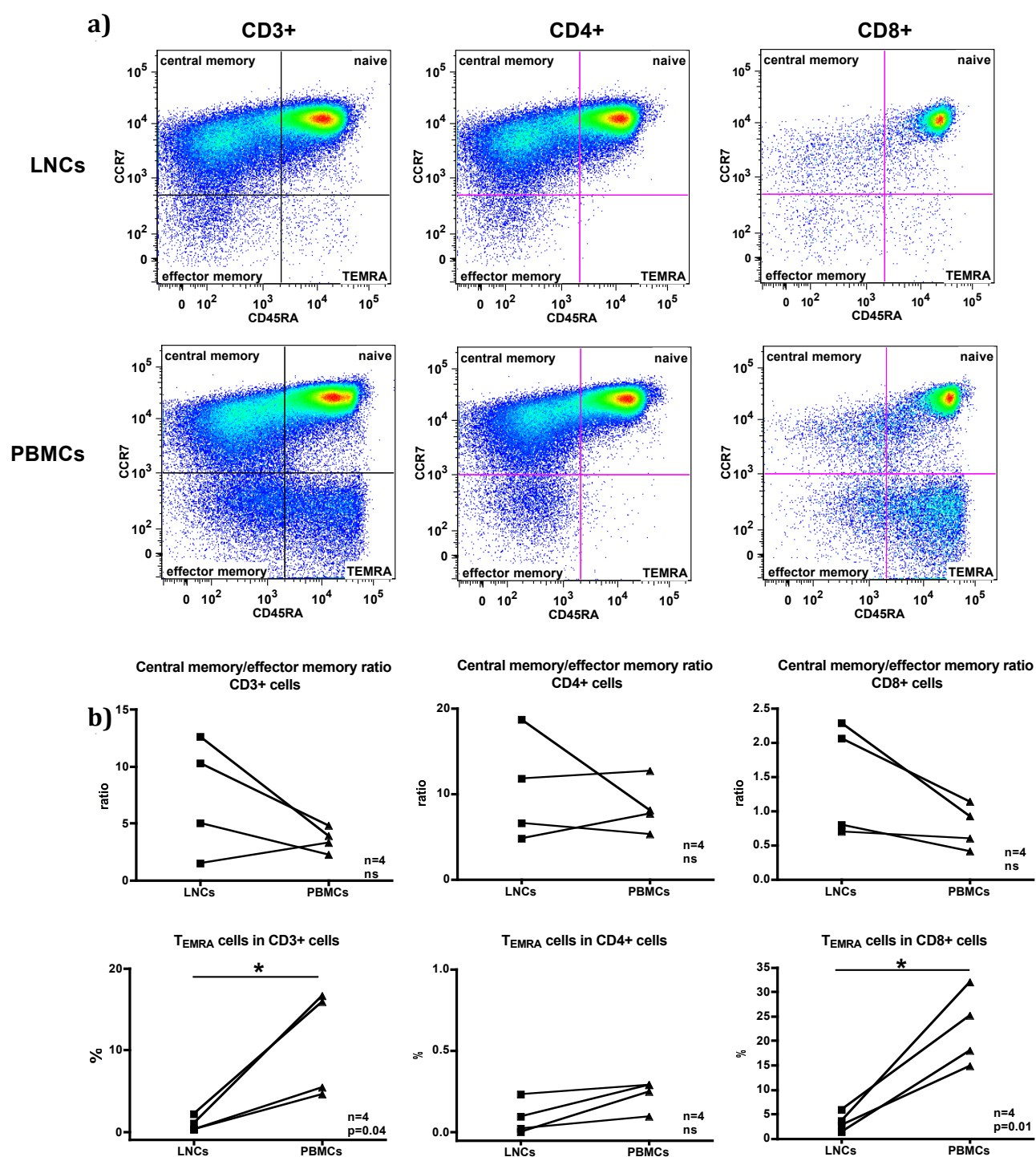


Figure 5-9. Flow cytometric analysis of CD45RA and CCR7 expression in the LN and in the blood. a) Representative example of flow cytometric analysis; b) summary graph of central memory/effector memory ratio in CD3+, CD4+ and CD8+ populations from 4 different healthy individuals at baseline; c) summary graph of the % of T_{EMRA} cells in CD3+, CD4+ and CD8+ populations from 4 different healthy individuals at baseline. Naïve = CD45RA⁺CCR7⁺, Central memory: CD45RA⁺CCR7⁺, Effector memory: CD45RA⁺CCR7⁻, TEMRA=CD45RA⁺CCR7⁺. Statistical test used: Paired samples t test.

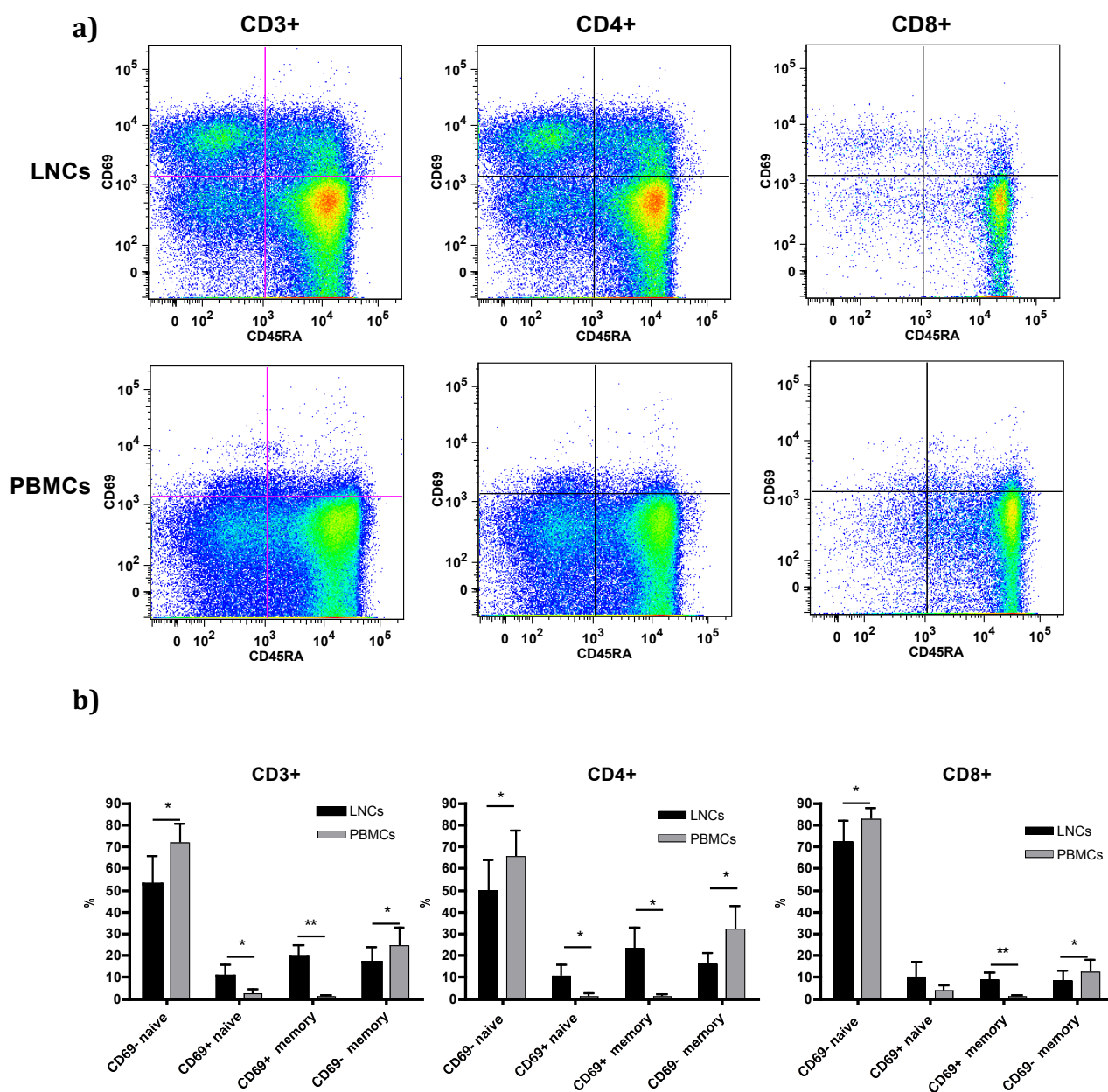


Figure 5-10. Flow cytometric analysis of CD45RA and CD69 expression in the LN and in the blood. a) Representative example of the flow cytometric analysis; b) summary graph of four populations of T cells: population I – CD69- naïve cells (CD45RA+CD69-), population II – CD69+ naïve cells (CD45RA+CD69+), population III – CD69+ memory (CD45RA-CD69+) and population IV – CD69- memory (CD45RA-CD69-), in CD3+, CD4+ and CD8+ population in the LN and blood.

	CD3			CD4+			CD8+		
	LNC	PBMC	p	LNC	PBMC	p	LNC	PBMC	p
Population 1	52.6±12.5	72.0±8.6	0.01	49.7±13.8	65.6±11.6	0.01	72.2±9.3	82.8±4.6	0.04
Population 2	10.8±4.8	2.4±1.9	0.01	10.8±4.8	1.3±1.2	0.01	10.3±6.7	3.8±2.2	0.08
Population 3	19.5±5.1	1.1±0.7	0.005	23.4±9.4	1.0±0.9	0.01	8.9±3.0	1.0±0.5	0.009
Population 4	17.1±6.5	21.8±5.3	0.03	16.1±4.7	32.1±10.4	0.01	8.6±4.5	12.4±5.5	0.04

Table 5-1. Comparison between distribution of four populations of T cells based on the expression of CD69 and CD45RA, in the LN and blood. Statistical test used: Paired sample T test.

Analysis of the expression of the skin homing receptors in the blood and the lymph node, showed no significant differences, with the exception of significantly higher expression of CCR4 and CLA in the CD8+ blood cells in comparison to the lymph node derived cells (p=0.01 and p=0.03, respectively)

- Figure 5-11.

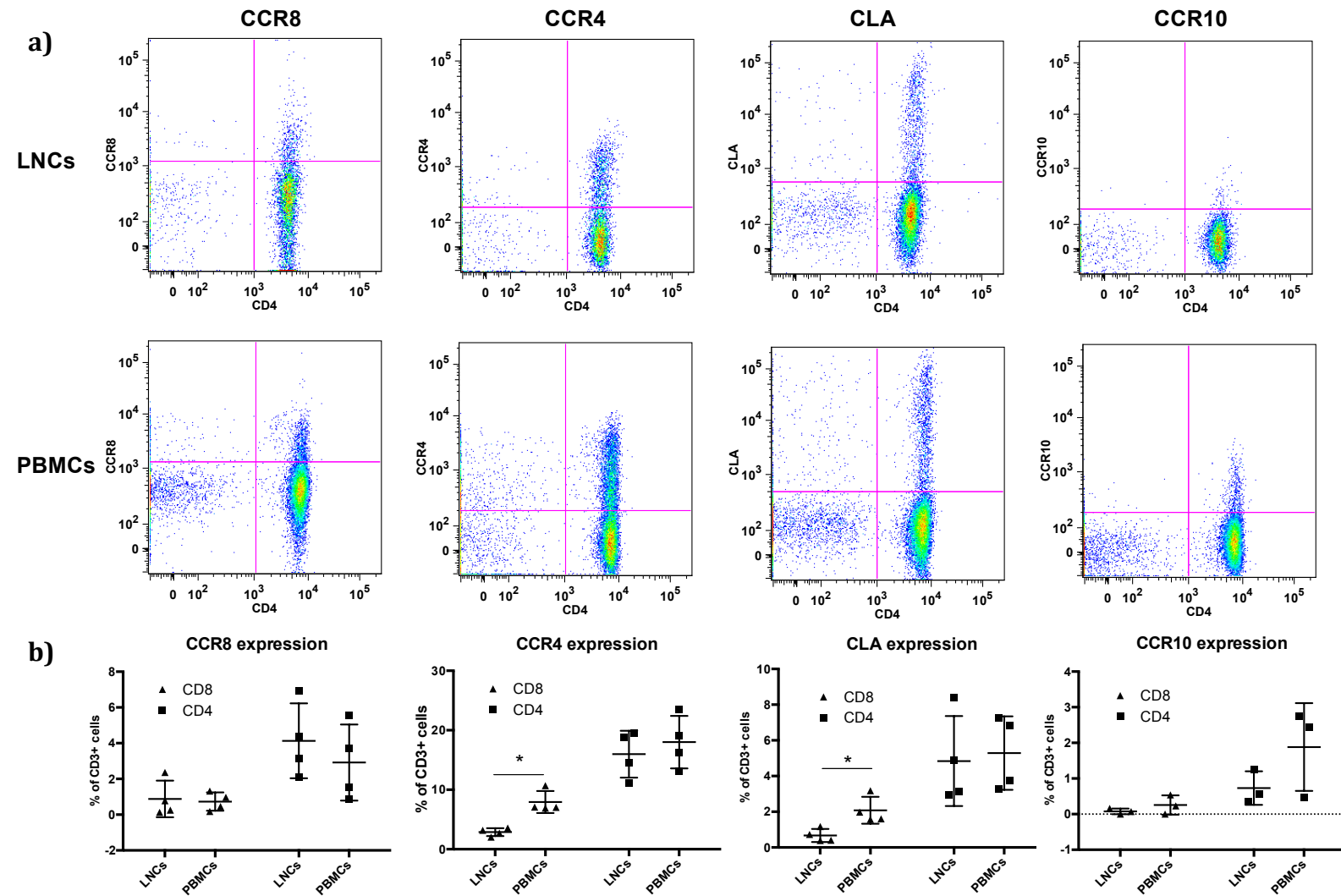


Figure 5-11. Flow cytometric analysis of skin homing receptors in the LN and in the blood. a) Representative example of the flow cytometric analysis; b) Summary graph of the expression of skin homing receptors in the skin and blood amongst CD4+ and CD8+ cells. CCR4 and CLA expression was significantly higher in the blood CD8+ cells ($p=0.01$ and $p=0.03$, respectively).

Interestingly, majority of CLA positive cells in the blood and the lymph node are central memory cells – Figure 5-12.

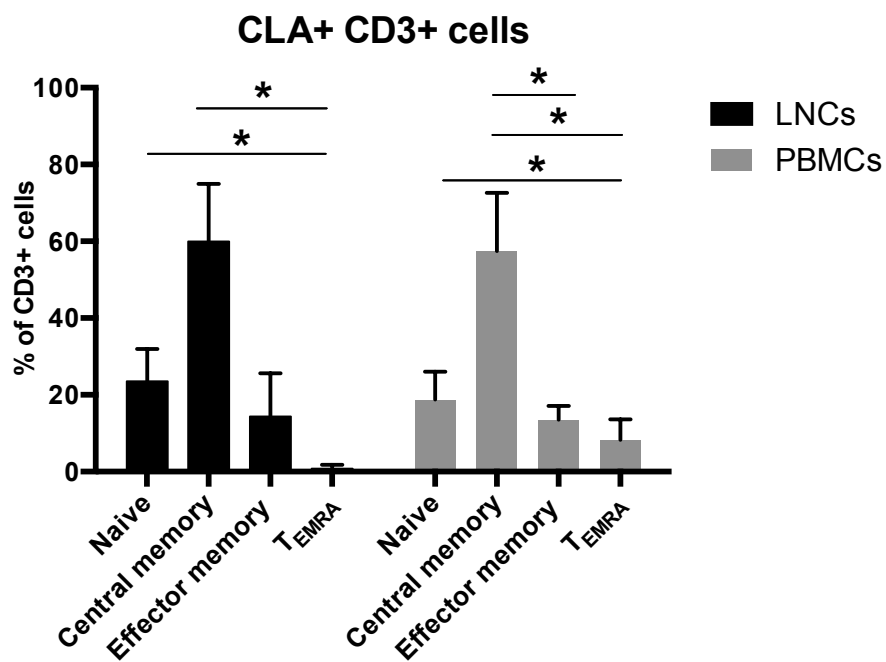


Figure 5-12. Comparison of naïve vs memory. Lymph node CD3+ cells (n=4, p=0.007); Blood derived CD3+ cells (n=4, p=0.007). Statistical test used: One-way ANOVA with the Tukey's multiple comparison test.

5.4.2 Response after two days of Tuberculin PPD injection

5.4.2.1 Lymph node size

I observed a significant increase in the ultrasonographically measured thickness of the lymph node cortex (before: 0.18 ± 0.03 cm; two days after: 0.24 ± 0.08 cm, $n=10$) – Figure 5-13.

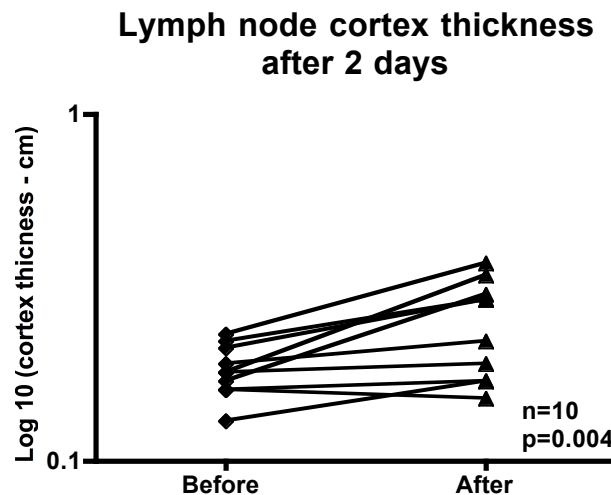


Figure 5-13. Lymph node cortex thickness at baseline and two days after Mantoux test. Statistical test used: Wilcoxon signed ranked test.

5.4.2.2 ELISPOT

To understand the process behind the response in the regional axillary lymph node after *in vivo* intradermal injection of 2TU Tuberculin PPD in the forearm, I used the ELISPOT assay designed to detect IFN- γ producing cells amongst lymph node cells (LNCs) and PBMCs collected before and after the injection. It involved incubation of cells in two different concentrations of Tuberculin PPD ($0.5 \mu\text{g/ml}$ and $5 \mu\text{g/ml}$) and control stimulants, $1 \mu\text{g/ml}$ PHA, 0.5u/ml Tetanus toxoid and viral peptide mix (VM) containing flu matrix protein (MP)₅₈₋₆₆ (GILGFVFTL), cytomegalovirus (CMV) pp65₄₉₅₋₅₀₃ (NLVPMVATV) and Epstein-Barr virus (EBV) BMLF1₂₈₀₋₂₈₈ (GLCTLVAML) at 20nM each (Chapter 2).

Representative examples of ELISPOT plates demonstrating a response of LNCs and PBMCs to the two different *in vitro* concentrations of Tuberculin PPD and control stimulants, before and two days after *in vivo* Tuberculin PPD injection, are shown in Figure 5-14, Figure 5-15. With the exception of viral mix (VM) response, all images are from the same person. Although derived from a different subject from the rest of the wells, VM responses in the blood and LN are originated from the same subject, to illustrate the comparison between the lymphocytes of a different origin.

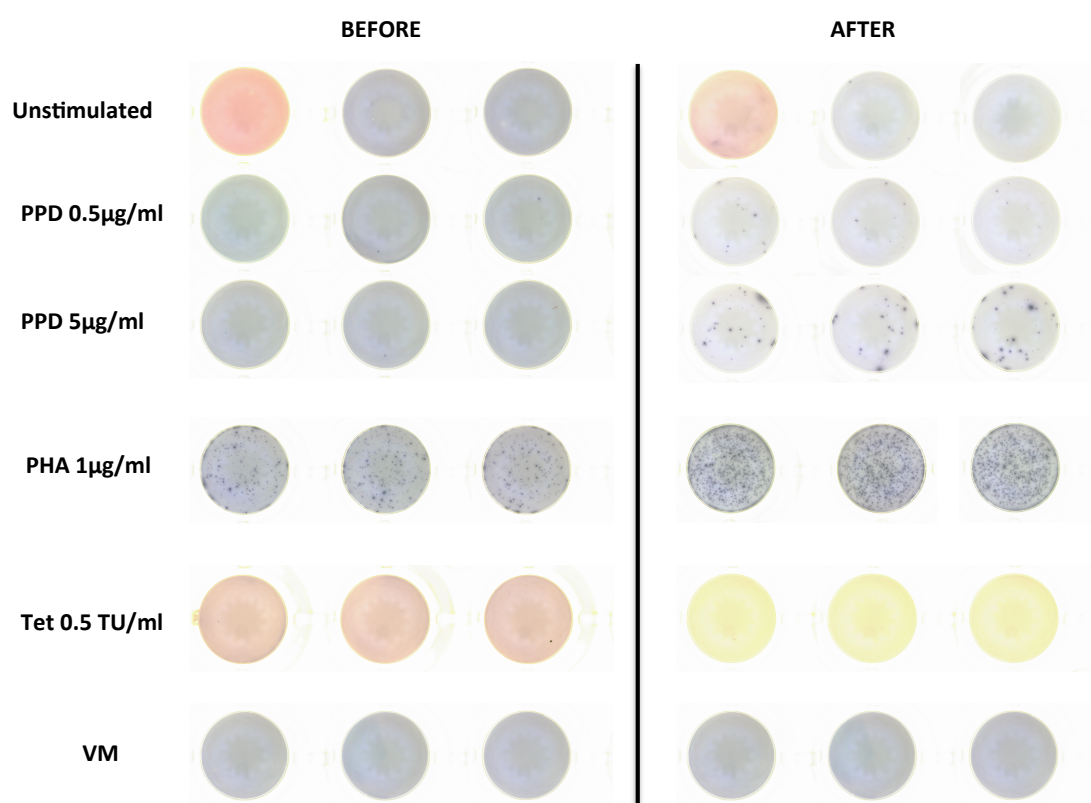


Figure 5-14. Representative example of the ELISPOT plate used for counting IFN γ producing cells in the suspension of lymph node aspirate cells (LNCs) before and two days after *in vivo* injection of Tuberculin PPD. 1×10^5 LNCs/well were plated.

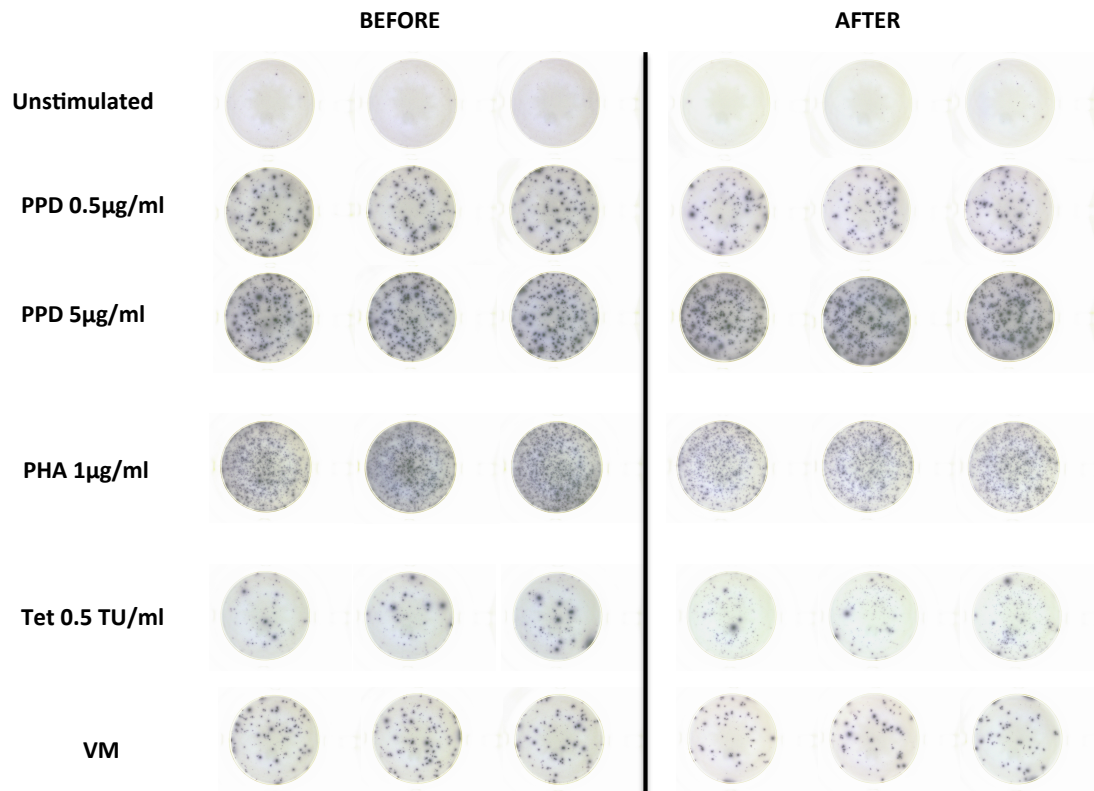


Figure 5-15. Representative example of the ELISPOT plate used for counting IFN γ producing cells in the suspension of PBMCs before and two days after *in vivo* injection of Tuberculin PPD. 2×10^5 PBMCs/well were plated. Wells illustrating VM response are not from the same person as the rest of the wells.

There was significant increase in IFN γ producing cells amongst LNCs after two day of Tuberculin PPD injection (Figure 5-16a), whilst the response in PBMCs remained unchanged (Figure 5-16b).

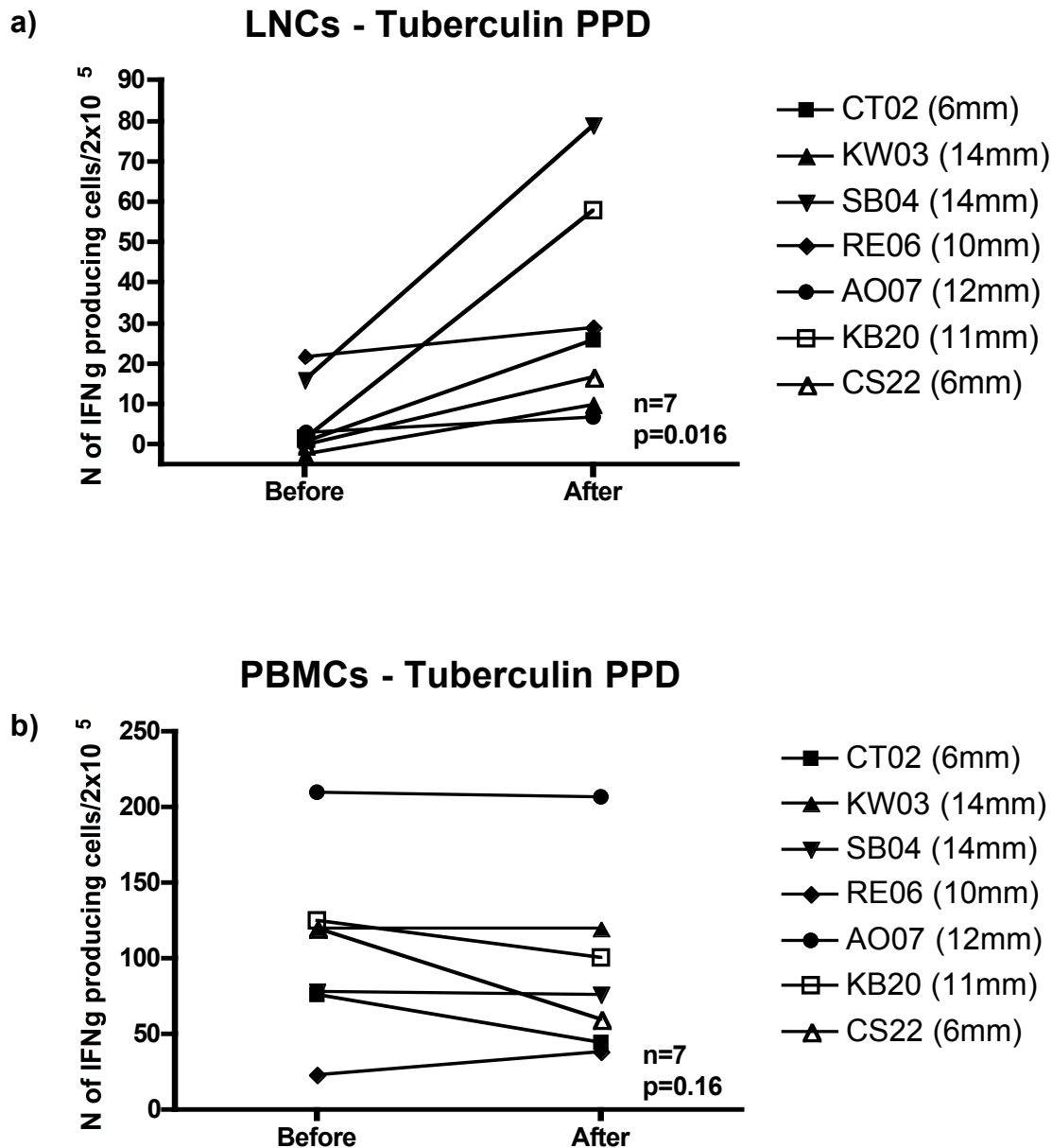


Figure 5-16. Summary of the ELISPOT response to *in vitro* Tuberculin PPD before and two days after *in vivo* injection. a) Number of IFN- γ producing cells per 2×10^5 cells from the lymph node aspirate before and two days after Tuberculin PPD injection ($n=7$, $p=0.016$). b) Number of IFN- γ producing cells per 2×10^5 PBMCs before and two days after Tuberculin PPD injection ($n=7$, $p=0.16$). The response of the each subject is shown as connected before-after points. Subjects' codes with their Montoux response in brackets are shown in the legend. Statistical test used: Wilcoxon signed ranked test.

LNCs showed significantly increased response to PHA following Tuberculin PPD injection (Figure 5-17a). This observation is most likely to be a non-specific response to the adjuvant-like elements in the PPD injection, rather than to PPD itself, given a lack of response to the specific stimulus Tetanus toxoid and mix of the viral peptides, used as control (Figure 5-17 b and c).

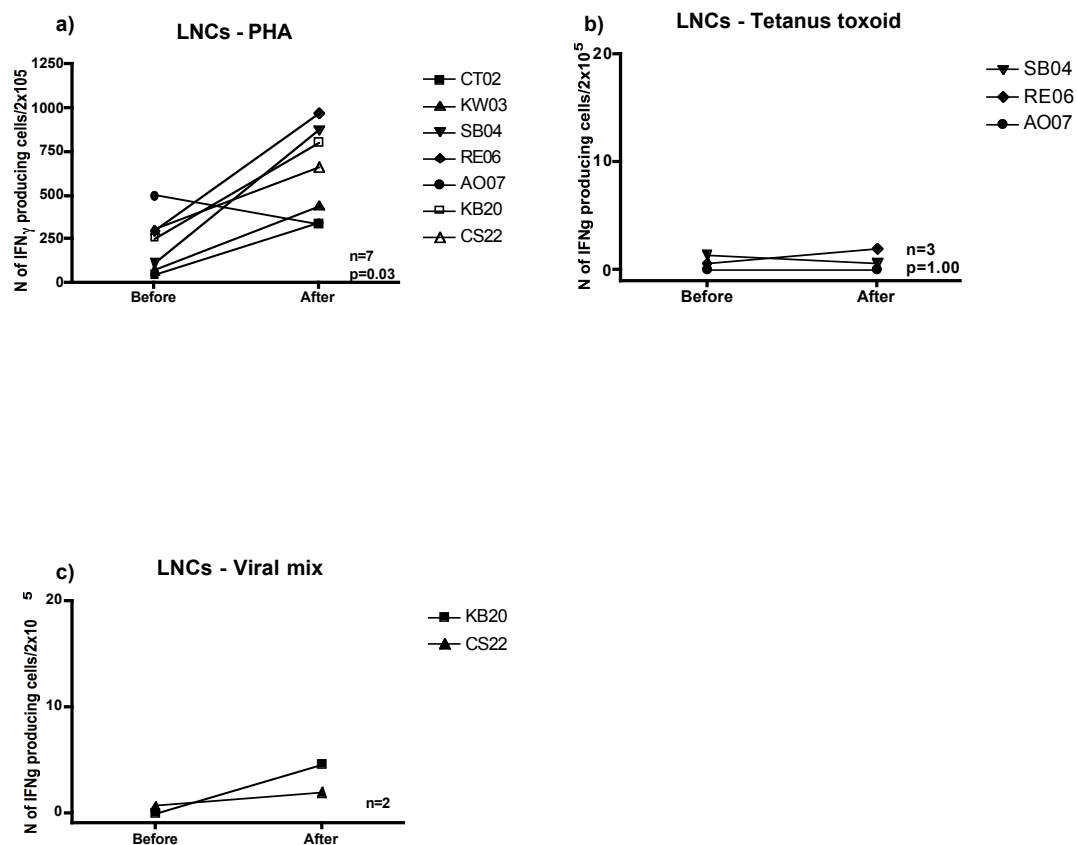


Figure 5-17. Summary of the ELISPOT response of LNCs to *in vitro* PHA, Tetanus toxoid and viral mix before and 48h after *in vivo* Tuberculin PPD injection. a) Response to PHA (n=7, p=0.03); b) Response to tetanus toxoid (n=3, p=1.00); c) Response to viral mix of CMV, ENV and flu peptides (n=2). The response of the each subject is shown as connected before-after points. Subjects' codes are shown in the legend. Statistical test used: Wilcoxon signed ranked test.

At the same time, I detected a response to Tetanus toxoid and the mix of viral peptides in the blood of the matching individuals, suggesting validity of the ELISPOT assay in subjects with immunity against these antigens. It remained unchanged before and after Tuberculin PPD injection – Figure 5-18.

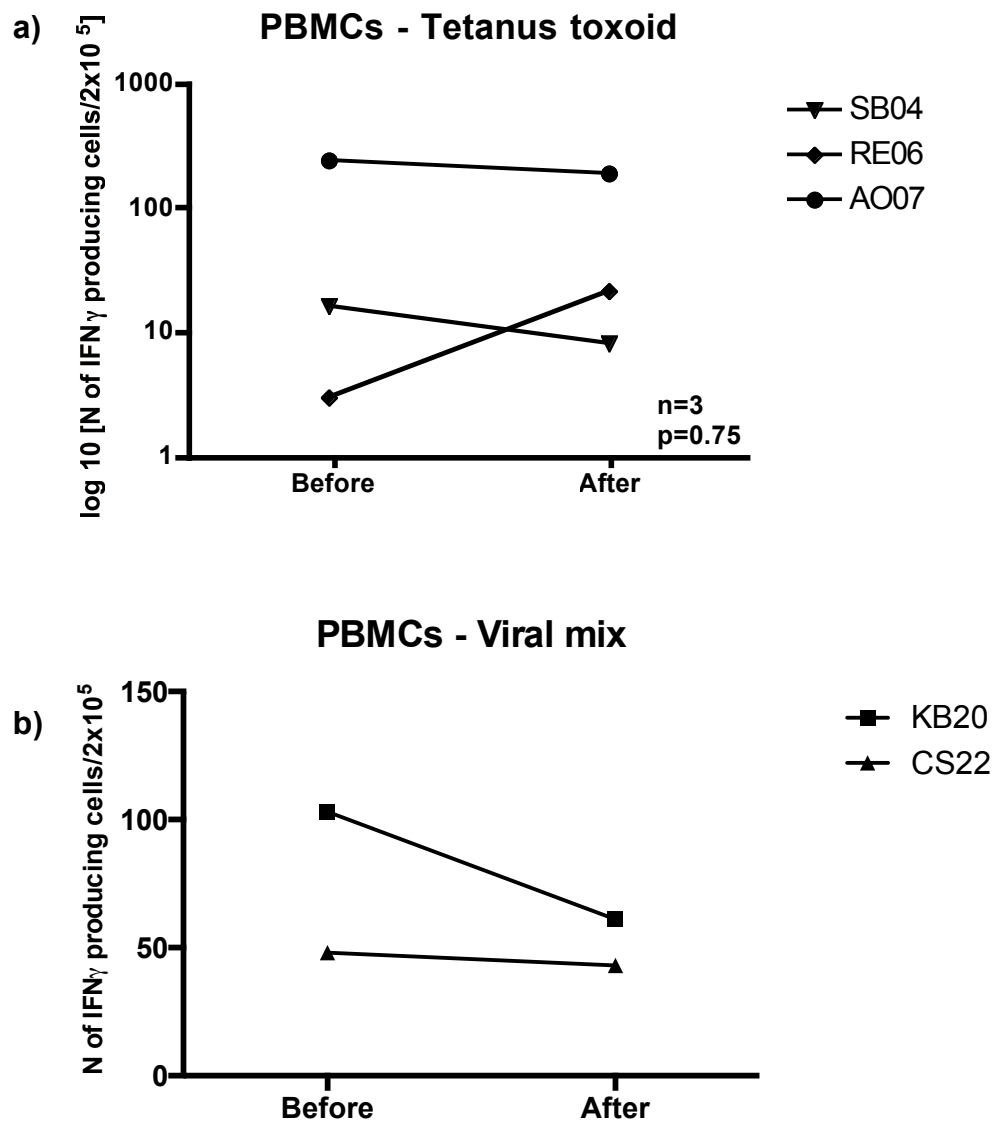


Figure 5-18. Summary of the ELISPOT response of PBMCs to *in vitro* control antigens before and two days after *in vivo* Tuberculin PPD injection. a) Tetanus toxoid ($n=3$, $p=0.75$). Statistical test used: Wilcoxon signed ranked test; b) Mix of the flu, CMV and EBV derived peptides ($n=2$). The response of the each subject is shown as connected before-after points. Subjects' codes are shown in the legend.

The response of PBMCs to PHA was very often so extensive that it was not possible to count (Figure 5-14, Figure 5-15), either manually or with a Bioreader, and therefore is not shown in the graphs.

5.4.2.3 Flow cytometry analysis

I used flow cytometry to assess changes in the number and profile of lymph node derived T cells and HLA-DR⁺ cells in comparison to their blood derived counterparts, before and two days after Tuberculin PPD injection.

With limited number of replicates (n=3), there was no change in the CD4⁺:CD8⁺ ratio after Mantoux test, neither in LNCs (Figure 5-19a) nor PBMCs (Figure 5-19b).

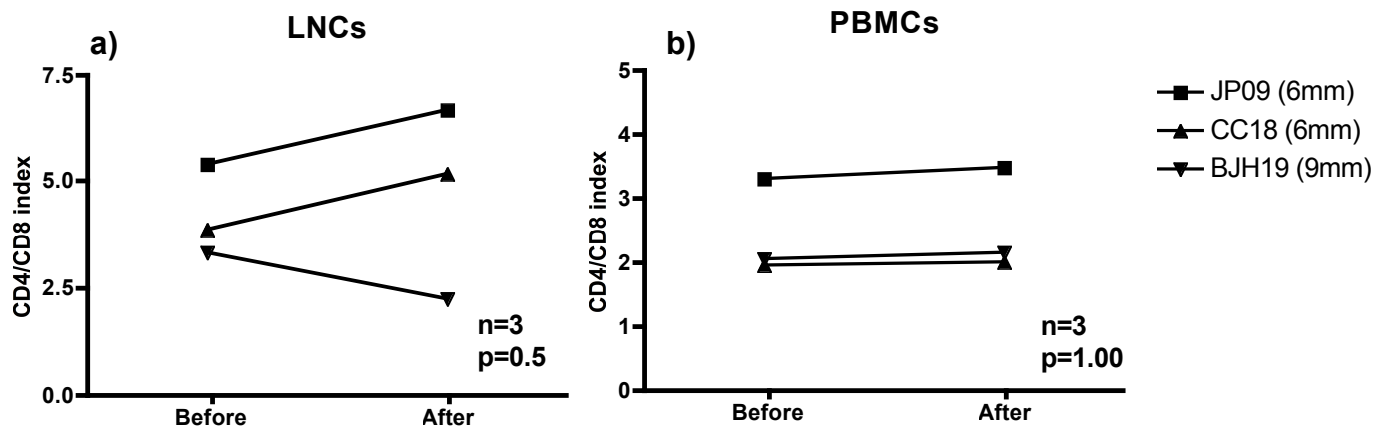


Figure 5-19. CD4⁺/CD8⁺ ratio before and two days after Tuberculin PPD. The ratio of the each subject is shown as connected before-after points. Subjects' codes with their Montoux response in brackets are shown in the legend. a) LNCs, n=3, p=0.5; b) PBMCs, n=3, p=1.00. Statistical test used: Wilcoxon signed ranked test.

There was no significant difference in the overall expression of marker CD69 in either blood or lymph node derived CD4⁺ or CD8⁺ cells, measured as MFI –

Table 5-2.

CD69 MFI	BEFORE	AFTER	n	p
CD4 ⁺ LNCs	625.7±244.0	450±81.59	3	1.00
CD8 ⁺ LNCs	373.3±175.0	241.3±104.9	3	1.00
CD4 ⁺ PBMCs	109.4±16.3	116.5±28.8	3	1.00
CD8 ⁺ PBMCs	137.3±21.5	144.7±41.0	3	1.00

Table 5-2. CD69 expression calculated as MFI on blood derived and lymph node derived T cells. Statistical test used: Wilcoxon signed ranked test.

The previously described large LN derived CD69⁺ population, appeared to show an increase in percentage two days after Tuberculin PPD injection, although with the small numbers tested, this did not reach statistical significance. No such a trend was observed in the blood – Figure 5-20, Figure 5-21.

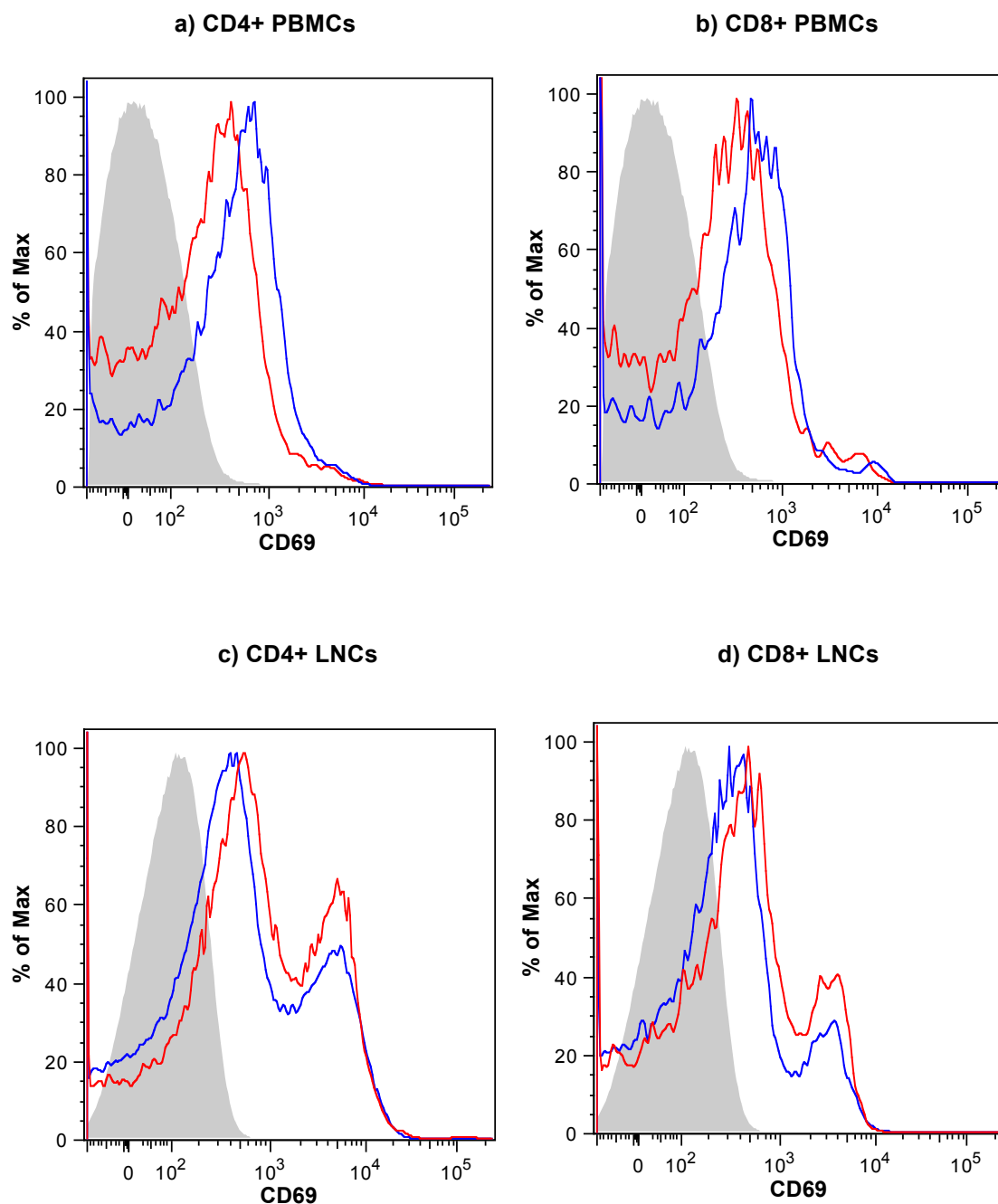


Figure 5-20. Representative example of CD69 expression on blood and lymph node derived T cells before and two days after Tuberculin PPD injection. Gates: gray solid – unstained live cells; blue line – baseline; red line – two days after Tuberculin PPD injection. a) CD4⁺PBMCs; b) CD8⁺ PBMCs; c) CD4⁺ LNCs; d) CD8⁺ LNCs.

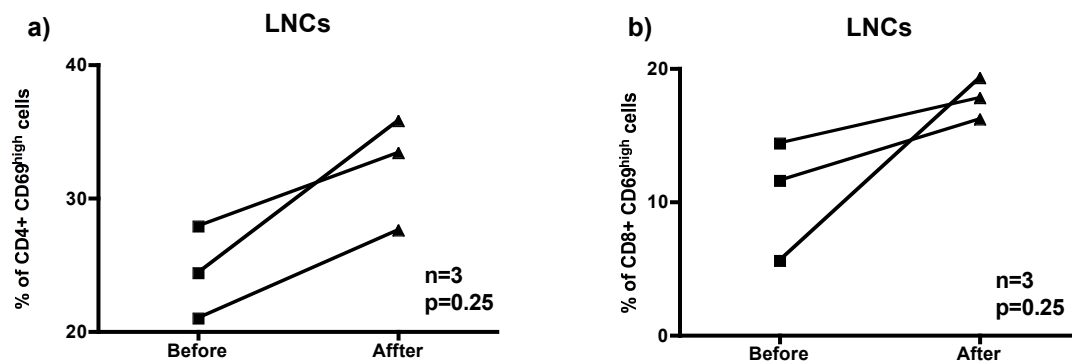


Figure 5-21. Percentage of CD69⁺ cells on lymph node derived T cells before and two days after Tuberculin PPD injection. a) CD4⁺ cells; b) CD8⁺ cells. Statistical test used: Wilcoxon signed ranked test

Expression of another activation marker, CD154, was generally low in both blood derived and lymph node derived T cells, with no increase after Tuberculin PPD injection – Table 5-3.

CD154 MFI	BEFORE	AFTER	n	p
CD4 ⁺ LNCs	62.2±27.6	45.3±18.3	3	0.75
CD8 ⁺ LNCs	29.8±45.5	9.6±16.6	3	0.75
CD4 ⁺ PBMCs	89.9±46.0	71.8±20.0	3	1.00
CD8 ⁺ PBMCs	66.0±47.6	53.5±25.6	3	1.00

Table 5-3. CD154 expression calculated as MFI on blood derived and lymph node derives T cells. Statistical test used: Wilcoxon signed ranked test.

I also did not observe any significant changes in the expression of HLA-DR on both B-cells (CD19⁺ HLA DR⁺ cells) or other HLA-DR expressing cells (CD19⁻ HLA-DR⁺ cells) – Table 5-4.

HLA DR MFI	BEFORE	AFTER	n	p
CD19 ⁺ HLA DR ⁺ LNCs	35531±4578	24048±8416	3	0.25
CD19 ⁺ HLA DR ⁻ LNCs	15660±5698	7672±1527	3	0.25
CD19 ⁺ HLA DR ⁺ PBMCs	24189±2931	21951±5981	3	0.59
CD19 ⁺ HLA DR ⁻ PBMCs	18256±873	16992±4451	3	0.75

Table 5-4. HLA-DR expression calculated as MFI on blood derived and lymph node derives T cells. Statistical test used: Wilcoxon signed ranked test.

5.4.3 Response after five days of Tuberculin PPD injection

5.4.3.1 Lymph node size

There was no significant increase in the ultrasonographically measured thickness of the lymph node cortex (before: 0.20 ± 0.04 cm; five days after: 0.22 ± 0.06 cm) – Figure 5-22.

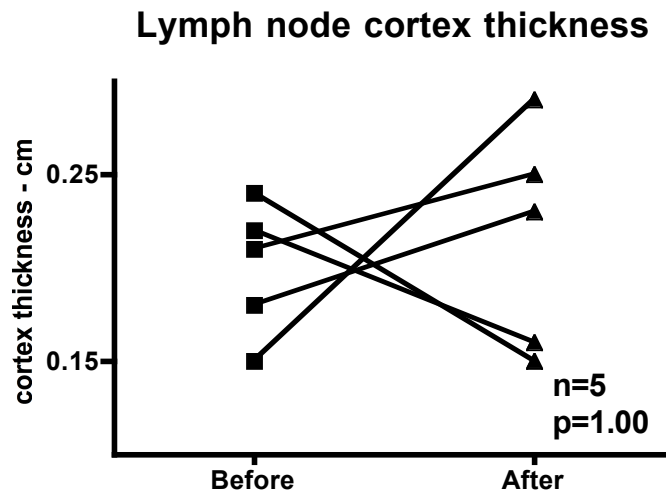


Figure 5-22. Lymph node thickness at baseline and five days after Mantoux test. Statistical test used: Wilcoxon signed ranked test.

5.4.3.2 ELISPOT

As with the two day time point, I again used the ELISPOT assay to detect IFN- γ producing cells amongst lymph node cells (LNCs) and PBMCs collected before and five days after Tuberculin PPD injection. This was performed in the separate group of subjects.

Contrary to the two day time-point, after five days of Tuberculin PPD injection, I did not detect an increase in IFN- γ producing cells in the LNCs suspension, in any, except one replicate – Figure 5-23 a. There was also no significant change in the blood - Figure 5-23 b.

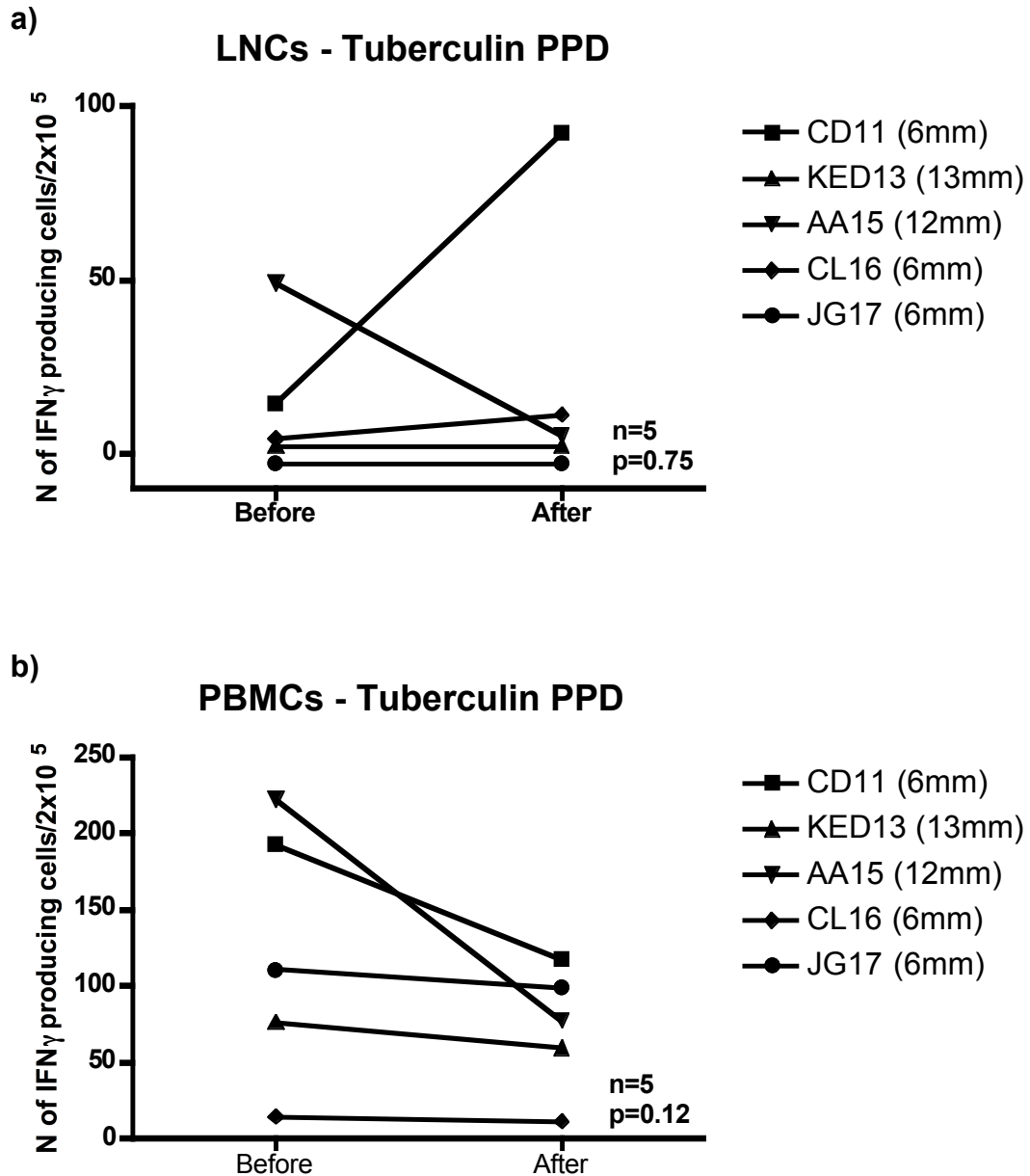


Figure 5-23. Summary of the ELISPOT response to *in vitro* Tuberculin PPD before and five days after *in vivo* injection. a) Number of IFN- γ producing cells per 2×10^5 cells from the lymph node aspirate before and five days after Tuberculin PPD injection (n=5, p=0.75); b) Number of IFN- γ producing cells per 2×10^5 PBMCs before and five days after Tuberculin PPD injection (n=5, p=0.12). The response of the each subject is shown as connected before-after points. Subjects' codes with their Mantoux response in brackets are shown in the legend. Statistical test used: Wilcoxon signed ranked test.

A consistent change of the non-specific response to PHA was lacking after five days (Figure 5-24a), which was also the case with the response to tetanus toxoid (Figure 5-24b).

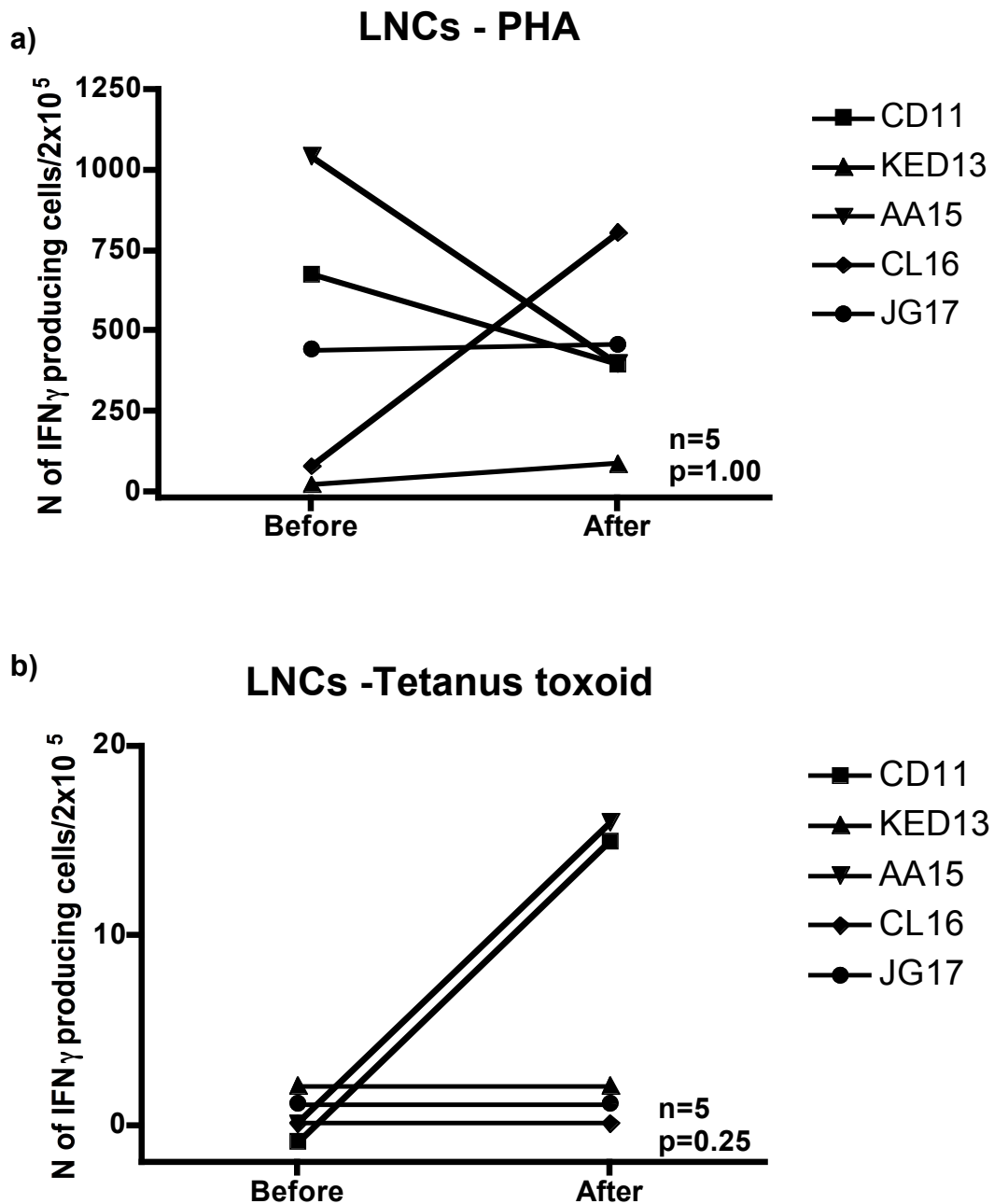


Figure 5-24. Summary of the ELISPOT response of LNCs to *in vitro* PHA and Tetanus toxoid before and five days after *in vivo* Tuberculin PPD injection. a) Response to PHA (n=5, p=1.00); b) Response to tetanus toxoid (n=3, p=0.25). The response of the each subject is shown as connected before-after points. Subjects' codes are shown in the legend. Statistical test used: Wilcoxon signed ranked test.

Again, I detected a response to Tetanus toxoid in the blood, which remained unchanged before and five days after Tuberculin PPD injection –

Figure 5-25.

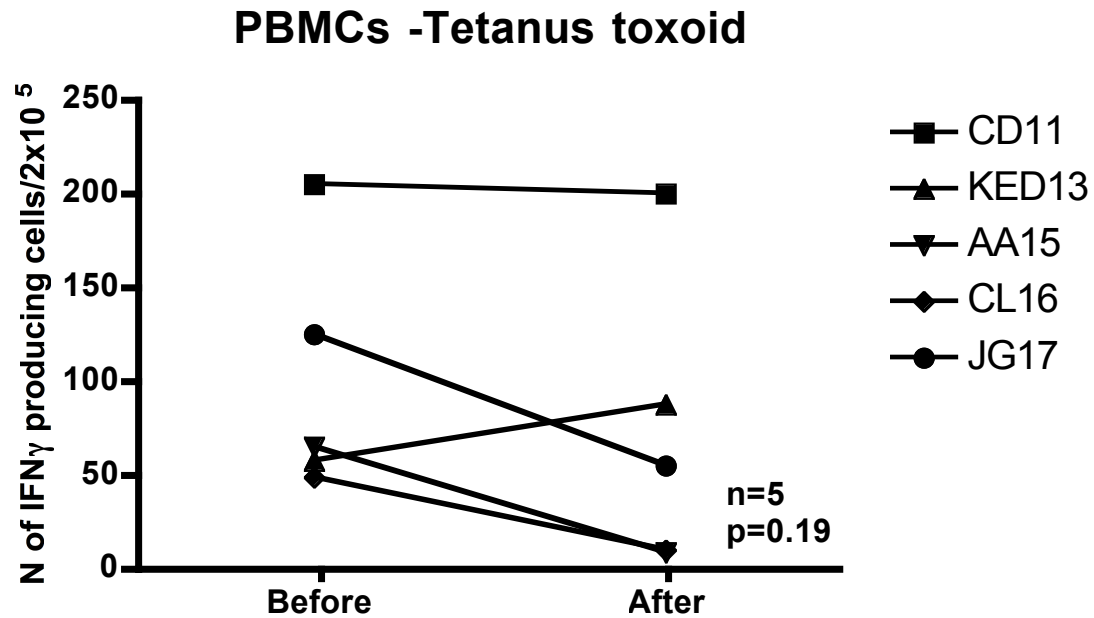


Figure 5-25. Summary of the ELISPOT response of PBMCs to *in vitro* Tetanus toxoid before and five days after *in vivo* Tuberculin PPD injection. n=3, p=0.19; The response of the each subject is shown as connected before-after points. Subjects' codes are shown in the legend. Statistical test used: Wilcoxon signed ranked test.

5.4.4 Mantoux negative subjects

Five subjects had a Mantoux negative test. They only had baseline investigations (two flowcytometry and five ELISPOT), without a post-treatment sample. Flowcytometric analysis performed in two individuals was included in the analysis of profile of LN cells presented in the beginning of this chapter. Other five subjects had baseline IFN γ ELISPOT.

At baseline, before *in vivo* challenge, I detected PPD specific IFN γ producing cells in the blood, even in Mantoux negative individuals – Figure 5-26.

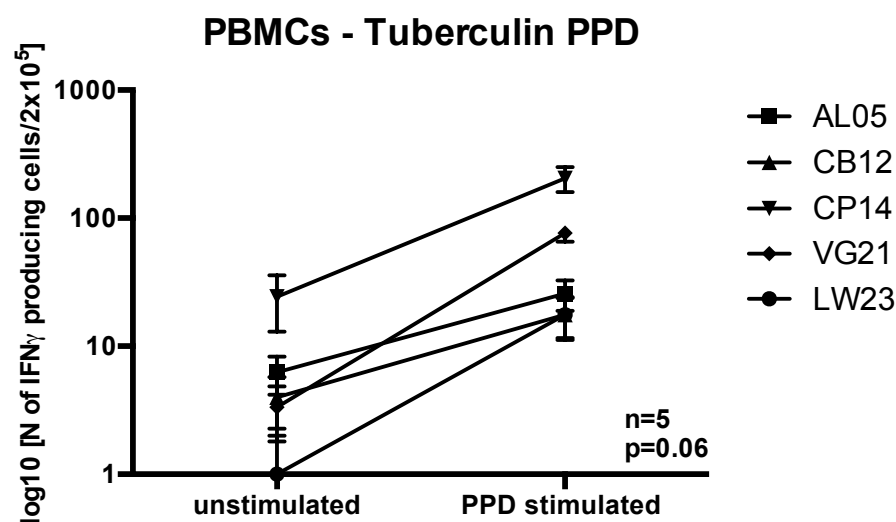


Figure 5-26. Summary of the baseline ELISPOT response of PBMCs to *in vitro* Tuberculin PPD at in Mantoux negative subjects. n=5, p=0.06; The response of the each subject is shown as connected before-after points. Subjects' codes are shown in the legend. Statistical test used: Wilcoxon signed ranked test.

5.5 Summary of findings

-
- 1 Ultrasound guided lymph node fine needle aspiration is minimally invasive procedure that provides a sufficient number of live and functional T cells for phenotypic analysis and functional assays.
 - 2 Hollow microneedle is reliable device for intradermal delivery of Tuberculin PPD.
 - 3 Fine needle aspiration of the lymph node is superior tool to the blood sampling, for the monitoring of the dynamics of the antigen-specific immune response following antigen skin delivery.
-

The results presented here show that lymph node fine needle aspiration provides a sufficient number of live and functional T cells to detect the cellular immune response after antigen skin delivery.

The hollow microneedle is an efficient intradermal delivery device as evidenced by clinically measurable and significant immune responses to Tuberculin PPD i.e. positive Mantoux test in 15 out of 22 treated subjects. The failure to elicit positive Mantoux test in 31% of participants is expected in the general British population with variable history of BCG vaccination and generally low exposure to *M. tuberculosis*.

Monitoring the early response in the draining lymph node following *in vivo* injection of Tuberculin PPD seems to provide more sensitivity than conventional monitoring in the blood.

Responses detected in blood most likely come from the PPD specific effector memory or even T_{EMRA} cells capable of rapid production of IFN γ . These cells patrol in the peripheral circulation of sensitive individuals in abundance (up to 1 in 1000 of PBMCs). The high baseline frequency of these cells prevented detection of possible small early changes after *in vivo* challenge. I and others

detected baseline IFN γ response even in the Mantoux negative individuals, which suggest a different origin and/or phenotype of cells involved in the skin response.[269]

Contrary to the peripheral circulation where the frequency of Tuberculin PPD specific IFN γ secreting cells was high, a low frequency of these cells at baseline in the lymph node and their accumulation following antigen challenge made their efficient detection possible.

Low level of the IFN γ production at baseline from the lymph node derived cells suggests an absence of effector memory in the lymph node. This was the case not only in response to Tuberculin PPD, but also to the control antigens, tetanus toxoid and mixed flu, EBV and CMV derived peptides. In both cases, this once again, contrasted with high levels of IFN γ producing cells responding to the same antigens in the same individual's peripheral blood. I can not exclude the possible need for longer cultures to prime lymph node T cells, as indicated in the study looking at baseline response to Tuberculin PPD where authors performed 7 days long incubations, rather than the overnight *in vitro* incubation, that I used in this study.[270]

I consistently detected an increase in PPD specific IFN γ producing LN cells two days after skin challenge in all six subjects included. An increase in the diameter of the lymph node cortex and the concomitant increase in the PHA response raised the possibility of non-specificity. One can speculate that there is a high level of baseline activation in the lymph node tissue, which may explain enhanced response to PHA after additional priming by potent adjuvant present in the Tuberculin PPD.

However, the lack of the amplification to the control antigens, tetanus toxoid and mix of viral peptides, argues that the final response is specific. Interestingly, five days after *in vivo* Tuberculin PPD, the increase in IFN γ producing LN cells was no longer consistent in all individuals. – Figure 23.

It is important to take into account the complex relationship between the skin, its draining lymph node and the peripheral blood to understand the type and phase of the response that is being captured by LN FNA.

This raises the question of the origin of the IFN γ that is being detected the lymph node two days after Tuberculin PPD challenge. It is unlikely to be the result of activated naïve cells, as this process requires a longer time. It is possible that one of the responses happening in the lymph node is the activation of central memory cells that recognise antigen on skin deriving DCs. Indeed, the majority of CLA expressing cells in the lymph node and blood are central memory cells that might have arrived in the lymph node via skin. However, this would be less likely to be detected by measuring IFN γ because central memory cells produce IL-2 rather than IFN γ upon activation.[252] The production of IFN γ suggests effector memory response, but it is not clear where these cells are coming from. Effector cells usually do not arrive to the lymph node directly from the blood, as they do not express CCR7 necessary for homing to the LN through HEV. It is more likely that these are effector cells arriving from the skin that are either *in situ* skin memory cells or blood derived memory cells, which travelled to the lymph node via skin. It is possible that they patrol in the blood, home in the skin guided by appropriate homing receptors, the expression of which is reduced once there. Some of these cells possibly continue to the regional lymph node where I saw reduced expression

of the skin homing receptors. The only significant difference that I observed to support this speculation was in the CD8⁺ population where I saw significant difference between expression of CLA and CCR4 amongst CD8⁺ cells, in favour of the blood.

Absence of CLA expression in the PPD specific blood cells in TB sufferers with negative Mantoux suggests that cells responsible for the skin reaction originate from the blood. It would be interesting to monitor parallel response in the lymph node in these individuals, which would certainly bring some light into the origin of PPD specific cells appearing early after antigen challenge in my study.[268]

Temporal histological changes in the skin following Mantoux test suggest that proliferating T cells appear at the site within 12 hrs, reaching their peak 7 days later.[133] Analysis of the cells generated through suction blister technique following Mantoux test, suggested that T cells start to reduce CLA expression approximately seven days after antigen challenge. At the same time, IFN γ and IL-2 production by PPD specific cells is again detected only at day seven. These data suggest that significant emigration from the skin, possibly of IFN γ and IL-2 producing cells happens at least 5-7 days after antigen challenge.[271] It remains unclear why this does not mirror the changes that I detected in the lymph node, i.e. consistent response after two days, tailing off end after five days. Possible explanations are that: 1) I was detecting “early bird” effector cells, and more would have been captured if a longer time after Mantoux was allowed, i.e. seven days and more; 2) antigen bearing DCs arrived early in the lymph node and activated local effector cells or blood derived ones, attracted by the presence of antigen in the LN. This latter option

is less likely given that absence of the CCR7 expression on the blood effector T cells. The possible scenarios of the skin-lymph node conversation following antigen skin delivery is summarised in the Figure 5-27.

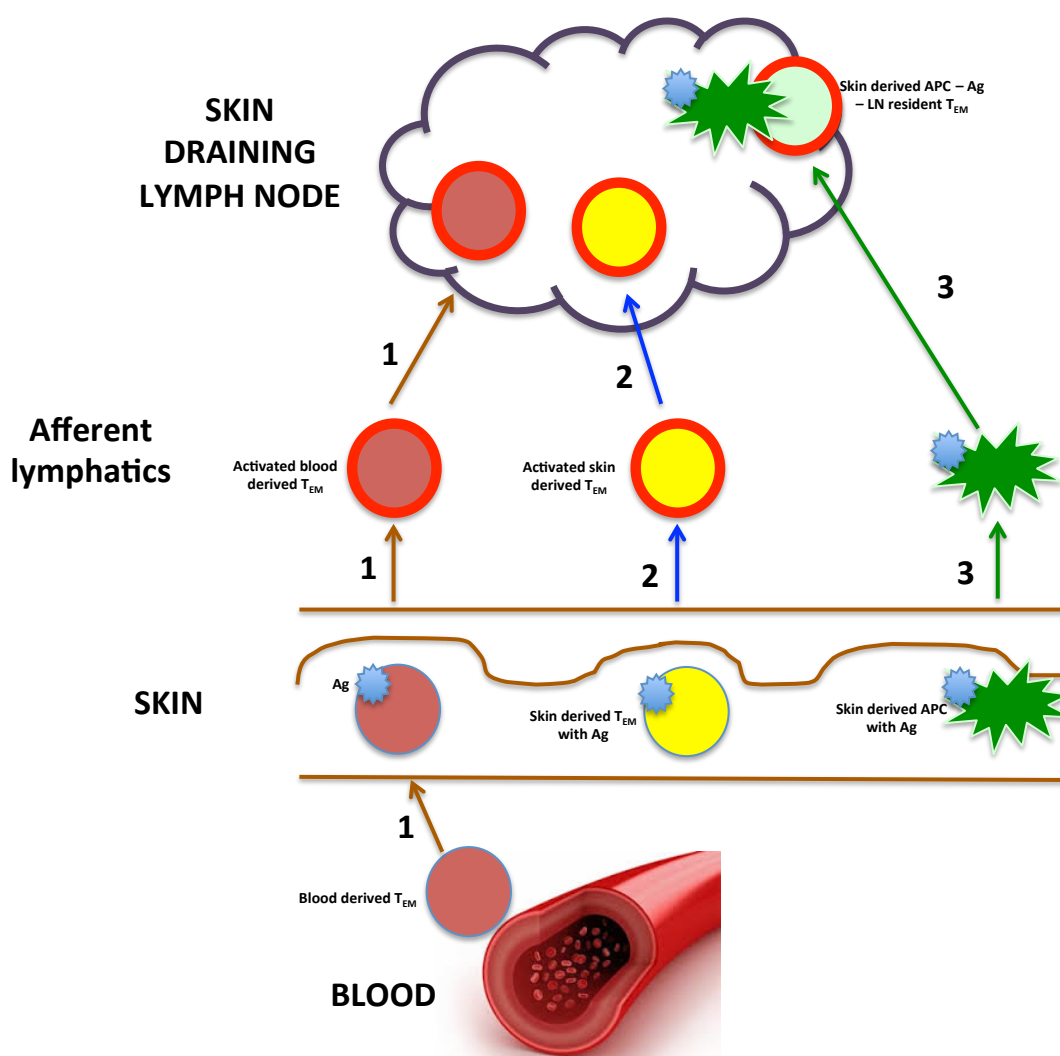


Figure 5-27. Interplay between skin and its regional draining lymph node following antigen skin delivery. 1) Arrival of blood derived T cells upon encounter with the antigen in the skin; 2) Arrival of skin derived T cells upon *in situ* activation by an antigen; 3) Antigen bearing skin DCs travel to LN where they activate local effector T cells. T_{EM}- effector T cells; Ag- antigen; APC – Antigen presenting cells.

LN FNA after Tuberculin PPD skin delivery allowed us a glimpse into the interplay between skin and its draining lymph node. Whether this technique will be equally successful in monitoring immune response after peptide

immunotherapy will be a subject of the future work. Contrary to the situation with the Tuberculin PPD, the frequency of self-antigen specific T cells in the peripheral circulation is low and often undetectable even with most sensitive methodology such as ELISPOT. Aggregation of activated antigen specific cells in the draining lymph node, coupled with the very low background response that I observed with the PPD challenge, could make the efficient detection possible.

Another difference to consider is the nature of the response following self-antigen challenge that will no doubt involve memory cells, Tregs and skin DCs. The abundance of a wide repertoire of memory cells and Tregs in the skin together with dendritic cells accessible to modulation towards tolerogenic antigen delivery is the solid basis for this expectation. However, this leaves us with the question, which part of this process will continue or happen in parallel in the regional lymph node, and what can we measure to help us in optimising the delivery antigen-specific immunotherapy without waiting for disease modulation.

The focus will be on detection of the tolerogenic self-antigen bearing skin DCs; memory cells, either resident or skin derived and/or Tregs, activated by resident or by migratory DCs or skin derived Tregs activated by locally injected self-antigen.

Chapter 6 NON-INVASIVE ASSESSMENT AND MONITORING OF CHANGES IN β -CELL FUNCTION

6.1 Introduction

Assuming the right type and the right delivery of the immune therapy, as well as the correct way of monitoring immune response following intervention, which has been discussed in previous chapters, the final piece in the jigsaw for this process, is knowing how to effectively monitor metabolic outcome.

Progressive β -cell destruction in type 1 diabetes leads to near absolute insulin deficiency. We now know that years of ongoing immunological attack, eventually lead to the metabolic abnormalities, starting with attenuated first phase insulin response (FPIR) approximately 1.5 to 5 years before diagnosis.[3] At the time of clinical presentation, it is estimated that 50-80% of β -cell function has been lost.[4] Further from this point, it seems that metabolic and immunological processes are different in the first year since clinical presentation, during which there is a steeper slope of β -- cell function loss (measured by standard MMTT), in comparison to the slower one during the second year. [5]

While less than 1% of subjects with Type 1 diabetes have levels of endogenous β -cell function above the fifth percentile for healthy individuals after 5 years, multiple cross-sectional studies and retrospective analysis of the Diabetes Control and Complication Trial (DCCT) cohort has repeatedly demonstrated the benefits of preservation of even minor levels of β -cell function [272], in regards to better control measured as HbA1c [273], less hypoglycaemia [274], less diabetic ketoacidosis [275] and reduced long-term complications [276, 277].

With a view to assessing the future potential of new treatments for Type 1 diabetes, there is a need for a simple, non-invasive, test for estimation and monitoring of the residual β -cell function in these patients. We are looking for the test that is sensitive enough to detect changes in the β -cell function over the time, and at the same time patient-friendly to allow frequent and repeated measurements in even a paediatric population. That will enable close monitoring and the detection of even subtle β -cell function changes that would prompt the intensification, the re-start or the change of the immunological intervention type. The concept of the treatment modification should be very similar to what has been happening for decades in cancer intervention, where the detection of the disease relapse quickly leads to the change of the treatment protocol.

6.1.1 Measuring residual β -cell function

Insulin production is complex and involves several steps. The final step includes cleavage of a larger precursor molecule into insulin and free C-peptide.[278] As a result, C-peptide is stored and realised in equal amounts with insulin. Unlike insulin, 50% of which is removed in the first pass through the liver, C-peptide is predominantly metabolised in the kidney, with, importantly, small but significantly measurable amounts passing into the urine. C-peptide has a half-life around six times longer than insulin, allowing it to circulate at around five times the concentrations of insulin. For this reason, it can be readily measured in both plasma and urine.

Tests that estimate β -cell function are currently used mainly as a research tool and include:

1	Fasting plasma C-peptide
2	Peak stimulated plasma C-peptide (glucagon or standardised mixed meal stimulation)
3	Area under the curve plasma C-peptide (following stimulation)
4	Urinary C-peptide

Although most convenient, fasting C-peptide seems to be relatively insensitive to the decline in stimulated insulin reserve around the time of diagnosis of Type 1 diabetes.[279]

Stimulated plasma C-peptide values seem to correlate well with number of functional islet cells in islet cell auto-transplantation studies.[280] C-peptide stimulation tests mainly include glucagon and mixed-meal stimulation, which correlate well. Although more time consuming, mixed meal tolerance test (MMTT) seem to be more reproducible and achieves higher levels of C-peptide.[281] Area under the curve rather than peak C-peptide is the standard for monitoring β -cell function in clinical trials, but the longer half-life of C-peptide compared to insulin means that C-peptide measurements may overestimate insulin secretion rates.[282]

Urinary C-peptide measurements are less invasive. Twenty-four hour urinary C-peptide measurements are shown to accurately assess β -cell secretory capacity and correlate with fasting and stimulated insulin and C-peptide.[283-286] On the other hand, they are impractical and often inaccurate in the non-observed setting. Post-mixed meal stimulated urinary C-peptide correlates

with serum insulin and plasma C-peptide in both non-diabetic [287] and insulin-treated diabetic patients [288].

It has been shown that second-void urinary C-peptide is a reproducible test, which correlates well with 24 hour urinary C-peptide, in healthy subjects. [289] An important question is whether this test is suitable for estimation of already depleted β - cell function in patients with diagnosed Type 1 diabetes and whether it can be used to track the change over time, which to my knowledge hasn't been addressed thus far.

Besser et al. reported that the two-hour urinary C-peptide response to a mixed meal correlates well with the standard MMTT, and hence can be used for estimation of β - cell reserve in patients with type 1 diabetes [131]. The ratio of urinary C-peptide to creatinine (UCPCR) was used to avoid the need for timed urine collections (UCPCR). In addition, the authors showed strong correlation between UCPCR stimulated by standard mixed meal and usual home meal without omitting regular insulin dose, which further simplifies the test, making it more acceptable for patients.

6.1.2 Practical application of tests for estimation of residual β -cell function

Tests that are described above are mainly research tools. Estimation of β -cell function is not routinely performed in the clinical management of Type 1 diabetes as the standard tests are invasive, time consuming and burdensome for patients. However, if a simple and reliable assessment were available, it would potentially have the following applications:

(1) to identify those individuals with very low levels of β -cell function in whom tight glycaemia control will be difficult to achieve, and who are at particular

risk of ketoacidosis[290] – this information may help guide choices of insulin treatment regimes and glycaemic targets

(2) to identify those patients with significant residual β -cell function to target for future β -cell protection therapies

(3) to sequentially monitor β - cell function to identify those patients who are losing β - cell function rapidly and prioritise them for immunointervention treatments, such as rituximab [107] and CTLA-4 IG [106]. This group is a particular priority, as rates of β - cell destruction vary widely and at present the predictors of disease progression are not robust [291].

(4) to monitor the response to immunointervention and perhaps detect benefit or the need for repeated intervention at an early stage.

Stimulated UCPCR is a good candidate test for this purpose, but there is no data to suggest that it is sensitive enough to detect loss of β -cell function in Type 1 diabetes over time. In particular, it would be of value to identify rapid progressors early – within 6 months if possible - to target intervention. The non-invasive nature of UCPCR testing provides the potential for repeated testing over time, which may be particularly valuable for early assessment of disease progression.

6.2 Hypothesis

I hypothesise that stimulated UCPCR is a reliable test for estimation and monitoring of the changing β - cell function over time.

6.3 Aims

1. To confirm in our center that standard mixed-meal stimulated UCPCR correlates well with gold standard MMTT.
2. To determine whether stimulated UCPCR can be used to monitor changing β - cell function over time.
3. To determine which form of stimulation is optimal for this purpose.

6.4 Results

6.4.1 Main study

Seventeen non-obese, adult patients with type 1 diabetes (duration of ≤ 5 years) were recruited in the Bristol area (UK), through the South West Newly Diagnosed Diabetes Collection database, after signing informed consent. Inclusion criteria: age 18-45 years, normal renal function, HbA1c < 10% (86 mmol/mol), daily insulin requirement of < 0.8 units/kg/day and detectable β -cell function measured at a post-meal UCPCR. Detailed methods are described in Chapter 2. Abbreviations used are shown in Table 6-1.

Abbreviation	Explanation
MMTT	Mixed Meal Tolerance Test
UCPCR	Urine C-peptide creatinine ratio
MM	Mixed meal
uCP	Urinary C-peptide
sCP	Serum C-peptide

Table 6-1. Abbreviations of the parameters used in the study.

Out of 17 eligible patients that were recruited into the study (13 males and 4 females), 16 completed the initial MMTT in hospital. Detailed progress of the study in terms of number of patients is shown in the flow diagram in Figure 6-1:

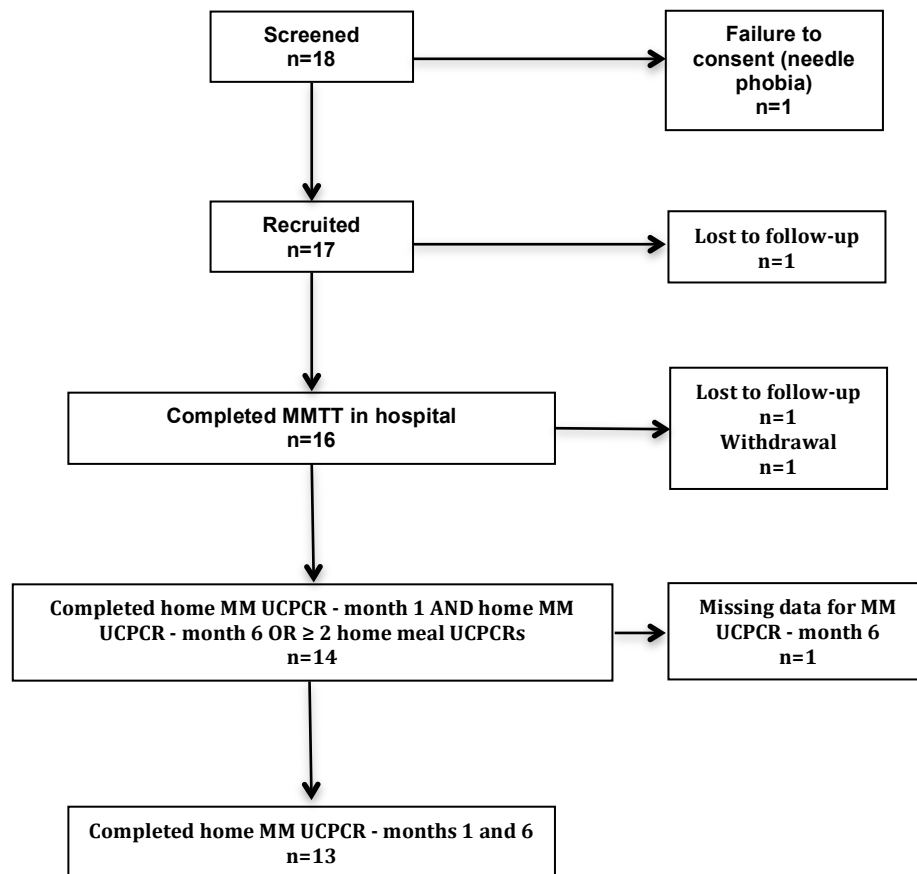


Figure 6-1. Flow-diagram of participants' progress during the study.

Demographic and clinical characteristics of the patients are shown in Table 6-2.

Age (years)	33.6±5.8
BMI (kg/m ²)	25.7±3.2
Duration of diabetes (years)	2.1±1.5
HbA1c (%(mmol/mol))	6.7±1.0 (50.1±11.1)
Daily insulin requirements (U/kg/day)	0.44±0.18
Peak C-peptide during MMTT (pmol/l)	918.00±994

Table 6-2. Demographic and diabetes related characteristics of the patients on entering the study.

6.4.1.1 Standard mixed meal stimulation of β -cell insulin production

Serum C-peptide (sCP) and glucose response to Ensure is shown in Figure 6-2. Participants with high C-peptide response demonstrated the most well-controlled and stable glucose levels over the 120 min of MMTT, and vice versa.

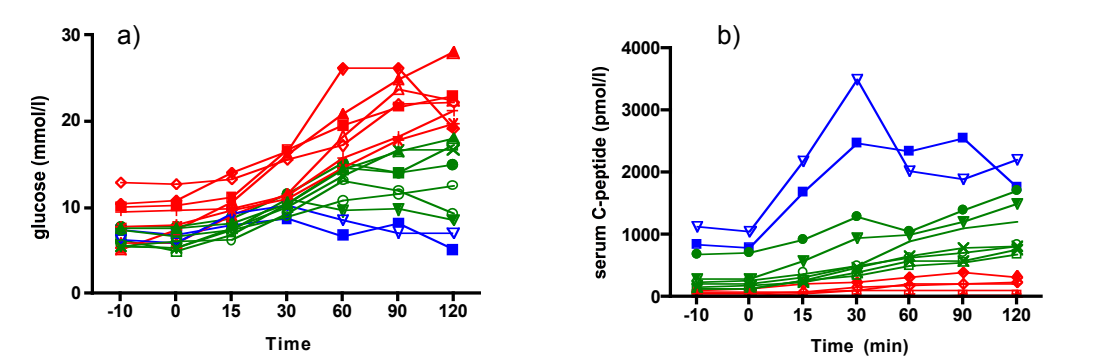


Figure 6-2. Serum C-peptide and glucose levels during 120 min of MMTT. a) glucose response b) serum C-peptide response; red lines – poor responders; green lines – intermediate responders; blue – good responders; n=16.

Peak sCP during the standard MMTT correlated strongly with the AUC sCP ($r=0.99$, 95% CI:0.97-0.99, $p<0.0001$, $n=16$) and was used as a representative estimate for β -cell insulin production (Figure 6-3).

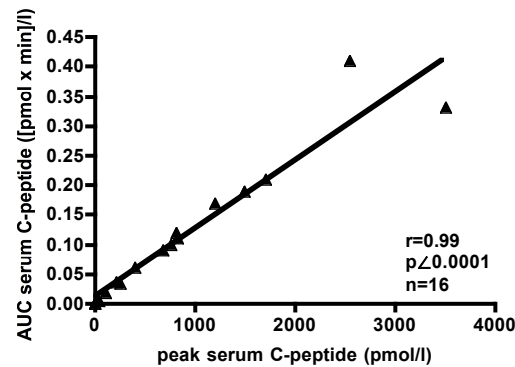


Figure 6-3. Peak serum C-peptide and AUC serum C-peptide during MMTT; AUC – area under the curve. Statistical test used: Spearman correlation.

Peak sCP during MMTT correlated well with the two-hour UCPCR done on the same occasion ($r=0.81$, 95% CI:0.51-0.93, $n=16$, $p=0.0002$, Figure 6-4 a), as well as the home MM-UCPCR month 1 measurement ($r=0.89$, 95% CI:0.69-0.96, $n=15$, $p<0.0001$, Figure 6-4 b). There was no significant difference between hospital MM-UCPCR and home MM-UCPCR month 1, undertaken 26.8 ± 14.1 days apart ($1.29\pm1.11\text{nmol/mmol}$ vs $0.96\pm0.97\text{nmol/mmol}$, respectively; $p=0.06$, $n=15$).

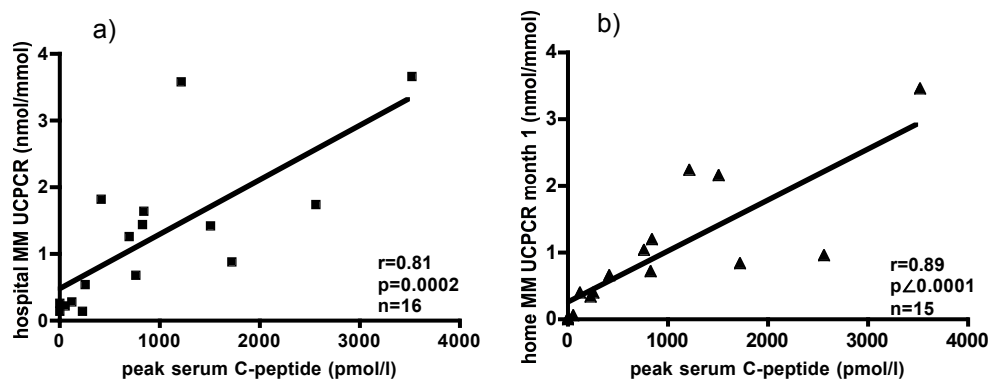


Figure 6-4. Correlation between peak serum C-peptide and MM-UCPCR. a) hospital based test; b) home based test. Statistical test used: Spearman correlation.

Peak sCP during MMTT correlated less well with the fasting UCPCR collected on the same occasion ($r=0.74$, 95% CI: 0.38-0.91, $n=16$, $p=0.001$, Figure 6-5).

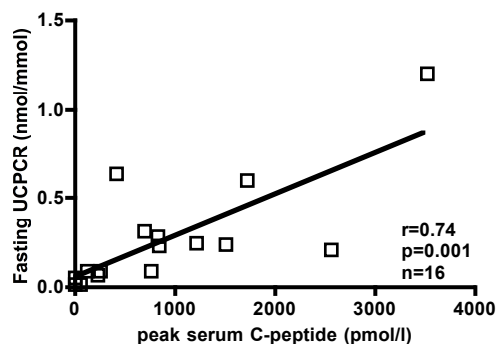


Figure 6-5. Correlation between peak serum C-peptide and fasting UCPCR measured from second morning void sample. Statistical test used: Spearman correlation.

6.4.1.2 Correlation of hospital MM UCPCR with the diabetes related parameters

Hospital MM UCPCR significantly negatively correlated with the patients' daily insulin requirements ($r=-0.76$, 95%CI: -0.92 to -0.42-, $n=16$, $p=0.0006$), but there was a non-significant (negative) trend only with HbA1c level ($r=-0.45$, 95%CI: -0.78 to 0.08, $n=16$, ns), with no definite correlation with time since diagnosis ($r=-0.29$, 95%CI: -0.69 to 0.26, $n=16$, ns) – Figure 6-6.

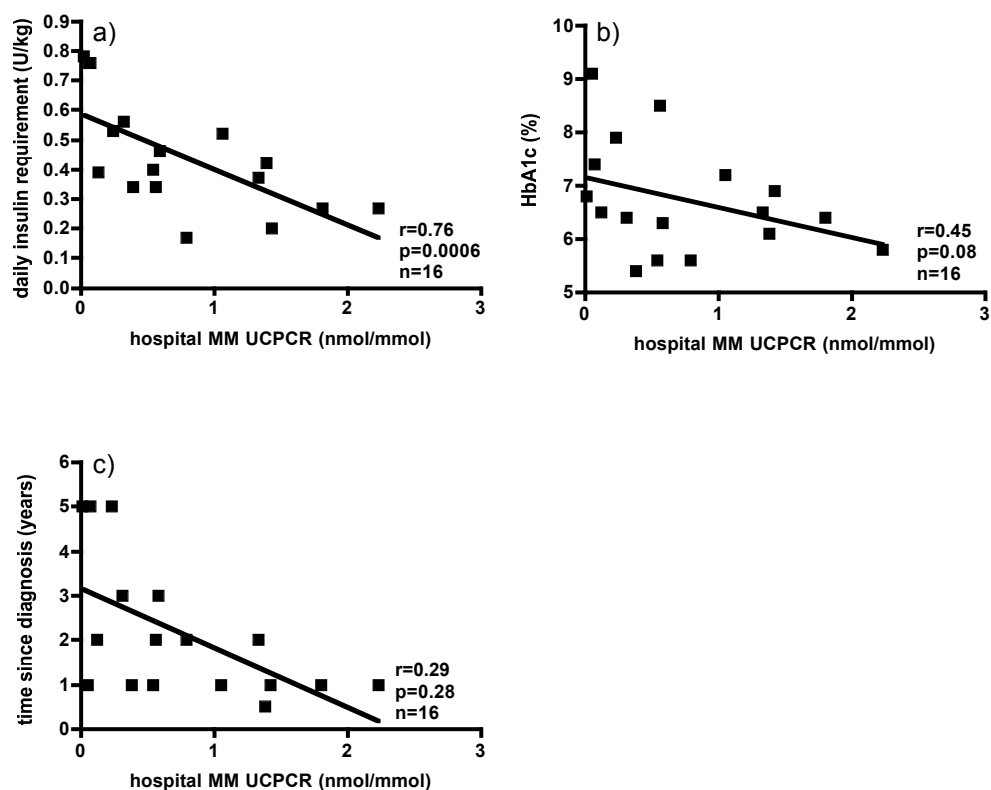


Figure 6-6. Correlation of hospital MM UCPCR with diabetes related parameters: a) daily insulin requirements (U/kg); b) HbA1c and c) time since diagnosis. Statistical test used: Spearman correlation.

6.4.1.3 Collection of repeated home UCPCR values and change of β - cell function over time

Of the 16 patients who provided paired data at baseline, 13 (81%) returned 2 or more home UCPCR post meal samples and 13 (81%) provided both a month 1 and a month 6 home UCPCR sample

The 4 patients who were lost to follow-up did not differ significantly in screening variables, such as age, BMI, duration of diabetes, HbA1c or daily insulin requirements at baseline. There was a large discrepancy in the peak

serum C-peptide, which was not significant due to low numbers and high variation (Table 6-3).

	Patients with the completed data	Lost to follow-up patients	p (Mann-Whitney)
N	13	4	
Age (years)	34.2±5.1	31.2±8.5	0.82
BMI (kg/m ²)	26.0±3.6	24.7±1.1	0.19
Duration of diabetes (years)	2.0±1.2	2.0±2.0	0.64
Insulin requirements (U/kg)	0.44±0.18	0.44±0.25	0.94
HbA1c (%)	6.7±1.1	6.8±0.7	0.46
Peak C-peptide during MMTT (pmol/l)	1056±1052	321.0±331.9	0.23 9(n=3)

Table 6-3. Comparison of patients with complete and incomplete data sets.

Patients showed significantly lower β -cell function on home MM-UCPCR month 6 ($0.71\pm0.86\text{nmol/mmol}$) in comparison with home MM-UCPCR month 1 performed on average 5.5 ± 1.0 months earlier ($1.08\pm0.98\text{nmol/mmol}$, $n=13$, $p=0.02$) – Figure 6-7.

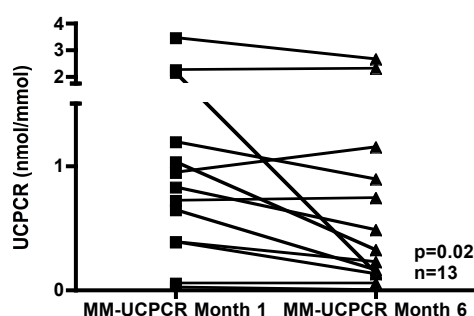


Figure 6-7. MM-UCPCR change over 6 months. Comparison was made between UCPCR collected after home meal stimulation (home MM-UCPCR) 1 month and 6 months after entering the study. Statistical test used: Wilcoxon signed rank test.

6.4.1.4 Home meal stimulation of β -cell insulin production

Home meal-UCPCR (HM UCPCR) collected 2.1 ± 1.1 months after hospital MMTT significantly correlated with peak sCP ($r=0.83$, 95% CI:0.50-0.95, $p=0.0005$, $n=13$) – Figure 6-8 a. The correlation became stronger when the maximal home meal-UCPCR value from all the serial monthly measurements was taken into account ($r=0.89$, 95% CI:0.67-0.97, $p<0.0001$, $n=13$) – Figure 6-8 b. Patients on average provided 2.6 ± 1.5 samples out of the 4 planned.

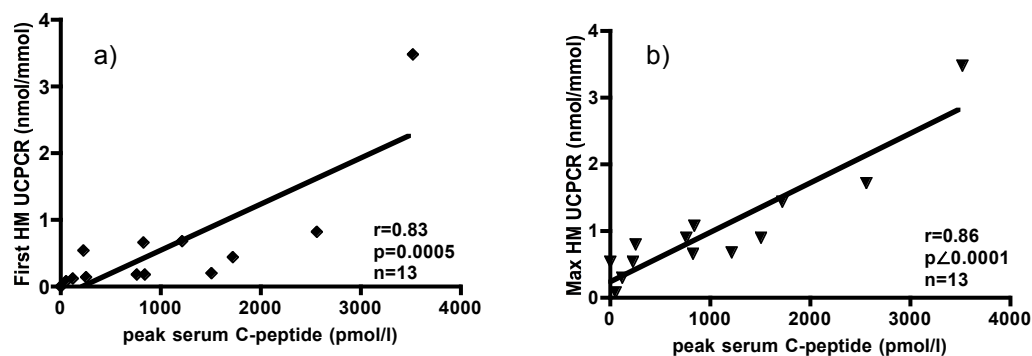


Figure 6-8. Correlation of peak serum C-peptide with home meal stimulated UCPCR (HM UCPCR). a) first collected HM-UCPCR; b) maximal HM-UCPCR value out of serial monthly measurement.

6.4.2 Additional samples

When data from the main study were pooled with the baseline data from the MonoPepT1De study (before intervention), correlation between peak sCP during MMTT and the two-hour UCPCR done on the same occasion was maintained ($r=0.52$, 95% CI:0.24-0.73, $n=38$, $p=0.0007$, Figure 6-9).

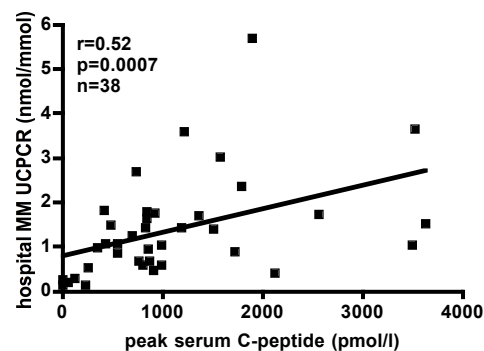


Figure 6-9. Correlation: Peak serum C-peptide and MM-UCPCR. Data from the main study and MonoPepT1De study were pooled. The tests in the both studies were done under the same conditions. Statistical test used: Spearman correlation.

The correlation between the change in MM-UCPCR and peak sCP was not evident after 3 months ($r=0.3$, 95% CI:-0.20-0.68, $n=18$, $p=0.2$, Figure 6-10 a), but reached significance after 6 months ($r=0.6$, 95% CI:0.08-0.86, $n=14$, $p=0.02$, Figure 6-10 b) of follow-up of the MonoPepT1De study subjects. I was only able to test the correlation of the change over time in these two parameters, given that it was performed before unblinding, with some of the subjects exposed to the study drug and some to the placebo.

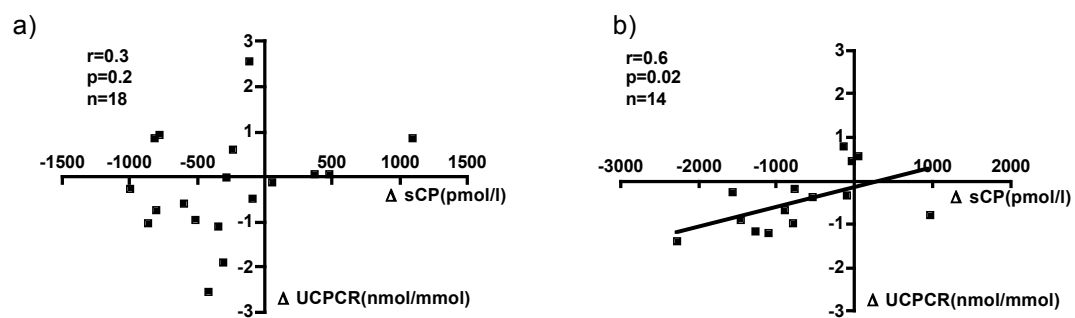


Figure 6-10 Correlation: Change in the peak serum C-peptide and the change in the MM-UCPCR. Δ sCP – change in the peak serum C-peptide during MMTT; Δ UCPCR – change in the MM stimulated UCPCR done at the same occasion. a) after 3 months; b) after 6 months. Statistical test used: Spearman correlation.

6.5 Summary of findings

-
1. Standard mixed meal stimulated UCPCR strongly correlated with gold standard MMTT for the estimation of residual β -cell function in patients with Type 1 diabetes within 5 years since diagnosis, in both hospital and home setting.
 2. The use of standard Mixed Meal stimulated UCPCR was proven to be a useful tool for the detection of a significant change in β -cell function over the six months long period of follow up.
 3. Best of the serial measurement of home meal stimulated UCPCR can be used as a reliable parameter for the estimation of β -cell function.
-

The importance of the effect of residual β -cell function on glycaemic control in Type 1 diabetes is reflected in the observation from standard MMTT during which highest C-peptide responders had near normal glucose levels, and vice versa. Significant negative correlation between residual β -cell function, measured as MM stimulated UCPCR, and daily insulin requirement supports this finding. The correlation with HbA1c and duration of diabetes lacks significance, possibly because of the effect of other parameters, such as compliance issues in the former and rate of disease progression in the latter.

Besser et al. demonstrated that stimulated UCPCR could be a practical alternative to the standard MMTT in estimating β -cell function.[131] Our study, conducted in patients much earlier in the disease process, all of whom had well controlled diabetes (HbA1c $6.7 \pm 1.0\%$, daily insulin requirements 0.44 ± 0.18 U/kg/day) and significant residual β -cell function (peak sCP during MMTT >200 pmol/l in 12 out of 16 patients - mean 918.00 ± 994 pmol/l), confirmed this finding, irrespective of the setting where the test was performed (hospital: $r=0.81$, $p=0.0002$; home $r=0.89$, $p<0.001$). Correlation remained significant when the data were pooled with the baseline results of the MMTT

test (serum and urine) from the MonoPepT1De study, performed at exactly the same conditions. The correlation was not as strong as in the Besser study. Higher rate of production and consequently wider range of C-peptide values in our cohort may be the explanation for this finding.

Although fasting UCPCR significantly correlated with the standard MMTT, the correlation was weaker and more diverse than with the stimulated one, suggesting that fasting UCPCR is less a reliable marker than stimulated one.

In addition, I was able to show a significant decline of β -cell function during the follow-up period using home UCPCR, suggesting that MM stimulated UCPCR is not only a good estimate of β -cell function at one particular time point, but also a useful tool for serial monitoring. It is unlikely that the patients who were lost to follow-up biased the results, because they did not differ significantly with the group with completed data in demographic and diabetes related parameters.

Potential use of stimulated UCPCR in the monitoring of β -cell function was additionally confirmed by the fact that the change in UCPCR correlated with the change in the gold standard MM stimulated sCP. The significance was achieved only when six months correlation was taken into account. It is possible that the three months change was not high and hence, sensitive enough.

Home meal stimulation of the UCPCR (as opposed to the use of proprietary standardised meal supplements, such as Ensure plus), although weaker, can

also be a comparable alternative to the standard MM stimulation. Our results also suggest for the first time that variation in the stimulus from home “main meals” could be overcome by serial measurements, followed by choosing the highest out of 2-3 measurements as representative of β -cell function without the requirement to fast, omit insulin or count carbohydrate content of the meal (increase in correlation coefficient from $r=0.83, p=0.0005$ to $r=0.89, p<0.0001$).

This approach has the potential to improve on the estimation of β -cell function without burdening subjects with a complex testing protocol, and should improve compliance rates. I suggest that this modification increases the accuracy of home meal stimulated UCPCR and makes it a potentially useful tool for assessment of residual β -cell function in large prospective cohort studies.

It has to be taken into account that this was a pilot study and therefore not sufficiently powered to draw solid conclusions about the efficacy of stimulated UCPCR in the estimation and monitoring of the β -cell function, but nevertheless, offers reasonable grounds for a larger definitive trial.

Chapter 7 GENERAL DISCUSSION AND CONCLUDING REMARKS

Success of peptide immunotherapy starts with the efficient delivery. Once the right peptide is delivered to the right cell, it is equally important to monitor the effect of such a therapy as closely and as precisely as possible, both in the regards to the immune and metabolic response.

Currently, clinical trials are designed in such a way that the effect of the study drug is measured at the end of the trial period, which can be months or even years later. *Ex-vivo* human models, such as skin organ bath culture, not being the subject of the extensive regulatory requirements, can provide rapid answers on the efficacy of the treatment, within its limitations. The idea is that the conclusions from murine models and *in-vitro* cultures can be tested for the proof of principle in the *ex-vivo* models, and if proven valuable, selected for assessment in clinical trials. Clinical trials and subsequent clinical practice would, on the other hand, be equipped with a monitoring techniques to detect early changes in immune and metabolic responses that would improve efficacy.

The ability to detect early immune responses to the study drug will allow early identification of the “responders”, followed by close monitoring of β -cell function. This would allow early recognition of changes in disease activity, and the potential need for a different treatment intensity and/or strategy.

Dilemmas on optimisation and potential advances in the each step of this process, from delivery to the metabolic response monitoring, achieved during this project are summarised in the Figure 7-1.

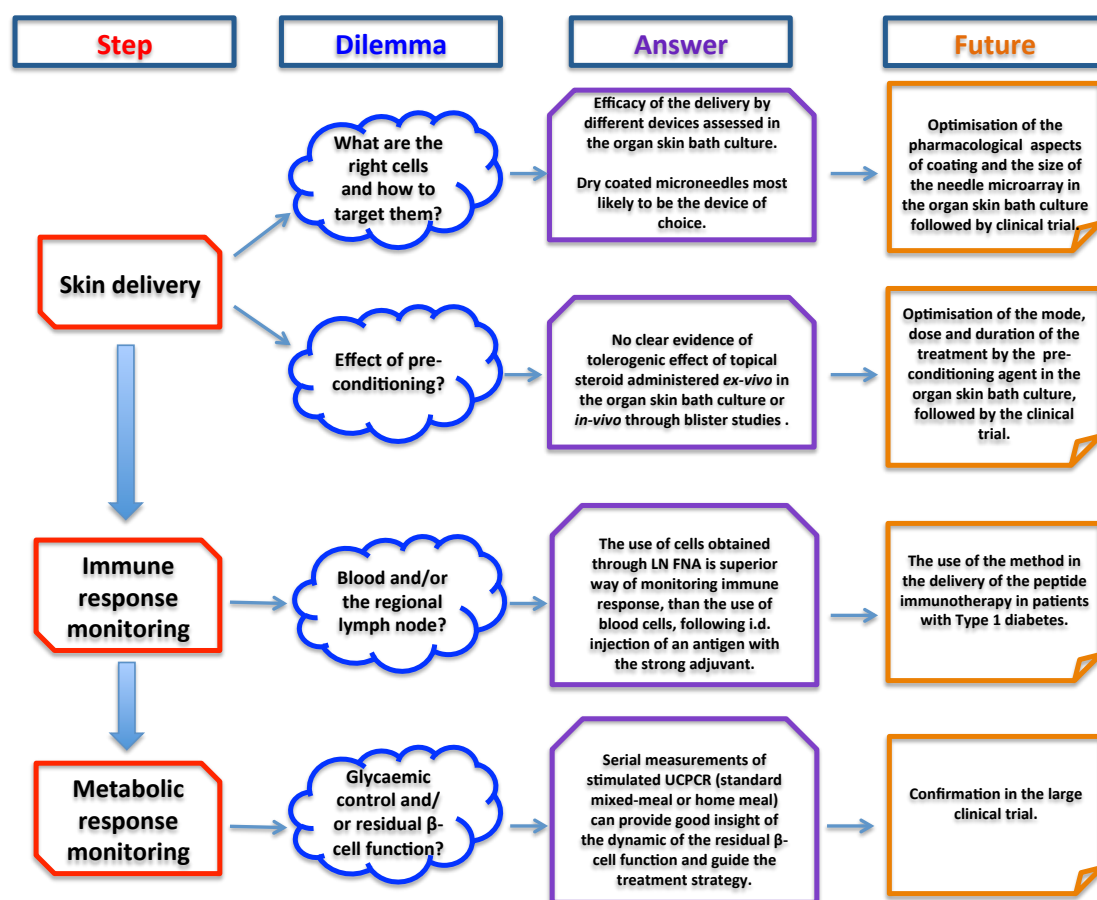


Figure 7-1. Dilemmas, answers and scope for the future in the optimisation of the efficacy of the peptide immunotherapy.

In this final chapter, I will further discuss advantages and disadvantages of the models and techniques that I developed, and link them with the ideas for the future work in this field.

7.1 Skin organ bath culture for the assessment of optimal antigen skin delivery

7.1.1 The skin organ bath culture model

I have shown that the skin organ bath culture is a useful *ex-vivo* model that permits the assessment of treatment agents delivered via different devices, through study of the phenotypic and functional characteristics of the cells targeted by such a treatment. This project led to the modification of the model to allow assessment at a particular time point of treatment, through rapid extraction of the dendritic cells of interest.

One of the advantages of the skin organ bath culture lies in the possibility to incubate the skin as a whole, following treatment, which mimics *in vivo* processes much better than *in vitro* cell cultures. In this model, an uptake of the delivered antigen is influenced by the full range of different cell types present in skin. It also has a potential to study the volume of distribution in the structures of skin and the access to the different skin layers.

Another advantage is the controlled duration of treatment being assessed, which is enabled by the rapid extraction of the epidermal cells from the skin. This is different from the majority of protocols that usually obtain DCs by the 'walk-out' method.[292] Although this provides purified, functional DCs, the issues with their number, maturity (that increases in the process of migration) and the potential to loose their captured antigen, makes it less favourable model for the purposes of this project. Enzymatic separation and digestion of epidermis makes the epidermal cell suspension rapidly available, with DCs in their less mature, nascent state.

Most importantly, the model allows assessment of various agents and devices without the regulatory limitations encountered in clinical trials.

However, the model carries certain disadvantages. These are particularly related to the fact that enzymatic process may cleave some of the cell membrane markers essential for the full potency of the cell. Indeed, failure to detect CD11c on the DCs obtained through this process, which was independent of antibody type or addition of fixative during preparation for the flow cytometry, is likely to have been a manifestation of this problem.

Finally, we have to take into account conditions in organ bath, such as the lack of circulation leading to the absence of the clearance of the administered agent from the local site, as would have happened *in vivo*. Also, hypoxia and high concentrations of metabolic by-products that would normally be cleared from the skin, remain *in situ* in this model and almost certainly would affect functionality of the cells.

There is certainly room for improvement that may be the subject of future research. One such improvement would involve purifying DC population, with elimination of dead cells and keratinocytes, by flow sorting or magnetic separation. This would eliminate potential non-specific influence of dead cells on reactions, and lead to more clear results, but at the expense of losing significant number of cells.

In conclusion, within its limitations, the design of the organ skin bath culture used in this project allows rapid answers to the questions particularly in regards to the optimal delivery of the antigens, without ethical boundaries

encountered in the clinic, which makes it an important translational filter to the *in-vivo* human studies.

7.1.2 Targeting epidermal dendritic cell in the peptide skin delivery

The skin organ bath model allowed me to investigate the efficacy of targeting epidermal DCs during antigen skin delivery. This set of experiments showed that both hollow and dry coated microneedles are comparable to standard intradermal 26G needles in targeting epidermal DCs, with some suggestion of superiority in the case of dry microneedles.

I found that the hollow microneedle is a comparable device to a standard 26G needle in targeting epidermis by measuring response of the cloned T-cells to the peptide presented by the DCs, loaded through *ex-vivo* delivery. However, even if needles of the hollow microneedle are positioned superficially in close proximity of epidermal/dermal junction, the 'jet effect' of the volume injected pushed the solution deeper in the dermis, away from the targeted epidermal cells. Both the hollow microneedle and the 26G needle are designed for intradermal drug administration, and the fact that antigen delivered by them reaches epidermal DCs is almost certainly due to flush-back of the solution, followed by diffusion throughout the skin layers including the epidermis. The advantage of the hollow microneedle perhaps lies in the fact that its short needles prevent accidental deeper administrations that are possible with the 26G needle.

I thought to overcome the problem of 'jet effect', by delivering the antigen using dry coated microneedles. In this way, arrays of 10 needles of 400µm duration are coated with peptide and positioned such that the majority of the

coated needle length would be in the epidermis. From here, the peptide will gradually dissolve in the interstitial fluid and diffuse into the tissue. Although, this mode of delivery again seemed comparable, if not better, than 26G needles, I encountered several problems. Firstly, to coat the peptide on the microneedle, I had to dissolve it in a solution that easily evaporates after coating, leaving the peptide only on the needle. Also, the coating solution should not change the peptide. Choosing the right coating solution that meets all of these criteria was the subject of PhD project of Ms Xin Zhao and I will not discuss it in detail here. Suffice to say that EBVP1 peptide, used in this model, is very hydrophobic, making the task of choosing the optimal coating solution difficult. For example, DMSO would resolve the problem of solubility, but I could not use it because of its poor evaporation, which would not allow the peptide to dry on the microneedle after coating. A solution of glacial acetic acid, 2-methylbuten-2-ol and 20mg/ml PVA 2000 (10:5:2 by volume) was found to be optimal for this purpose.

Once the needle was in the tissue, the hydrophobicity of the peptide played a role in the efficacy of the delivery. The small amount of interstitial fluid in a dense cellular tissue such as the epidermis reduced the dissolution from the needle into the aqueous interstitial tissue. As a consequence, 15 minutes of needle insertion only allowed less than 20% of delivery, which was comparable, if not better, than delivery via 26G needle.

Delivery can potentially be made more efficient by using the larger quantity from arrays consisting of more needles or increasing delivery time. Also, more soluble peptide will probably be delivered more efficiently.

Another improvement of this system would be to compare the proportion of peptide delivered to the epidermis and dermis via each device. Enzymatic digestion of the dermis or the 'walk out' method would be the way of obtaining dermal DCs. However, we have to bear in mind that epidermal DCs were obtained following peptide administration in the circular area of 0.8cm diameter. This provided approximately 3×10^5 EC (approximately 3000 DCs), enabling experiments that required 5×10^4 ECs (500 DCs) per well. It is very unlikely that I would be able to obtain a comparable number of dermal DCs from piece of dermis derived from a 0.8cm punch biopsy to enable the fair comparison. Indeed, when I tried to obtain dermal DCs in such a way (48h 'walk out'), I only obtained 10,000 live cells per one 0.8cm punch biopsy. According to the flow data, only 7% of these cells were $CD1a^+HLA-DR^+$, providing approximately 700 cells per one punch biopsy, which is not nearly enough to set up an experiment - Figure 7-2. However, optimising the model to allow dermal/epidermal comparisons this could be the subject of future work.

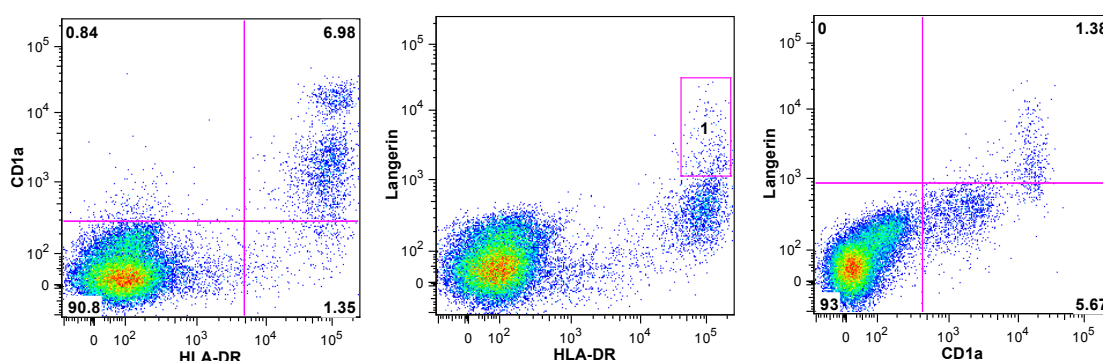


Figure 7-2. Flow cytometry profile of the dermal dendritic cells. a) CD1a/HLA-DR staining; b) Langerin/CD1a staining; c) Langerin/CD1a staining.

This project gave a suggestion that dry microneedle can be more efficient in targeting epidermis than established intradermal devices. This is because

they are designed to anatomically and chemically (slow diffusion from the needle to the surrounding space) target the epidermis, as opposed to the intradermal devices that rely on flash back to deliver to the epidermal DCs. The efficacy of the delivery by dry coated microneedles could be further improved by the use of devices with more densely packed arrays and water soluble peptides. One such peptide is C19-A3 peptide, currently tested in a Phase Ib trial. To study the efficacy of C19-A3 peptide delivery via dry microneedles, the antigen would be coated on the dry microneedle array and delivered to the skin *ex-vivo*. Subsequently, skin derived dendritic cells (either in epidermal cell suspension or purified as previously discussed) would be co-cultured with C19-A3 specific cloned T cells. If proven efficient in comparison to standard 26G, this mode of delivery can be used in later phases of clinical trials on C19-A3 peptide, subject to regulatory approvals and a positive safety outcome from ongoing Ib phase.

7.1.3 Enhancement of tolerogenic environment in preparation for peptide immunotherapy

The skin organ bath culture allowed the analysis of the effect of topical steroid on the tolerogenic potential of epidermal DCs. When complemented with the *in vivo* blister studies, data indicate that topical steroid treatment induced changes in the skin DCs responsible for their weaker capacity to activate responder T cells in the MLR type reactions. Although suggested by the *ex vivo* model, *in vivo* data are less supportive of pro-tolerogenic effects. Instead, generally weaker activation signal is more likely explanation for this phenomenon.

One can argue that a lack of circulation and effective clearance of steroid from the tissue allowed the effect to be evident after only 24h, which may not be the case *in vivo*, and would certainly require separate titration of the optimal treatment duration. However, reduced expression of co-stimulatory markers on skin DCs and the reduced capacity to drive proliferation in MECLR might mean an enhancement of the tolerogenic nature of these cells. I have not been able to demonstrate a mechanism of tolerance by using cultures of epidermal cells exposed to steroid and allogeneic donor CD4+ naïve T cells, aiming to assess the phenotype and the suppression capacity of T cells cultivated in such a way. The reason was the small number of cell cultivated in this experiment, which could be due to the old age of skin donors and adverse *ex-vivo* conditions affecting DCs, as previously discussed. When a similar protocol was applied with the use of *in vivo* steroid exposed DCs (obtained via suction blister), no clear tolerance was shown. A generally weaker signal delivered by steroid exposed cells is the more likely explanation.

Beside topical steroid, I tested the effect of locally injected IL-10, both in pure form and attached to nanoparticles, in the skin organ bath culture. The absence of strong suppression in the *ex vivo* model, previously observed *in vitro*, is most likely to be due to the large individual variation in the response to locally injected IL-10 on the background of a weaker MLR type reaction, short duration of incubation to allow for the IL-10 effect and insufficient dose of locally injected IL-10. However, the *ex-vivo* trends on the background of the significant *in vitro* data, were suggestive that a small dose of locally injected IL-10 has the potential to modulate skin DCs into a pro-tolerogenic profile, particularly if used as an enhancer to peptide immunotherapy. To draw any

solid conclusion, this protocol would need to be optimised, particularly in regards to IL-10 dose and duration of effect, assessment of different types of nanoparticles to which IL-10 is linked and purification of DCs used in the cultures.

In summary, despite limitations, the skin organ bath culture is a useful system for studying treatment effects of variety of *ex-vivo* delivered agents that bridges the *in vitro* models and *in vivo* studies in humans, which are restricted for ethical reasons. When used to study the optimal delivery of peptides, it indicated a potential role of dry coated microneedles in targeting epidermal DCs, important because of their endogenous tolerogenic potential. I have also shown that, due to the accessibility of epidermal DCs, they can be modified by topical treatments and locally injected agents. Whether true tolerogenic potential can be achieved in such a way, is subject to further studies designed to optimise the type, dose and the duration of the treatment by the conditioning agent.

7.2 Monitoring immunological and metabolic outcomes

7.2.1 Immune response monitoring after skin antigen delivery

In most studies in humans, immune responses are assessed in blood-derived cells due to their ready availability. However, the immune response is a dynamic process that starts in the primary tissue (skin in the case of this study) and subsequently takes part mainly in lymphoid organs, such as lymph nodes and spleen. It is very important to be able to monitor immune response following skin antigen delivery, in order to assess its efficacy. However the induced antigen-specific T cells are only present at very low levels in the blood, as the cells only pass briefly through the blood, travelling from the primary source of the antigen to the lymphoid site, or between two lymphoid sites. Hence, studies assessing blood derived immune cells have a high risk of false negative results, and any beneficial effect of peptide immunotherapy may be missed. On the contrary, looking at the immune processes in the lymphoid organ is the default method in animal models. This project explored the concept of translating this approach into humans by using minimally invasive ultrasound guided fine needle aspiration (FNA) of the regional lymph node (LN), a technique commonly used in clinical practice for cancer diagnostics.

Our results show that LN FNA is acceptable to subjects, can be repeatedly and reliably performed by a skilled operator and provides a sufficient number of live and functional T cells to detect the cellular immune response after antigen skin delivery. The question that immediately arose was triggered by the failure to detect baseline IFN γ response to specific antigens, which

suggests reduced effector memory response in the quiet lymph node. On the contrary, a specific IFN γ response following Mantoux test, as detected in the draining lymph node, points towards effector memory, but it is not clear where these cells are coming from. They might have been 'early bird' effector cells arriving from the skin that are either *in situ* skin memory cells or blood derived memory cells, which travelled to the lymph node via skin; or local effector cells activated by the antigen bearing DCs arrived early in the lymph node from the skin.

Future research should aim to characterise the groups of cells, in particular T cells, residing and arriving in the lymph node following *in vivo* antigen stimulation, by means of flow-cytometry. This would particularly relate to the groups of cells such as central (CD45RA⁻ CCR7⁺) and effector memory cells (CD45RA⁺ CCR7⁻), naïve T cells (CD45RA⁺) and cells equipped with the machinery to home in the skin (CLA⁺) and/or lymph node (CCR7⁺).

This 'proof of principle' study indicated that LN FNA is a feasible method for detecting IFN γ immune response in humans, elicited by the antigen linked to the strong adjuvant. Future research should follow to detect responses to peptide immunotherapy, which does not involve strong adjuvants, as was the case with Tuberculin PPD. This would require a different approach in choosing read-outs. Whilst Tuberculin PPD is potent stimulator, response to which is very likely to be recorded through detection of cells producing an abundance of the pro-inflammatory cytokine IFN γ , responses to peptide immunotherapy are likely to be more subtle, and involve generation of Tregs. They recognise the administered autoantigen/peptide and have an immune regulatory phenotype, which they achieve through production of IL-10 and

TGF- β , amongst other proposed mechanisms. Hence, detection of, for example, IL-10 producing cells and flowcytometric analysis of the change in the proportion of Tregs following PIT delivery, would be a good starting approach for a follow-up study.

7.2.2 Monitoring of the metabolic outcome

This study confirmed earlier findings that stimulated UCPCR could be a practical alternative to the standard MMTT in estimating β -cell function. In addition, it extended the application of the method to patients much earlier in the disease process, with well controlled diabetes and significant residual β -cell function.

In addition, I was able to show a significant decline of β -cell function during the follow-up period using home UCPCR, suggesting that MM stimulated UCPCR is not only a good estimate of β -cell function at one particular time point, but also a useful tool for serial monitoring.

Home meal stimulation of the UCPCR, although weaker, can also be a comparable alternative to the standard MM stimulation, particularly when choosing the highest out of 2-3 serial measurements as representative of β -cell function, without the requirement to fast, omit insulin or count the carbohydrate content of the meal.

This approach has the potential to improve the estimation of β -cell function without burdening subjects with a complex testing protocol, and should improve compliance rates.

In summary, lymph node fine needle aspiration biopsy is a feasible non-invasive method suitable for monitoring the cellular immune responses after antigen skin delivery. Subject to confirmatory study, it has a potential to find immediate application as an efficient and reliable tool for monitoring immune response after antigen-specific immunotherapy in clinical trials. Once recognised as ‘immune responders’ in such a way, participants in clinical trials can be subjected to the monitoring of the metabolic response to the immune intervention, by measuring β -cell function via stimulated UCPCR as a non-invasive and more compliant-prone alternative to the standard MMTT.

References

1. Eisenbarth, G.S., *Type I diabetes mellitus. A chronic autoimmune disease*. N Engl J Med, 1986. **314**(21): p. 1360-8.
2. Sherry, N.A., E.B. Tsai, and K.C. Herold, *Natural history of beta-cell function in type 1 diabetes*. Diabetes, 2005. **54 Suppl 2**: p. S32-9.
3. Sosenko, J.M., et al., *Acceleration of the loss of the first-phase insulin response during the progression to type 1 diabetes in diabetes prevention trial-type 1 participants*. Diabetes, 2013. **62**(12): p. 4179-83.
4. Tsai, E.B., et al., *The rise and fall of insulin secretion in type 1 diabetes mellitus*. Diabetologia, 2006. **49**(2): p. 261-70.
5. Greenbaum, C.J., et al., *Fall in C-peptide during first 2 years from diagnosis: evidence of at least two distinct phases from composite Type 1 Diabetes TrialNet data*. Diabetes, 2012. **61**(8): p. 2066-73.
6. Ziegler, A.G. and G.T. Nepom, *Prediction and pathogenesis in type 1 diabetes*. Immunity, 2010. **32**(4): p. 468-78.
7. Parikka, V., et al., *Early seroconversion and rapidly increasing autoantibody concentrations predict prepubertal manifestation of type 1 diabetes in children at genetic risk*. Diabetologia, 2012. **55**(7): p. 1926-36.
8. Ziegler, A.G., E. Bonifacio, and B.-B.S. Group, *Age-related islet autoantibody incidence in offspring of patients with type 1 diabetes*. Diabetologia, 2012. **55**(7): p. 1937-43.
9. Yu, L., et al., *Antiislet autoantibodies usually develop sequentially rather than simultaneously*. J Clin Endocrinol Metab, 1996. **81**(12): p. 4264-7.
10. Long, A.E., et al., *Rising incidence of type 1 diabetes is associated with altered immunophenotype at diagnosis*. Diabetes, 2012. **61**(3): p. 683-6.
11. Winkler, C., et al., *Is islet autoimmunity related to insulin sensitivity or body weight in children of parents with type 1 diabetes?* Diabetologia, 2009. **52**(10): p. 2072-8.
12. Ziegler, A.G., et al., *Seroconversion to multiple islet autoantibodies and risk of progression to diabetes in children*. JAMA, 2013. **309**(23): p. 2473-9.
13. Decochez, K., et al., *IA-2 autoantibodies predict impending type I diabetes in siblings of patients*. Diabetologia, 2002. **45**(12): p. 1658-66.
14. Elding Larsson, H., et al., *Children followed in the TEDDY study are diagnosed with type 1 diabetes at an early stage of disease*. Pediatr Diabetes, 2014. **15**(2): p. 118-26.
15. Bonifacio, E., et al., *A strategy to find gene combinations that identify children who progress rapidly to type 1 diabetes after islet autoantibody seroconversion*. Acta Diabetol, 2014. **51**(3): p. 403-11.
16. Keskinen, P., et al., *First-phase insulin response in young healthy children at genetic and immunological risk for Type I diabetes*. Diabetologia, 2002. **45**(12): p. 1639-48.
17. Bingley, P.J., *Interactions of age, islet cell antibodies, insulin autoantibodies, and first-phase insulin response in predicting risk of progression to IDDM in ICA+ relatives: the ICARUS data set. Islet Cell Antibody Register Users Study*. Diabetes, 1996. **45**(12): p. 1720-8.
18. Mrena, S., et al., *Staging of preclinical type 1 diabetes in siblings of affected children. Childhood Diabetes in Finland Study Group*. Pediatrics, 1999. **104**(4 Pt 1): p. 925-30.

19. Anderson, M.S. and J.A. Bluestone, *The NOD mouse: a model of immune dysregulation*. Annu Rev Immunol, 2005. **23**: p. 447-85.
20. Willcox, A., et al., *Analysis of islet inflammation in human type 1 diabetes*. Clin Exp Immunol, 2009. **155**(2): p. 173-81.
21. Imagawa, A., et al., *Immunological abnormalities in islets at diagnosis paralleled further deterioration of glycaemic control in patients with recent-onset Type 1 (insulin-dependent) diabetes mellitus*. Diabetologia, 1999. **42**(5): p. 574-8.
22. Coppieters, K.T., et al., *Demonstration of islet-autoreactive CD8 T cells in insulinitic lesions from recent onset and long-term type 1 diabetes patients*. J Exp Med, 2012. **209**(1): p. 51-60.
23. Coppieters, K.T., et al., *Persistent glucose transporter expression on pancreatic beta cells from longstanding type 1 diabetic individuals*. Diabetes Metab Res Rev, 2011. **27**(8): p. 746-54.
24. Murphy, K., et al., *Janeway's immunobiology*. 7th ed. 2008, New York: Garland Science. xxi, 887 p.
25. Fedoric, B. and R. Krishnan, *Rapamycin downregulates the inhibitory receptors ILT2, ILT3, ILT4 on human dendritic cells and yet induces T cell hyporesponsiveness independent of FoxP3 induction*. Immunol Lett, 2008. **120**(1-2): p. 49-56.
26. Korn, T., et al., *IL-21 initiates an alternative pathway to induce proinflammatory T(H)17 cells*. Nature, 2007. **448**(7152): p. 484-7.
27. Lohr, J., et al., *T-cell tolerance and autoimmunity to systemic and tissue-restricted self-antigens*. Immunol Rev, 2005. **204**: p. 116-27.
28. Apostolou, I., et al., *Origin of regulatory T cells with known specificity for antigen*. Nat Immunol, 2002. **3**(8): p. 756-63.
29. Abbas, A.K., et al., *Regulatory T cells: recommendations to simplify the nomenclature*. Nat Immunol, 2013. **14**(4): p. 307-8.
30. Apostolou, I. and H. von Boehmer, *In vivo instruction of suppressor commitment in naive T cells*. J Exp Med, 2004. **199**(10): p. 1401-8.
31. Kretschmer, K., et al., *Inducing and expanding regulatory T cell populations by foreign antigen*. Nat Immunol, 2005. **6**(12): p. 1219-27.
32. Roncarolo, M.G., et al., *Interleukin-10-secreting type 1 regulatory T cells in rodents and humans*. Immunol Rev, 2006. **212**: p. 28-50.
33. Wong, F.S. and C.M. Dayan, *Regulatory T cells in autoimmune endocrine diseases*. Trends Endocrinol Metab, 2008. **19**(8): p. 292-9.
34. Sakaguchi, S., et al., *Immunologic self-tolerance maintained by activated T cells expressing IL-2 receptor alpha-chains (CD25). Breakdown of a single mechanism of self-tolerance causes various autoimmune diseases*. J Immunol, 1995. **155**(3): p. 1151-64.
35. McNeill, A., E. Spittle, and B.T. Backstrom, *Partial depletion of CD69^{low}-expressing natural regulatory T cells with the anti-CD25 monoclonal antibody PC61*. Scand J Immunol, 2007. **65**(1): p. 63-9.
36. Read, S., V. Malmstrom, and F. Powrie, *Cytotoxic T lymphocyte-associated antigen 4 plays an essential role in the function of CD25⁽⁺⁾CD4⁽⁺⁾ regulatory cells that control intestinal inflammation*. J Exp Med, 2000. **192**(2): p. 295-302.

37. Takahashi, T., et al., *Immunologic self-tolerance maintained by CD25(+)CD4(+) regulatory T cells constitutively expressing cytotoxic T lymphocyte-associated antigen 4*. J Exp Med, 2000. **192**(2): p. 303-10.
38. McHugh, R.S., et al., *CD4(+)CD25(+) immunoregulatory T cells: gene expression analysis reveals a functional role for the glucocorticoid-induced TNF receptor*. Immunity, 2002. **16**(2): p. 311-23.
39. Huang, C.T., et al., *Role of LAG-3 in regulatory T cells*. Immunity, 2004. **21**(4): p. 503-13.
40. Seddiki, N., et al., *Expression of interleukin (IL)-2 and IL-7 receptors discriminates between human regulatory and activated T cells*. J Exp Med, 2006. **203**(7): p. 1693-700.
41. Hori, S., T. Nomura, and S. Sakaguchi, *Control of regulatory T cell development by the transcription factor Foxp3*. Science, 2003. **299**(5609): p. 1057-61.
42. Fontenot, J.D., M.A. Gavin, and A.Y. Rudensky, *Foxp3 programs the development and function of CD4+CD25+ regulatory T cells*. Nat Immunol, 2003. **4**(4): p. 330-6.
43. Khattri, R., et al., *An essential role for Scurfin in CD4+CD25+ T regulatory cells*. Nat Immunol, 2003. **4**(4): p. 337-42.
44. Corthay, A., *How do regulatory T cells work?* Scand J Immunol, 2009. **70**(4): p. 326-36.
45. Petrich de Marquesini, L.G., et al., *IFN-gamma and IL-10 islet-antigen-specific T cell responses in autoantibody-negative first-degree relatives of patients with type 1 diabetes*. Diabetologia, 2010. **53**(7): p. 1451-60.
46. Arif, S., et al., *Autoreactive T cell responses show proinflammatory polarization in diabetes but a regulatory phenotype in health*. J Clin Invest, 2004. **113**(3): p. 451-63.
47. Mallone, R., et al., *Immunology of Diabetes Society T-Cell Workshop: HLA class I tetramer-directed epitope validation initiative T-Cell Workshop Report-HLA Class I Tetramer Validation Initiative*. Diabetes Metab Res Rev, 2011. **27**(8): p. 720-6.
48. James, E.A., et al., *Immunology of Diabetes Society T-Cell Workshop: HLA class II tetramer-directed epitope validation initiative*. Diabetes Metab Res Rev, 2011. **27**(8): p. 727-36.
49. Yamazaki, S., et al., *Direct expansion of functional CD25+ CD4+ regulatory T cells by antigen-processing dendritic cells*. J Exp Med, 2003. **198**(2): p. 235-47.
50. Yu, P., et al., *Specific T regulatory cells display broad suppressive functions against experimental allergic encephalomyelitis upon activation with cognate antigen*. J Immunol, 2005. **174**(11): p. 6772-80.
51. Sundstedt, A., et al., *Role for IL-10 in suppression mediated by peptide-induced regulatory T cells in vivo*. J Immunol, 2003. **170**(3): p. 1240-8.
52. Green, E.A., et al., *CD4+CD25+ T regulatory cells control anti-islet CD8+ T cells through TGF-beta-TGF-beta receptor interactions in type 1 diabetes*. Proc Natl Acad Sci U S A, 2003. **100**(19): p. 10878-83.
53. Grossman, W.J., et al., *Human T regulatory cells can use the perforin pathway to cause autologous target cell death*. Immunity, 2004. **21**(4): p. 589-601.

54. Tree, T.I., et al., *Naturally arising human CD4 T-cells that recognize islet autoantigens and secrete interleukin-10 regulate proinflammatory T-cell responses via linked suppression*. Diabetes, 2010. **59**(6): p. 1451-60.
55. Mellor, A.L. and D.H. Munn, *IDO expression by dendritic cells: tolerance and tryptophan catabolism*. Nat Rev Immunol, 2004. **4**(10): p. 762-74.
56. Huehn, J., et al., *Developmental stage, phenotype, and migration distinguish naive- and effector/memory-like CD4+ regulatory T cells*. J Exp Med, 2004. **199**(3): p. 303-13.
57. Derbinski, J., et al., *Promiscuous gene expression in thymic epithelial cells is regulated at multiple levels*. J Exp Med, 2005. **202**(1): p. 33-45.
58. Cai, C.Q., et al., *Both polymorphic variable number of tandem repeats and autoimmune regulator modulate differential expression of insulin in human thymic epithelial cells*. Diabetes, 2011. **60**(1): p. 336-44.
59. Atkinson, M.A., et al., *How does type 1 diabetes develop?: the notion of homicide or beta-cell suicide revisited*. Diabetes, 2011. **60**(5): p. 1370-9.
60. Redondo, M.J. and G.S. Eisenbarth, *Genetic control of autoimmunity in Type 1 diabetes and associated disorders*. Diabetologia, 2002. **45**(5): p. 605-22.
61. Yu, L., et al., *Diabetes Prevention Trial 1: prevalence of GAD and ICA512 (IA-2) autoantibodies by relationship to proband*. Ann N Y Acad Sci, 2002. **958**: p. 254-8.
62. Bluestone, J.A., K. Herold, and G. Eisenbarth, *Genetics, pathogenesis and clinical interventions in type 1 diabetes*. Nature, 2010. **464**(7293): p. 1293-300.
63. Erlich, H., et al., *HLA DR-DQ haplotypes and genotypes and type 1 diabetes risk: analysis of the type 1 diabetes genetics consortium families*. Diabetes, 2008. **57**(4): p. 1084-92.
64. Roark, C.L., et al., *Multiple HLA epitopes contribute to type 1 diabetes susceptibility*. Diabetes, 2014. **63**(1): p. 323-31.
65. Todd, J.A., et al., *Robust associations of four new chromosome regions from genome-wide analyses of type 1 diabetes*. Nat Genet, 2007. **39**(7): p. 857-64.
66. Barrett, J.C., et al., *Genome-wide association study and meta-analysis find that over 40 loci affect risk of type 1 diabetes*. Nat Genet, 2009. **41**(6): p. 703-7.
67. Atkinson, M.A. and G.S. Eisenbarth, *Type 1 diabetes: new perspectives on disease pathogenesis and treatment*. Lancet, 2001. **358**(9277): p. 221-9.
68. Eringsmark Regnell, S. and A. Lernmark, *The environment and the origins of islet autoimmunity and Type 1 diabetes*. Diabet Med, 2013. **30**(2): p. 155-60.
69. Coppieters, K.T. and M.G. von Herrath, *Viruses and cytotoxic T lymphocytes in type 1 diabetes*. Clin Rev Allergy Immunol, 2011. **41**(2): p. 169-78.
70. Stene, L.C., et al., *Enterovirus infection and progression from islet autoimmunity to type 1 diabetes: the Diabetes and Autoimmunity Study in the Young (DAISY)*. Diabetes, 2010. **59**(12): p. 3174-80.
71. Kondrashova, A., et al., *A six-fold gradient in the incidence of type 1 diabetes at the eastern border of Finland*. Ann Med, 2005. **37**(1): p. 67-72.
72. *Infections and vaccinations as risk factors for childhood type 1 (insulin-dependent) diabetes mellitus: a multicentre case-control investigation. EURODIAB Substudy 2 Study Group*. Diabetologia, 2000. **43**(1): p. 47-53.

73. Lempainen, J., et al., *Interplay between PTPN22 C1858T polymorphism and cow's milk formula exposure in type 1 diabetes*. J Autoimmun, 2009. **33**(2): p. 155-64.
74. Zipitis, C.S. and A.K. Akobeng, *Vitamin D supplementation in early childhood and risk of type 1 diabetes: a systematic review and meta-analysis*. Arch Dis Child, 2008. **93**(6): p. 512-7.
75. Hypponen, E., et al., *Intake of vitamin D and risk of type 1 diabetes: a birth-cohort study*. Lancet, 2001. **358**(9292): p. 1500-3.
76. Mallone, R., V. Brezar, and C. Boitard, *T cell recognition of autoantigens in human type 1 diabetes: clinical perspectives*. Clin Dev Immunol, 2011. **2011**: p. 513210.
77. Di Lorenzo, T.P., M. Peakman, and B.O. Roep, *Translational mini-review series on type 1 diabetes: Systematic analysis of T cell epitopes in autoimmune diabetes*. Clin Exp Immunol, 2007. **148**(1): p. 1-16.
78. Nakayama, M., et al., *Prime role for an insulin epitope in the development of type 1 diabetes in NOD mice*. Nature, 2005. **435**(7039): p. 220-3.
79. Peakman, M., et al., *Naturally processed and presented epitopes of the islet cell autoantigen IA-2 eluted from HLA-DR4*. J Clin Invest, 1999. **104**(10): p. 1449-57.
80. Thrower, S.L., et al., *Proinsulin peptide immunotherapy in type 1 diabetes: report of a first-in-man Phase I safety study*. Clin Exp Immunol, 2009. **155**(2): p. 156-65.
81. Yang, J., et al., *CD4+ T cells recognize diverse epitopes within GAD65: implications for repertoire development and diabetes monitoring*. Immunology, 2013. **138**(3): p. 269-79.
82. Kawasaki, E., et al., *Definition of multiple ICA512/phogrin autoantibody epitopes and detection of intramolecular epitope spreading in relatives of patients with type 1 diabetes*. Diabetes, 1998. **47**(5): p. 733-42.
83. Naserke, H.E., et al., *Early development and spreading of autoantibodies to epitopes of IA-2 and their association with progression to type 1 diabetes*. J Immunol, 1998. **161**(12): p. 6963-9.
84. Brooks-Worrell, B., et al., *Intermolecular antigen spreading occurs during the preclinical period of human type 1 diabetes*. J Immunol, 2001. **166**(8): p. 5265-70.
85. Ryden, A.K., et al., *Non-antigenic and antigenic interventions in type 1 diabetes*. Hum Vaccin Immunother, 2013. **10**(4).
86. Tian, J. and D.L. Kaufman, *Antigen-based therapy for the treatment of type 1 diabetes*. Diabetes, 2009. **58**(9): p. 1939-46.
87. Skyler, J.S., et al., *Effects of oral insulin in relatives of patients with type 1 diabetes: The Diabetes Prevention Trial--Type 1*. Diabetes Care, 2005. **28**(5): p. 1068-76.
88. Harrison, L.C., et al., *Pancreatic beta-cell function and immune responses to insulin after administration of intranasal insulin to humans at risk for type 1 diabetes*. Diabetes Care, 2004. **27**(10): p. 2348-55.
89. Nanto-Salonen, K., et al., *Nasal insulin to prevent type 1 diabetes in children with HLA genotypes and autoantibodies conferring increased risk of disease: a double-blind, randomised controlled trial*. Lancet, 2008. **372**(9651): p. 1746-55.

90. Rewers, M. and P. Gottlieb, *Immunotherapy for the prevention and treatment of type 1 diabetes: human trials and a look into the future*. Diabetes Care, 2009. **32**(10): p. 1769-82.
91. Skyler, J.S., *Primary and secondary prevention of Type 1 diabetes*. Diabet Med, 2013. **30**(2): p. 161-9.
92. Bougneres, P.F., et al., *Limited duration of remission of insulin dependency in children with recent overt type I diabetes treated with low-dose cyclosporin*. Diabetes, 1990. **39**(10): p. 1264-72.
93. Jenner, M., et al., *Cyclosporin A treatment of young children with newly-diagnosed type 1 (insulin-dependent) diabetes mellitus*. London Diabetes Study Group. Diabetologia, 1992. **35**(9): p. 884-8.
94. Gottlieb, P.A., et al., *Failure to preserve beta-cell function with mycophenolate mofetil and daclizumab combined therapy in patients with new-onset type 1 diabetes*. Diabetes Care, 2010. **33**(4): p. 826-32.
95. Chatenoud, L., et al., *Corticosteroid inhibition of the OKT3-induced cytokine-related syndrome--dosage and kinetics prerequisites*. Transplantation, 1991. **51**(2): p. 334-8.
96. Li, B., et al., *Construction and characterization of a humanized anti-human CD3 monoclonal antibody 12F6 with effective immunoregulation functions*. Immunology, 2005. **116**(4): p. 487-98.
97. Herold, K.C., et al., *Anti-CD3 monoclonal antibody in new-onset type 1 diabetes mellitus*. N Engl J Med, 2002. **346**(22): p. 1692-8.
98. Herold, K.C., et al., *A single course of anti-CD3 monoclonal antibody hOKT3gamma1(Ala-Ala) results in improvement in C-peptide responses and clinical parameters for at least 2 years after onset of type 1 diabetes*. Diabetes, 2005. **54**(6): p. 1763-9.
99. Bisikirska, B., et al., *TCR stimulation with modified anti-CD3 mAb expands CD8+ T cell population and induces CD8+CD25+ Tregs*. J Clin Invest, 2005. **115**(10): p. 2904-13.
100. Herold, K.C., et al., *Teplizumab (Anti-CD3 mAb) Treatment Preserves C-Peptide Responses in Patients With New-Onset Type 1 Diabetes in a Randomized Controlled Trial: Metabolic and Immunologic Features at Baseline Identify a Subgroup of Responders*. Diabetes, 2013. **62**(11): p. 3766-74.
101. Sherry, N., et al., *Teplizumab for treatment of type 1 diabetes (Protege study): 1-year results from a randomised, placebo-controlled trial*. Lancet, 2011. **378**(9790): p. 487-97.
102. Hagopian, W., et al., *Teplizumab preserves C-peptide in recent-onset type 1 diabetes: two-year results from the randomized, placebo-controlled Protege trial*. Diabetes, 2013. **62**(11): p. 3901-8.
103. Ambery, P., et al., *Efficacy and safety of low-dose oteelixizumab anti-CD3 monoclonal antibody in preserving C-peptide secretion in adolescent type 1 diabetes: DEFEND-2, a randomized, placebo-controlled, double-blind, multi-centre study*. Diabet Med, 2014. **31**(4): p. 399-402.
104. Keymeulen, B., et al., *Insulin needs after CD3-antibody therapy in new-onset type 1 diabetes*. N Engl J Med, 2005. **352**(25): p. 2598-608.
105. Keymeulen, B., et al., *Four-year metabolic outcome of a randomised controlled CD3-antibody trial in recent-onset type 1 diabetic patients*

- depends on their age and baseline residual beta cell mass. *Diabetologia*, 2010. **53**(4): p. 614-23.
106. Orban, T., et al., *Co-stimulation modulation with abatacept in patients with recent-onset type 1 diabetes: a randomised, double-blind, placebo-controlled trial*. *Lancet*, 2011. **378**(9789): p. 412-9.
 107. Pescovitz, M.D., et al., *Rituximab, B-lymphocyte depletion, and preservation of beta-cell function*. *N Engl J Med*, 2009. **361**(22): p. 2143-52.
 108. Herold, K.C., et al., *Increased T cell proliferative responses to islet antigens identify clinical responders to anti-CD20 monoclonal antibody (rituximab) therapy in type 1 diabetes*. *J Immunol*, 2011. **187**(4): p. 1998-2005.
 109. Zhao, Y., et al., *Circulating T follicular helper cell and regulatory T cell frequencies are influenced by B cell depletion in patients with granulomatosis with polyangiitis*. *Rheumatology (Oxford)*, 2014. **53**(4): p. 621-30.
 110. Mandrup-Poulsen, T., L. Pickersgill, and M.Y. Donath, *Blockade of interleukin 1 in type 1 diabetes mellitus*. *Nat Rev Endocrinol*, 2010. **6**(3): p. 158-66.
 111. Moran, A., et al., *Interleukin-1 antagonism in type 1 diabetes of recent onset: two multicentre, randomised, double-blind, placebo-controlled trials*. *Lancet*, 2013. **381**(9881): p. 1905-15.
 112. Long, S.A., et al., *Rapamycin/IL-2 combination therapy in patients with type 1 diabetes augments Tregs yet transiently impairs beta-cell function*. *Diabetes*, 2012. **61**(9): p. 2340-8.
 113. Weinberg, A., et al., *Effect of abatacept on immunogenicity of vaccines in individuals with type 1 diabetes*. *Vaccine*, 2013. **31**(42): p. 4791-4.
 114. Ruderman, E.M., *Overview of safety of non-biologic and biologic DMARDs*. *Rheumatology (Oxford)*, 2012. **51 Suppl 6**: p. vi37-43.
 115. Kroll, J.L., et al., *Reactivation of latent viruses in individuals receiving rituximab for new onset type 1 diabetes*. *J Clin Virol*, 2013. **57**(2): p. 115-9.
 116. Larche, M. and D.C. Wraith, *Peptide-based therapeutic vaccines for allergic and autoimmune diseases*. *Nat Med*, 2005. **11**(4 Suppl): p. S69-76.
 117. Brewer, J.M., et al., *In interleukin-4-deficient mice, alum not only generates T helper 1 responses equivalent to freund's complete adjuvant, but continues to induce T helper 2 cytokine production*. *Eur J Immunol*, 1996. **26**(9): p. 2062-6.
 118. Ludvigsson, J., et al., *GAD treatment and insulin secretion in recent-onset type 1 diabetes*. *N Engl J Med*, 2008. **359**(18): p. 1909-20.
 119. Wherrett, D.K., et al., *Antigen-based therapy with glutamic acid decarboxylase (GAD) vaccine in patients with recent-onset type 1 diabetes: a randomised double-blind trial*. *Lancet*, 2011. **378**(9788): p. 319-27.
 120. Ludvigsson, J., et al., *GAD65 antigen therapy in recently diagnosed type 1 diabetes mellitus*. *N Engl J Med*, 2012. **366**(5): p. 433-42.
 121. Boettler, T., et al., *The clinical and immunological significance of GAD-specific autoantibody and T-cell responses in type 1 diabetes*. *J Autoimmun*, 2013. **44**: p. 40-8.
 122. von Herrath, M., M. Peakman, and B. Roep, *Progress in immune-based therapies for type 1 diabetes*. *Clin Exp Immunol*, 2013. **172**(2): p. 186-202.
 123. Raz, I., et al., *Beta-cell function in new-onset type 1 diabetes and immunomodulation with a heat-shock protein peptide (DiaPep277): a*

- randomised, double-blind, phase II trial. Lancet*, 2001. **358**(9295): p. 1749-53.
124. Lazar, L., et al., *Heat-shock protein peptide DiaPep277 treatment in children with newly diagnosed type 1 diabetes: a randomised, double-blind phase II study. Diabetes Metab Res Rev*, 2007. **23**(4): p. 286-91.
 125. Raz, I., et al., *Treatment of Recent-Onset Type 1 Diabetic Patients With DiaPep277: Results of a Double-Blind, Placebo-Controlled, Randomized Phase 3 Trial. Diabetes Care*, 2014. **37**(5): p. 1392-400.
 126. Pozzilli, P., et al., *Evaluation of long-term treatment effect in a type 1 diabetes intervention trial: differences after stimulation with glucagon or a mixed meal. Diabetes Care*, 2014. **37**(5): p. 1384-91.
 127. Gottlieb, P., et al., *Clinical optimization of antigen specific modulation of type 1 diabetes with the plasmid DNA platform. Clin Immunol*, 2013. **149**(3): p. 297-306.
 128. Bresson, D., et al., *Anti-CD3 and nasal proinsulin combination therapy enhances remission from recent-onset autoimmune diabetes by inducing Tregs. J Clin Invest*, 2006. **116**(5): p. 1371-81.
 129. Jaber-Douraki, M., M. Pietropaolo, and A. Khadra, *Predictive models of type 1 diabetes progression: understanding T-cell cycles and their implications on autoantibody release. PLoS One*, 2014. **9**(4): p. e93326.
 130. Buzzetti, R., et al., *C-peptide response and HLA genotypes in subjects with recent-onset type 1 diabetes after immunotherapy with DiaPep277: an exploratory study. Diabetes*, 2011. **60**(11): p. 3067-72.
 131. Besser, R.E., et al., *Urine C-peptide creatinine ratio is a noninvasive alternative to the mixed-meal tolerance test in children and adults with type 1 diabetes. Diabetes Care*, 2011. **34**(3): p. 607-9.
 132. Roep, B.O. and M. Peakman, *Surrogate end points in the design of immunotherapy trials: emerging lessons from type 1 diabetes. Nat Rev Immunol*, 2010. **10**(2): p. 145-52.
 133. Vukmanovic-Stejic, M., et al., *The kinetics of CD4+Foxp3+ T cell accumulation during a human cutaneous antigen-specific memory response in vivo. J Clin Invest*, 2008. **118**(11): p. 3639-50.
 134. Prunieras, M., M. Regnier, and D. Woodley, *Methods for cultivation of keratinocytes with an air-liquid interface. J Invest Dermatol*, 1983. **81**(1 Suppl): p. 28s-33s.
 135. Boyce, S.T. and R.G. Ham, *Calcium-regulated differentiation of normal human epidermal keratinocytes in chemically defined clonal culture and serum-free serial culture. J Invest Dermatol*, 1983. **81**(1 Suppl): p. 33s-40s.
 136. Amel Kashipaz, M.R., et al., *Human autologous mixed lymphocyte reaction as an in vitro model for autoreactivity to apoptotic antigens. Immunology*, 2002. **107**(3): p. 358-65.
 137. Sontheimer, R.D., *The mixed epidermal cell-lymphocyte reaction. II. Epidermal Langerhans cells are responsible for the enhanced allogeneic lymphocyte-stimulating capacity of normal human epidermal cell suspensions. J Invest Dermatol*, 1985. **85**(1 Suppl): p. 21s-26s.
 138. Gillespie, K.M., et al., *HLA class II typing of whole genome amplified mouth swab DNA. Tissue Antigens*, 2000. **56**(6): p. 530-8.

139. Krishnamurthy, S., *Current applications and future prospects of fine-needle aspiration biopsy of locoregional lymph nodes in the management of breast cancer*. Cancer, 2009. **117**(6): p. 451-62.
140. Schmittel, A., et al., *Application of the IFN-gamma ELISPOT assay to quantify T cell responses against proteins*. J Immunol Methods, 2001. **247**(1-2): p. 17-24.
141. Haselden, B.M., A.B. Kay, and M. Larche, *Immunoglobulin E-independent major histocompatibility complex- restricted T cell peptide epitope-induced late asthmatic reactions*. J Exp Med, 1999. **189**(12): p. 1885-94.
142. Kanitakis, J., *Anatomy, histology and immunohistochemistry of normal human skin*. Eur J Dermatol, 2002. **12**(4): p. 390-9; quiz 400-1.
143. Spetz, A.L., J. Strominger, and V. Groh-Spies, *T cell subsets in normal human epidermis*. Am J Pathol, 1996. **149**(2): p. 665-74.
144. Mbongue, J., et al., *The role of dendritic cells in tissue-specific autoimmunity*. J Immunol Res, 2014. **2014**: p. 857143.
145. Valladeau, J. and S. Saeland, *Cutaneous dendritic cells*. Semin Immunol, 2005. **17**(4): p. 273-83.
146. Stingl, G., K. Tamaki, and S.I. Katz, *Origin and function of epidermal Langerhans cells*. Immunol Rev, 1980. **53**: p. 149-74.
147. Valladeau, J., et al., *Langerin, a novel C-type lectin specific to Langerhans cells, is an endocytic receptor that induces the formation of Birbeck granules*. Immunity, 2000. **12**(1): p. 71-81.
148. Ebner, S., et al., *Expression of C-type lectin receptors by subsets of dendritic cells in human skin*. Int Immunol, 2004. **16**(6): p. 877-87.
149. Tang, A., et al., *Adhesion of epidermal Langerhans cells to keratinocytes mediated by E-cadherin*. Nature, 1993. **361**(6407): p. 82-5.
150. Borkowski, T.A., et al., *A role for endogenous transforming growth factor beta 1 in Langerhans cell biology: the skin of transforming growth factor beta 1 null mice is devoid of epidermal Langerhans cells*. J Exp Med, 1996. **184**(6): p. 2417-22.
151. Hunger, R.E., et al., *Langerhans cells utilize CD1a and langerin to efficiently present nonpeptide antigens to T cells*. J Clin Invest, 2004. **113**(5): p. 701-8.
152. Merad, M., F. Ginhoux, and M. Collin, *Origin, homeostasis and function of Langerhans cells and other langerin-expressing dendritic cells*. Nat Rev Immunol, 2008. **8**(12): p. 935-47.
153. Geijtenbeek, T.B., et al., *Identification of DC-SIGN, a novel dendritic cell-specific ICAM-3 receptor that supports primary immune responses*. Cell, 2000. **100**(5): p. 575-85.
154. Klechevsky, E. and J. Banchereau, *Human dendritic cells subsets as targets and vectors for therapy*. Ann N Y Acad Sci, 2013. **1284**: p. 24-30.
155. Bursch, L.S., et al., *Identification of a novel population of Langerin+ dendritic cells*. J Exp Med, 2007. **204**(13): p. 3147-56.
156. Fukunaga, A., et al., *Langerhans cells serve as immunoregulatory cells by activating NKT cells*. J Immunol, 2010. **185**(8): p. 4633-40.
157. Azukizawa, H., et al., *Steady state migratory RelB+ langerin+ dermal dendritic cells mediate peripheral induction of antigen-specific CD4+ CD25+ Foxp3+ regulatory T cells*. Eur J Immunol, 2011. **41**(5): p. 1420-34.

158. Romani, N., B.E. Clausen, and P. Stoitzner, *Langerhans cells and more: langerin-expressing dendritic cell subsets in the skin*. Immunol Rev, 2010. **234**(1): p. 120-41.
159. Guillelliams, M., et al., *From skin dendritic cells to a simplified classification of human and mouse dendritic cell subsets*. Eur J Immunol, 2010. **40**(8): p. 2089-94.
160. van der Aar, A.M., et al., *Langerhans Cells Favor Skin Flora Tolerance through Limited Presentation of Bacterial Antigens and Induction of Regulatory T Cells*. J Invest Dermatol, 2013.
161. Chu, C.C., et al., *Resident CD141 (BDCA3)+ dendritic cells in human skin produce IL-10 and induce regulatory T cells that suppress skin inflammation*. J Exp Med, 2012. **209**(5): p. 935-45.
162. Kenney, R.T., et al., *Dose sparing with intradermal injection of influenza vaccine*. N Engl J Med, 2004. **351**(22): p. 2295-301.
163. Davis, S.P., et al., *Hollow metal microneedles for insulin delivery to diabetic rats*. IEEE Trans Biomed Eng, 2005. **52**(5): p. 909-15.
164. Van Damme, P., et al., *Safety and efficacy of a novel microneedle device for dose sparing intradermal influenza vaccination in healthy adults*. Vaccine, 2009. **27**(3): p. 454-9.
165. Martanto, W., et al., *Transdermal delivery of insulin using microneedles in vivo*. Pharm Res, 2004. **21**(6): p. 947-52.
166. Fukushima, K., et al., *Pharmacokinetic and pharmacodynamic evaluation of insulin dissolving microneedles in dogs*. Diabetes Technol Ther, 2010. **12**(6): p. 465-74.
167. Gupta, J., E.I. Felner, and M.R. Prausnitz, *Minimally invasive insulin delivery in subjects with type 1 diabetes using hollow microneedles*. Diabetes Technol Ther, 2009. **11**(6): p. 329-37.
168. Gupta, J., E.I. Felner, and M.R. Prausnitz, *Rapid pharmacokinetics of intradermal insulin administered using microneedles in type 1 diabetes subjects*. Diabetes Technol Ther, 2011. **13**(4): p. 451-6.
169. Harvey, A.J., et al., *Microneedle-based intradermal delivery enables rapid lymphatic uptake and distribution of protein drugs*. Pharm Res, 2011. **28**(1): p. 107-16.
170. Daddona, P.E., et al., *Parathyroid hormone (1-34)-coated microneedle patch system: clinical pharmacokinetics and pharmacodynamics for treatment of osteoporosis*. Pharm Res, 2011. **28**(1): p. 159-65.
171. Fernando, G.J., et al., *Potent immunity to low doses of influenza vaccine by probabilistic guided micro-targeted skin delivery in a mouse model*. PLoS One, 2010. **5**(4): p. e10266.
172. Matriano, J.A., et al., *Macroflux microprojection array patch technology: a new and efficient approach for intracutaneous immunization*. Pharm Res, 2002. **19**(1): p. 63-70.
173. Koyama, Y., et al., *Sex differences in the densities of epidermal Langerhans cells of the mouse*. J Invest Dermatol, 1987. **88**(5): p. 541-4.
174. Hong, X., et al., *Dissolving and biodegradable microneedle technologies for transdermal sustained delivery of drug and vaccine*. Drug Des Devel Ther, 2013. **7**: p. 945-952.

175. Beran, J., et al., *Intradermal influenza vaccination of healthy adults using a new microinjection system: a 3-year randomised controlled safety and immunogenicity trial*. BMC Med, 2009. **7**: p. 13.
176. Bal, S.M., et al., *In vivo assessment of safety of microneedle arrays in human skin*. Eur J Pharm Sci, 2008. **35**(3): p. 193-202.
177. Fernando, G.J., et al., *Nanopatch targeted delivery of both antigen and adjuvant to skin synergistically drives enhanced antibody responses*. J Control Release, 2012. **159**(2): p. 215-21.
178. Ruutu, M.P., et al., *Increasing mechanical stimulus induces migration of Langerhans cells and impairs the immune response to intracutaneously delivered antigen*. Exp Dermatol, 2011. **20**(6): p. 534-6.
179. Novak, N., et al., *Human skin and oral mucosal dendritic cells as 'good guys' and 'bad guys' in allergic immune responses*. Clin Exp Immunol, 2010. **161**(1): p. 28-33.
180. Steinman, R.M., D. Hawiger, and M.C. Nussenzweig, *Tolerogenic dendritic cells*. Annu Rev Immunol, 2003. **21**: p. 685-711.
181. Bedoui, S., et al., *Cross-presentation of viral and self antigens by skin-derived CD103+ dendritic cells*. Nat Immunol, 2009. **10**(5): p. 488-95.
182. Bianchi, T., et al., *Maintenance of peripheral tolerance through controlled tissue homing of antigen-specific T cells in K14-mOVA mice*. J Immunol, 2009. **182**(8): p. 4665-74.
183. Thepaut, M., et al., *Structural studies of langerin and Birbeck granule: a macromolecular organization model*. Biochemistry, 2009. **48**(12): p. 2684-98.
184. Schuler, G., N. Romani, and R.M. Steinman, *A comparison of murine epidermal Langerhans cells with spleen dendritic cells*. J Invest Dermatol, 1985. **85**(1 Suppl): p. 99s-106s.
185. Klitz, W., et al., *New HLA haplotype frequency reference standards: high-resolution and large sample typing of HLA DR-DQ haplotypes in a sample of European Americans*. Tissue Antigens, 2003. **62**(4): p. 296-307.
186. Gill, H.S., et al., *Effect of microneedle design on pain in human volunteers*. Clin J Pain, 2008. **24**(7): p. 585-94.
187. Haq, M.I., et al., *Clinical administration of microneedles: skin puncture, pain and sensation*. Biomed Microdevices, 2009. **11**(1): p. 35-47.
188. Norman, J.J., et al., *Microneedle patches: usability and acceptability for self-vaccination against influenza*. Vaccine, 2014. **32**(16): p. 1856-62.
189. Coquerelle, C. and M. Moser, *DC subsets in positive and negative regulation of immunity*. Immunol Rev, 2010. **234**(1): p. 317-34.
190. Yamazaki, S., et al., *CD8+ CD205+ splenic dendritic cells are specialized to induce Foxp3+ regulatory T cells*. J Immunol, 2008. **181**(10): p. 6923-33.
191. Nikolic, T., et al., *Plasmacytoid dendritic cells in autoimmune diabetes - potential tools for immunotherapy*. Immunobiology, 2009. **214**(9-10): p. 791-9.
192. De Smedt, T., et al., *Regulation of dendritic cell numbers and maturation by lipopolysaccharide in vivo*. J Exp Med, 1996. **184**(4): p. 1413-24.
193. Sallusto, F. and A. Lanzavecchia, *Efficient presentation of soluble antigen by cultured human dendritic cells is maintained by granulocyte/macrophage colony-stimulating factor plus interleukin 4 and downregulated by tumor necrosis factor alpha*. J Exp Med, 1994. **179**(4): p. 1109-18.

194. Inaba, K., et al., *The formation of immunogenic major histocompatibility complex class II-peptide ligands in lysosomal compartments of dendritic cells is regulated by inflammatory stimuli*. J Exp Med, 2000. **191**(6): p. 927-36.
195. Caux, C., et al., *Activation of human dendritic cells through CD40 cross-linking*. J Exp Med, 1994. **180**(4): p. 1263-72.
196. Inaba, K., et al., *The tissue distribution of the B7-2 costimulator in mice: abundant expression on dendritic cells in situ and during maturation in vitro*. J Exp Med, 1994. **180**(5): p. 1849-60.
197. Granucci, F., et al., *Inducible IL-2 production by dendritic cells revealed by global gene expression analysis*. Nat Immunol, 2001. **2**(9): p. 882-8.
198. Sallusto, F., et al., *Distinct patterns and kinetics of chemokine production regulate dendritic cell function*. Eur J Immunol, 1999. **29**(5): p. 1617-25.
199. Langenkamp, A., et al., *Kinetics of dendritic cell activation: impact on priming of TH1, TH2 and nonpolarized T cells*. Nat Immunol, 2000. **1**(4): p. 311-6.
200. Kushwah, R. and J. Hu, *Role of dendritic cells in the induction of regulatory T cells*. Cell Biosci, 2011. **1**(1): p. 20.
201. Jonuleit, H., et al., *Induction of interleukin 10-producing, nonproliferating CD4(+) T cells with regulatory properties by repetitive stimulation with allogeneic immature human dendritic cells*. J Exp Med, 2000. **192**(9): p. 1213-22.
202. Salomon, B., et al., *B7/CD28 costimulation is essential for the homeostasis of the CD4+CD25+ immunoregulatory T cells that control autoimmune diabetes*. Immunity, 2000. **12**(4): p. 431-40.
203. Cella, M., et al., *A novel inhibitory receptor (ILT3) expressed on monocytes, macrophages, and dendritic cells involved in antigen processing*. J Exp Med, 1997. **185**(10): p. 1743-51.
204. Liang, B., et al., *Regulatory T cells inhibit dendritic cells by lymphocyte activation gene-3 engagement of MHC class II*. J Immunol, 2008. **180**(9): p. 5916-26.
205. Carvalheiro, T., et al., *Tolerogenic versus inflammatory activity of peripheral blood monocytes and dendritic cells subpopulations in systemic lupus erythematosus*. Clin Dev Immunol, 2012. **2012**: p. 934161.
206. Nuyts, A., et al., *Dendritic cells in multiple sclerosis: key players in the immunopathogenesis, key players for new cellular immunotherapies?* Mult Scler, 2013. **19**(8): p. 995-1002.
207. Nikolic, T. and B.O. Roep, *Regulatory multitasking of tolerogenic dendritic cells - lessons taken from vitamin d3-treated tolerogenic dendritic cells*. Front Immunol, 2013. **4**: p. 113.
208. Rutella, S., S. Danese, and G. Leone, *Tolerogenic dendritic cells: cytokine modulation comes of age*. Blood, 2006. **108**(5): p. 1435-40.
209. Boks, M.A., et al., *IL-10-generated tolerogenic dendritic cells are optimal for functional regulatory T cell induction--a comparative study of human clinical-applicable DC*. Clin Immunol, 2012. **142**(3): p. 332-42.
210. Adorini, L. and G. Penna, *Induction of tolerogenic dendritic cells by vitamin D receptor agonists*. Handb Exp Pharmacol, 2009(188): p. 251-73.

211. Adorini, L., et al., *Dendritic cells as key targets for immunomodulation by Vitamin D receptor ligands*. J Steroid Biochem Mol Biol, 2004. **89-90**(1-5): p. 437-41.
212. van Halteren, A.G., et al., *Redirection of human autoreactive T-cells Upon interaction with dendritic cells modulated by TX527, an analog of 1,25 dihydroxyvitamin D(3)*. Diabetes, 2002. **51**(7): p. 2119-25.
213. Penna, G. and L. Adorini, *1 Alpha,25-dihydroxyvitamin D3 inhibits differentiation, maturation, activation, and survival of dendritic cells leading to impaired alloreactive T cell activation*. J Immunol, 2000. **164**(5): p. 2405-11.
214. van Halteren, A.G., et al., *1alpha,25-dihydroxyvitamin D3 or analogue treated dendritic cells modulate human autoreactive T cells via the selective induction of apoptosis*. J Autoimmun, 2004. **23**(3): p. 233-9.
215. Unger, W.W., et al., *Induction of Treg by monocyte-derived DC modulated by vitamin D3 or dexamethasone: differential role for PD-L1*. Eur J Immunol, 2009. **39**(11): p. 3147-59.
216. Farias, A.S., et al., *Vitamin D3 induces IDO(+) tolerogenic DCs and enhances Treg, reducing the severity of EAE*. CNS Neurosci Ther, 2013. **19**(4): p. 269-77.
217. Piemonti, L., et al., *Glucocorticoids affect human dendritic cell differentiation and maturation*. J Immunol, 1999. **162**(11): p. 6473-81.
218. Matasic, R., A.B. Dietz, and S. Vuk-Pavlovic, *Dexamethasone inhibits dendritic cell maturation by redirecting differentiation of a subset of cells*. J Leukoc Biol, 1999. **66**(6): p. 909-14.
219. Rea, D., et al., *Glucocorticoids transform CD40-triggering of dendritic cells into an alternative activation pathway resulting in antigen-presenting cells that secrete IL-10*. Blood, 2000. **95**(10): p. 3162-7.
220. Chamorro, S., et al., *TLR triggering on tolerogenic dendritic cells results in TLR2 up-regulation and a reduced proinflammatory immune program*. J Immunol, 2009. **183**(5): p. 2984-94.
221. Ferreira, G.B., et al., *1,25-Dihydroxyvitamin D3 alters murine dendritic cell behaviour in vitro and in vivo*. Diabetes Metab Res Rev, 2011. **27**(8): p. 933-41.
222. Stoop, J.N., et al., *Therapeutic effect of tolerogenic dendritic cells in established collagen-induced arthritis is associated with a reduction in Th17 responses*. Arthritis Rheum, 2010. **62**(12): p. 3656-65.
223. Volchenkov, R., et al., *Type 1 regulatory T cells and regulatory B cells induced by tolerogenic dendritic cells*. Scand J Immunol, 2013. **77**(4): p. 246-54.
224. Kleijwegt, F.S., et al., *Tolerogenic dendritic cells impede priming of naive CD8(+) T cells and deplete memory CD8(+) T cells*. Eur J Immunol, 2013. **43**(1): p. 85-92.
225. Karagiannidis, C., et al., *Glucocorticoids upregulate FOXP3 expression and regulatory T cells in asthma*. J Allergy Clin Immunol, 2004. **114**(6): p. 1425-33.
226. Azab, N.A., et al., *CD4+CD25+ regulatory T cells (TREG) in systemic lupus erythematosus (SLE) patients: the possible influence of treatment with corticosteroids*. Clin Immunol, 2008. **127**(2): p. 151-7.

227. Xu, L., Z. Xu, and M. Xu, *Glucocorticoid treatment restores the impaired suppressive function of regulatory T cells in patients with relapsing-remitting multiple sclerosis*. Clin Exp Immunol, 2009. **158**(1): p. 26-30.
228. Zhang, Q., et al., *Expression of surface markers on peripheral CD4+CD25high T cells in patients with atopic asthma: role of inhaled corticosteroid*. Chin Med J (Engl), 2008. **121**(3): p. 205-12.
229. Xystrakis, E., et al., *Reversing the defective induction of IL-10-secreting regulatory T cells in glucocorticoid-resistant asthma patients*. J Clin Invest, 2006. **116**(1): p. 146-55.
230. Majak, P., B. Rychlik, and I. Stelmach, *The effect of oral steroids with and without vitamin D3 on early efficacy of immunotherapy in asthmatic children*. Clin Exp Allergy, 2009. **39**(12): p. 1830-41.
231. Sbiera, S., et al., *Influence of short-term glucocorticoid therapy on regulatory T cells in vivo*. PLoS One, 2011. **6**(9): p. e24345.
232. Kang, Y., et al., *Cutting edge: Immunosuppressant as adjuvant for tolerogenic immunization*. J Immunol, 2008. **180**(8): p. 5172-6.
233. Zheng, G., et al., *Dexamethasone promotes tolerance in vivo by enriching CD11clo CD40lo tolerogenic macrophages*. Eur J Immunol, 2013. **43**(1): p. 219-27.
234. Enioutina, E.Y., D. Bareyan, and R.A. Daynes, *Vitamin D3-mediated alterations to myeloid dendritic cell trafficking in vivo expand the scope of their antigen presenting properties*. Vaccine, 2007. **25**(7): p. 1236-49.
235. van der Aar, A.M., et al., *Vitamin D3 targets epidermal and dermal dendritic cells for induction of distinct regulatory T cells*. J Allergy Clin Immunol, 2011. **127**(6): p. 1532-40 e7.
236. Lindenberg, J.J., et al., *IL-10 conditioning of human skin affects the distribution of migratory dendritic cell subsets and functional T cell differentiation*. PLoS One, 2013. **8**(7): p. e70237.
237. Bastus, N.G., et al., *Peptides conjugated to gold nanoparticles induce macrophage activation*. Mol Immunol, 2009. **46**(4): p. 743-8.
238. Villiers, C., et al., *Analysis of the toxicity of gold nano particles on the immune system: effect on dendritic cell functions*. J Nanopart Res, 2010. **12**(1): p. 55-60.
239. Kennedy, L.C., et al., *T cells enhance gold nanoparticle delivery to tumors in vivo*. Nanoscale Res Lett, 2011. **6**(1): p. 283.
240. Thompson, C.D., et al., *The therapeutic role of interleukin-10 after spinal cord injury*. J Neurotrauma, 2013. **30**(15): p. 1311-24.
241. Marlow, G.J., D. van Gent, and L.R. Ferguson, *Why interleukin-10 supplementation does not work in Crohn's disease patients*. World J Gastroenterol, 2013. **19**(25): p. 3931-41.
242. Creed, T.J., et al., *The effects of cytokines on suppression of lymphocyte proliferation by dexamethasone*. J Immunol, 2009. **183**(1): p. 164-71.
243. Jurynczyk, M., et al., *Immune regulation of multiple sclerosis by transdermally applied myelin peptides*. Ann Neurol, 2010. **68**(5): p. 593-601.
244. O'Rahilly, R. and F. Müller, *Basic human anatomy : a regional study of human structure*. 1983, Philadelphia: Saunders. xi, 566 p.

245. Forster, R., A. Braun, and T. Worbs, *Lymph node homing of T cells and dendritic cells via afferent lymphatics*. Trends Immunol, 2012. **33**(6): p. 271-80.
246. Jiang, A., et al., *Disruption of E-cadherin-mediated adhesion induces a functionally distinct pathway of dendritic cell maturation*. Immunity, 2007. **27**(4): p. 610-24.
247. Ratzinger, G., et al., *Matrix metalloproteinases 9 and 2 are necessary for the migration of Langerhans cells and dermal dendritic cells from human and murine skin*. J Immunol, 2002. **168**(9): p. 4361-71.
248. Tomura, M., et al., *Monitoring cellular movement in vivo with photoconvertible fluorescence protein "Kaede" transgenic mice*. Proc Natl Acad Sci U S A, 2008. **105**(31): p. 10871-6.
249. van de Ven, R., et al., *Characterization of four conventional dendritic cell subsets in human skin-draining lymph nodes in relation to T-cell activation*. Blood, 2011. **118**(9): p. 2502-10.
250. Angel, C.E., et al., *Distinctive localization of antigen-presenting cells in human lymph nodes*. Blood, 2009. **113**(6): p. 1257-67.
251. Gunn, M.D., et al., *A chemokine expressed in lymphoid high endothelial venules promotes the adhesion and chemotaxis of naive T lymphocytes*. Proc Natl Acad Sci U S A, 1998. **95**(1): p. 258-63.
252. Sallusto, F., et al., *Two subsets of memory T lymphocytes with distinct homing potentials and effector functions*. Nature, 1999. **401**(6754): p. 708-12.
253. Baron, J.L., et al., *Surface expression of alpha 4 integrin by CD4 T cells is required for their entry into brain parenchyma*. J Exp Med, 1993. **177**(1): p. 57-68.
254. Sallusto, F., C.R. Mackay, and A. Lanzavecchia, *Selective expression of the eotaxin receptor CCR3 by human T helper 2 cells*. Science, 1997. **277**(5334): p. 2005-7.
255. Wu, L., et al., *CCR5 levels and expression pattern correlate with infectability by macrophage-tropic HIV-1, in vitro*. J Exp Med, 1997. **185**(9): p. 1681-91.
256. Peters, J.H., et al., *Human secondary lymphoid organs typically contain polyclonally-activated proliferating regulatory T cells*. Blood, 2013. **122**(13): p. 2213-23.
257. Kupper, T.S. and R.C. Fuhlbrigge, *Immune surveillance in the skin: mechanisms and clinical consequences*. Nat Rev Immunol, 2004. **4**(3): p. 211-22.
258. Clark, R.A., et al., *The vast majority of CLA+ T cells are resident in normal skin*. J Immunol, 2006. **176**(7): p. 4431-9.
259. Kunkel, E.J., et al., *Expression of the chemokine receptors CCR4, CCR5, and CXCR3 by human tissue-infiltrating lymphocytes*. Am J Pathol, 2002. **160**(1): p. 347-55.
260. Clark, R.A. and T.S. Kupper, *IL-15 and dermal fibroblasts induce proliferation of natural regulatory T cells isolated from human skin*. Blood, 2007. **109**(1): p. 194-202.
261. Sanchez Rodriguez, R., et al., *Memory regulatory T cells reside in human skin*. J Clin Invest, 2014. **124**(3): p. 1027-36.

262. Hirahara, K., et al., *The majority of human peripheral blood CD4⁺CD25^{high}Foxp3⁺ regulatory T cells bear functional skin-homing receptors*. J Immunol, 2006. **177**(7): p. 4488-94.
263. Turk, J.L., *Delayed hypersensitivity*. 3d rev. ed. Research monographs in immunology. 1980, Amsterdam ; New YorkNew York: Elsevier/North-Holland Biomedical Press ;sole distributors for the U.S.A. and Canada, Elsevier North-Holland. xii, 295 p.
264. Platt, J.L., et al., *Immune cell populations in cutaneous delayed-type hypersensitivity*. J Exp Med, 1983. **158**(4): p. 1227-42.
265. Poulter, L.W., et al., *Immunohistological analysis of delayed-type hypersensitivity in man*. Cell Immunol, 1982. **74**(2): p. 358-69.
266. Vukmanovic-Stejic, M., et al., *Mantoux Test as a model for a secondary immune response in humans*. Immunol Lett, 2006. **107**(2): p. 93-101.
267. Muller, H.K., et al., *Tuberculin anergy in clinically normal individuals. I. Lymphokine and lymphocyte transformation studies*. Int Arch Allergy Appl Immunol, 1983. **70**(1): p. 65-70.
268. Magnani, Z.I., et al., *Circulating, Mycobacterium tuberculosis-specific lymphocytes from PPD skin test-negative patients with tuberculosis do not secrete interferon-gamma (IFN-gamma) and lack the cutaneous lymphocyte antigen skin-selective homing receptor*. Clin Exp Immunol, 2000. **119**(1): p. 99-106.
269. Black, G.F., et al., *Relationship between IFN-gamma and skin test responsiveness to Mycobacterium tuberculosis PPD in healthy, non-BCG-vaccinated young adults in Northern Malawi*. Int J Tuberc Lung Dis, 2001. **5**(7): p. 664-72.
270. Jobe, O., et al., *Proviral load and immune function in blood and lymph node during HIV-1 and HIV-2 infection*. Clin Exp Immunol, 1999. **116**(3): p. 474-8.
271. Akbar, A.N., et al., *Investigation of the cutaneous response to recall antigen in humans in vivo*. Clin Exp Immunol, 2013. **173**(2): p. 163-72.
272. Torn, C., et al., *Prognostic factors for the course of beta cell function in autoimmune diabetes*. J Clin Endocrinol Metab, 2000. **85**(12): p. 4619-23.
273. *Effect of intensive therapy on residual beta-cell function in patients with type 1 diabetes in the diabetes control and complications trial. A randomized, controlled trial. The Diabetes Control and Complications Trial Research Group*. Ann Intern Med, 1998. **128**(7): p. 517-23.
274. *Hypoglycemia in the Diabetes Control and Complications Trial. The Diabetes Control and Complications Trial Research Group*. Diabetes, 1997. **46**(2): p. 271-86.
275. Madsbad, S., et al., *Role of residual insulin secretion in protecting against ketoacidosis in insulin-dependent diabetes*. Br Med J, 1979. **2**(6200): p. 1257-9.
276. Steffes, M.W., et al., *Beta-cell function and the development of diabetes-related complications in the diabetes control and complications trial*. Diabetes Care, 2003. **26**(3): p. 832-6.
277. Panero, F., et al., *Fasting plasma C-peptide and micro- and macrovascular complications in a large clinic-based cohort of type 1 diabetic patients*. Diabetes Care, 2009. **32**(2): p. 301-5.

278. Marques, R.G., M.J. Fontaine, and J. Rogers, *C-peptide: much more than a byproduct of insulin biosynthesis*. *Pancreas*, 2004. **29**(3): p. 231-8.
279. Sosenko, J.M., et al., *Patterns of metabolic progression to type 1 diabetes in the Diabetes Prevention Trial-Type 1*. *Diabetes Care*, 2006. **29**(3): p. 643-9.
280. Teuscher, A.U., et al., *Successful islet autotransplantation in humans: functional insulin secretory reserve as an estimate of surviving islet cell mass*. *Diabetes*, 1998. **47**(3): p. 324-30.
281. Greenbaum, C.J., et al., *Mixed-meal tolerance test versus glucagon stimulation test for the assessment of beta-cell function in therapeutic trials in type 1 diabetes*. *Diabetes Care*, 2008. **31**(10): p. 1966-71.
282. Steele, C., et al., *Insulin secretion in type 1 diabetes*. *Diabetes*, 2004. **53**(2): p. 426-33.
283. Horwitz, D.L., A.H. Rubenstein, and A.I. Katz, *Quantitation of human pancreatic beta-cell function by immunoassay of C-peptide in urine*. *Diabetes*, 1977. **26**(1): p. 30-5.
284. Gjessing, H.J., et al., *Fasting plasma C-peptide, glucagon stimulated plasma C-peptide, and urinary C-peptide in relation to clinical type of diabetes*. *Diabetologia*, 1989. **32**(5): p. 305-11.
285. Gjessing, H.J., et al., *Correlations between fasting plasma C-peptide, glucagon-stimulated plasma C-peptide, and urinary C-peptide in insulin-treated diabetics*. *Diabetes Care*, 1987. **10**(4): p. 487-90.
286. Huttunen, N.P., et al., *Clinical significance of urinary C-peptide excretion in children with insulin-dependent diabetes mellitus*. *Acta Paediatr Scand*, 1989. **78**(2): p. 271-7.
287. Hoogwerf, B.J., et al., *Urinary C-peptide as a measure of beta-cell function after a mixed meal in healthy subjects: comparison of four-hour urine C-peptide with serum insulin and plasma C-peptide*. *Diabetes Care*, 1983. **6**(5): p. 488-92.
288. Koskinen, P., et al., *Plasma and urinary C-peptide in the classification of adult diabetics*. *Scand J Clin Lab Invest*, 1986. **46**(7): p. 655-63.
289. McDonald, T.J., et al., *Stability and reproducibility of a single-sample urinary C-peptide/creatinine ratio and its correlation with 24-h urinary C-peptide*. *Clin Chem*, 2009. **55**(11): p. 2035-9.
290. Mortensen, H.B., et al., *Multinational study in children and adolescents with newly diagnosed type 1 diabetes: association of age, ketoacidosis, HLA status, and autoantibodies on residual beta-cell function and glycemic control 12 months after diagnosis*. *Pediatr Diabetes*, 2010. **11**(4): p. 218-26.
291. Boggetti, E., et al., *Growth changes in children and adolescents with short-term diabetes*. *Diabetes Care*, 1998. **21**(8): p. 1226-9.
292. Richters, C.D., et al., *Isolation and characterization of migratory human skin dendritic cells*. *Clin Exp Immunol*, 1994. **98**(2): p. 330-6.

Appendix – sources of materials

Reagents

Name	Content	Company
[³H] thymidine	6.2µCi/ml in 5%FCS in supplemented RPMI 1640	Perkin Elmer, Cambridge, UK
2-methylbuten-2-ol		Sigma-Aldrich, Poole, UK
5-TAMRA (carboxytetramethylthodamine) – GLCTLVAML – EBVP1 peptide	≥95% purity	GL Biochem (Shanghai) Ltd.,PRC
Agarose, powder		Geneflow, Lichfield, UK
AIM-V®+AlbuMAX BSA serum free media		Gibco, Paisley, UK
Bovine serum albumin (BSA)		Promega. Madison, USA
CD4+CD25+CD127_ Regulatory T cell Isolation Kit II, human		Miltenyi Biotec GmbH, Surrey, UK
Collagenase I	210 U/mg	Invitrogen, Paisley, UK
Compensation particles set, anti-mouse Ig k/negative control FBS		BD Pharmigen, Oxford, UK
Deoxyribonuclease I (DNA-sel) from bovine pancreas	≥400Kunitsz/mg	Invitrogen, Paisley, UK
DiproSone® cream	0.05%w/w betamethasone (as dipropionate)	Merck Sharp&Dohme Ltd, Hoddesdon, UK
Dispase II (neutral protease, grade II)	0.89U/mg	Roche, Burgess Hill, UK
DNA ladder	100bp	Thermoscientific, Loughborough, UK
DRB1*0101-0103 primers	100µM	Invitrogen, Paisley, UK
Dulbecco's Modified Eagle Medium (DMEM)		Gibco, Paisley, UK
Dulbecco's Phosphate Buffered Saline (PBS)		Sigma-Aldrich, Poole, UK
EDTA (ethylenediaminetetraacetic acid)	0.5M	Sigma-Aldrich, Poole, UK
ELISA substrate solution (IFNgamma and IL-10)	1Xtetramethylbenzidine (TMB) solution	E-bioscience, Hatfield, UK
ELISA Substrate Solution MIP-1β, BDOptEIA™	Two part substrate solution: Reagent A – H ² O ² , reagent B – TMB.	BD Biosciences, Oxford, UK
Ensure Plus®		Abbott Nutrition, Illinois, USA
Ethidium bromide	Stock 10mg/ml in dH ₂ O	Sigma-Aldrich, Poole, UK

ExtraAvidin® Alkaline Phosphatase		Sigma-Aldrich, Poole, UK
Ficoll-Paque PLUS	1.077±0.001 g/ml, +20°C	GE Healthcare Biosciences, Uppsala, Sweden
Foetal calf serum (FCS)		Biosera, Boussens, France
Glacial acetic acid		Fisher Scientific, Loughborough, UK
Glycerol		Fisher Scientific, Loughborough, UK
Gold nanoparticles (NP)	325 µg/ml of gold	Midatech, Abingdon, UK
Hemagglutinin (306-318) Influenza A virus peptide PKYVKQNTLKLAT (FP1)	≥97% purity	Mimotopes Pty Ltd, Australia
Heparin Sodium solution	1,000 IU/ml	Wockhardt UK Ltd, Wrexham, UK
HLA-DR1 and control primers for HLA DR1 typing		Invitrogen, Paisley, UK
Human AB serum		PAA, Pasching, Austria
Human anti IL10- antibody	1mg/ml	Miltenyi Biotec, Surrey, UK
Human C-peptide ELISA		Mercodia, Milton Keynes, UK
Human IFNgamma ELISA Ready-Set-Go!		E-bioscience, Hatfield, UK
Human IL-10		Cell Signaling Technology, Danvers, USA
Human IL-10 ELISA Ready-Set-Go!		E-bioscience, Hatfield, UK
Human IL-10 nanoparticles	62.5µg/ml IL-10, 227µg/ml gold	Midatech, Abingdon, UK
Human IL-15, research grade	2x10 ⁶ iu/ml	Miltenyi Biotec, Bergisch Gladbach, UK
Human IL-2, research grade	5x10 ⁶ iu/ml	Miltenyi Biotec, Bergisch Gladbach, UK
Human MIB-1β DuoSet® ELISA kit		R&D Systems, Abingdon, UK
IFNγ ELISPOT Biotinylated detection antibody		U-CyTech biosciences, Utrecht, The Netherlands
IFNγ ELISPOT coating antibody		U-CyTech biosciences, Utrecht, The Netherlands
L-glutamine	200mM	Gibco, Paisley, UK
Lytic protein BMLF-1 (280-288) Epstein-Barr virus peptide GLCTLVAML (EBVP1)	≥90% purity	Mimotopes Pty Ltd, Australia
Naïve CD4+ T cell isolation kit II, human		Miltenyi Biotec GmbH, Surrey, UK
Nitric acid		Fisher Scientific, Loughborough, UK

Orange G sodium		Sigma-Aldrich, Poole, UK
Ortho-phosphoric acid		Fisher Scientific, Loughborough, UK
Paraformaldehyde		Fisher Scientific, Loughborough, UK
Penicillin-Streptomycin solution	5,000 units/ml of penicillin	Gibco, Paisley, UK
	5,000 µg/ml of streptomycin	
Penicillin-Streptomycin-Neomycin solution	5,000 units/ml of penicillin	Sigma-Aldrich, Poole, UK
	5,000 µg/ml of streptomycin	
	10,000 µg/ml of neomycin	
Phytohemagglutinin PHA-P, lyophilized powder		Sigma-Aldrich, Poole, UK
Polyvinyl alcohol (PVA 2000)		Sigma-Aldrich, Poole, UK
RPMI 1640, without glutamine		Gibco, Paisley, UK
SIGMA FAST™ BCIP/NBT tablets	5-Bromo-4-chloro-3-indolyl-phosphate/Nitro blue tetrazolium (BCIP/NBT)	Sigma-Aldrich, Poole, UK
Tetanol Pur® Tetanus toxoid	80IU/ml	Novartis, Holzkirchen, Germany
Tris (hydroxymethyl)-methylamine		Fisher Scientific, Loughborough, UK
Trypan blue, solution	0.4% w/v	Sigma-Aldrich, Poole, UK
Trypsin-EDTA solution	0.25% w/v	Sigma-Aldrich, Poole, UK
Tuberculin PPD RT23, for <i>in vivo</i> use	2TU in 0.1ml	Serum Statens Institute, Copenhagen, Denmark
Tuberculin PPD, for <i>in vitro</i> use	1mg/ml	Serum Statens Institute Copenhagen, Denmark
Tween 20, solution		Fisher Scientific, Loughborough, UK
Xylocaine 1% w/v, local anaesthetic		Astra Zeneca, London, UK

Solutions and buffers

1X TAE buffer	40 mM Tris, 20mM acetic acid and 1mM EDTA in DI water
Complete RPMI1640	10% human AB serum v/v 0.5mM L-glutamine, 50IU/ml penicillin, 0.05mg/ml streptomycin and 0.1mg/ml neomycin
DI water	Deionized water
ELISA stop solution	2M H ₂ SO ₄
ELISA wash buffer	0.05% Tween 20 in PBS
Flow-cytometry buffer (FCB)	0.5% (v/v) FCS and 0.01% (w/v) Na-azide in PBS
Flow-cytometry fixative (FCF)	1% (v/v) paraformaldehyde in PBS
MACS buffer	2mM EDTA in 0.5% (w/v) BSA in 1xPBS
Name	Content
Orange G PCR loading buffer	0.25g of OrangeG in 30%glycerol in water
Supplemented RPMI1640	0.5mM L-glutamine, 50IU/ml penicillin, 0.05mg/ml streptomycin and 0.1mg/ml neomycin

Software and hardware

Name	Content	Company
1450 Micro Beta Tri Lux Microplate scintillation counter		Perkin Elmer, Cambridge, UK
ELISPOT plate BioReader		ByoSys, Karben, Germany
FACS Canto II flow-cytometer		BD biosciences, Oxford, UK
Flow Jo 8.8.6 software		Leland, Stanford, UK
Gammacell 1000 Elite Blood Irradiator		MDS Norton, US
GE HealthCare Ultrasound Logiq E9	Linear probe ML1 6-15Hz	GE Healthcare Life Sciences, UK
GraphPad Prism, version 4a for Macintosh		GraphPad Software, SanDiego, USA
NanoVue Plus Spectrophotometer		GE Healthcare Life Sciences, UK
Photometer – Opsys MR™ Microplate Reader		Dynex Technologies, Chantilly, USA
PTC-200 DNA Engine thermocycler		MJ Research, Ramsey, USA
Suction pump machine		Eschmann, UK

Equipment

Name	Content	Company
Cell culture inserts, for 24-well plate		Fisher Scientific, Loughborough, UK
Cell culture strainer 70µm for 50ml centrifuge tube		Fisher Scientific, Loughborough, UK
CryoTube	1ml	Thermo Scientific, Cramlington, UK
Dry stainless steel microneedle		Cardiff School of Engineering, Cardiff, UK
ELISA plate, Coat Corning Costar 9018 96-well plate		Lifesciences, Tewksbury, USA
ELISPOT filter plates	High-Protein Binding Immobilon-P Membrane	Millipore, Billerica, USA
Harris Uni-Core™ skin sampling tool for PCR	0.5mm	Ted Pella, Redding, Canada
LD columns for magnetic separation		Miltenyi Biotec, Surrey, UK
Micronjet 600 Needle, hollow microneedle		Nanopass Technologies, Nes Ziona, Israel
MidiMacs Separator	For holding the columns	Miltenyi Biotec, Surrey, UK
MiniMacs Separator	For holding the columns	Miltenyi Biotec, Surrey, UK
MS columns for magnetic separation		Miltenyi Biotec, Surrey, UK
MultiStand	For holding separators	Miltenyi Biotec, Surrey, UK
PCR tube	0.2ml	Eppendorf UK Limited, Stevenage, UK
Punch biopsy 0.8cm		Kai Medical, Seki, Japan
Round-bottom polypropylene tubes	14ml; with dual-position snap cap	Fisher Scientific, Loughborough, UK
SST blood collection tube	5ml (13x100mm)	BD Vacutainer, Oxford, England
Suction blister cup		UHBristol NHS Foundation Trust Medical Engineering Department, Bristol, UK
Surgical blade	Removal of blister roof	Swann Morton Ltd, Sheffield, UK